B.ERPEK

ATILIM UNIVERSITY 2022

STRENGTHENING DEFICIENT RC BUILDINGS
USING EXTERNAL STEEL BRACES

THE GRADUATE SCHOOL OF NATURAL AND APPLIED SCIENCES
OF
ATILIM UNIVERSITY

BERK ERPEK

A MASTER OF SCIENCE THESIS
IN
THE DEPARTMENT OF CIVIL ENGINEERING

JUNE 2022

STRENGTHENING DEFICIENT RC BUILDINGS
USING EXTERNAL STEEL BRACES

A THESIS SUBMITTED TO
THE GRADUATE SCHOOL OF NATURAL AND APPLIED SCIENCES
OF
ATILIM UNIVERSITY

BY

BERK ERPEK

IN PARTIAL FULFILLMENT OF THE REQUIRMENT
FOR
THE DEGREE OF MASTER OF SCIENCE
IN
THE DEPARMENT OF CIVIL ENGINEERING

JUNE 2022

Approval of the Graduate School of Natural and Applied Sciences, Atilim University.

Prof. Dr. Ender KESKİNKILIÇ
Director

I certify that this thesis satisfies all the requirements as a thesis for the degree of **Master of Science in Civil Engineering Department, Atılım University**.

Prof. Dr. Yakup DARAMA

Head of Department

This is to certify that we have read the thesis “STRENGTHENING DEFICIENT RC BUILDINGS USING EXTERNAL STEEL BRACES” submitted by BERK ERPEK and that in our opinion it is fully adequate, in scope and quality, as a thesis for the degree of Master of Science.

Asst. Prof. Dr. Halit Cenan MERTOL

Supervisor

Examining Committee Members:

Assoc. Prof. Dr. Rıza Secer Orkun KESKİN
Civil Eng. Department, TED University

Asst. Prof. Dr. Halit Cenan MERTOL
Civil Eng. Department, Atılım University

Asst. Prof. Dr. Gökhan TUNÇ
Civil Eng. Department, Atılım University

Date: 10.06.2022

I hereby declare that all information in this document has been obtained and presented in accordance with academic rules and ethical conduct. I also declare that, as required by these rules and conduct, I have fully cited and referenced all material and results that are not original to this work.

Berk ERPEK

ABSTRACT

STRENGTHENING DEFICIENT RC BUILDINGS USING EXTERNAL STEEL BRACES

Erpek, Berk
M. S., Department of Civil Engineering
Supervisor: Asst. Prof. Halit Cenan Mertol

June 2022, 196 pages

Based on Ministry of Environment and Urbanization of Turkey, there are 5 million earthquake resistant apartments out of a total of 19,5 million apartments in Turkey. Seven million apartments need urgent action for a strengthening solution or shall be demolished immediately. It is not possible to demolish and rebuild all these deficient structures. Strengthening them includes many complications. One of the most important complications is the replacement of the occupants from the deficient buildings during the construction process.

Strengthening of existing reinforced concrete structures using external steel braces method is getting popular worldwide since it may be performed faster, cheaper and without impacting the inhabitants who live in these structures. The purpose of this research is to determine the effectiveness of external strengthening using steel braces for existing reinforced concrete buildings.

Four building models having number of stories 3, 6, 9, and 12 were analytically investigated. These building models were designed as deficient buildings according to Turkish design codes. The performances of the deficient building models were evaluated using three different methods, Equivalent Static Earthquake Load, Pushover Analysis, and Time History Analysis. These deficient buildings were strengthened using external steel braces and the performances were evaluated using these methods.

The results indicated all building models can effectively be strengthened using inverted-V configured external steel bracing system. Buildings up to 9 stories can be effectively strengthened using X configured steel bracing system. The most cost-effective strengthening system was the one having one steel frame on each side of the building.

Keywords: Strengthening against Seismic Load, Equivalent Earthquake Load, Pushover Analysis, Time History Analysis, Reinforced Concrete Buildings, External Steel Braces.

ÖZ

YETERLİ DAYANIMA SAHİP OLMAYAN BETONARME BİNALARIN ÇAPRAZ ÇELİK PROFİLLER KULLANILARAK GÜÇLENDİRİLMESİ

Erpek, Berk
Yüksek Lisans, İnşaat Mühendisliği Bölümü
Tez Yöneticisi: Dr. Öğr. Üyesi Halit Cenan Mertol

Haziran 2022, 196 sayfa

Türkiye Cumhuriyeti Çevre, Şehircilik ve İklim Değişikliği Bakanlığı'na göre, Türkiye'deki toplam 19,5 milyon binadan sadece 5 milyonu depreme dayanıklıdır. Yedi milyon bina acil olarak güçlendirilmeli veya yıkılmalıdır. Yeterli dayanıma sahip olmayan binaların hepsini yıkıp yeniden inşa etmek mümkün gözükmemektedir. Güçlendirme süreci birçok komplikasyon içerir. En önemli komplikasyonlardan biri, güçlendirme çalışmaları yapılan binalarda oturanların tahliye edilmesidir.

Mevcut betonarme binaların dıştan çelik çapraz yöntemi ile güçlendirilmesi, daha hızlı, daha ucuz ve bu binalarda yaşayan, çalışan veya kullananları etkilemeden yapılabilmesi nedeniyle dünya çapında popüler hale gelmektedir. Bu araştırmanın amacı, mevcut betonarme binalar için dıştan çelik çaprazlar kullanılarak güçlendirme yönteminin verimliliğini değerlendirmektir.

Bu çalışmada 3, 6, 9 ve 12 katlı dört betonarme bina model analitik olarak incelenmiştir. Kullanılan betonarme bina modelleri, tasarım kodlarına göre yeterli dayanıma sahip olmayan binalar olarak tasarlanmıştır. Yeterli dayanıma sahip olmayan bina modellerinin performansları, Eşdeğer Statik Deprem Yükü, İtme Analizi ve Zaman Tanım Alanında Deprem Yer Hareketi Analizi olmak üzere üç farklı yöntemle değerlendirilmiştir. Bu binalar daha sonra dıştan çelik çaprazlarla güçlendirilmiş ve performansları aynı üç yöntemle değerlendirilmiştir. Sonuçlara göre, tüm betonarme bina modellerinin ters V konfigüre edilmiş dış çelik destek sistemi kullanılarak etkin bir şekilde güçlendirilebileceğini anlaşılmıştır. 9 kata kadar olan betonarme binaların ise X konfigürasyonlu çelik çaprazlama sistemi ile etkin bir şekilde güçlendirilebileceği sonucuna ulaşılmıştır. Binanın her iki yanında birer çelik çerçeveye sahip olan sistemin, maliyet açısından en uygun güçlendirme sistem olduğu görülmüştür.

Anahtar Kelimeler: Depreme Karşı Güçlendirme, Eşdeğer Deprem Yükü Yöntemi, İtme Analizi, Zaman Tanım Alanında Deprem Yer Hareketi Analizi, Betonarme Binalar, Dış Çelik Çaprazlar.

DEDICATION

To all readers

ACKNOWLEDGEMENTS

I would like to express my special thanks to my supervisor, Assist. Prof. Dr. Halit Cenan Mertol, who guided me about thesis and gave this opportunity to work with himself. Also, I learnt lots of information especially engineering and computer programming from him. I am glad working with him.

I would like to thanks who worked on this topic. I used their ideas, thesis, articles and studies to develop myself and my thesis.

I would like to thanks to committee of Atılım University, who gave my scholarship to study. Also, I would like to thanks to academic personal of Department of Civil Engineering of Atılım University be a part of my bachelor degree.

Finally, I would like to special thanks to my parents and my friends. They gave me this opportunity with their supports and their works and ideas always be supportive to me.

TABLE OF CONTENTS

LIST OF TABLES

TABLES

LIST OF FIGURES

FIGURES

CHAPTER 1

1. INTRODUCTION

1.1 General Information

Earthquakes always be a part of mankind's life. People lost their lives and structures were collapsed or damaged seriously due to earthquakes. Also, earthquakes lead to massive economic losses for building new structures or recovery costs of damaged buildings.

Many earthquakes happened in Turkey which affected people's lives and country's economy, such as Düzce Earthquake (1999), Gölcük Earthquake (1999), and İzmir Earthquake (2020) [1]. Earthquake Map of Turkey [2] is presented in the Figure 1.1, which corresponds to an earthquake having a probability of exceeding 10% in 50 years and recurrence period is 475 years. Based on this map, 92% of surface area of our country is in seismic zones and 95% of the population is under earthquake threat. Additionally, 98% of huge industrial centers and 93% of dams are located in these seismically active areas [3].

According to data of Ministry of Environment, Urbanization and Climate Change of Republic of Turkey, there are 19,5 million apartments in Turkey [4]. However, only 5 million apartments are earthquake resistant according to Turkish Earthquake Code (2007) [5]. Seven million apartments shall be strengthened against earthquake or destroyed immediately. Since the thread may happen anytime, these structures need a fast solution of strengthening or demolishing.

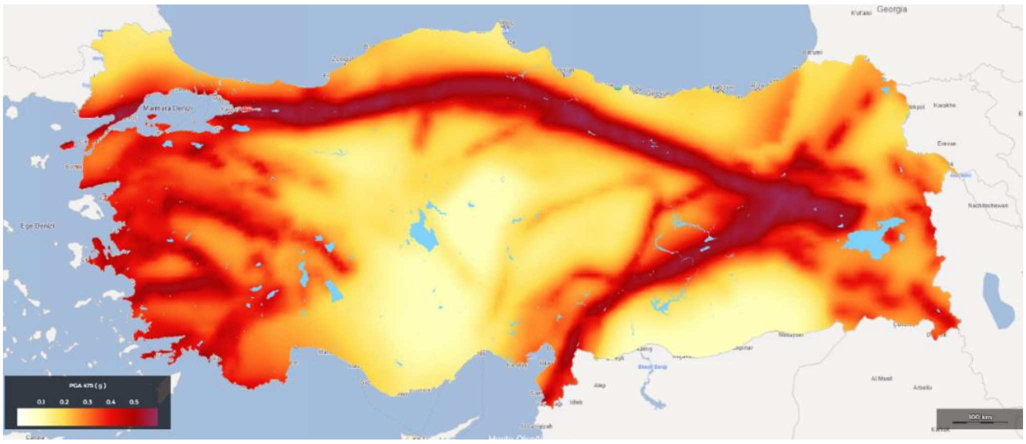

Figure 1.1 Earthquake Map of Turkey [2]

There are many strengthening methods that can be applied on reinforced concrete structures. Out of these methods, strengthening of existing reinforced concrete structures using external steel braces is getting popular worldwide. One of example of strengthening using external steel braces method is shown Figure 1.2. When this method is compared to other strengthening methods, it may be performed faster, cheaper and without impacting the inhabitants who live in, work in, or use these structures. In this study, the effectiveness of external strengthening method using steel braces is investigated against seismic loads.

Figure 1.2 Strengthening of Existing Reinforced Concrete Parking Garage Using External Steel Braces [6]

1.2 Problem Definition

Based on the report published by Ministry of Environment, Urbanization and Climate Change of Republic of Turkey [2], 7 million apartments are deficient against seismic loads determined according to the Turkish Earthquake Code (2007) [5]. It looks impossible that all these structures to demolish and rebuild because of economic conditions and lack of time.

1.3 Scope

The purpose of this research is to determine the effectiveness of external strengthening method using steel braces for existing reinforced concrete buildings that would not disturb/replace the occupants of the building during the construction process.

For this purpose, three different methods were used to evaluate the effectiveness of this strengthening method, determine the benefits of different modelling systems for this strengthening method. SAP2000 Analysis Software [7] was used for this study. The scope can be summarized as follows:

- Four buildings having number of stories 3, 6, 9, and 12 were investigated.
- The structural members (beams, columns, slabs, etc.) of the building models were designed based on TS500 (2000) [8] and the latest Turkish Building Earthquake Code (2018) [11]. These models were converted to deficient buildings by reducing the dimensions of all columns in the building by 10% in both directions which corresponds to an area reduction of 19%.
- The performances of the deficient building models were evaluated using three different methods, Equivalent Static Earthquake Load, Pushover Analysis, and Time History Analysis.
- These deficient buildings were strengthened using external steel braces designed based on AISC 360-10 [9] and the performances were evaluated using the same three methods.

1.4 Organization of Thesis

This thesis has five chapters. First chapter contains the introduction, problem statement and scope of thesis.

Second chapter contains, a literature review related to strengthening methods using external steel braces in different countries and different models.

Third chapter contains the description of building models and applied loads on these models based on TS500 (2000) [8], TS498 (1987) [10], and TBEC (2018) [11].

Results of analysis and design of the models were presented in Chapter 4. Three different methods, Equivalent Earthquake Load Method based on TBEC (2018) [11], Pushover Analysis Method, and Time History Analysis Method using past earthquakes, were used to determine the effectiveness of strengthening of deficient buildings using external steel braces.

Last chapter of this thesis, Chapter 5 contained conclusions related to strengthening of deficient buildings using external steel braces. Recommendations and thoughts on future work were also stated.

CHAPTER 2

2. LITERATURE REVIEW

In this chapter, previous studies related to strengthening of buildings using steel braces are presented.

Balagopal [12] investigated the efficiency of a diagonal curved brace system as an alternate to retrofit existing steel moment frame structures. The modelling was performed using SAP2000 Structural Analysis Software [7]. Two different building layouts (square and rectangular) having different building heights (ranging from 21 to 50 stories) and three arc-formed external bracing systems were used in the analysis. The results were compared based on deflections, drift ratios, and economy. It was concluded that the diagonal curved brace form worked efficiently in producing minimal drift in buildings as tall as 21 stories with a square layout, however not in taller buildings or buildings with a rectangular layout. Based on economy, it was stated that huge amount of money can be saved by strengthening moment frame structures using curved braced system and achieve minimal deflection.

Haikal and Muca [13] analyzed and strengthened an existing 7 story structure consisting of prefabricated concrete and steel elements in Stockholm. MIDAS GEN [14] Analysis Software was used in the analysis. Various strengthening techniques including steel bracing and reinforced concrete shear walls were compared. The results indicated that the strengthening method using steel braces provided the greatest reduction of displacements in the x- and y-direction remarkably. It was suggested that a combination of innovative seismic retrofitting methods would be more effective, achieving a more resistant building under seismic hazards, by improving the stability and ductility of the structure.

Abou-Elfath and Ghobarah [15] investigated the seismic performance of low-rise non-ductile reinforced concrete buildings strengthened using concentric steel bracing. Three-story building strengthened using steel bracing was analyzed using various ground motion records. The effect of the distribution of the steel bracing along the height of the RC frames on the seismic performance of the rehabilitated building was also studied. The performance of the building was evaluated in terms of global and story drifts and damage indices. A simplified approach was proposed for selecting the proper brace distribution. It was concluded that the degree of improvement in the seismic performance of the strengthened building depended significantly on the level of increase in the load carrying capacity as well as the changes in the seismic demand that result from the associated stiffness increase. It was also indicated that adding steel bracing uniformly along the height of an existing non-ductile building may not represent the optimum solution. Special arrangement of the lateral strength distribution along the frame height to force most of the building stories was stated as a better solution.

Agar [16] analytically investigated the use of steel bracing for the strengthening of low, intermediate, and relatively high rise reinforced concrete frames. Three building heights (3, 5, and 8 stories), four column dimensions (300×300, 400×400, 500×500, and 650×650 mm), and four concrete types (C16, C20, C25, and C30) were used as the variables of seven models produced in SAP2000 Structural Analysis Software [7]. The ultimate lateral load capacities of the strengthened frames were determined by a load controlled push-over analysis. It was concluded that it was possible to increase the lateral load capacities of existing reinforced concrete frame structures by up to 20 times using a bracing system composed of steel X-bracing and an enclosing steel frame around it in the frame bays and without even anchoring them into the existing R/C frame structure. It was also indicated that the concrete strength had a positive influence on the degree of improvement provided by steel bracing.

Balkaya [17] used structural building jacketing system (exterior steel bracing) to strengthen existing reinforced concrete structures against seismic loads. The main advantage of this strengthening method was stated as strengthening without disturbing their serviceability. Three-dimensional scaled models of RC buildings with and without the jacketing system were tested under static cyclic pushover loading to understand three-dimensional behavior. X and inverted -V steel braces were used in the investigation. Experimental and analytical results were compared to verify the models. The results indicated that structures strengthened using the jacketing system increased the seismic capacity by a factor of four. Application of this system to a 10-story housing in Istanbul was also discussed.

CHAPTER 3

3. DESCRIPTION OF BUILDING MODELS AND LOADS

3.1 Introduction

Description of models to evaluate the earthquake behavior of external steel bracing system is presented in this chapter. There were four different structure models in this study. All the plan views and story heights were same for all the models. The difference was in the story numbers. The investigated models had 3, 6, 9, and 12 stories. In the previous earthquakes in Turkey, it was seen that the severely damaged or collapsed buildings had story numbers between 3 and 12 [18]. The selection of the number of stories were made based on this information. Therefore, 3, 6, 9, and 12 stories were used to simulate low-rise, intermediate-rise, relatively high-rise, and high rise buildings, respectively.

The plan view of the models is shown in Figure 3.1. The plan views of the buildings were square-shaped having 5-bays in X-direction and 5-bays in Y-direction. The length of the bays in X- and Y-directions were equal each other and was equal to 6 meters. Total plan area of each story was equal to 900 m^2.

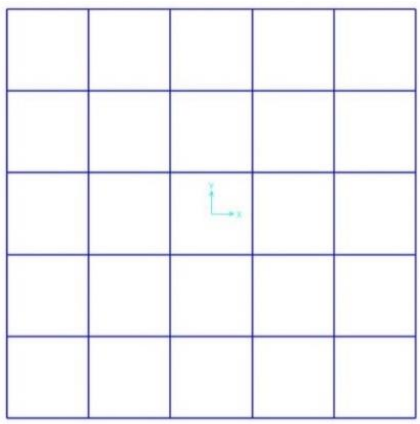

Figure 3.1 Plan View of Existing Structure Model

The cross-sectional view of the 3-story building is shown in Figure 3.2. Story heights of all the buildings were identical and equal to 3 meters. Total heights of the buildings were 9, 18, 27, and 36 meters for 3-, 6-, 9-, and 12-story building models, respectively. The cross-sectional views of other buildings are shown in between Figure 3.3 and Figure 3.5.

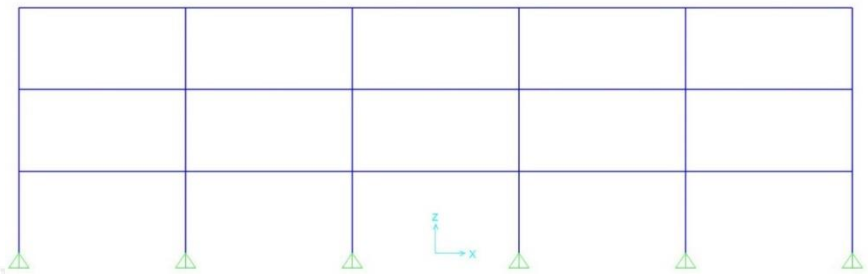

Figure 3.2 Cross-Sectional Views of 3-Story Structure

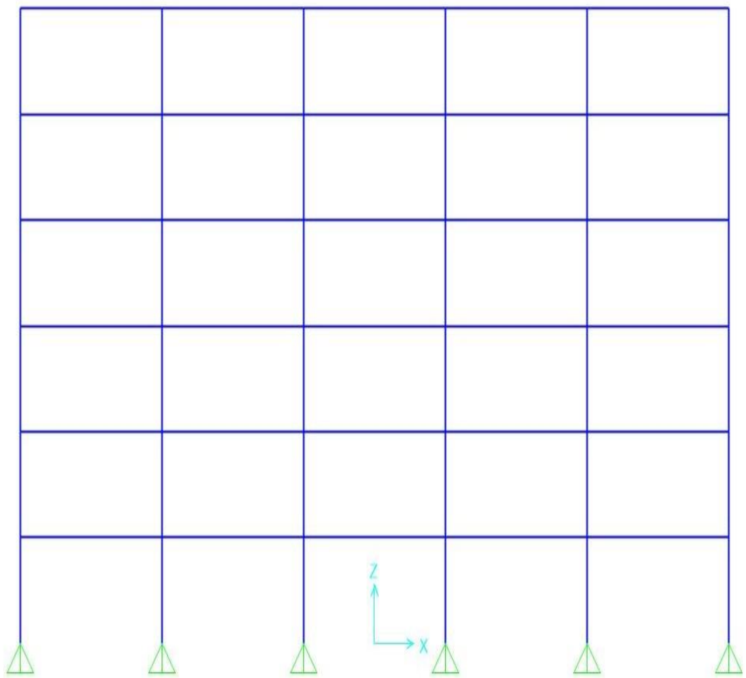

Figure 3.3 Cross-Sectional Views of 6-Story Structure

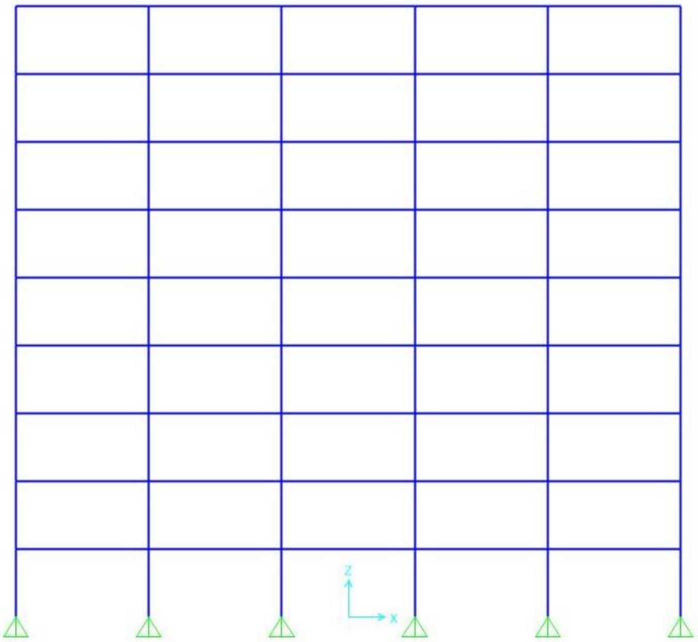

Figure 3.4 Cross-Sectional Views of 9-Story Structure

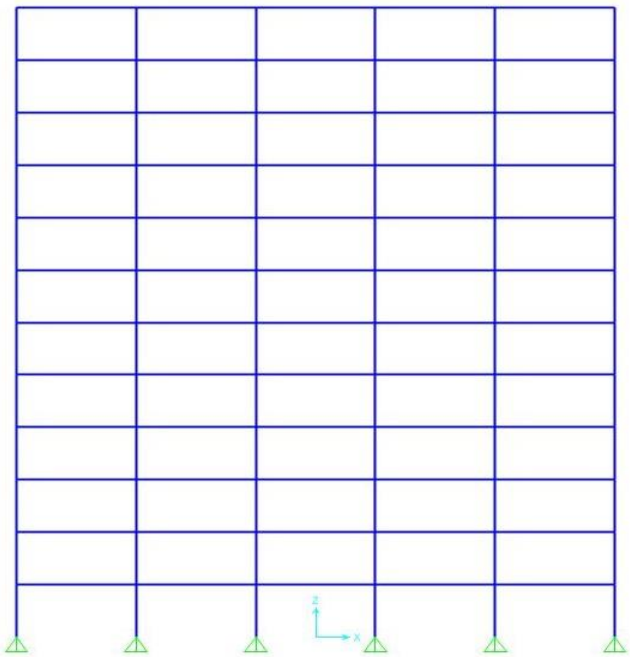

Figure 3.5 Cross-Sectional Views of 12-Story Structure

3.2 Assumptions

In this study, following assumptions were made:

- The building was assumed to be located in Üsküdar Province in İstanbul, Turkey. The aim of this selection was apply large earthquake loads and evaluate the effectiveness of strengthening using external steel braces better.

- The building was assumed to be located on a ZC local site class. This class represent very dense soil and soft rock.
- When earthquake happens, the bottom ends of the first story columns are converted to hinges due to the applied earthquake loads. Therefore, the connections between the first story columns and foundation were assumed to be hinges in all the models.
- Moment of inertias of structural reinforced concrete members (columns and beams) were not reduced in the analysis. This resulted in lower deflections of the deficient models, making the deficient models behave better. After strengthening, the deflections were all controlled by the deflections of the steel braces. Therefore, the results indicated that using the unreduced moment of inertias did not have any significant effects in the analysis and design.
- The connections between the structural steel sections and reinforced concrete joints were assumed to be perfectly fixed. Problems related to the construction of these connections were ignored. This assumption was modelled using assignment of joint constraints between connection joints in SAP2000 [7] and is shown in Figure 3.6.

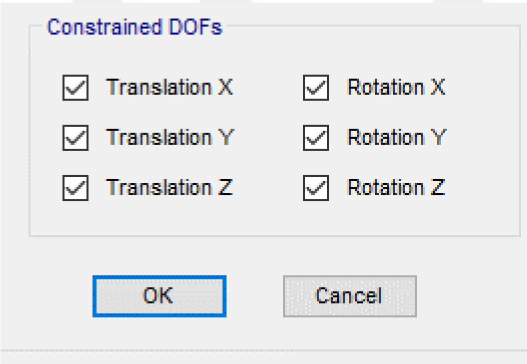

Figure 3.6 Joint Constraints between Structural Members

- The connections between the structural steel sections were assumed to be bolted connection. Examples of these types of connections are shown in Figure 3.7 and Figure 3.8. Bolted connections require less labor and less working area. These connections do not require special skilled workers.

Figure 3.7 Example of Bolded Connection

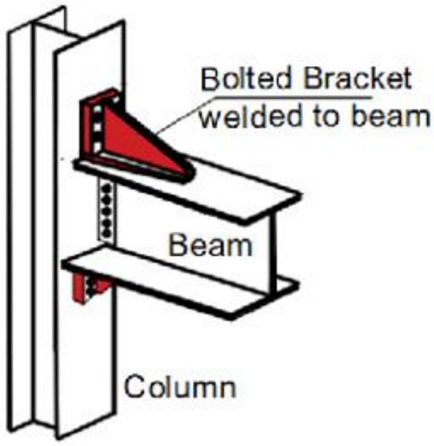

Figure 3.8 Details of Connection between Structural Members

- This study was performed for buildings having only frames.
- For the steel braces used in strengthening, the sections were changed in the increments of 3 stories: e.g. The cross-sectional dimensions of structural steel sections used for the first three stories were reduced in the next three stories.

3.3 Materials

Since the building models were simulating the existing (old) buildings, a low strength was used for concrete. The class of concrete used in the models was C16. All the properties related to concrete class were calculated using TS500 (2000) [8]. The values related to C16 concrete are shown in Table 3.1.

Table 3.1 C16 Concrete Properties based on TS500 (2000) [8]

Concrete Class	Characteristic Compressive Strength f_{ck} (MPa)	Equivalent Cube Compressive Strength (MPa)	Characteristic Tensile Strength f_{ctk} (MPa)	Elastic Modulus E_c (MPa)
C16	16	20	1,4	27000

Since the building models were simulating the existing (old) buildings, a low strength was also used for reinforcing steel. The type of both the longitudinal and transverse steel reinforcement steel used in the models was S220. All the properties related to steel type were calculated using TS500 (2000) [8]. The values related to S220 steel reinforcement are shown in Table 3.2.

Table 3.2 S220 Reinforcement Properties based on TS500 (2000) [8]

Mechanical Characteristics	Values (MPa)
Minimum Yield Strength, f_{yk}	220
Minimum Rupture Strength, f_{su}	340
Elastic Modulus, E_s	200000

The type of steel used for external steel braces (I-shaped steel sections) was A992Fy50. All the properties related to steel type were obtained using ASTM A992 [19]. The values related to A992Fy50 steel are shown in Table 3.3.

Table 3.3 Steel Section Properties based on ASTM A992 [19]

Mechanical Characteristic	Values (MPa)
Modulus of Elasticity, E	200000
Minimum Yield Stress (MPa)	345
Minimum Tensile Stress (MPa)	448

3.4 Design Parameters

3.4.1 Location of Structure

Location of structure is important to calculate loads especially for earthquake and snow load based on Turkish Building Earthquake Code 2018 [11] and TS 498 [10]. A location producing large earthquake loads was selected to evaluate the effectiveness of strengthening method better. Based on this criteria, Üsküdar Province in İstanbul, Turkey was selected as the location of the models. The selected location of the models is shown in Figure 3.9.

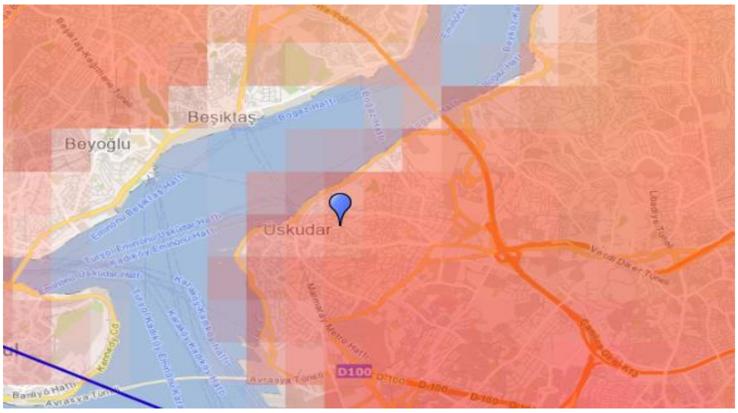

Figure 3.9 Location of Structure

Ground motion data for Üsküdar province in İstanbul, Turkey were obtained from Earthquake Map of Turkey from AFAD [2]. S_S, S_1, peak ground acceleration (PGA), and peak ground velocity (PGV) are shown in Table 3.4. Based on the assumption for soil class of building location (which is ZC), S_{DS} and S_{D1} are calculated as shown in Table 3.5.

Table 3.4 Design Data Based on Location of Structure

S_S	0,885
S_1	0,246
PGA (g)	0,363
PGV (cm/sec)	22,542

Table 3.5 Design Data Based on Soil Properties

S_{DS}	1,062
S_{D1}	0,369

3.4.1 Columns

Three different types of columns were defined for the models such as corner, edge, and inner columns. The defined columns on the plan view of the models are shown in Figure 3.10. The columns in red, yellow, and blue rectangles are defined as corner, edge, and inner columns, respectively.

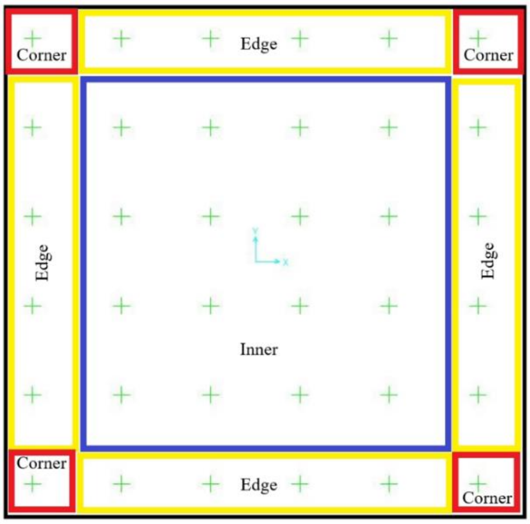

Figure 3.10 Plan View of Column Types

Cross sections of columns are calculated using the following expression specified by TBEC (2018) [11].

$$A_c \geq N_{dm} / (0{,}4 \times f_{ck}) \qquad \text{Equation 3-1}$$

Using the expression above, the column dimensions for all the buildings were calculated as shown in Table 3.6. These values were reduced by 10% in both directions (corresponding to an area reduction of 19%) to simulate the columns of an earthquake deficient building. The column dimensions of the structurally deficient building models against earthquake are shown in Table 3.7. Only the earthquake deficient building models were used in this study.

Table 3.6 Column Dimensions of Building Models based on TBEC (2018) [11]

Models	**Cross-Sectional Dimensions(mm×mm)**		
	Corner Columns	**Edge Columns**	**Inner Columns**
3-Story Apartment	300×300	450×450	600×600
6-Story Apartment	450×450	650×650	800×800
9-Story Apartment	600×600	800×800	1000×1000
12-Story Apartment	750×750	950×950	1200×1200

Table 3.7 Column Dimensions of Earthquake Deficient Building Models

Models	**Cross-Sectional Dimensions(mm×mm)**		
	Corner Columns	**Edge Columns**	**Inner Columns**
3-Story Apartment	270×270	405×405	540×540
6-Story Apartment	405×405	585×585	720×720
9-Story Apartment	540×540	720×720	900×900
12-Story Apartment	675×675	855×855	1080×1080

3.4.2 Beams

The beam dimensions of the models were determined using TS500 (2000) [8] (Table 3.8). Based on this standard, the cross-sectional dimensions of beams were determined as 300×600 mm in all models.

Table 3.8 Criteria of Beam Dimensions based on TS 500 (2000) [8]

Member	Simple Support	Exterior Span	Interior Span	Cantilever
One-way slab	L/20	L/25	L/30	L/10
Two-way slab	L/25	L/30	L/35	-
Joist slab	L/15	L/18	L/20	L/8
Beam	L/10	L/12	L/15	L/5

3.4.3 Slabs

The slab thickness of the models was determined using TS500 (2000) [8] (Equation 3-2 and Equation 3-3). Based on this standard, the slab thickness was determined as 150 mm in all models as shown in Table 3.9.

$$h \geq \frac{lsn}{15+(\frac{20}{m})} \times (1 - \frac{\alpha s}{4}) \qquad \text{Equation 3-2}$$

$$h \geq 150 \text{ mm} \qquad \text{Equation 3-3}$$

Table 3.9 Slab Dimensions of Building Models based on TS500 (2000) [8]

Slab Type	α_s	m	l_{sn} (mm)	h (mm)	Selected h (mm)
Corner Slabs	0,5	1	6000	150	**150**
Edge Slabs	0,75	1	6000	139	
Inner Slabs	1	1	6000	128	

3.4.4 Walls

Three different types of walls were used in the models. The surrounding walls of the building were defined as the outer walls. The outer walls consisted of 300 mm wide brick having an outer plaster of 30 mm and inner plaster of 24 mm. The separator walls inside the building were named as inner walls. The inner walls consisted of 200 mm wide brick having plaster of 24 mm on both sides. The 1-meter-high walls along the edge of the roof were named as parapet walls. The parapet walls consisted of 300 mm wide brick having plaster of 6 mm on both sides.

3.5 Loads

Dead, live, snow, wind, and earthquake loads were used in the analysis of the models. The calculation of these loads were performed using TS498 (1987) [10] and TBEC (2018) [11].

3.5.1 Dead Loads

The own weight of columns, beams, slabs, walls, and external steel braces are categorized as dead loads. Unit weights of each of the materials used to calculate the dead loads were obtained from TS498 (1987) [10] and TS ISO9194 (1997) [20].

The calculation of dead loads of 150 mm thick slabs are shown in Table 3.10. The superimposed dead load on the slab due to marble, plain concrete, and plaster was calculated as shown in Table 3.11.

Table 3.10 Dead Load Calculation for Slabs

Element	**Thickness (m)**	**Unit Weight of Material (kN/m^3)**	**Slab Weight (kN/m^2)**
Slabs	0,15	25	**3,75**

Table 3.11 Dead Load Calculation due to Materials used for Slabs

Material	**Height (m)**	**Unit Weight of Material (kgf/m^3)**	**Distributed Load (kN/m^2)**
Plain Concrete	0,05	2200	1,078
Marble	0,02	2700	0,529
Plaster	0,02	2000	0,392
		Total	**2,000**

The calculation of dead load of a 300×600 mm beam having a length of 6 meters is shown in Table 3.12. This value shall be multiplied by the total number of beams to calculate the total dead load of all the beams.

Table 3.12 Dead Load Calculation for Beams

Element	**Cross Sectional Area (m^2)**	**Width (m)**	**Unit Weight of Material (kN/m^3)**	**Beam Weight (kN)**
Beams	0,18	6	25	**27**

The dimension and height of each column were used to calculate the dead load of each column. These calculations are shown in Table 3.13. These values shall be multiplied by the total number of each type of columns to calculate the total dead load of all the columns.

Table 3.13 Dead Load Calculations for Columns

Column Types	Cross Sectional Area (m^2)	Height (m)	Unit Weight of Material (kN/m^3)	Column Weight (kN)
3-STORY				
Corner Columns	0,073	3	25	**5,468**
Edge Columns	0,164	3	25	**12,302**
Inner Columns	0,292	3	25	**21,870**
6-STORY				
Corner Columns	0,164	3	25	**12,302**
Edge Columns	0,342	3	25	**25,667**
Inner Columns	0,518	3	25	**38,880**
9-STORY				
Corner Columns	0,292	3	25	**21,870**
Edge Columns	0,518	3	25	**38,880**
Inner Columns	0,810	3	25	**60,750**
12-STORY				
Corner Columns	0,456	3	25	**34,172**
Edge Columns	0,731	3	25	**54,827**
Inner Columns	1,166	3	25	**87,480**

The dead load calculations related to outer, inner, and parapet walls are shown in tables between Table 3.14 and Table 3.16.

Table 3.14 Dead Load Calculations for Outer Walls

Material	Thickness (m)	Height (m)	Unit Weight of Material (kN/m^3)	Total Weight (kN/m)
Brick Wall	0,300	2,4	9,8	7,056
Plaster (Outer)	0,030	3,0	19,6	1,764
Plaster (Inner)	0,024	2,4	19,6	1,117
			Total=	**9,94**

Table 3.15 Dead Load Calculations for Inner Walls

Material	Thickness (m)	Height (m)	Unit Weight of Material (kN/m^3)	Total Weight (kN/m)
Brick Wall	0,200	2,4	9,8	7,056
Plaster(Outer)	0,024	2,4	19,6	1,117
Plaster(Inner)	0,024	2,4	19,6	1,117
			Total=	**6,94**

Table 3.16 Dead Load Calculations for Parapet Walls at Roof Level

Material	Thickness (m)	Height (m)	Unit Weight of Material (kN/m^3)	Total Weight (kN/m)
Brick Wall	0,300	1,0	9,8	2,94
Plaster(Outer)	0,006	1,0	19,6	1,117
Plaster(Inner)	0,006	1,0	19,6	1,117
			Total=	**5,17**

3.5.2 Live Loads

Live load value for residential buildings, which is equal to 2 kN/m^2, specified by TS498 (1987) [10] was used in all the models at every story. The application of live load on the slabs is shown in Figure 3.11.

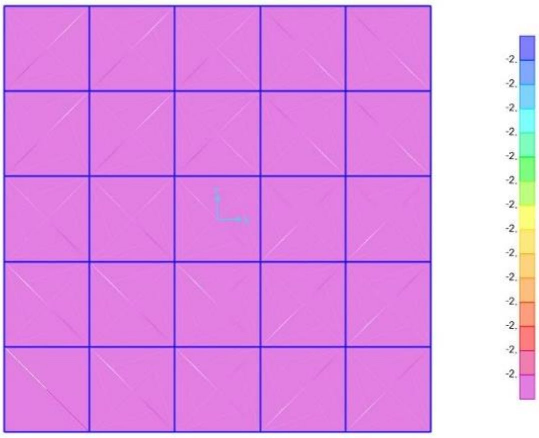

Figure 3.11 Application of Live Load on Slabs (kN/m2)

3.5.3 Snow Loads

Snow load was considered as a live load in all the analyses. Snow loads were calculated using Equation 3-3 specified by TS498 (1987) [10].

$$P_k = m \times P_{k0} \qquad \text{Equation 3-3}$$

where P_{k0} is the value of the snow load based on location and altitude of the structure, snow load reduction factor based on slope of the roof, and P_k is the value to be applied on the model. The m values can be determined using Table 3.17. In this table α represents the slope of the roof in degrees. In all the models, slope of the roof was selected as zero which represents a horizontal roof. Therefore, the value of m was used as 1. The buildings in this study were located in Üsküdar, İstanbul whose altitude is equal to 30 meters. Therefore, P_k was calculated as 0,75 kN/m^2. The application of snow load on the roof slab is shown in Figure 3.12 .

Table 3.17 m - Snow Load Coefficient due to Slope of Roof Table from TS498 (1987) [10]

α	0°	1°	2°	3°	4°	5°	6°	7°	8°	9°
0-30°	1,0									
30°	1,00	0,97	0,95	0,92	0,90	0,87	0,85	0,82	0,80	0,77
40°	0,75	0,72	0,70	0,67	0,65	0,62	0,60	0,57	0,55	0,52
50°	0,50	0,47	0,45	0,42	0,40	0,37	0,35	0,32	0,30	0,27
60°	0,25	0,22	0,20	0,17	0,15	0,12	0,10	0,07	0,05	0,02
70-90°										

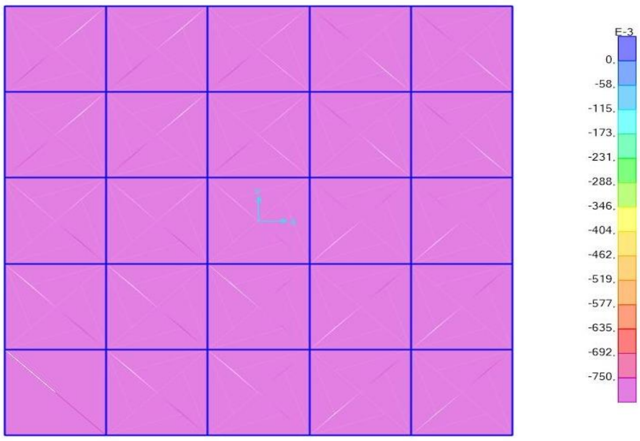

Figure 3.12 Application of Snow Load on Roof Slab (kN/m^2)

3.5.4 Wind Loads

The wind load changes along the height of the structures. Wind loads were calculated using Table 3.18 and Figure 3.13 as specified by TS498 (1987) [10].

Table 3.18 Pressure and Suction Values for Various Heights from Basement TS498 (1987) [10]

Height from Basement (m)	Suction, q (kN/m^2)
0-8	0,5
9-20	0,8
21-100	1,1
>100	1,3

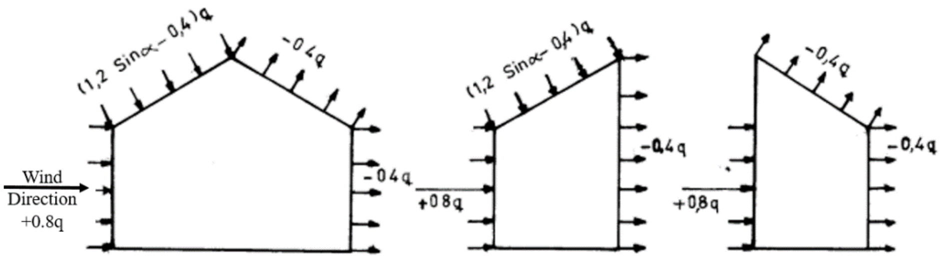

Figure 3.13 Pressure and Suction Values of Wind Load based on TS498 (1987) [10]

3.5.5 Effects of Earthquake Loads

The effects of earthquake loads were calculated using three different methods in this study. These methods are explained in details in this section.

3.4.5.1 Equivalent Earthquake Load Method

In this section, method of determine the effectiveness of strengthening method is introduced. Equivalent Earthquake Load Method is a linear analysis method. In this method, earthquake loads (total base shear) were calculated as a portion of the seismic weight of the structure. The total base shear was distributed to the floor levels as an equivalent earthquake load at each story level. This distribution produced an inverted triangular shape for earthquake loads. This means that first story of structure begins with a smaller earthquake load and the earthquake load increases at each story reaching a maximum earthquake load at the top story of structure. The distributed seismic load at each story level was applied to the mass center of that floor.

In this study, the procedure specified by Turkish Earthquake Building Code (2018) [11] was used to calculate the equivalent earthquake loads. Some important variables used to calculate this earthquake load are location of structure, soil site class, purpose of occupancy of structure, and material used such as concrete class and reinforcing steel type, etc.

The horizontal elastic response spectrum shown in Figure 3.14 was used in this study. This spectrum was modified using the selected soil type and ground motion level of earthquake (Table 3.19) according to the data provided by AFAD (2022) [2]. The modified horizontal elastic response spectrum is shown in Figure 3.15.

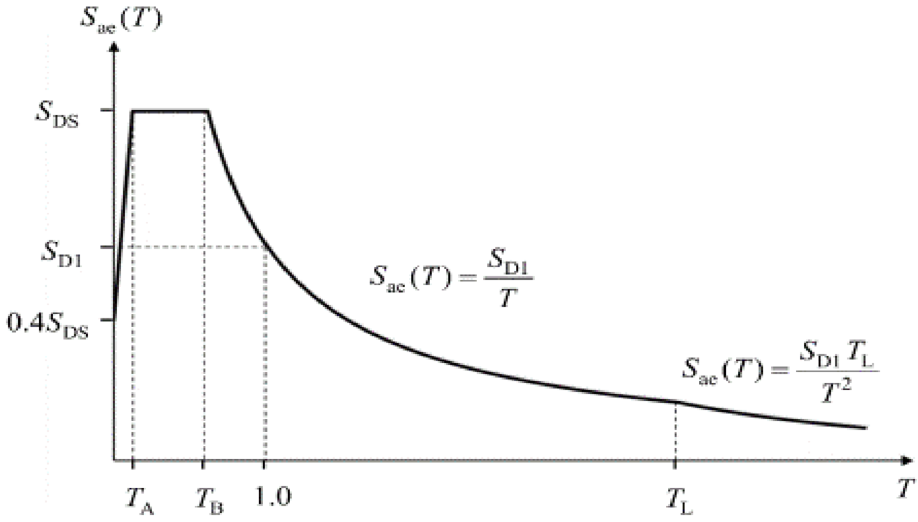

Figure 3.14 Horizontal Elastic Response Spectrum based on TBEC (2018) [11]

Table 3.19 Soil Characteristic of Structure's Location

S_{DS}	S_{D1}	T_A (s)	T_B (s)	T_L (s)
1,062	0,369	0,069	0,347	6,0

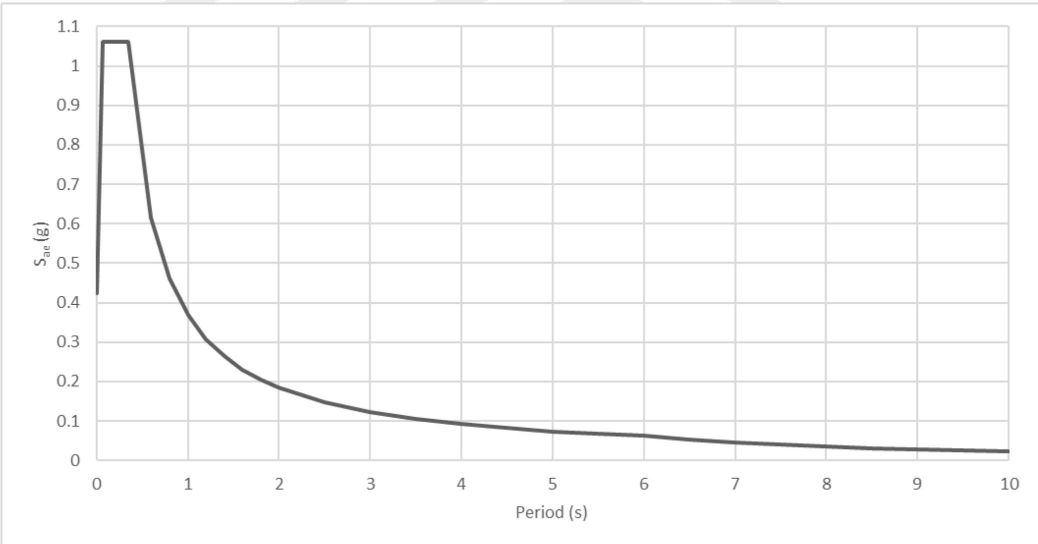

Figure 3.15 Horizontal Elastic Response Spectrum used in Analysis

In the Equivalent Earthquake Load Method, seismic design forces along any principle direction are calculated using a design horizontal seismic coefficient of the seismic weight of structure. The design horizontal seismic coefficient depends on zone factor of structure location, purpose of occupancy of structure, period of structure, and response reduction factor of the lateral load resisting frames. Dead loads and some part of live loads produces the seismic weight of structure. Live load participation factor changes according to the purpose of occupancy of the structure.

The first step to calculate the earthquake load using TBEC (2018) [11] is to determine the class of structure and its importance factor. In this study, structure models were all residential buildings. Therefore, the importance factor was used as 1,0 (Table 3.20).

Table 3.20 Importance Factor of Structure based on TBEC (2018) [11]

Purpose of Occupancy of Building	**Importance Factor(I)**
Other structures Residence, hotels, business centers, etc.	1,0

Second step is to determine the structural behavior. The deficient structures were assumed to have limited ductility level and when calculating the seismic load of the deficient structure, the coefficient of structural behavior and over-strength factor was used as 4 and 2,5, respectively. The strengthened structures were assumed to have high ductility level and when calculating the seismic load of the strengthened structure, the coefficient of structural behavior and over-strength factor was used as 8 and 3, respectively. The values used in this study are shown in Table 3.21.

Table 3.21 Coefficient of Structural Behavior based on TBEC(2018) [11]

Building Structural System	**Coefficient of Structural Behavior R**	**Over Strength Factor D**
High ductility level building in which seismic loads are fully resisted by frames	8	3
Limited ductility level building in which seismic loads are fully resisted by frames	4	2,5

The earthquake load reduction coefficient, $R_a(T)$, is calculated using Equation 3-4 and Equation 3-5.

$R_a(T) = \frac{R}{I}$ $\quad T>T_B \quad$ Equation 3-4

$R_a(T) = D + \left(\frac{R}{I} - D\right) \times \frac{T}{\mathrm{Tb}}$ $\quad T \leq T_B \quad$ Equation 3-5

$S_{aR}(T)$ is defined as reduced acceleration spectrum value based on the structural system of the building. Equation 3-6 was used to calculating $S_{aR}(T)$.

$S_{aR}(T) = \frac{Sae(T)}{Ra(T)}$ Equation 3-6

Seismic weight of structure is calculated using Equation 3-7. The live load participation factor used in this study was equal to 0,3 since the building model used in this study was a residential building (Table 3.22).

$w_j^{(S)} = w_{G,j}^{(S)} + n \times w_{Q,j}^{(S)}$ Equation 3-7

Table 3.22 Live Load Participation Factor based on TBEC (2018) [11]

Purpose of Occupancy of Building	**Live Load Participation Factor, n**
Residence, office, hotel, hospital, etc.	0,3

Finally, the total base shear is calculated using Equation 3-8. This load was distributed to each story using Equation 3-9, Equation 3-10, and Equation 3-11.

$V_{tE}^{(H)} = m_t \times S_{aR}(T_p^{(H)})$ Equation 3-8

$V_{tE}^{(H)} = \Delta F_{NE}^{(H)} + \sum F_{iE}^{(H)}$ Equation 3-9

$\Delta F_{NE}^{(H)} = 0,0075 \times N \times V_{tE}^{(H)}$ Equation 3-10

$F_{iE}^{(H)} = (V_{tE}^{(H)} - \Delta F_{NE}^{(H)}) \times \frac{mi \times Hi}{\sum_{j=1}^{N} mj \times Hj}$ Equation 3-11

3.4.5.2 Pushover Analysis Method

Pushover analysis is one of the most accurate analysis method and getting more popular in recent years to determine the performance of structure under the determined loads. One of the main advantages of nonlinear pushover analysis is being easier and direct than any other methods that uses lateral displacements. The purpose of nonlinear pushover analysis is to determine the resultant base shear against the monitored displacement response. In other words, capacity curve of a structure can be determined using pushover analysis. A demand spectrum is established using soil properties. With the help of seismic demands of structure, peak roof drift values, story drift ratios, local deformations and details related to plastic hinges can be calculated, which may be an advantage to make a decision for design.

3.4.5.2.1 Capacity Spectrum Method

The capacity spectrum method, a nonlinear static pushover analysis provides a graphical representation of the forces and displacement of the capacity curve of the structure. Capacity spectrum method is beneficial to evaluate the behavior of strengthened existing reinforced concrete structures. The earthquake ground motions are reduced in this method to represent the damping of structures. The reduced response spectrums may be defined as demand of the earthquake. Also the capacity curve is produced which is a graphical presentation of roof displacement versus the acceleration applied at the roof level.

The intersection point of capacity curve and the demand curve shows the performance point of structure. Performance point represent the behavior of structure under the applied earthquake ground motion. Typical capacity and demand curves and their performance point is shown in Figure 3.16

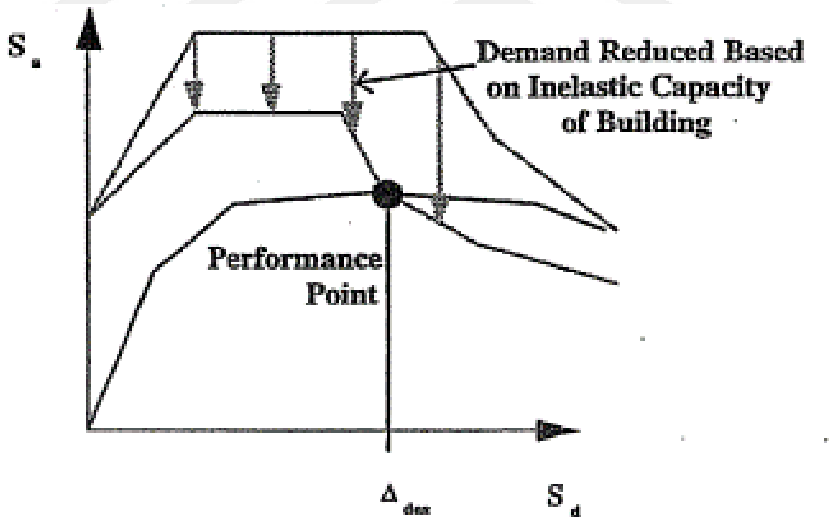

Figure 3.16 Definition of Performance Point based on ATC-40 [22]

The demand spectrum (Figure 3.17) was produced based on ATC-40 [22] document using coefficients (C_A and C_V) of site properties (Equation 3-12 and 3-13).

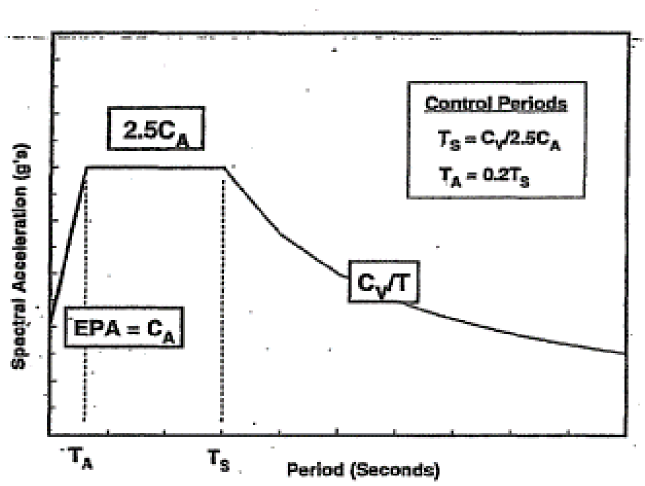

Figure 3.17 Demand Spectrum based on ATC-40 [22]

$C_A = 0,4 \times S_{MS}$ Equation 3-12

$C_V = S_{M1}$ Equation 3-13

where S_{MS} is defined as spectral acceleration in the short-period range and S_{M1} is defined as spectral acceleration at a 1.0 second period. Spectral acceleration values, S_{MS} and S_{M1}, were obtained using Turkish Earthquake Risk Map of AFAD [2]. S_{MS} was equal to 1,062 and S_{M1} was equal to 0,369 for the selected construction location of the building models. These values were calculated using Equation 3-12 and Equation 3-13, and defined in SAP2000 [7] as shown in Figure 3.18.

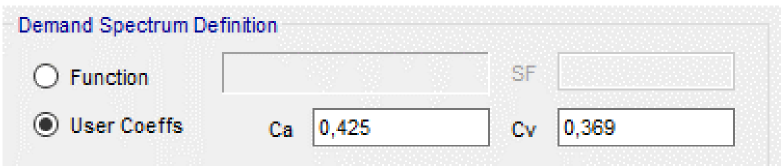

Figure 3.18 Defined Parameters for Demand Spectrum in SAP2000 [7]

3.4.5.2.2 P-Δ Effect on Frames

P-Δ effects occur due to geometric nonlinearity when the members are slender. P-Δ effect is used in pushover analysis to reach more accurate results. Axial compressive forces generally cause an increase in lateral displacements and it effects the lateral load resistance of the frames. In this study, P-Δ effects were considered in all the analyses of all the building models. A typical P-Δ effect description on columns is shown in Figure 3.19.

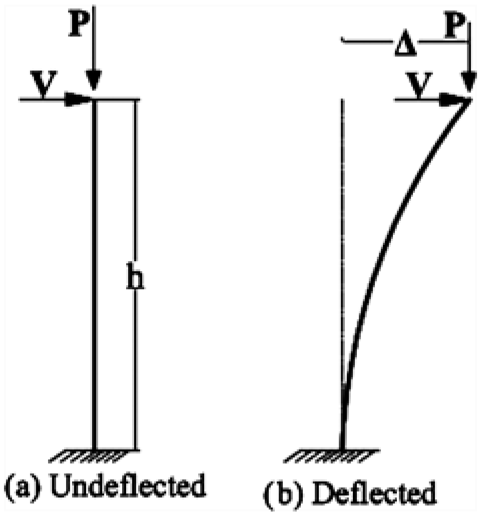

Figure 3.19 P-Δ Effect on Columns

3.4.5.2.3 Plastic Hinges

Plastic hinges shall be defined to obtain the pushover curve of the structure in pushover analysis method. Plastic hinges shall be assumed at the ends of columns and beams based on criteria of TBEC (2018) [11]. Hinges may be categorized based on material type (concrete and steel) and structural member (columns, beams, and braces).

Detailed information related to hinge assignment to structural elements in SAP2000 [7] is explained in this section. Five different hinges were defined in building models of this study based on ASCE 41-13[23] . These hinges were for concrete columns, concrete beams, steel columns, steel beams, and steel braces. Details related to these hinges are shown in figures between Figure 3.20 and Figure 3.24.

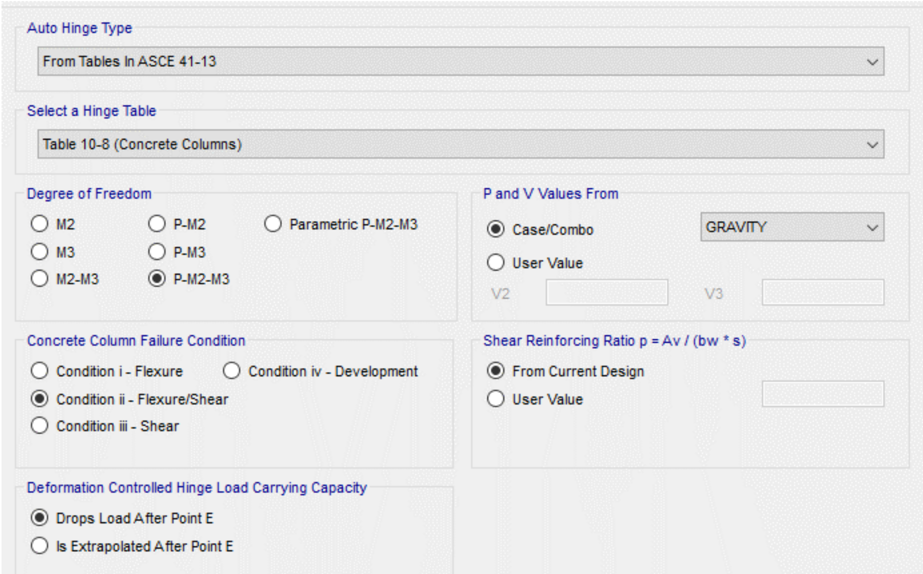

Figure 3.20 Assigned Hinge Properties for Concrete Columns

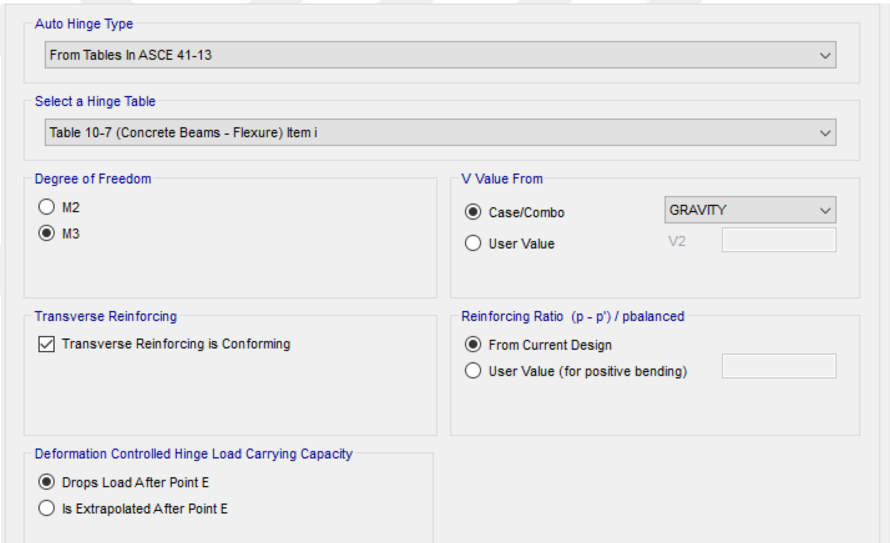

Figure 3.21 Assigned Hinge Properties for Concrete Beams

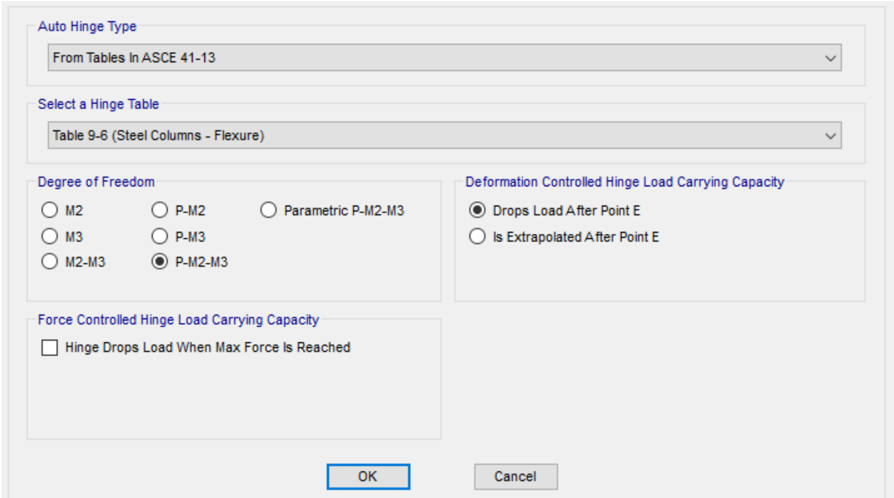

Figure 3.22 Assigned Hinge Properties for Steel Columns

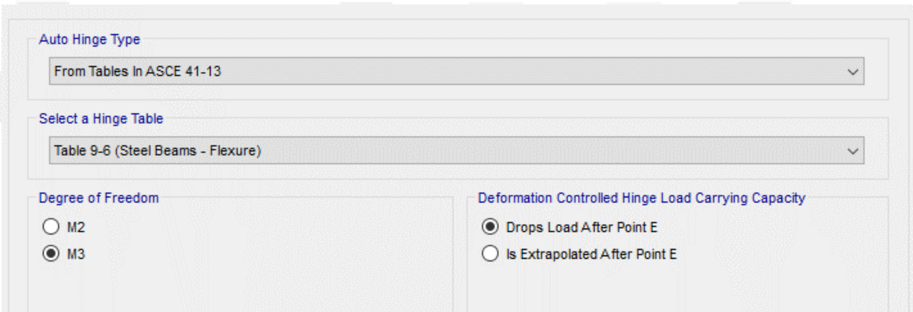

Figure 3.23 Assigned Hinge Properties for Steel Beams

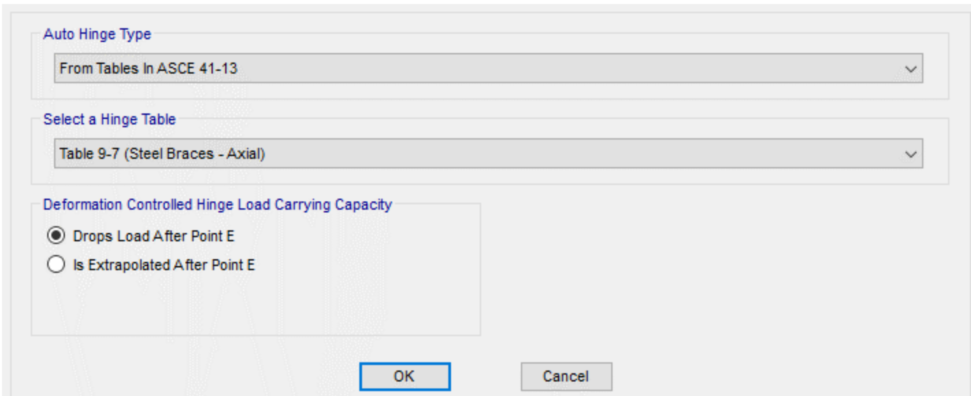

Figure 3.24 Assigned Hinge Properties for Steel Braces

3.4.5.2.4 Steps of Pushover Analysis using SAP2000 [7]

SAP2000 [7] was used to perform the pushover analysis on all building models. In this section, a step by step procedure is explained for pushover analysis of structure.

Initially, the load case of gravity was defined to start the analysis from initial the state of structure. P-Δ effect was selected and applied loads were selected as dead, live and snow with scale factors based on seismic weight of structure.

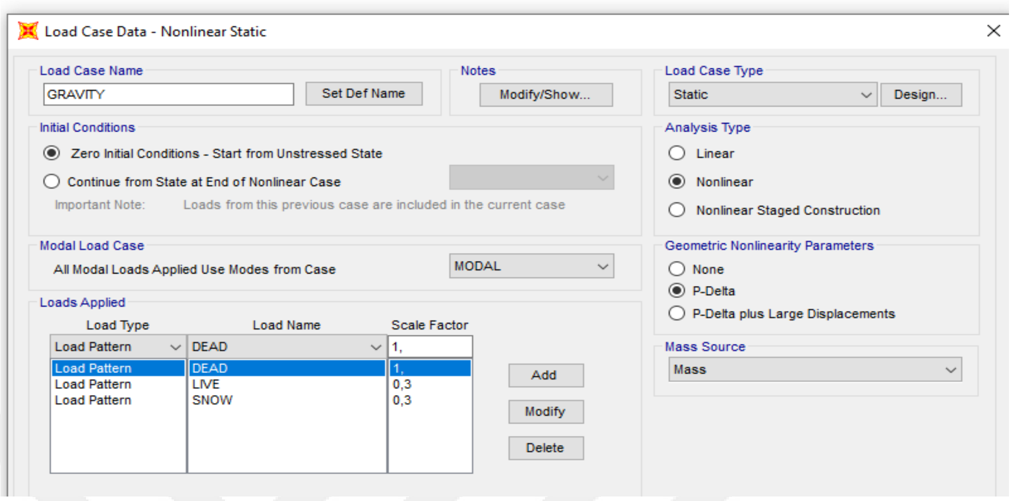

Figure 3.25 Definition of Gravity Load Case

In the second step, load cases, Push X and Push Y, were defined. In these load cases, initial conditions started from the Gravity load case. It means that analysis starts from the initial state of structure after the gravity loads are applied. Then the pushover starts by applying the displacements in X- and Y-directions as shown in Figure 3.26 and Figure 3.27.

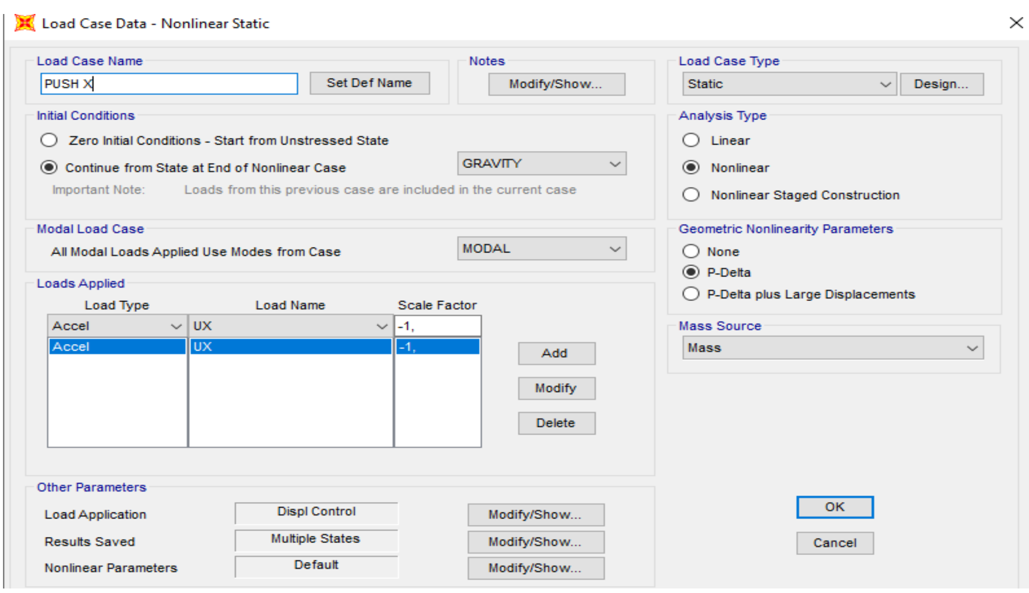

Figure 3.26 Definition of Push X Load Case in X-Direction

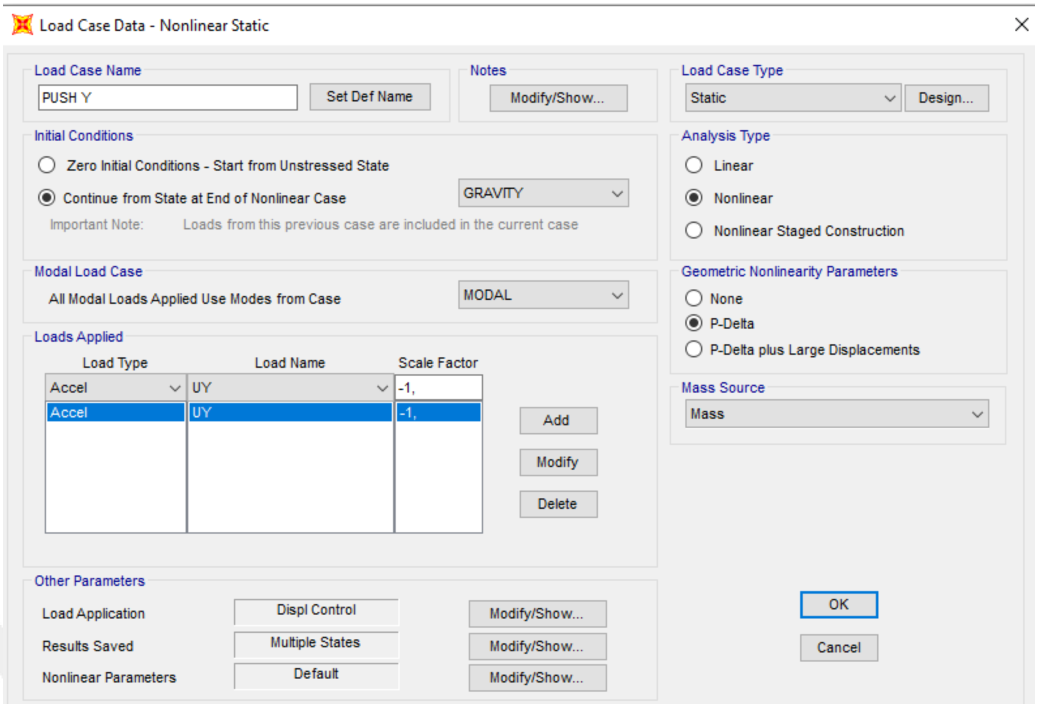

Figure 3.27 Definition of Push Y Load Case in Y-Direction

In this third step, conditions of load application control for nonlinear static analysis were defined. Load application control was selected as “displacement control” to produce capacity spectrum curve of the structure (Figure 3.28). Also, the type of displacement control was selected as “use monitored displacement” (Figure 3.28) to check the displacement until it reached the target displacement at the selected node (Figure 3.29, Figure 3.30, Figure 3.31, and Figure 3.32). For pushover analysis in X-direction, degree of freedom was selected as U1. For pushover analysis in Y-direction, degree of freedom was selected as U2. Load to a monitored displacement magnitude was used as default.

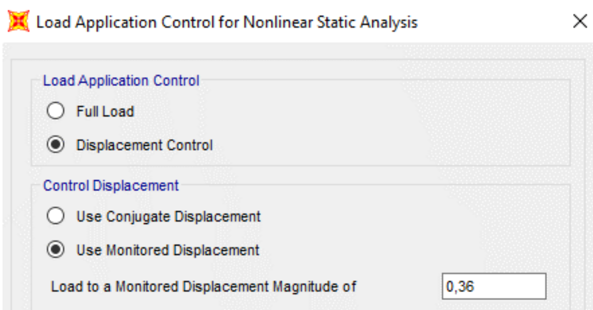

Figure 3.28 Applied Load Definition for Pushover Analysis

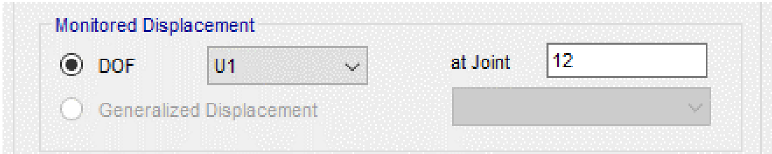

Figure 3.29 Monitored Displacement Definition for Pushover Analysis in X-Direction

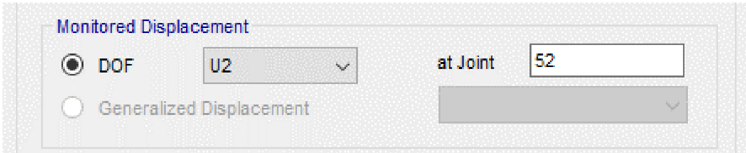

Figure 3.30 Monitored Displacement Definition for Pushover Analysis in Y-Direction

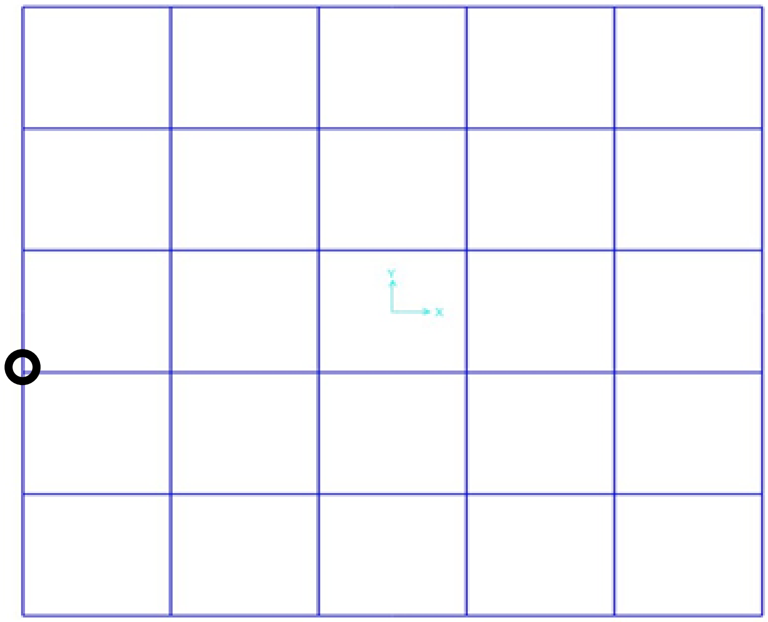

Figure 3.31 Selection of Monitored Joint (Joint 12) for Pushover Analysis in X-Direction

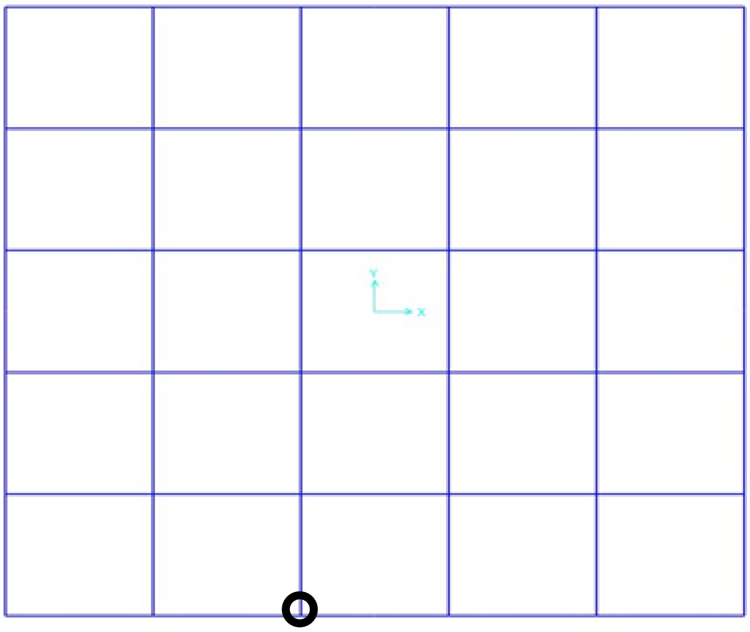

Figure 3.32 Selection of Monitored Joint (Joint 52) for Pushover Analysis in Y-Direction

In Figure 3.33, final state only and multiple states are two option for saving the results of pushover analysis in X- and Y-directions. The option “final state only” shows the final step of the load cases. When this option is selected, only the last results of displacements and forces are recorded. In “multiple states”, all the results of intermediate steps are also recorded. In this study, multiple states were selected using 10 and 100 for minimum and maximum number of saved stages, respectively.

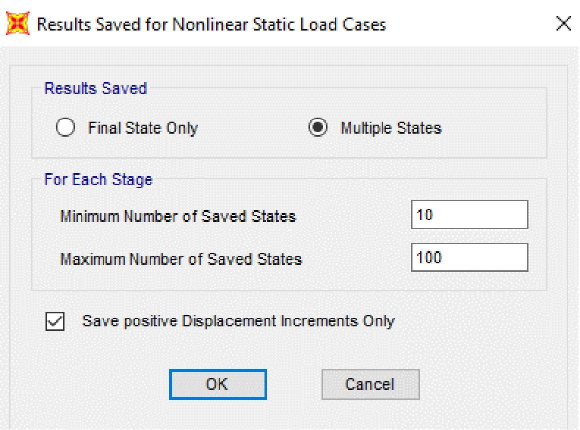

Figure 3.33 Defined Values of Saved Results for Nonlinear Static Load Cases

3.4.5.2.5 Performance Levels

Pushover curve is a graphical representation between horizontal displacement in selected direction and base shear. Performance point of the structure can have various stages. These stages are shown in Figure 3.34. These stages play an important role to determine condition of the structure.

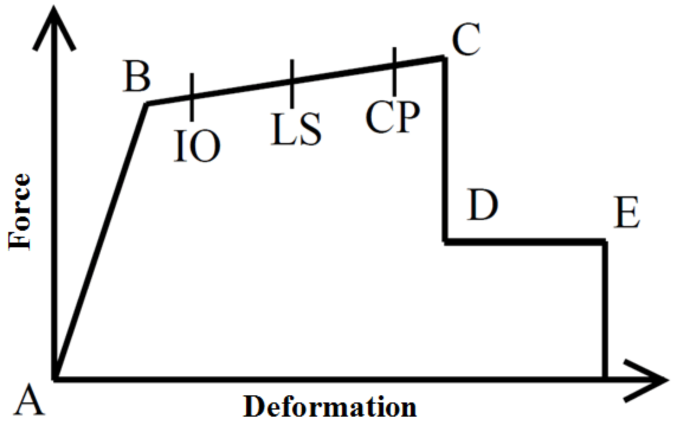

Figure 3.34 Definition of Performance Points [24]

In this figure, the section between A and B represents the elastic range of structure. The IO represents the immediate occupancy, LS represents life safety, CP represents collapse prevention. Point C represents that the structure has reached to ultimate strength and the load of hinges start to drop after this point. Point D represents the initiation of the residual strength plateau. And finally, at Point E structure reaches the maximum deformation capacity.

3.4.5.3 Time History Analysis Method

Ground motion is the movement of earth's surface due to earthquakes. Strong motion duration, soil properties of structure location, magnitude, peak ground acceleration, etc. are defined as basis characteristics of ground motion. Ground motion characteristics are effective for nonlinear dynamic analysis of structure.

Strong ground motion data used in this study were retrieved from open sources of Pacific Earthquake Engineering Research (PEER) Ground Motion Database [25]. Data obtained from PEER was scaled using Turkish Building Earthquake Code (2018) [11].

Selection of ground motion and earthquakes is controversial process. The selected data of ground motions due to earthquakes effect the analysis results. Based on TBEC (2018) [11], at least 11 different earthquake time history data shall be used in analysis. Therefore, 11 strong ground motion data was used in this study. Each of these ground motions were different from each other. In this selection process, same earthquakes were used to make a comparison between peak ground accelerations and different earthquakes were selected to observe the effectiveness of magnitude of earthquakes. The information related to the selected ground motions are shown in Table 3.23. Earthquake records of the selected ground motions are shown in figures between Figure 3.35 and Figure 3.45.

Table 3.23 Information related to Selected Ground Motions

No	Earthquake Name	Year	Station	Magnitude(M_w)	PGA(g)
1	San Fernando	1971	Pearblossom Pump	6,61	0,0545
2	San Fernando	1971	Santa Anita Dam	6,61	0,0597
3	Imperial Valley	1979	Superstition Mountains	6,53	0,0801
4	Loma Prieta	1989	APEEL 7 - Pulgas	6,93	0,0614
5	Loma Prieta	1989	APEEL 9 - Crystal Springs Res	6,93	0,0487
6	Loma Prieta	1989	Fremont - Mission San Jose	6,93	0,0809
7	Loma Prieta	1989	Palo Alto - SLAC Lab	6,93	0,0907
8	Northridge-01	1994	Lake Hughes	6,69	0,0789
9	Northridge-01	1994	Pasadena	6,69	0,1536
10	Northridge-01	1994	San Gabriel - E Grand Ave	6,69	0,0756
11	Düzce	1999	Lamont 1061	7,14	0,0531

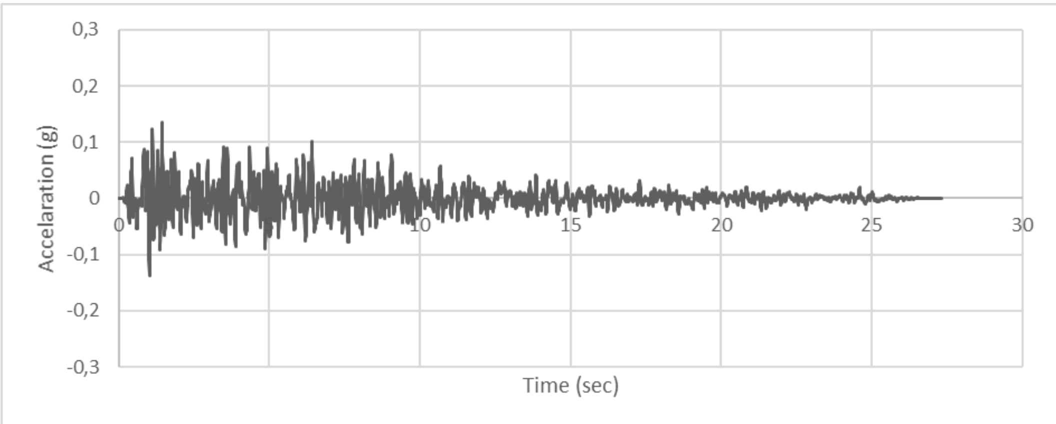

Figure 3.35 San Fernando EQ (Pearblossom Pump) Record (EQ1)

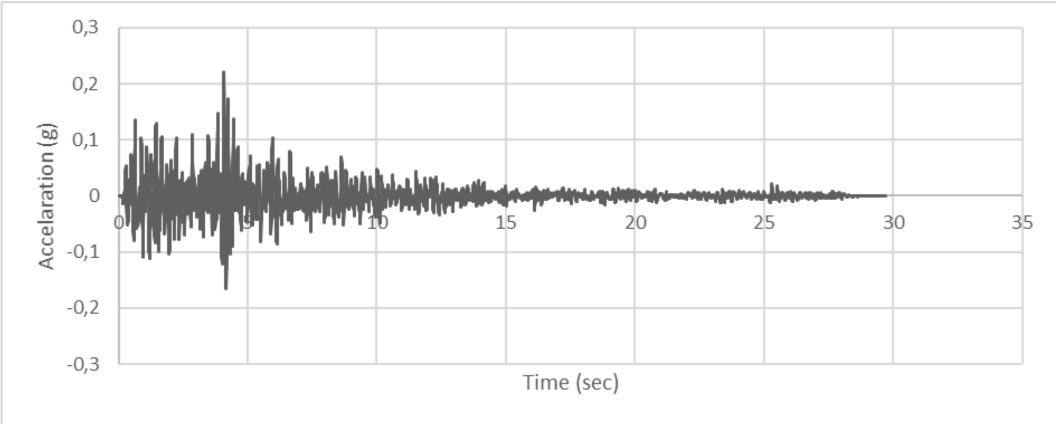

Figure 3.36 San Fernando EQ (Santa Anita Dam) Record (EQ2)

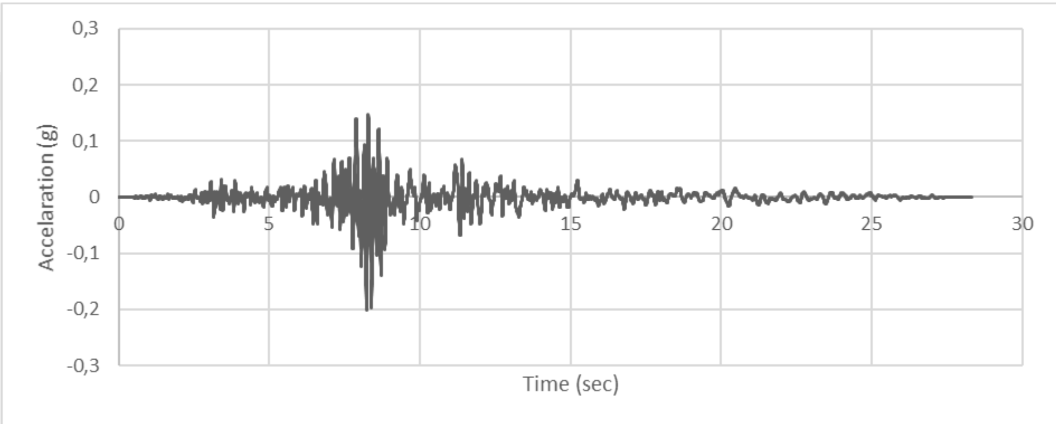

Figure 3.37 Imperial Valley EQ (Superstition Mountains) Record (EQ3)

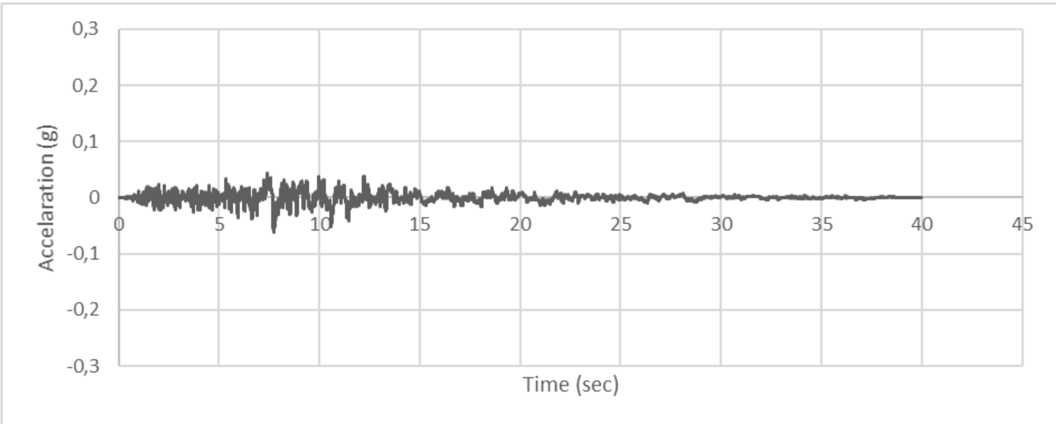

Figure 3.38 Loma Prieta EQ (APEEL 7 - Pulgas) Record (EQ4)

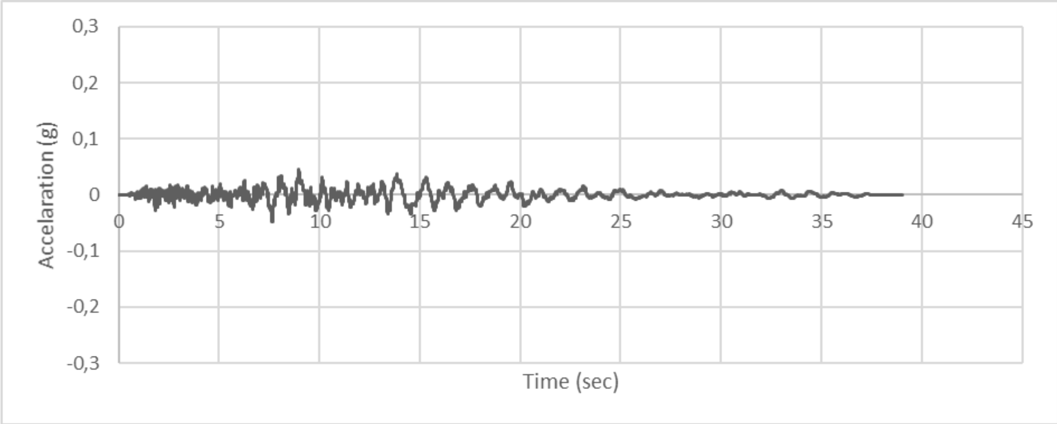

Figure 3.39 Loma Prieta EQ (APEEL 9 - Crystal Springs Res) Record (EQ5)

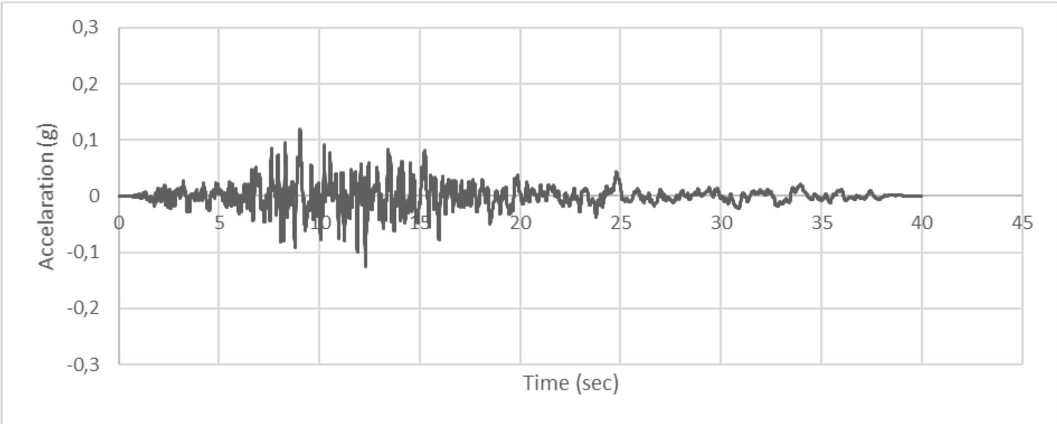

Figure 3.40 Loma Prieta EQ (Fremont Mission San Jose) Record (EQ6)

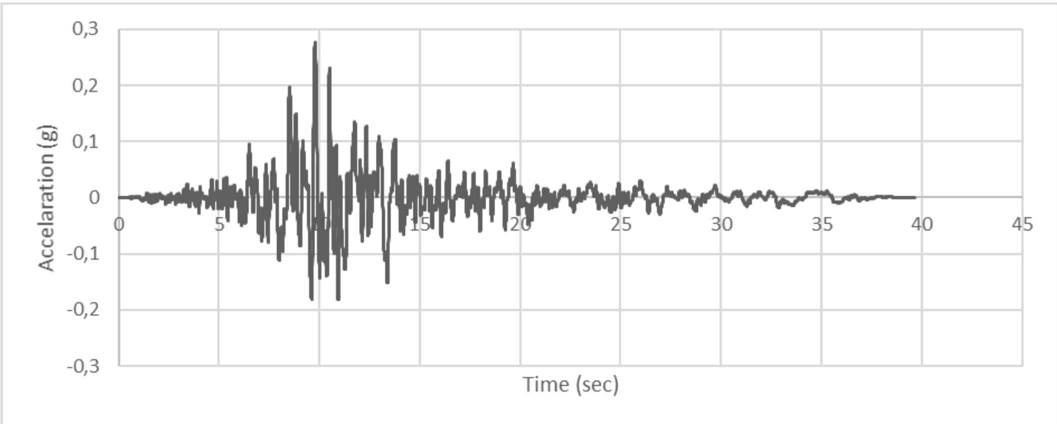

Figure 3.41 Loma Prieta EQ (Palo Alto) Record (EQ7)

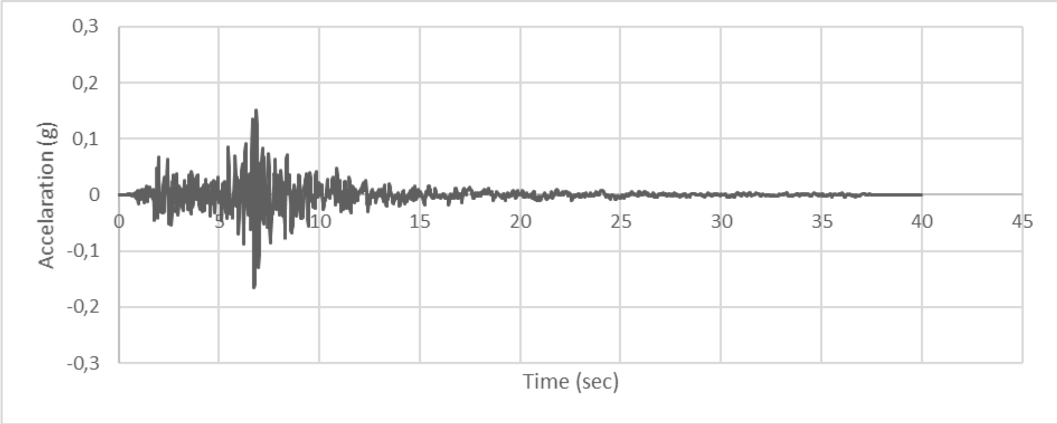

Figure 3.42 Northridge-01 EQ (Lake Hughes) Record (EQ8)

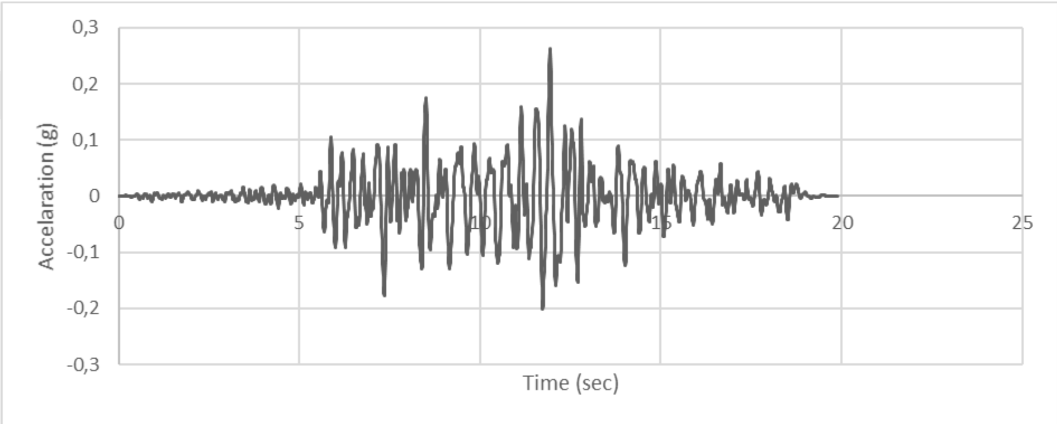

Figure 3.43 Northridge-01 EQ (Pasadena) Record (EQ9)

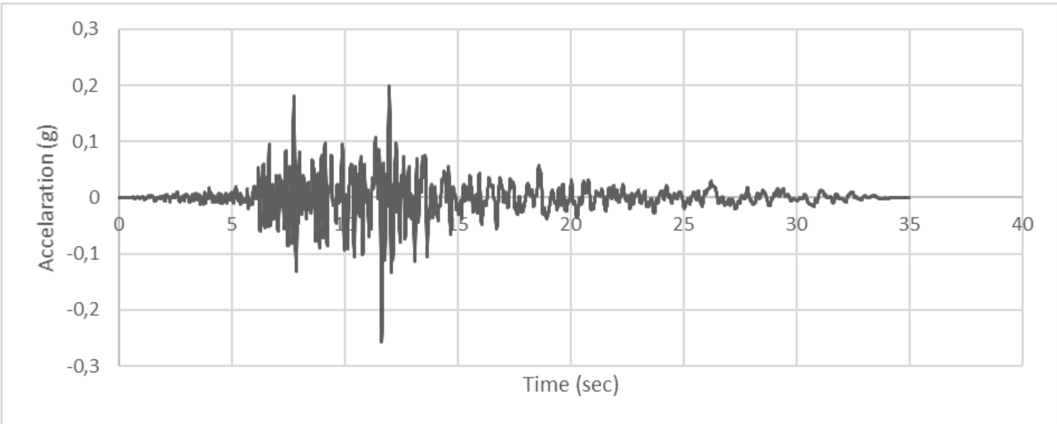

Figure 3.44 Northridge-01 EQ (San Gabriel) Record (EQ10)

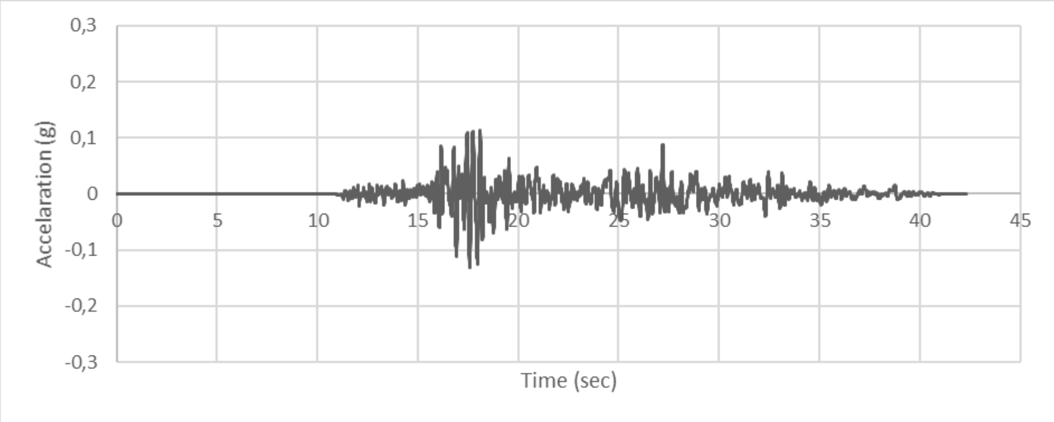

Figure 3.45 Düzce EQ (Lamont 1061) Record (EQ11)

There are various methods to scale the ground motion data for the desired earthquake effect. In this study, ground motion data was scaled using the tool available in SAP2000 V22 [26]. Initially, the elastic response spectrum (Figure 3.15) used Equivalent Earthquake Load Method was defined in the program as shown in Figure 3.46. The program scaled each of the earthquake records to have the same earthquake effect as the elastic response spectrum as shown in Figure 3.47 and Figure 3.48.

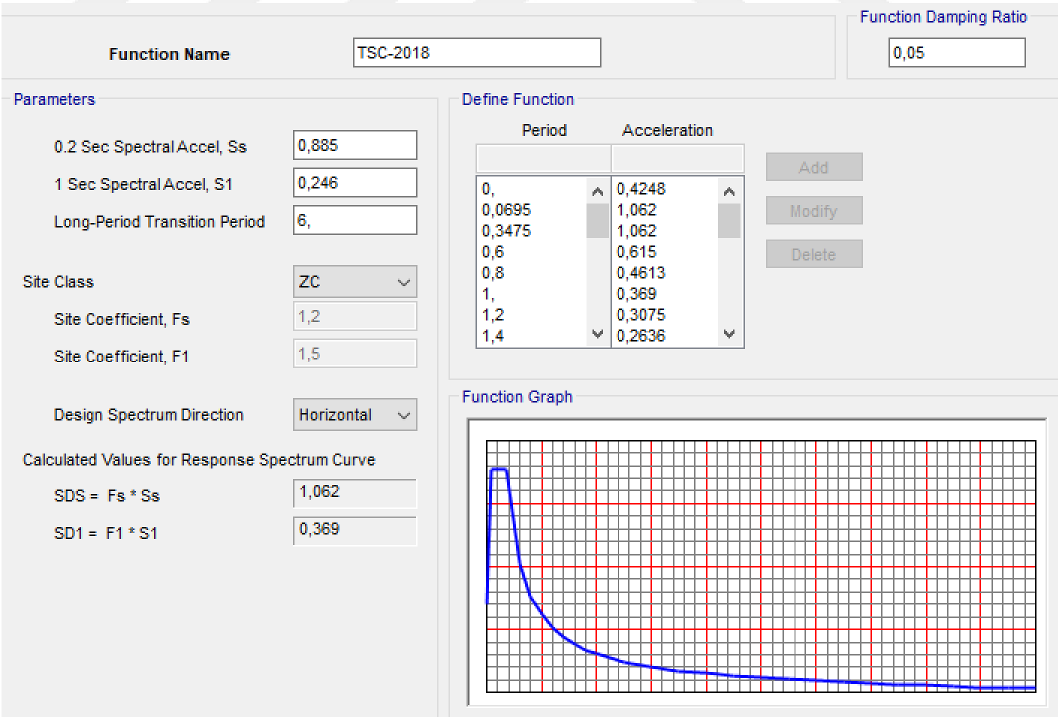

Figure 3.46 Defined Target Response Spectrum in SAP2000 V22 [26]

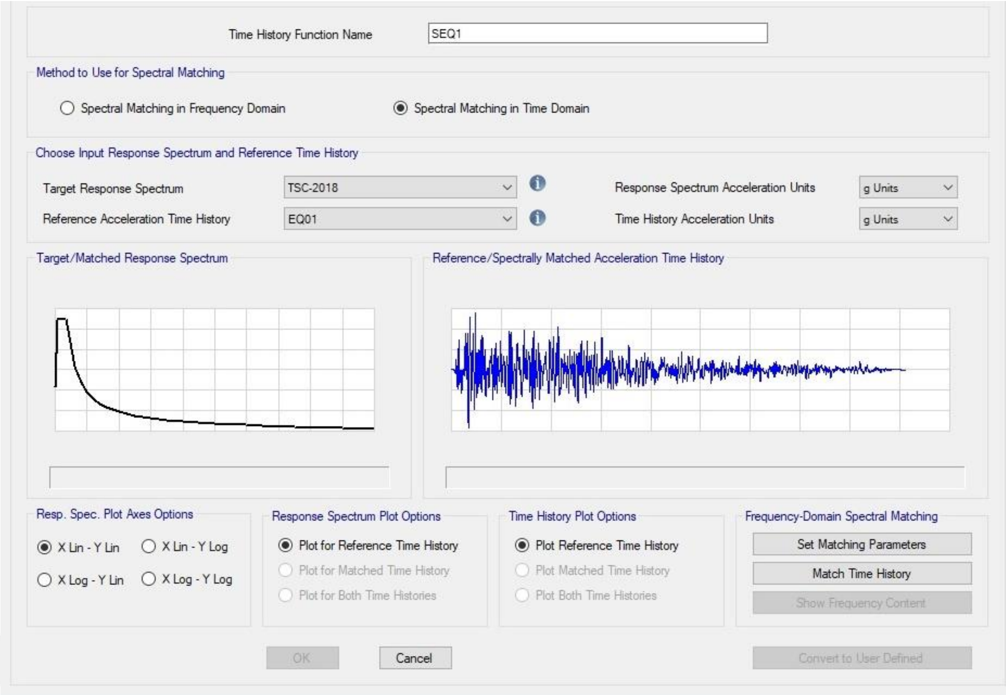

Figure 3.47 Method of Scaling in SAP2000 V22 [26]

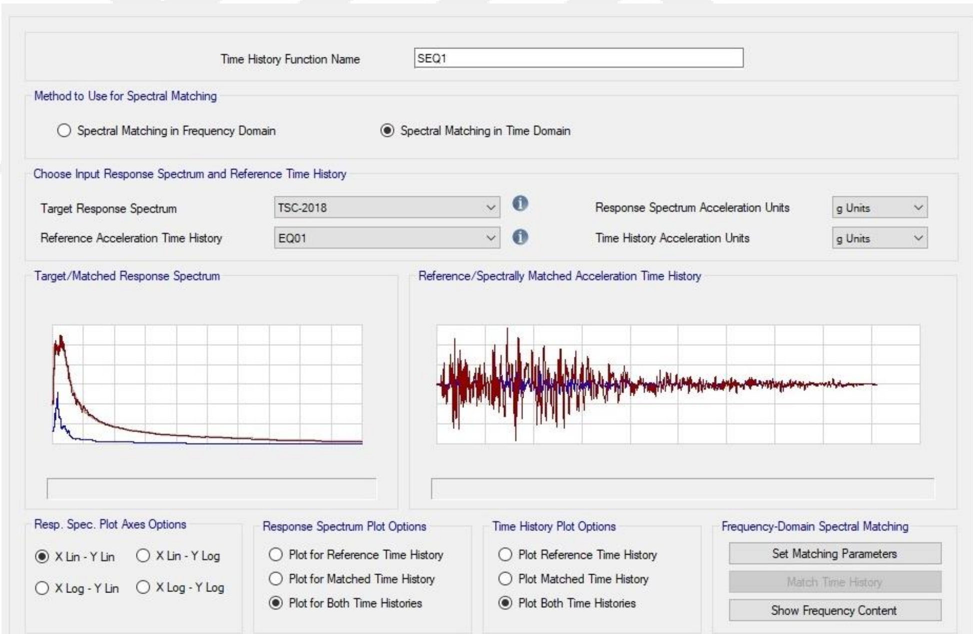

Figure 3.48 Results of Scaling in SAP2000 V22 [26]

This scaling process was performed for all the strong ground motion graphs. Scaled ground motions were used in the analysis. Scaled earthquake records of the selected ground motions are shown in figures between Figure 3.35 and Figure 3.45.

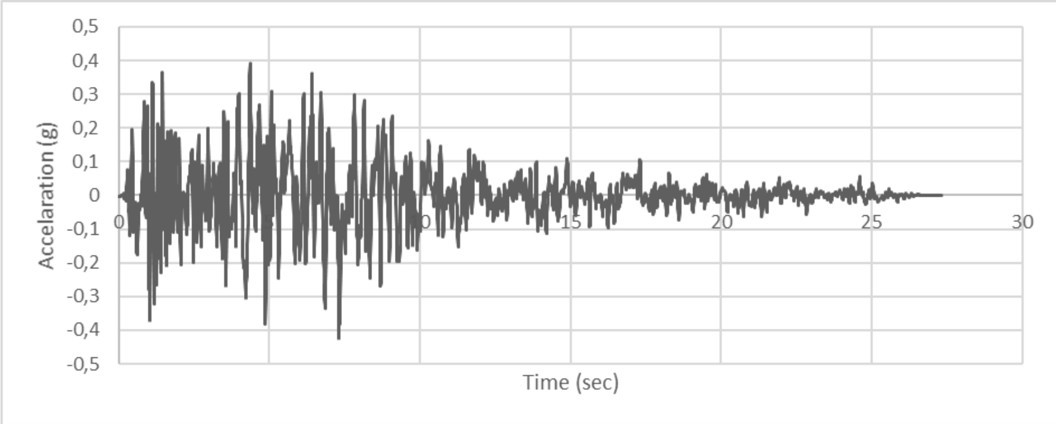

Figure 3.49 San Fernando EQ (Pearblossom Pump) Record (Scaled EQ1)

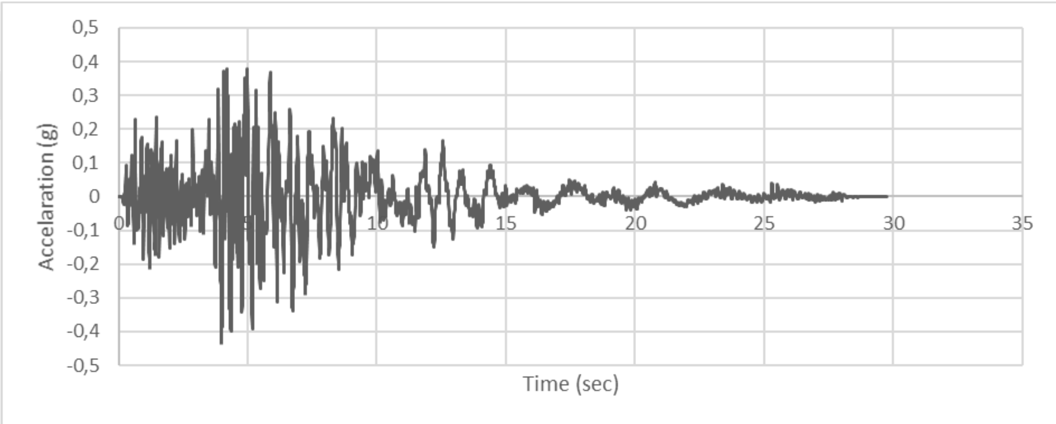

Figure 3.50 San Fernando EQ (Santa Anita Dam) Record (Scaled EQ2)

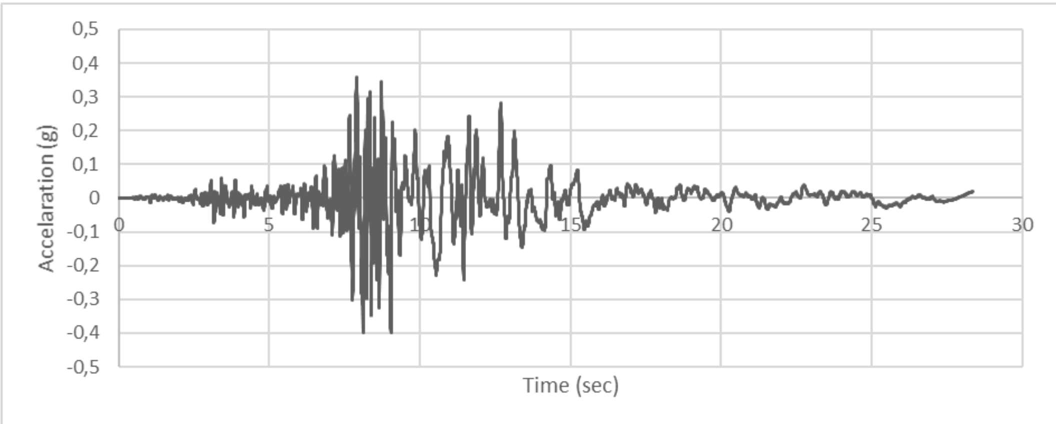

Figure 3.51 Imperial Valley EQ (Superstition Mountains) Record (Scaled EQ3)

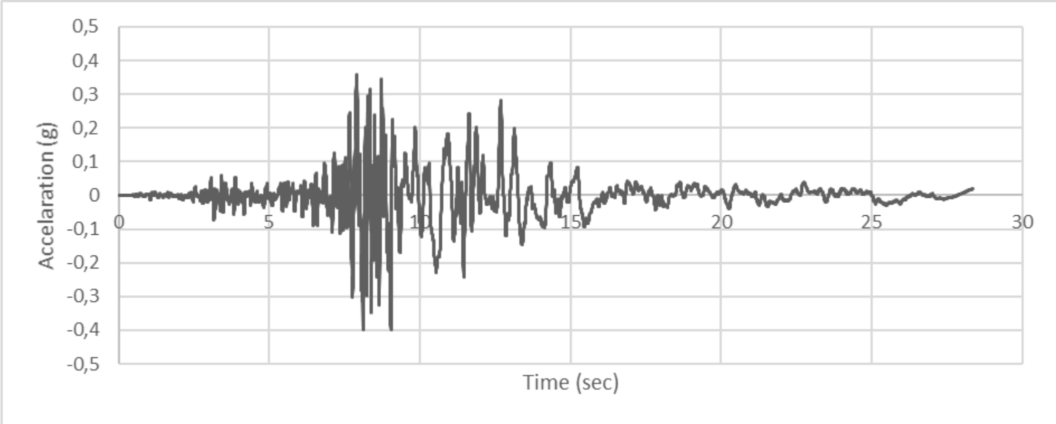

Figure 3.52 Loma Prieta EQ (APEEL 7 - Pulgas) Record (Scaled EQ4)

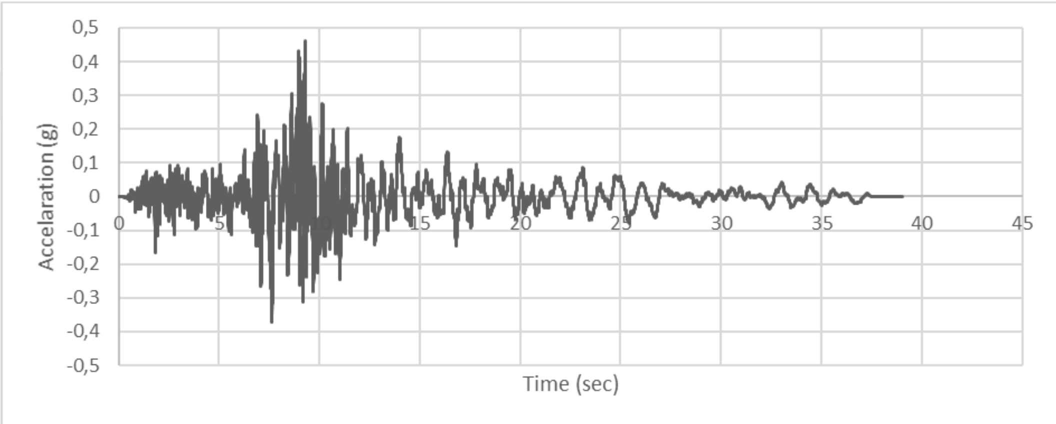

Figure 3.53 Loma Prieta EQ (APEEL 9 - Crystal Springs Res) Record (Scaled EQ5)

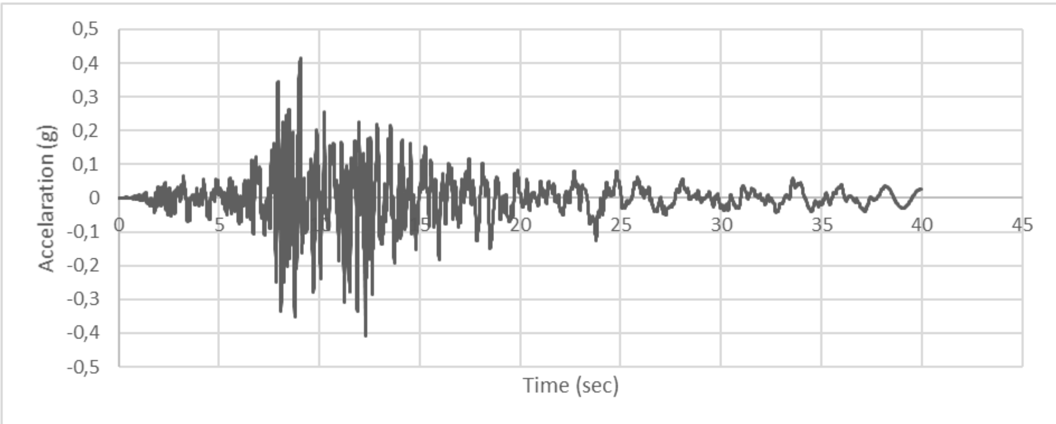

Figure 3.54 Loma Prieta EQ (Fremont Mission San Jose) Record (Scaled EQ6)

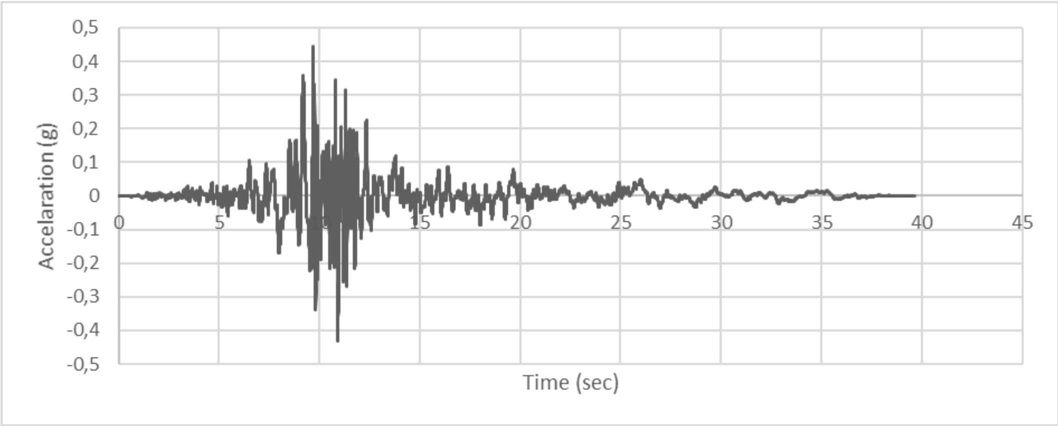

Figure 3.55 Loma Prieta EQ (Palo Alto) Record (Scaled EQ7)

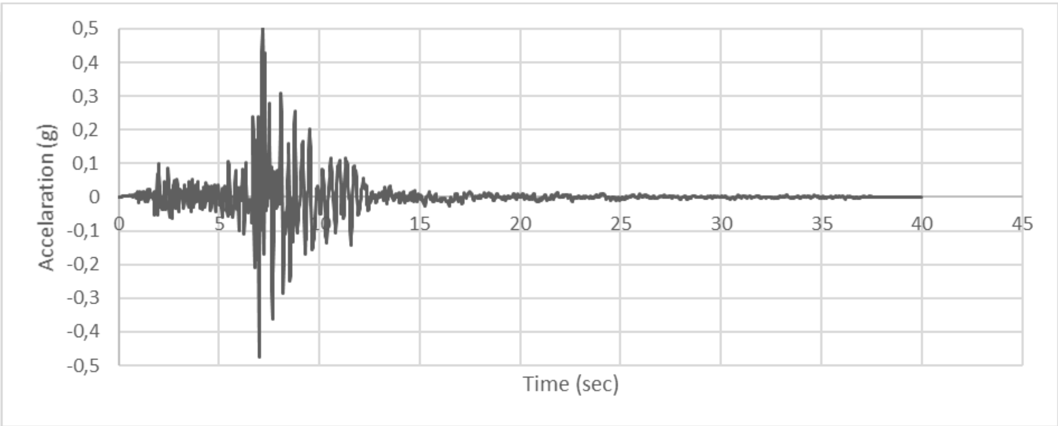

Figure 3.56 Northridge-01 EQ (Lake Hughes) Record (Scaled EQ8)

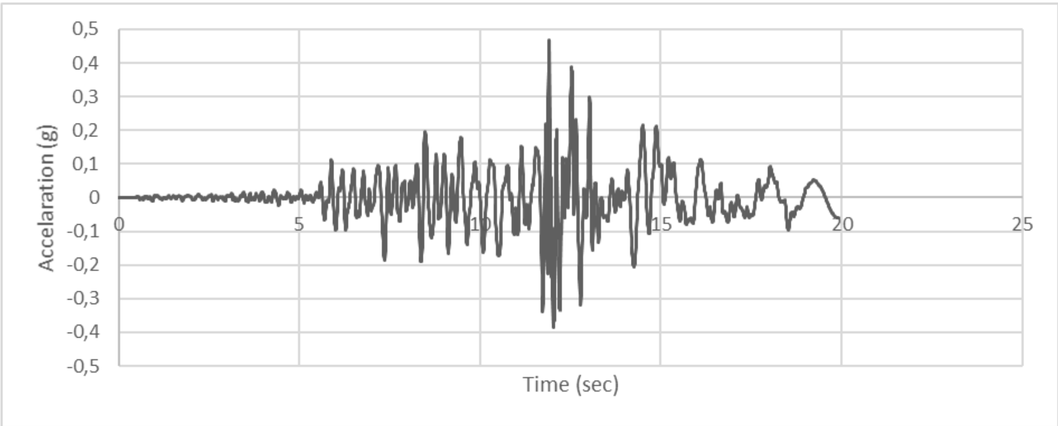

Figure 3.57 Northridge-01 EQ (Pasadena) Record (Scaled EQ9)

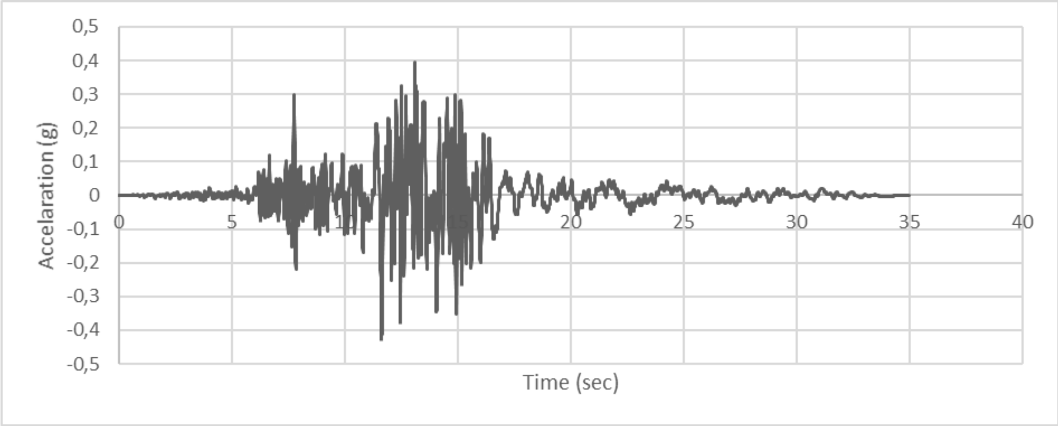

Figure 3.58 Northridge-01 EQ (San Gabriel) Record (Scaled EQ10)

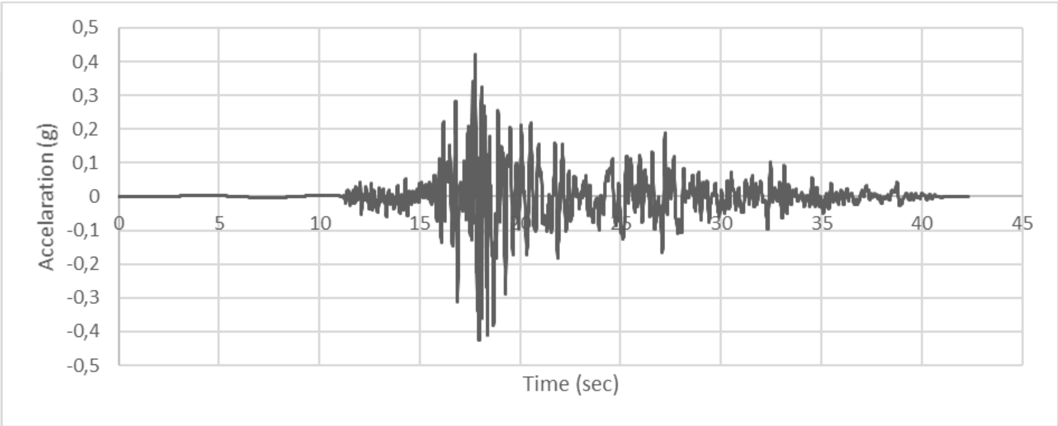

Figure 3.59 Düzce EQ (Lamont 1061) Record (Scaled EQ11)

3.4.5.3.1 Time History Analysis using SAP2000 [7]

SAP2000 Analysis Software [7] was used to perform nonlinear dynamic analysis of building models. The first step was to define a new load case as shown in Figure 3.60. The analysis started from the initial conditions of Gravity load case.

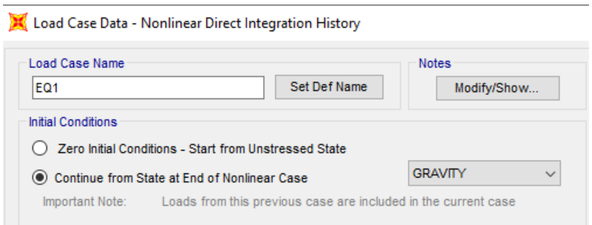

Figure 3.60 Initial Conditions for Time History Analysis

In the second step, accelerations in X- and Y-directions were defined as shown in Figure 3.61 based on Turkish Building Earthquake Code (2018) [11]. Scale factor in SAP2000 [7] was determined in the Equation 3-6.

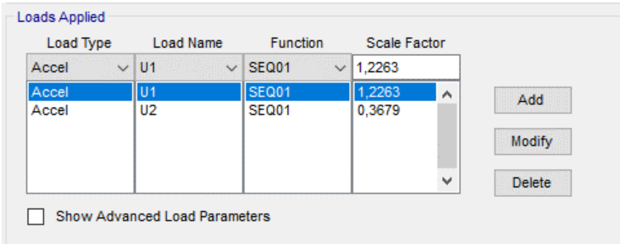

Figure 3.61 Applied Acceleration Loads for Time History Analysis

In the third step, analysis type was selected as nonlinear and P-Δ effect was included in the analysis.

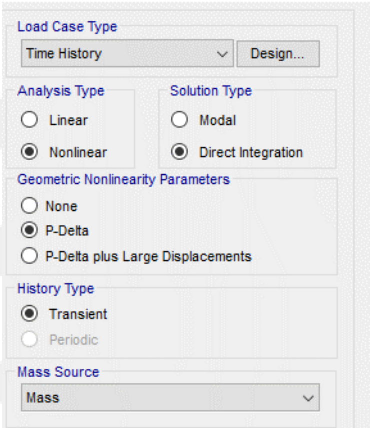

Figure 3.62 Definition of Time History Load Case

In the last step, damping was defined as 5% and time integration method was selected as Newmark as shown in Figure 3.63.

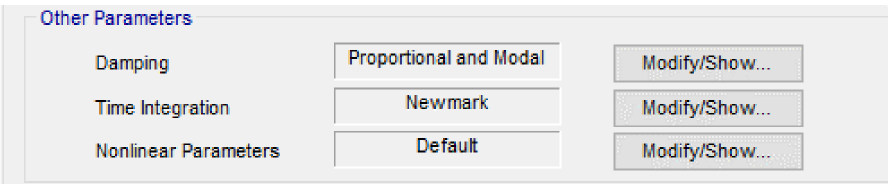

Figure 3.63 Defined Parameters for Time History Analysis

Input/output steps and step sizes were the limitations of the calculated strong ground motion data. Output steps and step sizes shall match the initial strong ground motion data.

Table 3.24 Definitions of Earthquake Data

Case	Input Steps	Output Steps	Step Size	Damping
EQ1	2734	2734	0,01	0,05
EQ2	2974	2974	0,01	0,05
EQ3	5669	5669	0,005	0,05
EQ4	7998	7998	0,005	0,05
EQ5	7811	7811	0,005	0,05
EQ6	7998	7998	0,005	0,05
EQ7	7930	7930	0,005	0,05
EQ8	2000	2000	0,02	0,05
EQ9	1991	1991	0,01	0,05
EQ10	3499	3499	0,01	0,05
EQ11	4233	4233	0,01	0,05

3.5 Load Combinations

The earthquake load effects were combined based on TBEC (2018) [11]. When considering the earthquake load effects in X-direction, the full effect of earthquake loads in X-direction was combined with 30% of the earthquake loads in Y-direction. The same logic was followed when considering the earthquake load effects in Y-direction. The expressions for this criteria are shown in Equation 3-14 and Equation 3-15. Additionally, 30% of the vertical earthquake load effects were also added to these combinations.

$$E_d^{(H)} = E_d^{(X)} + 0,3 \times E_d^{(Y)} \qquad \text{Equation 3-14}$$

$$E_d^{(H)} = 0,3 \times E_d^{(X)} + E_d^{(Y)} \qquad \text{Equation 3-15}$$

Load combinations specified by TS500 (2000) [8] and TBEC (2018) [11] were used in the analyses. These combinations are shown in Table 3.25.

Table 3.25 Load Combinations

1,4DL+1,6LL	0,9DL+1,3WINDY
1,0DL+1,0LL+1,0EQX-E+0,3EQY+0,3EQZ	0,9DL-1,3WINDY
1,0DL+1,0LL+1,0EQY+E+0,3EQX+0,3EQZ	0,9DL+1,0EQX+0,3EQY-0,3EQZ
1,0DL+1,0LL+1,0EQY-E+0,3EQX+0,3EQZ	0,9DL-1,0EQX+0,3EQY-0,3EQZ
1,0DL+1,0LL-1,0EQX+E+0,3EQY+0,3EQZ	0,9DL+1,0EQX+E+0,3EQY-0,3EQZ
1,0DL+1,0LL-1,0EQX-E+0,3EQY+0,3EQZ	0,9DL-1,0EQX+E+0,3EQY-0,3EQZ
1,0DL+1,0LL-1,0EQY+E+0,3EQX+0,3EQZ	0,9DL+1,0EQX-E+0,3EQY-0,3EQZ
1,0DL+1,0LL-1,0EQY-E+0,3EQX+0,3EQZ	0,9DL-1,0EQX-E+0,3EQY-0,3EQZ
1,0DL+1,3LL+1,3WINDX	0,9DL+1,0EQY+0,3EQX-0,3EQZ
1,0DL+1,3LL-1,3WINDX	0,9DL-1,0EQY+0,3EQX-0,3EQZ
1,0DL+1,3LL+1,3WINDY	0,9DL+1,0EQY+E+0,3EQX-0,3EQZ
1,0DL+1,3LL-1,3WINDY	0,9DL-1,0EQY+E+0,3EQX-0,3EQZ
0,9DL+1,3WINDX	0,9DL+1,0EQY-E+0,3EQX-0,3EQZ
0,9DL-1,3WINDX	0,9DL-1,0EQY-E+0,3EQX-0,3EQZ
1,0DL+1,0LL+0,2SL+1,0EQX+0,3EQY+0,3EQZ	1,0DL+1,0LL+0,2SL+1,0EQY+0,3EQX+0,3EQZ

CHAPTER 4

4. RESULTS AND DISCUSSIONS

The deficient and strengthened models were analyzed using Equivalent Earthquake Load Method, Pushover Analysis Method, and Time History Analysis using past earthquakes. Based on these three method, the results of total base shear, seismic weights, maximum horizontal deflections, performance points V and Δ, and seismic loads due to time history analysis of past earthquake ground motions are presented in this chapter.

4.1 Analysis and Design of Deficient Buildings

The models of the deficient buildings were first analyzed using the Equivalent Earthquake Load Method specified by TBEC (2018) [11]. The load combinations shown in Table 3.25 was also used in the analysis. The periods, total base shears, and maximum horizontal deflections were obtained at the end of this analysis. The obtained values for deficient buildings are shown in Table 4.1, Table 4.2, and Table 4.3.

Table 4.1 General Characteristics of Structures

Modal	L_x (m)	Span X (m)	L_y (m)	Span Y (m)	# of Story	T_x (sec)	T_y (sec)
310	30	6	30	6	3	0,74	0,74
610	30	6	30	6	6	1,02	1,02
910	30	6	30	6	9	1,38	1,38
1210	30	6	30	6	12	1,79	1,79

Table 4.2 Base Shear Forces of Structures

Models	Total Base Shear X-Direction (kN)	Total Base Shear Y-Direction (kN)
3-Story Apartment	3882,716	3882,716
6-Story Apartment	6144,666	6144,666
9-Story Apartment	7258,191	7258,191
12-Story Apartment	7943,665	7943,665

Table 4.3 Seismic Weights and Maximum Horizontal Deflections of Structures

Modal	Seismic Weight (kN)	Max.U_x (mm)	Load Combination for U_x	Max.U_y (mm)	Load Combination for U_y
310	30251	25,887	1,0DL+1,0LL+1,0EQX+E +0,3EQY+0,3EQZ	25,887	1,0DL+1,0LL+1,0EQY+E +0,3EQX+0,3EQZ
610	65617	39,759	1,0DL+1,0LL+1,0EQX+E +0,3EQY+0,3EQZ	39,759	1,0DL+1,0LL+1,0EQY+E +0,3EQX+0,3EQZ
910	104839	57,041	1,0DL+1,0LL+1,0EQX+E +0,3EQY+0,3EQZ	57,041	1,0DL+1,0LL+1,0EQY+E +0,3EQX+0,3EQZ
1210	148843	76,43	1,0DL+1,0LL+1,0EQX+E +0,3EQY+0,3EQZ	76,43	1,0DL+1,0LL+1,0EQY+E +0,3EQX+0,3EQZ

The deficient models were also analyzed using the Pushover Analysis Method and Time History Analysis Method using past earthquakes. The total base shears and deflections at performance points obtained from the Pushover Analysis Method is shown in Table 4.4. The total base shear forces and maximum deflections (U_x and U_y) in both directions calculated using Time History Analysis Method are shown in Table 4.5 and Table 4.6.

Table 4.4 Results of Pushover Analysis of Deficient Buildings

	PUSH X		PUSH Y	
Modal	Performance Point V (kN)	Performance Point Δ (mm)	Performance Point V (kN)	Performance Point Δ (mm)
310	4639	70	4665	70
610	10320	85	10319	85
910	13684	115	13700	115
1210	21639	172	21641	172

Table 4.5 Base Shear Force Results of Time History Analysis of Deficient Buildings

EARTHQUAKES		MODELS			
		310	610	910	1210
EQ1	Fx (kN)	2460	3969	4598	4549
	Fy (kN)	738	1191	1379	1365
EQ2	Fx (kN)	2665	4606	5384	5835
	Fy (kN)	800	1382	1615	1750
EQ3	Fx (kN)	3017	4020	4642	4643
	Fy (kN)	905	1206	1392	1393
EQ4	Fx (kN)	3310	3999	4352	4401
	Fy (kN)	992	1200	1306	1320
EQ5	Fx (kN)	2565	4170	3937	4187
	Fy (kN)	770	1251	1181	1256
EQ6	Fx (kN)	2546	3313	4242	4646
	Fy (kN)	764	994	1273	1394
EQ7	Fx (kN)	2854	4633	4961	6009
	Fy (kN)	856	1390	1488	1803
EQ8	Fx (kN)	3010	5029	6450	5055
	Fy (kN)	904	1509	1935	1516
EQ9	Fx (kN)	3078	4105	3989	5126
	Fy (kN)	923	1231	1197	1538
EQ10	Fx (kN)	3002	4186	4998	5925
	Fy (kN)	901	1256	1499	1778
EQ11	Fx (kN)	3074	3640	5664	5022
	Fy (kN)	922	1092	1699	1507

Table 4.6 Deflection Results of Time History Analysis of Deficient Buildings

EARTHQUAKES		MODELS			
		310	610	910	1210
EQ1	Δ_X (mm)	15,037	19,755	30,000	39,922
	Δ_Y (mm)	4,511	5,946	9,022	12,003
EQ2	Δ_X (mm)	15,262	24,751	29,134	34,148
	Δ_Y (mm)	4,590	7,444	8,764	10,268
EQ3	Δ_X (mm)	17,411	23,891	36,810	46,613
	Δ_Y (mm)	5,234	7,186	11,067	14,013
EQ4	Δ_X (mm)	18,335	23,537	29,658	37,834
	Δ_Y (mm)	5,510	7,080	8,920	11,375
EQ5	Δ_X (mm)	14,197	21,800	25,211	39,401
	Δ_Y (mm)	4,270	6,559	7,585	11,846
EQ6	Δ_X (mm)	14,382	19,277	29,969	38,307
	Δ_Y (mm)	4,307	5,802	9,013	11,517
EQ7	Δ_X (mm)	16,265	22,019	27,467	42,053
	Δ_Y (mm)	4,891	6,625	8,262	12,644
EQ8	Δ_X (mm)	17,173	25,263	36,659	50,657
	Δ_Y (mm)	5,161	7,598	11,021	15,225
EQ9	Δ_X (mm)	17,090	25,286	27,561	38,473
	Δ_Y (mm)	5,118	7,605	8,290	11,567
EQ10	Δ_X (mm)	16,745	23,801	32,894	44,400
	Δ_Y (mm)	5,035	7,160	9,890	13,346
EQ11	Δ_X (mm)	17,853	21,472	27,246	46,117
	Δ_Y (mm)	5,367	6,460	8,195	13,862

The analyzed structure models were then designed (beams and columns) using SAP2000 [7]. The design code used was TS500 (2000) [8]. The details of the code and coefficients used in the design are shown in Figure 4.1.

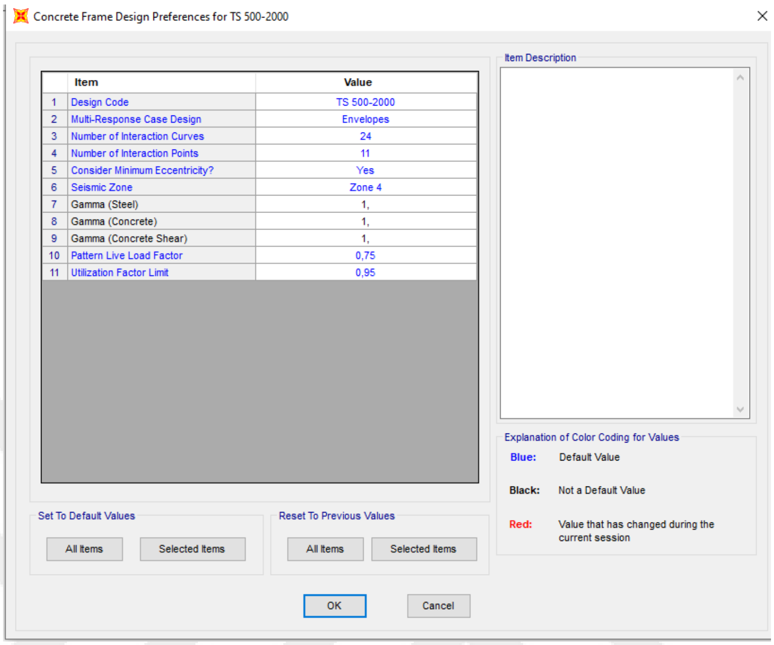

Figure 4.1 Concrete Frame Design Preferences for TS500 (2000)

Based on the design results of SAP2000 [7], some of the columns and beams of deficient structures were not sufficient to resist the load combinations used in this study. The design results of 3-, 6-, 9-, and 12-story structure models are shown in Figure 4.2, Figure 4.3, Figure 4.4, and Figure 4.5, respectively. In these figures, the orange elements represent the sufficient frame elements under the applied loads and the red elements represent the insufficient frame elements. Inıtially, axial forces on columns and moments on beams were the reasons for the deficiency of columns and beams, respectively. Detailed design data of columns and beams of deficient and strengthened structures are shown in figures available in Appendix A. These deficient structures shall be strengthened, if strengthening is not possible, structures shall be demolished and reconstructed for safety purposes.

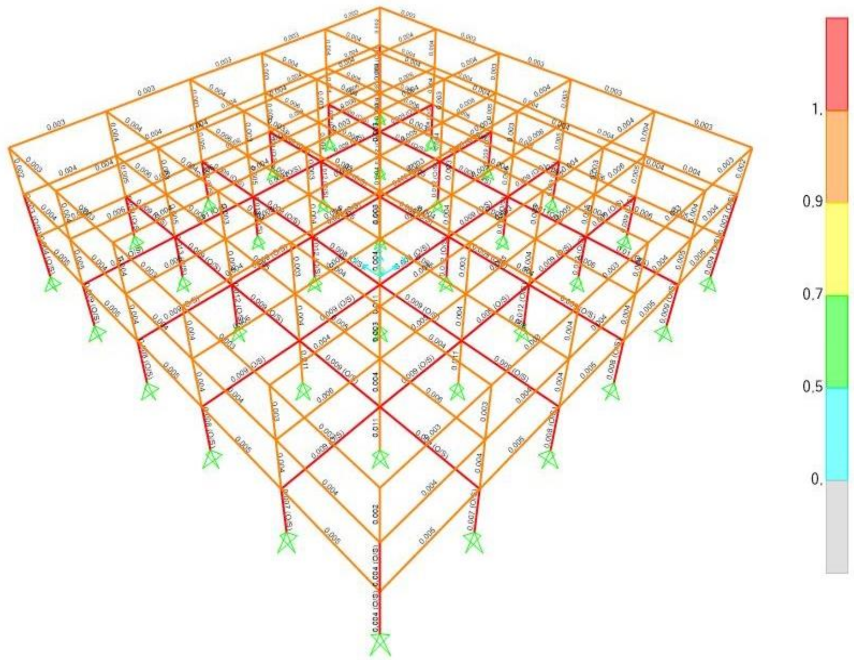

Figure 4.2 Results of Concrete Frame Design of Deficient 3-Story Model

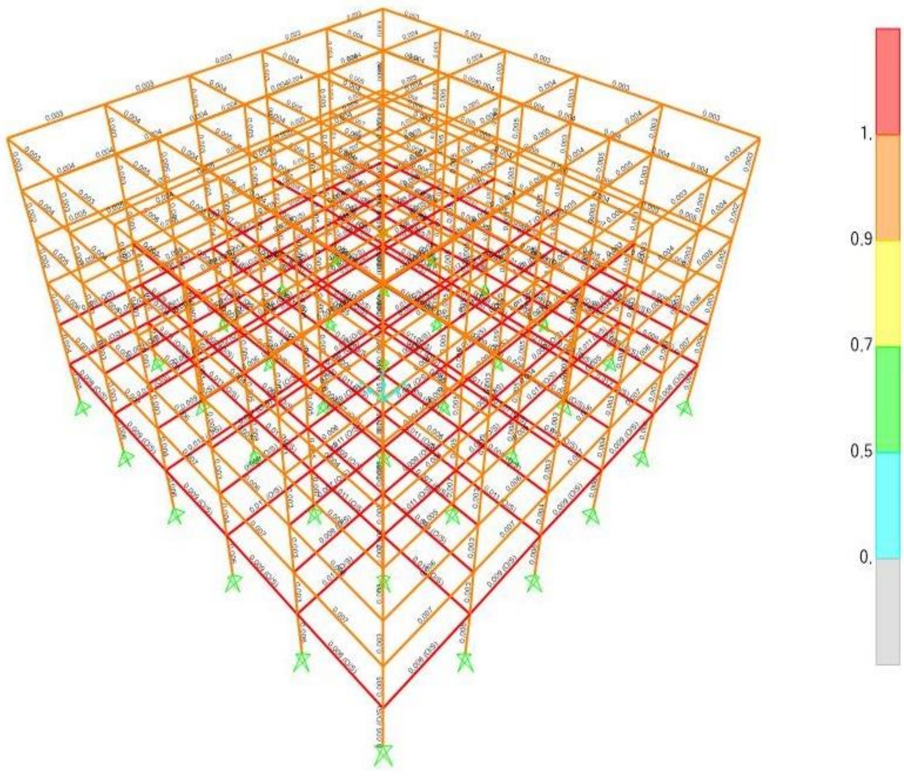

Figure 4.3 Results of Concrete Frame Design of Deficient 6-Story Model

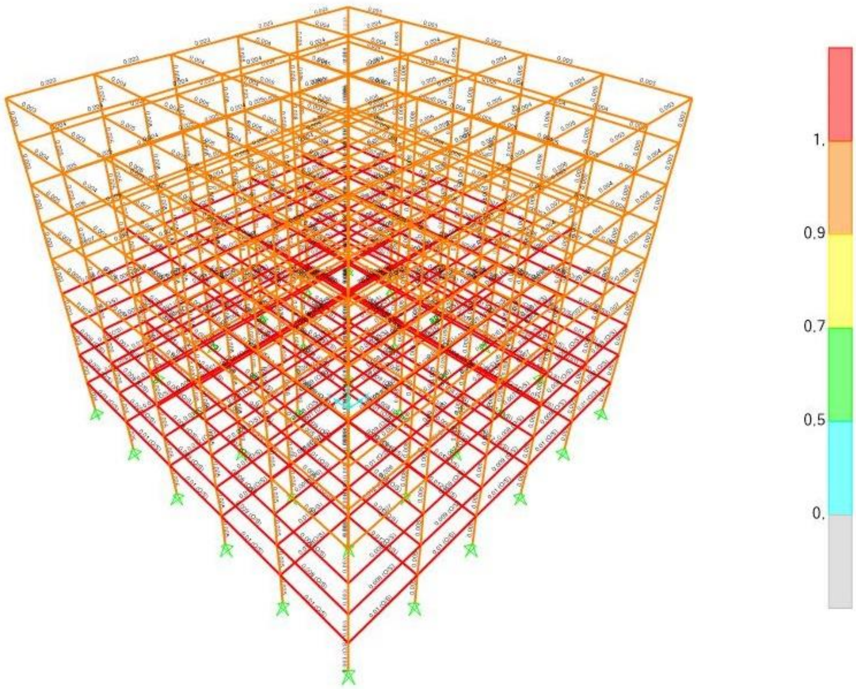

Figure 4.4 Results of Concrete Frame Design of Deficient 9-Story Model

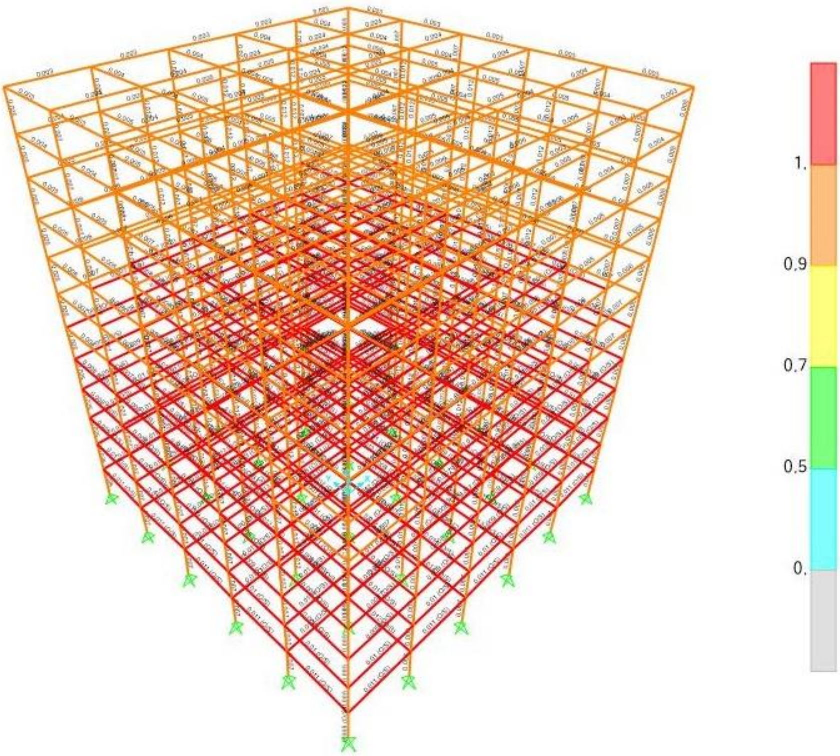

Figure 4.5 Results of Concrete Frame Design of Deficient 12-Story Model

4.2 Strengthening Configuration and Method

In this study, external steel braces were used to strengthen the deficient building models. The purpose of using strengthening is to decrease the lateral displacements of structural elements, decrease the drift ratio of structures, increase the performance of structure, and sufficient against the earthquake loads.

Two different configuration of external steel braces were used in this research. These configurations of external steel braces were inverted V and X, as shown in Figure 4.6 and in Figure 4.7, respectively. The width of the bracing systems was equal to 6 meters which was similar to the length of any bay in any direction of the building models. Also, the height of the bracing systems (one portion) was equal to 3 meters which was similar to the height of each story. Note that, the strengthening system was applied to a height of the total elevation of the building structure, from the foundation to roof level.

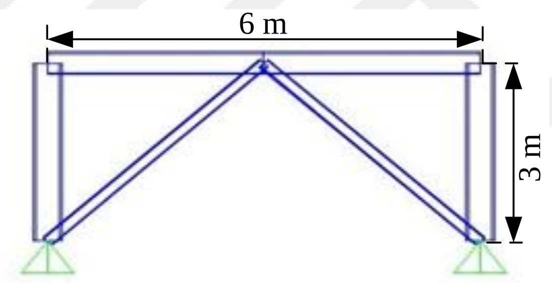

Figure 4.6 Configuration of Inverted V-Braces

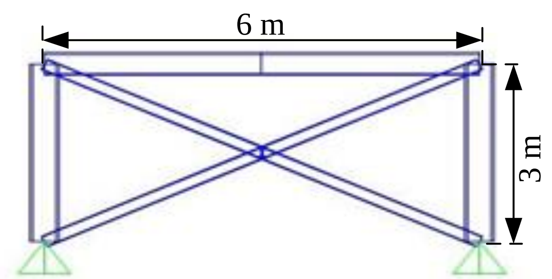

Figure 4.7 Configuration of X-Braces

Three different model types were used for strengthening and to compare the performance and effectiveness of different designs. In the first model type, one frame system of external steel braces was used at all sides around the perimeter of the structure. If the configuration of this type of brace was an inverted v-brace, then the brace type would be named as V11. If the configuration of this type of brace was an X-brace, then the brace type would be named as X11.

In the second type, two frame systems of external steel braces were used on two opposite sides, whereas one frame system of external steel braces was used on the rest of the sides around the perimeter of the structure. If the configuration of this type of brace was an inverted v-brace, then the brace type would be named as V21. If the configuration of this type of brace was an x-brace, then the brace type would be named as X21.

In the third model type, two frame system of external steel braces were used at all sides of around the perimeter of the structure. If the configuration of this type of brace was an inverted v-brace, then the brace type would be named as V22. If the configuration of this type of brace was an x-brace, then the brace type would be named as X22. All external steel bracing systems were located approximately 0,35 meters away from the deficient structures. Plan and 3D views of different types of strengthening are shown in Figure 4.8 and Figure 4.9.

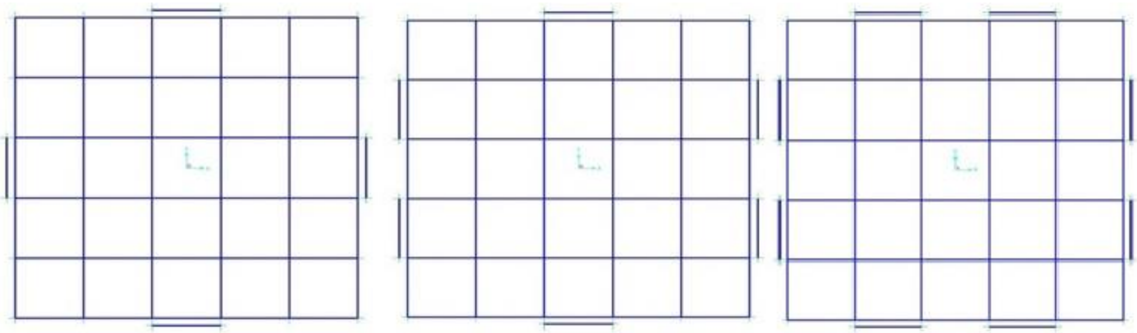

a) One Frame at All Sides | b) Two Frames at Opposite Sides and One Frame at Rest | c) Two Frames at All Sides

Figure 4.8 Plan Views of Strengthening Types

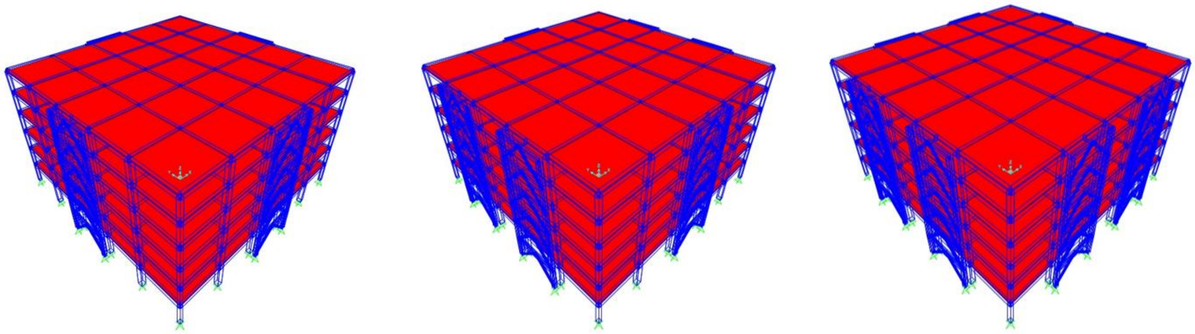

a) One Frame at All Sides | b) Two Frames at Opposite Sides and One Frame at Rest | c) Two Frames at All Sides

Figure 4.9 Strengthening Configurations along Building Heights

Several structural steel sections were used in this research. These structural steel sections and their dimensions based on European Standards (1993) [21] are shown in Table 4.7. Three different analysis methods, Equivalent Earthquake Load, Pushover Analysis and Time History Analysis Method using past earthquakes, were used to evaluate the effectiveness of the strengthening against to earthquake loads in both directions. All the buildings were designed and validated for each of these methods successfully. After the design process, general information related to periods of the building models in X- and Y-directions, total steel weights of the strengthening systems, and steel bracing weight ratio based on total area of structure models are shown in Table 4.8.

Table 4.7 Dimensions of Structural Steel Sections

Section Name	Material	Shape	t_3 (m)	t_2 (m)	t_f (m)	t_w (m)	t_{2b} (m)	t_{fb} (m)
H400X237	A992Fy50	I/Wide Flange	0,381	0,395	0,0305	0,0185	0,395	0,0305
H400X262			0,387	0,397	0,0335	0,0205	0,397	0,0335
H400X288			0,393	0,399	0,0365	0,0230	0,399	0,0365
H400X314			0,400	0,400	0,040	0,0245	0,400	0,0400
H400X340			0,406	0,403	0,0429	0,0265	0,403	0,0429
H400X347			0,407	0,404	0,0435	0,0275	0,404	0,0435
H400X383			0,416	0,406	0,048	0,03	0,406	0,048
H400X393			0,419	0,407	0,0492	0,0306	0,407	0,0492
H400X422			0,425	0,409	0,0525	0,033	0,409	0,0525
H400X463			0,435	0,412	0,0575	0,0355	0,412	0,0575
H400X467			0,437	0,412	0,058	0,0359	0,412	0,058
H400X509			0,445	0,416	0,0622	0,0395	0,416	0,0622
H400X551			0,455	0,418	0,0675	0,0425	0,418	0,0675
H400X593			0,465	0,421	0,0725	0,0445	0,421	0,0725
H400X634			0,475	0,423	0,0775	0,047	0,423	0,0775
H400X678			0,484	0,427	0,082	0,0505	0,427	0,082
H400X744			0,499	0,431	0,0895	0,0545	0,431	0,0895
H400X818			0,514	0,437	0,097	0,0605	0,437	0,097
H400X900			0,531	0,442	0,106	0,0659	0,442	0,106
H400X990			0,55	0,448	0,115	0,0719	0,448	0,115
HE100A			0,096	0,1	0,008	0,005	0,1	0,008
HE120A			0,114	0,12	0,008	0,005	0,12	0,008
HE140A			0,133	0,14	0,0085	0,0055	0,14	0,0085
HE160A			0,152	0,16	0,009	0,006	0,16	0,009
HE180A			0,171	0,18	0,0095	0,006	0,18	0,0095
HE200A			0,19	0,2	0,01	0,0065	0,2	0,01
HE220A			0,21	0,22	0,011	0,007	0,22	0,011
HE240A			0,23	0,24	0,012	0,0075	0,24	0,012
HE260A			0,25	0,26	0,0125	0,0075	0,26	0,0125
HE280A			0,27	0,28	0,013	0,008	0,28	0,013
HE300A			0,29	0,3	0,014	0,0085	0,3	0,014
HE320A			0,31	0,3	0,0155	0,009	0,3	0,0155
HE340A			0,33	0,3	0,0165	0,0095	0,3	0,0165
HE360A			0,35	0,3	0,0175	0,01	0,3	0,0175
HE400A			0,39	0,3	0,019	0,011	0,3	0,019
HE450A			0,44	0,3	0,021	0,0115	0,3	0,021
HE500A			0,49	0,3	0,023	0,012	0,3	0,023
HE550A			0,54	0,3	0,024	0,0125	0,3	0,024
HE600A			0,59	0,3	0,025	0,013	0,3	0,025
HE650A			0,64	0,3	0,026	0,0135	0,3	0,026
HE700A			0,69	0,3	0,027	0,0145	0,3	0,027
HE800A			0,79	0,3	0,028	0,015	0,3	0,028
HE900A			0,89	0,3	0,03	0,016	0,3	0,03
HE1000A			0,99	0,3	0,031	0,0165	0,3	0,031

Table 4.8 General Characteristics of Models

Modal	Lx (m)	Span X(m)	Ly (m)	Span Y(m)	# of Story	Tx (sec)	Ty (sec)	Bracing Type	Bracing Weight(kN)	Bracing Weight/ Total Area (kN/m²)
310	30	5	30	5	3	0,74	0,74	-	-	-
310V11	30	5	30	5	3	0,47	0,47	K11	439	0,16
310X11	30	5	30	5	3	0,49	0,49	X11	455	0,17
310V21	30	5	30	5	3	0,50	0,42	K21	627	0,23
310X21	30	5	30	5	3	0,46	0,40	X21	681	0,25
310V22	30	5	30	5	3	0,41	0,41	K22	849	0,31
310X22	30	5	30	5	3	0,39	0,39	X22	911	0,34
610	30	5	30	5	6	1,02	1,02	-	-	-
610V11	30	5	30	5	6	0,75	0,75	K11	974	0,18
610X11	30	5	30	5	6	0,75	0,75	X11	1023	0,19
610V21	30	5	30	5	6	0,77	0,69	K21	1467	0,27
610X21	30	5	30	5	6	0,75	0,69	X21	1483	0,27
610V22	30	5	30	5	6	0,68	0,68	K22	1885	0,35
610X22	30	5	30	5	6	0,68	0,68	X22	1969	0,36
910	30	5	30	5	9	1,38	1,38	-	-	-
910V11	30	5	30	5	9	1,03	1,03	K11	1737	0,21
910X11	30	5	30	5	9	1,02	1,02	X11	1844	0,23
910V21	30	5	30	5	9	1,00	0,88	K21	2605	0,32
910X21	30	5	30	5	9	1,00	0,88	X21	2766	0,34
910V22	30	5	30	5	9	0,93	0,93	K22	3370	0,42
910X22	30	5	30	5	9	0,87	0,87	X22	3687	0,46
1210	30	5	30	5	12	1,79	1,79	-	-	-
1210V11	30	5	30	5	12	1,31	1,31	K11	2914	0,27
1210X11	30	5	30	5	12	1,30	1,30	X11	2933	0,27
1210V21	30	5	30	5	12	1,29	1,14	K21	4197	0,39
1210X21	30	5	30	5	12	1,23	1,20	X21	4835	0,45
1210V22	30	5	30	5	12	1,18	1,18	K22	6965	0,64
1210X22	30	5	30	5	12	1,17	1,17	X22	6102	0,57

4.3 Analysis and Design of Strengthened Buildings Using Equivalent Earthquake Load Method

Turkish Building Earthquake Code (2018) [11] was used to calculate the earthquake for the strengthened buildings. In this section, general characteristic, total base shears in both X- and Y- directions, seismic weights, and maximum horizontal deflections in both X- and Y-directions of structures are shown in Table 4.9. The results of the deficient building models were also presented in this table for comparison purposes. The results indicated that the deflection of the building models in both directions decreases significantly when the models were strengthened.

Table 4.9 Joint Displacements and Bracing Weights for Equivalent Earthquake Load Method based on TBEC (2018) [11]

Modal	Seismic Weight (kN)	T_x (sec)	T_y (sec)	Total Base Shear X (kN)	Total Base Shear Y (kN)	Bracing Weight (kN)	Max. U_x (mm)	Load Combination for U_x	Max. U_y (mm)	Load Combination for U_y
310	30251	0,74	0,74	3882,716	3882,716	-	25,887	1,0DL+1,0LL+1,0EQX+E+0,3EQY+E+0,3EQZ	25,887	1,0DL+1,0LL+1,0EQY+E+0,3EQX+E+0,3EQZ
310V11	30690	0,47	0,47	3107,84	3107,84	439	7,932		7,932	
310X11	30706	0,49	0,49	2982,32	2982,32	455	11,837		11,837	
310V21	30878	0,50	0,42	2986,629	3453,055	627	8,174		7,155	
310X21	30932	0,46	0,40	3249,089	3650,364	681	10,312		6,854	
310V22	31100	0,41	0,41	3602,803	3602,803	849	7,034		7,034	
310X22	31162	0,39	0,39	3793,91	3793,91	911	9,993		9,993	
610	65617	1,02	1,02	6144,666	6144,666	-	39,759		39,759	
610V11	66591	0,75	0,75	4236,563	4236,563	974	14,836		14,836	
610X11	66640	0,75	0,75	4237,759	4237,759	1023	17,263		17,263	
610V21	67084	0,77	0,69	4195,193	4597,035	1467	15,005		13,706	
610X21	67100	0,75	0,69	4296,79	4606,33	1483	16,541		16,58	
610V22	67502	0,68	0,68	4729,963	4729,963	1885	13,371		13,371	
610X22	67586	0,68	0,68	4735,357	4735,357	1969	15,33		15,33	
910	104839	1,38	1,38	7258,191	7258,191	-	57,041		57,041	
910V11	106576	1,03	1,03	4938,165	4938,165	1737	21,917		21,917	
910X11	106683	1,02	1,02	4991,229	4991,229	1844	23,543		23,543	
910V21	107444	1,00	0,88	5186,666	5769,804	2605	21,391		19,42	
910X21	107605	1,00	0,88	5193,866	5777,814	2766	22,6		19,361	
910V22	108209	0,93	0,93	5548,349	5548,349	3370	19,856		19,856	
910X22	108526	0,87	0,87	5947,075	5947,075	3687	20,676		20,676	
1210	148843	1,79	1,79	7943,665	7943,665	-	76,43		76,43	
1210V11	151757	1,31	1,31	5529,287	5529,287	2914	29,142		29,142	
1210X11	151776	1,30	1,30	5572,308	5572,308	2933	29,153		29,153	
1210V21	153040	1,29	1,14	5725,83	6347,296	4197	28,544		25,617	
1210X21	153678	1,23	1,20	5968,246	6092,55	4835	28,201		26,603	
1210V22	155808	1,18	1,18	6296,008	6296,008	6965	26,453		26,453	
1210X22	154945	1,17	1,17	6315,802	6315,802	6102	27,598		27,598	

Total drift ratio of a structure is defined as the ratio of deflections (U_x and U_y in Table 4.9) over total height of structures. The total drift ratio is calculated using the expression shown in Equation 4-1.

$$\text{Total Drift Ratio} = \frac{Uh}{Total\ Height\ of\ Structure} \qquad \text{Equation 4-1}$$

The total drift ratios of all structures are shown in Table 4.10 and the comparisons of these drift ratios for 3-, 6-, 9-, and 12-story building models are shown in figures between Figure 4.10 and Figure 4.17.

Table 4.10 Drift Ratios According to Equivalent Earthquake Load Method

Modal	Max. U_x (mm)	Max. U_y (mm)	Drift Ratios	
			X	Y
310	25,887	25,887	2,88E-03	2,88E-03
310V11	7,932	7,932	8,81E-04	8,81E-04
310X11	11,837	11,837	1,32E-03	1,32E-03
310V21	8,174	7,155	9,08E-04	7,95E-04
310X21	10,312	6,854	1,15E-03	7,62E-04
310V22	7,034	7,034	7,82E-04	7,82E-04
310X22	9,993	9,993	1,11E-03	1,11E-03
610	39,759	39,759	2,21E-03	2,21E-03
610V11	14,836	14,836	8,24E-04	8,24E-04
610X11	17,263	17,263	9,59E-04	9,59E-04
610V21	15,005	13,706	8,34E-04	7,61E-04
610X21	16,541	16,58	9,19E-04	9,21E-04
610V22	13,371	13,371	7,43E-04	7,43E-04
610X22	15,33	15,33	8,52E-04	8,52E-04
910	57,041	57,041	2,11E-03	2,11E-03
910V11	21,917	21,917	8,12E-04	8,12E-04
910X11	23,543	23,543	8,72E-04	8,72E-04
910V21	21,391	19,42	7,92E-04	7,19E-04
910X21	22,6	19,361	8,37E-04	7,17E-04
910V22	19,856	19,856	7,35E-04	7,35E-04
910X22	20,676	20,676	7,66E-04	7,66E-04
1210	76,43	76,43	2,12E-03	2,12E-03
1210V11	29,142	29,142	8,10E-04	8,10E-04
1210X11	29,153	29,153	8,10E-04	8,10E-04
1210V21	28,544	25,617	7,93E-04	7,12E-04
1210X21	28,201	26,603	7,83E-04	7,39E-04
1210V22	26,453	26,453	7,35E-04	7,35E-04
1210X22	27,598	27,598	7,67E-04	7,67E-04

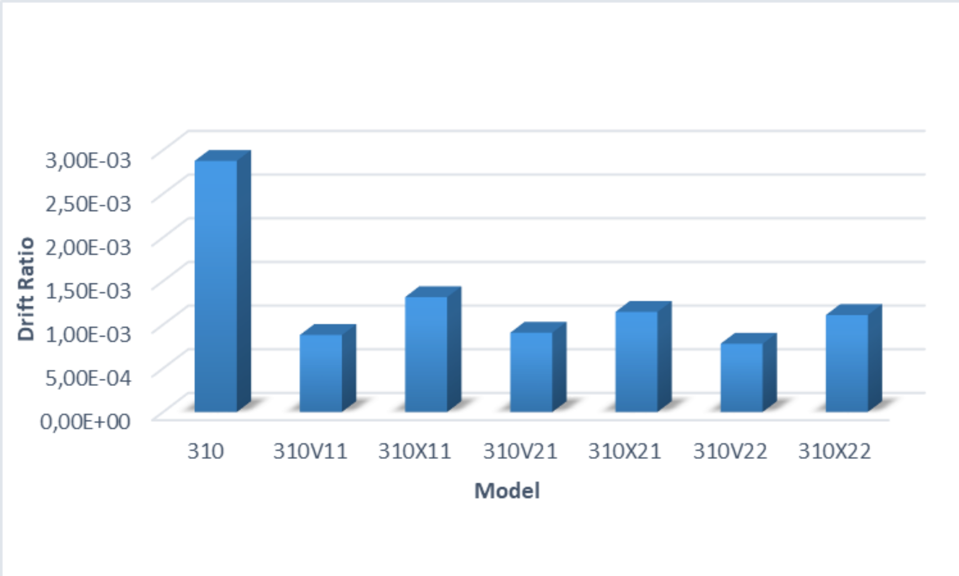

Figure 4.10 Drift Ratios for 3-Story Building Models based on Equivalent Earthquake Load Method in X-Direction

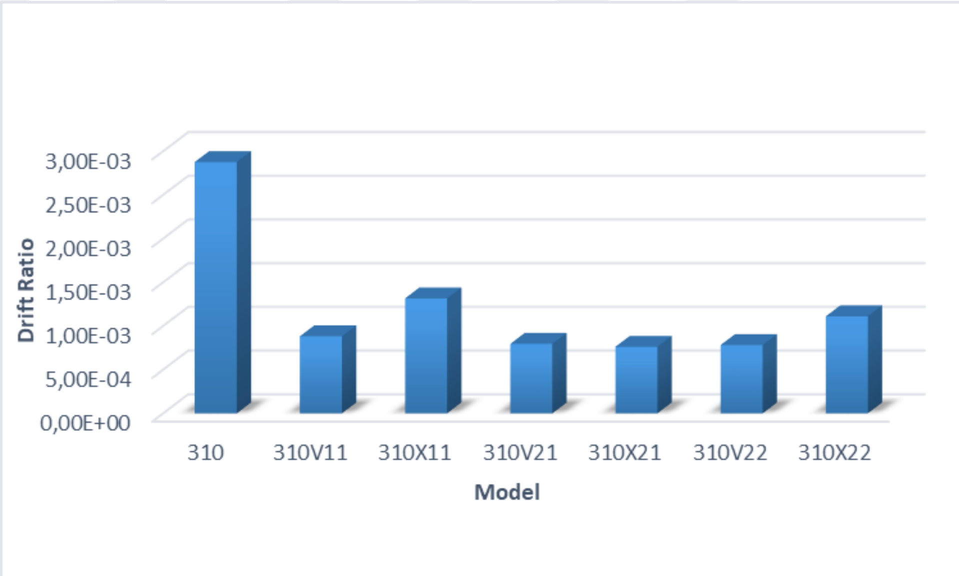

Figure 4.11 Drift Ratios for 3-Story Building Models based on Equivalent Earthquake Load Method in Y-Direction

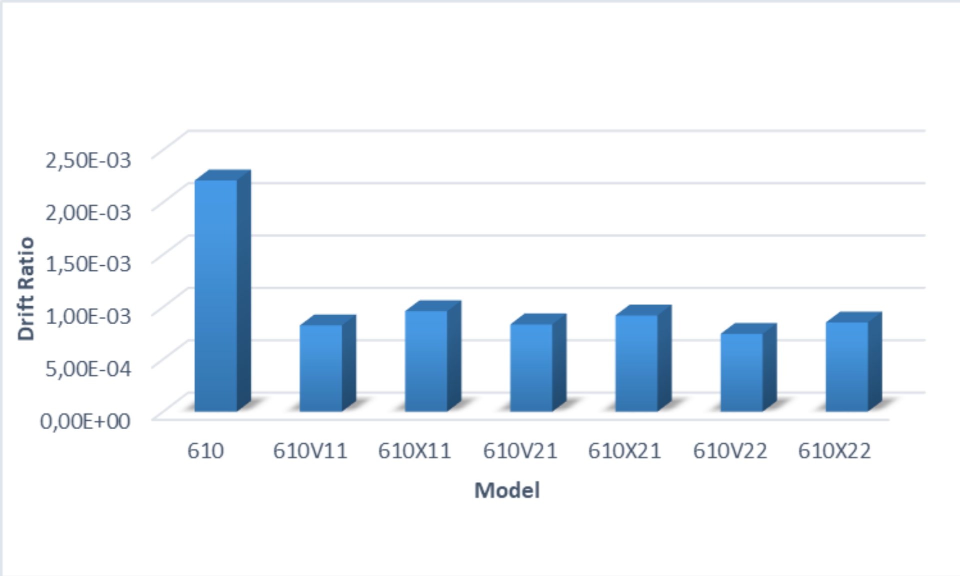

Figure 4.12 Drift Ratios for 6-Story Building Models based on Equivalent Earthquake Load Method in X-Direction

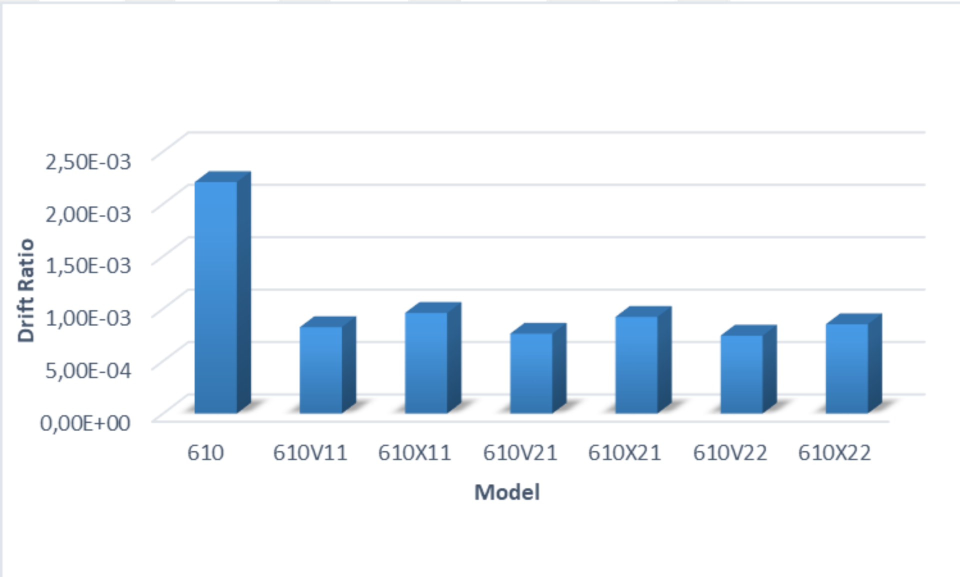

Figure 4.13 Drift Ratios for 3-Story Building Models based on Equivalent Earthquake Load Method in Y-Direction

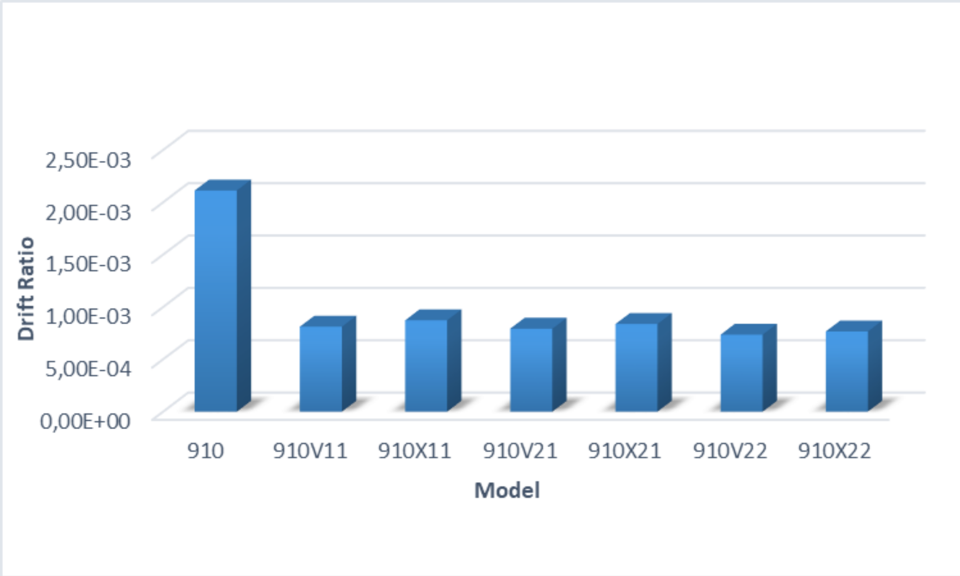

Figure 4.14 Drift Ratios for 9-Story Building Models based on Equivalent Earthquake Load Method in X-Direction

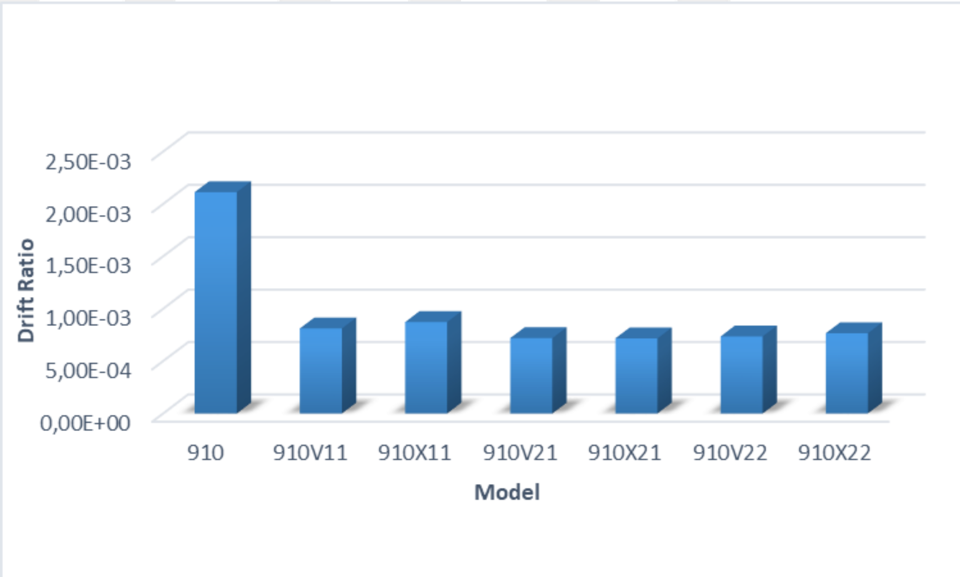

Figure 4.15 Drift Ratios for 9-Story Building Models based on Equivalent Earthquake Load Method in Y-Direction

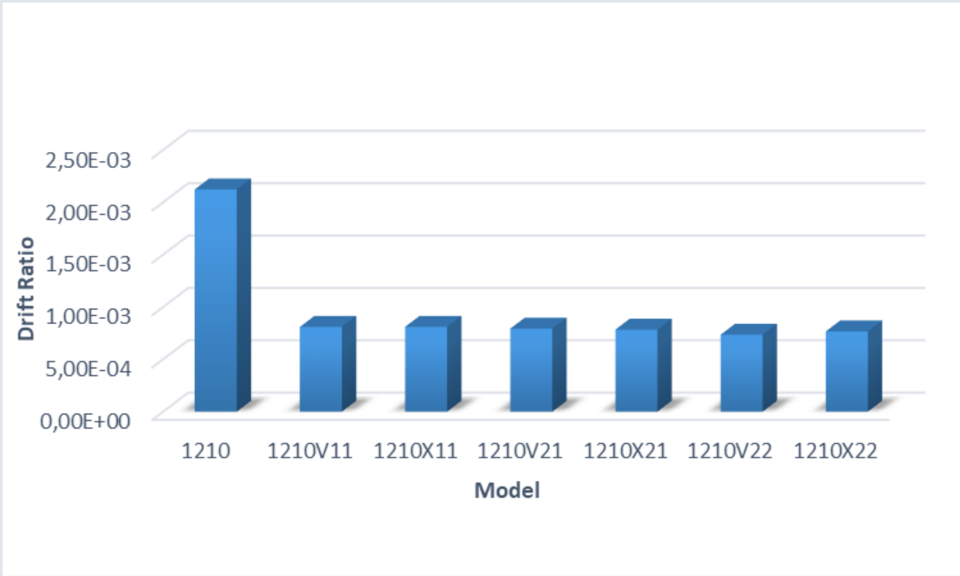

Figure 4.16 Drift Ratios for 12-Story Building Models based on Equivalent Earthquake Load Method in X-Direction

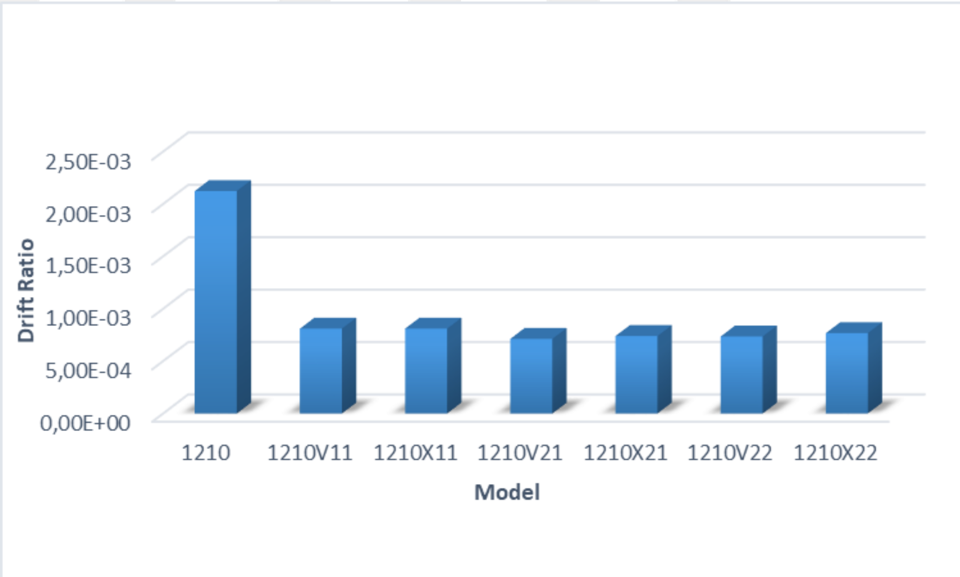

Figure 4.17 Drift Ratios for 12-Story Building Models based on Equivalent Earthquake Load Method in Y-Direction

The analyzed structure models were then designed (beams and columns) using SAP2000 [7]. The design code used was TS500 (2000) [8]. The details of the code and coefficients used in the design are shown in Figure 4.18.

Concrete Frame Design Preferences for TS 500-2000

	Item	Value
1	Design Code	TS 500-2000
2	Multi-Response Case Design	Envelopes
3	Number of Interaction Curves	24
4	Number of Interaction Points	11
5	Consider Minimum Eccentricity?	Yes
6	Seismic Zone	Zone 4
7	Gamma (Steel)	1,15
8	Gamma (Concrete)	1,5
9	Gamma (Concrete Shear)	1,25
10	Pattern Live Load Factor	0,75
11	Utilization Factor Limit	0,95

Set To Default Values: All Items | Selected Items

Reset To Previous Values: All Items | Selected Items

Figure 4.18 Concrete Frame Design Preferences for TS500 (2000) [8]

Based on the design results of SAP2000 [7], all the columns and beams of the strengthened structure models were sufficient to resist the load combinations used in this study. The design results of 3-, 6-, 9-, and 12-story structure models are shown in figures between Figure 4.19 and Figure 4.42. In these figures, the orange elements represent the sufficient frame elements under the applied loads and the red elements represent the insufficient frame elements. Note that there are no insufficient frame elements in the designed models.

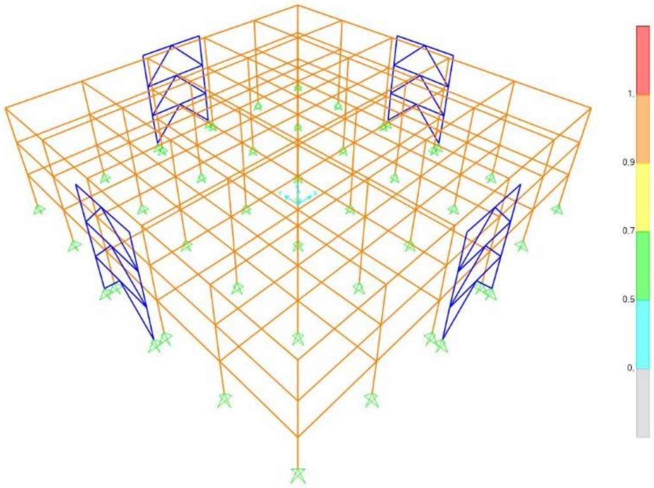

Figure 4.19 Results of Concrete Frame Design of Model 310V11

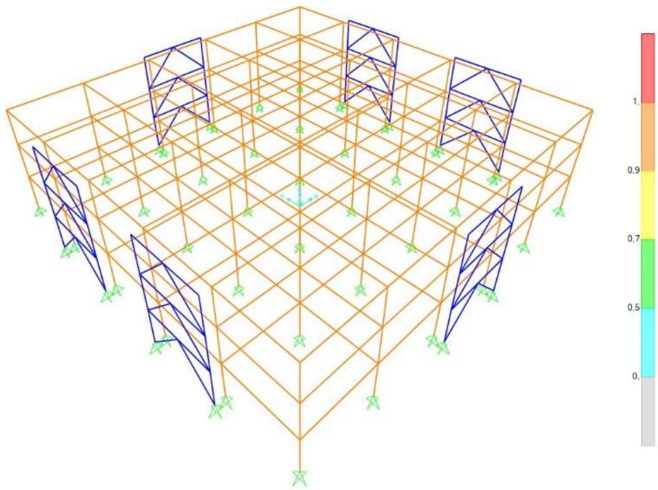

Figure 4.20 Results of Concrete Frame Design of Model 310V21

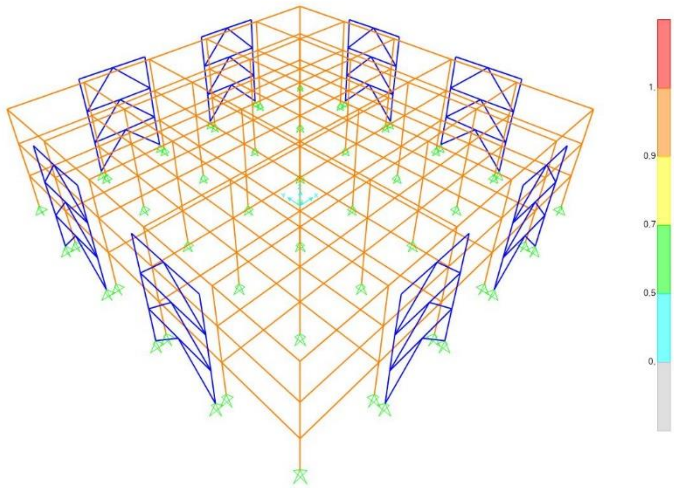

Figure 4.21 Results of Concrete Frame Design of Model 310V22

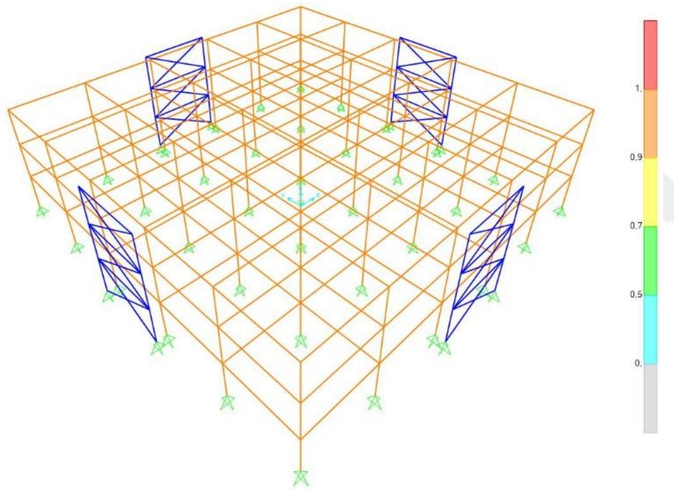

Figure 4.22 Results of Concrete Frame Design of Model 310X11

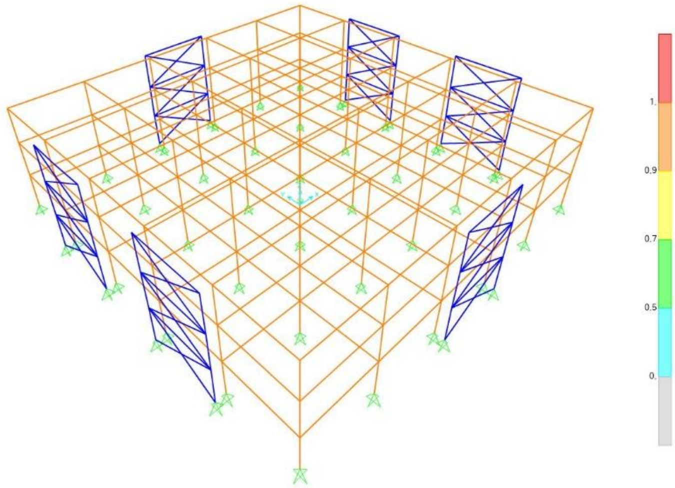

Figure 4.23 Results of Concrete Frame Design of Model 310X21

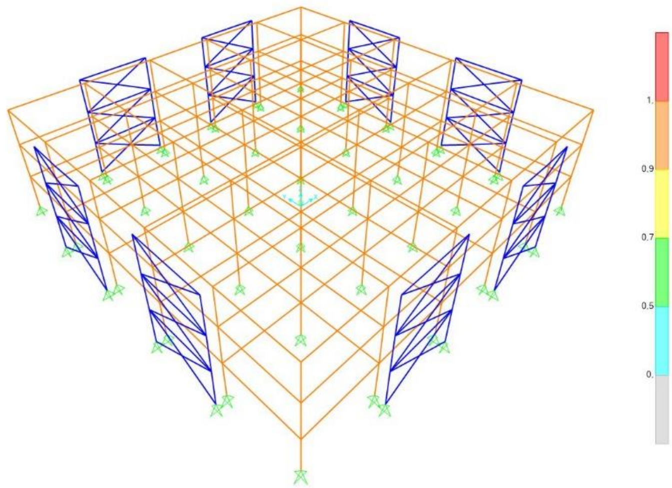

Figure 4.24 Results of Concrete Frame Design of Model 310X22

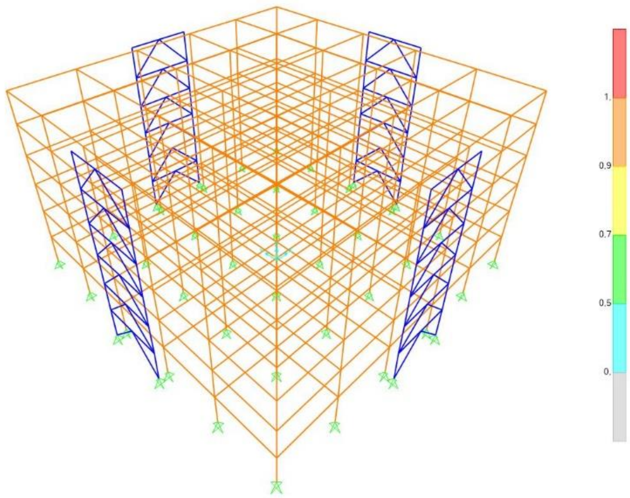

Figure 4.25 Results of Concrete Frame Design of Model 610V11

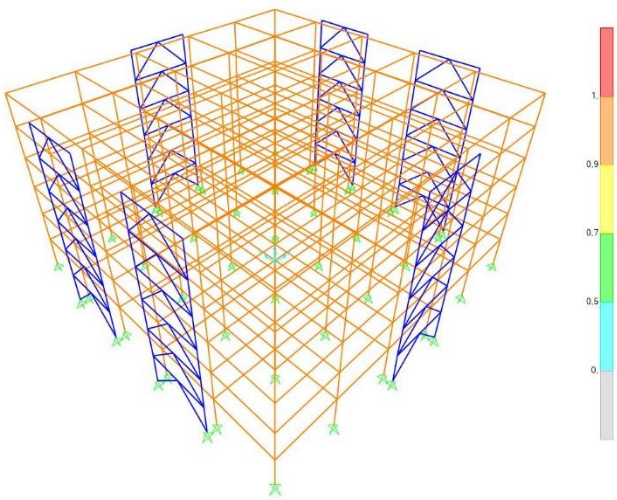

Figure 4.26 Results of Concrete Frame Design of Model 610V21

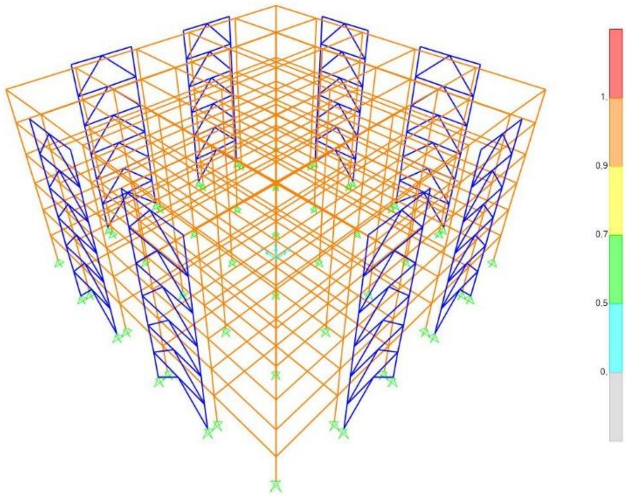

Figure 4.27 Results of Concrete Frame Design of Model 610V22

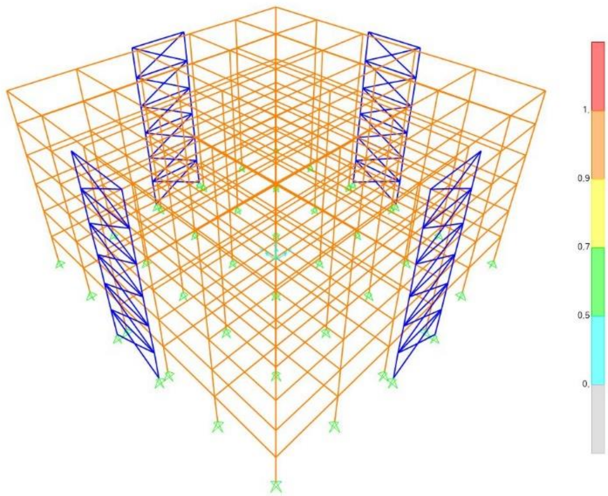

Figure 4.28 Results of Concrete Frame Design of Model 610X11

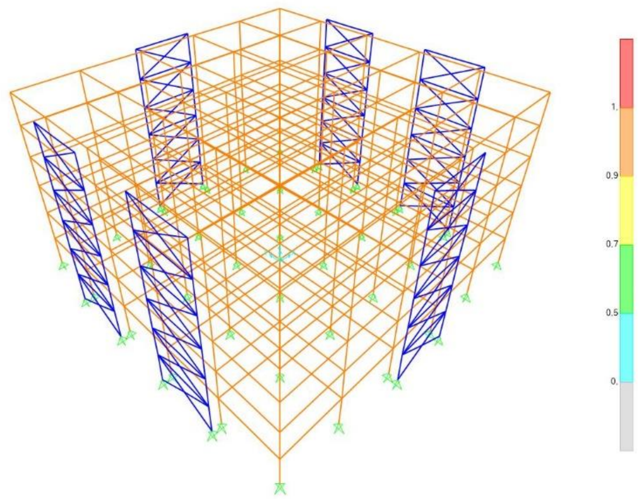

Figure 4.29 Results of Concrete Frame Design of Model 610X21

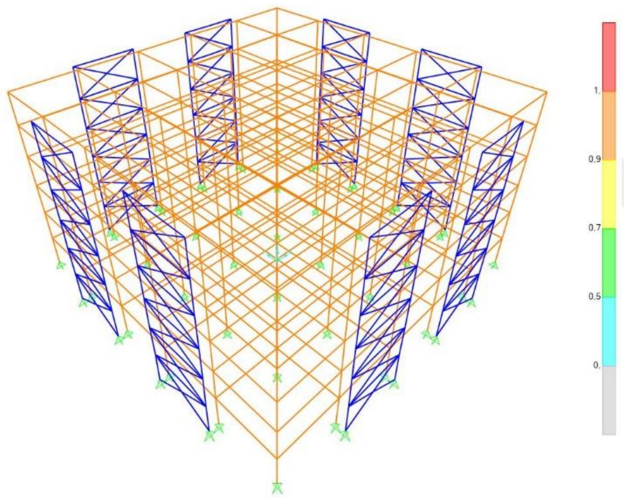

Figure 4.30 Results of Concrete Frame Design of Model 610X22

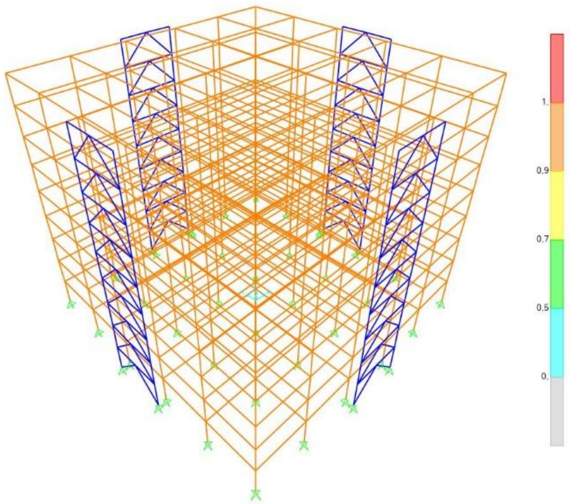

Figure 4.31 Results of Concrete Frame Design of Model 910V11

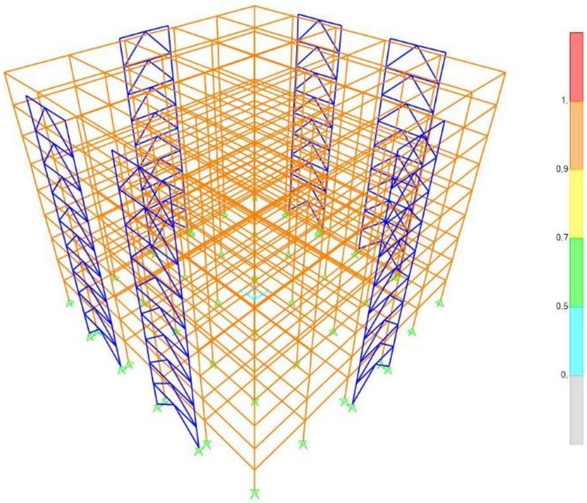

Figure 4.32 Results of Concrete Frame Design of Model 910V21

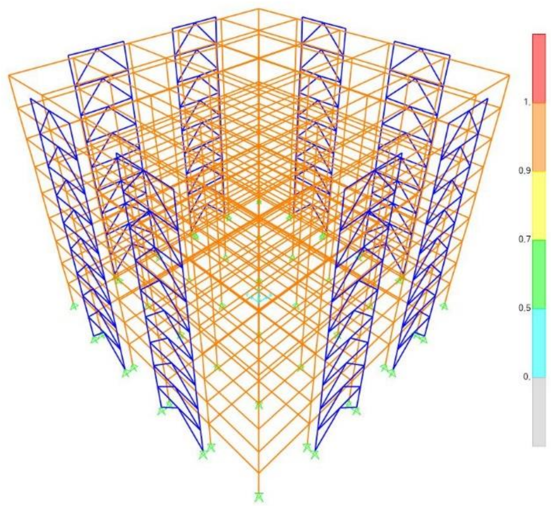

Figure 4.33 Results of Concrete Frame Design of Model 910V22

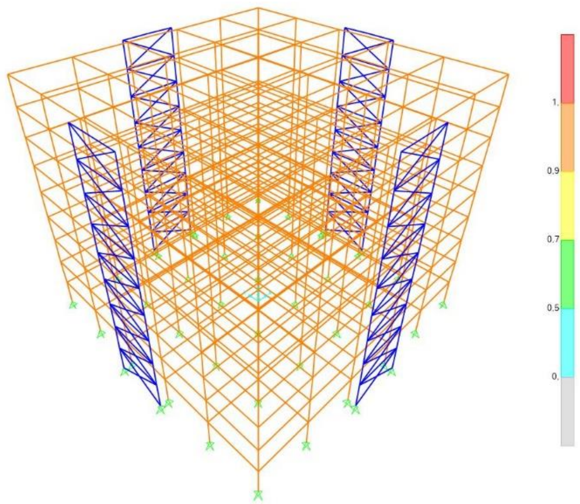

Figure 4.34 Results of Concrete Frame Design of Model 910X11

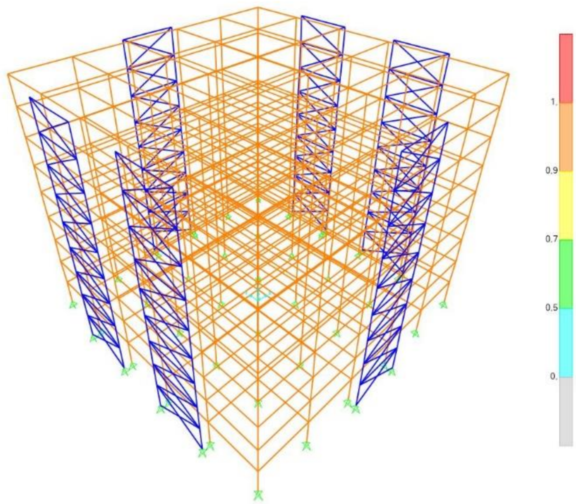

Figure 4.35 Results of Concrete Frame Design of Model 910X21

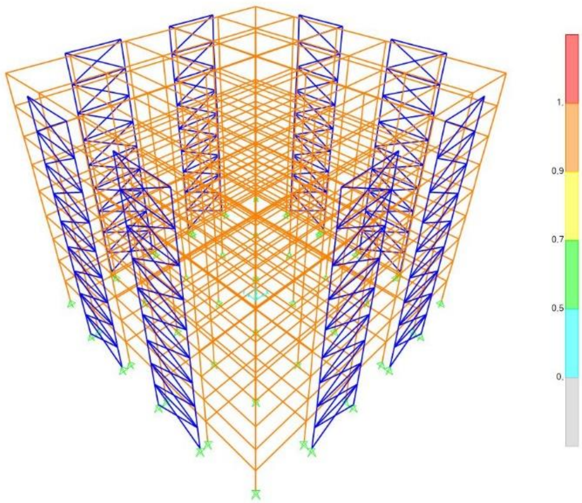

Figure 4.36 Results of Concrete Frame Design of Model 910X22

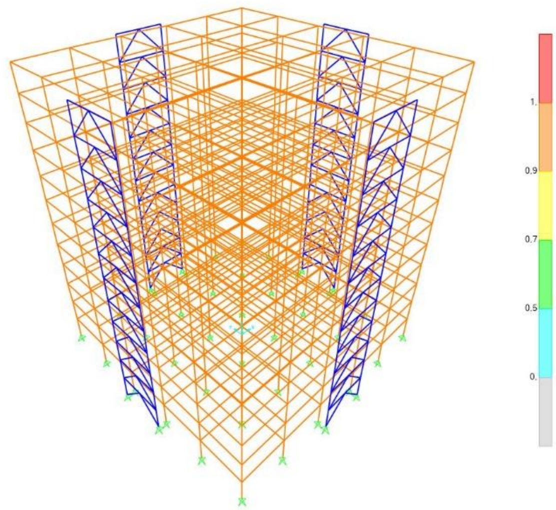

Figure 4.37 Results of Concrete Frame Design of Model 1210V11

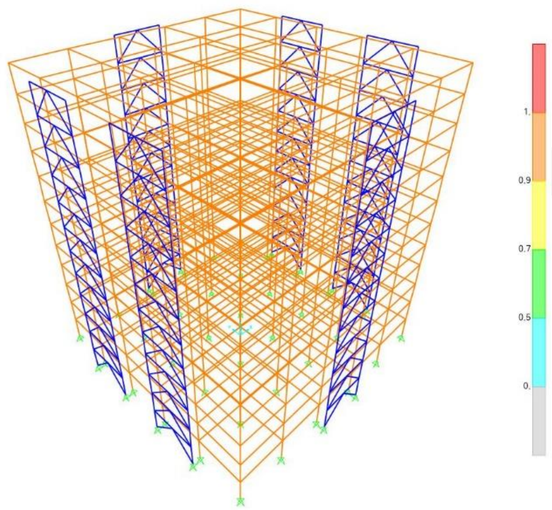

Figure 4.38 Results of Concrete Frame Design of Model 1210V21

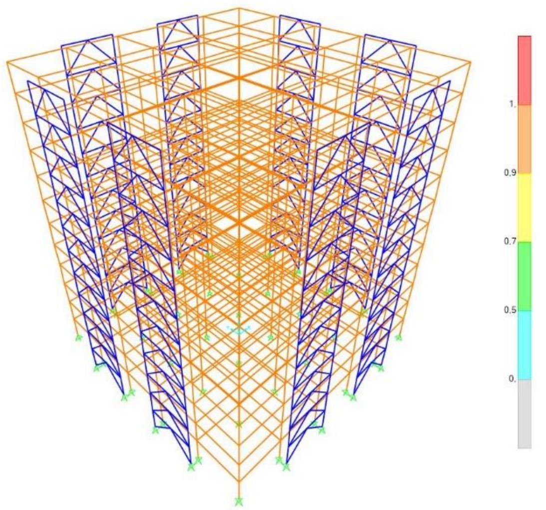

Figure 4.39 Results of Concrete Frame Design of Model 1210V22

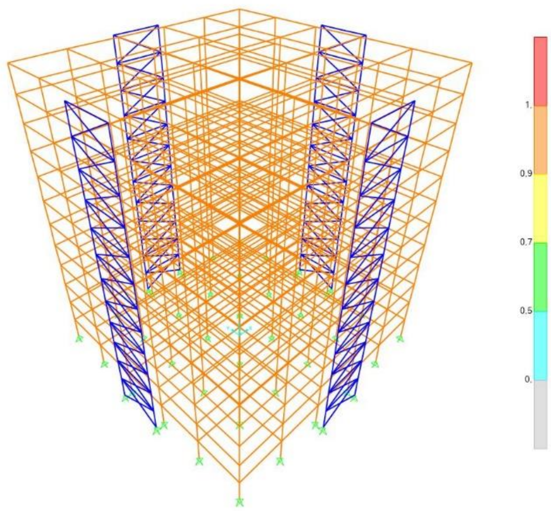

Figure 4.40 Results of Concrete Frame Design of Model 1210X11

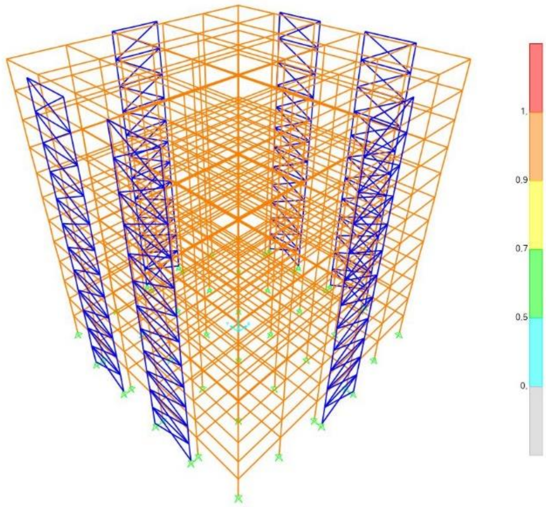

Figure 4.41 Results of Concrete Frame Design of Model 1210X21

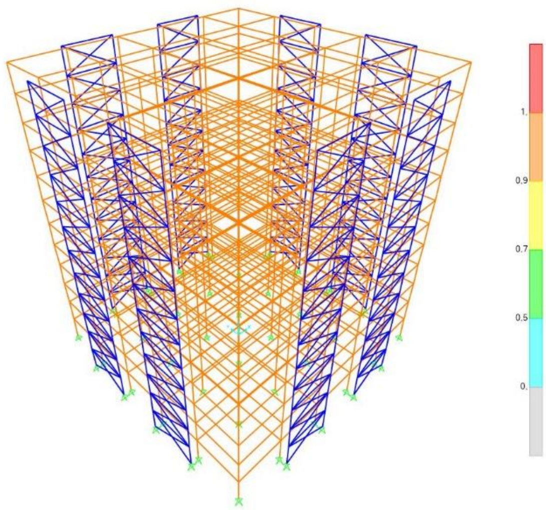

Figure 4.42 Results of Concrete Frame Design of Model 1210X22

4.4 Analysis and Design of Strengthened Building Using Pushover Analysis Method

Pushover Analysis Method was used to calculate the earthquake load effect for the strengthened buildings. In this section, performance points V and Δ based on ATC-40 [22] of all strengthened structure models are shown in Table 4.9. The results of the deficient building models were also presented in this table for comparison purposes. The results indicated that the performances of structure models as shear, V, increases significantly and deflections, Δ, decreases significantly when the models were strengthened.

Demand curve was defined based on spectral accelerations C_A and C_V. Performance points of models were determined where the capacity curve intersected with the demand curve. Based on these criteria, performance points V and Δ of all building models were obtained as shown in Table 4.11.

Table 4.11 Results of Model Performances for Pushover Analysis

Model	PUSH X		PUSH Y	
	Performance Point, V (kN)	Performance Point, Δ (mm)	Performance Point, V (kN)	Performance Point, Δ (mm)
310	4639	70	4665	70
310V11	10412	44	10312	43
310X11	10990	44	10926	43
310V21	9590	48	12973	40
310X21	13094	45	17697	41
310V22	13580	39	13568	39
310X22	17978	37	17946	37
610	10320	85	10319	85
610V11	16024	72	15838	72
610X11	16070	73	16100	74
610V21	14710	82	18462	66
610X21	15424	77	18356	70
610V22	19229	65	19242	65
610X22	19617	70	19617	70
910	13684	115	13700	115
910V11	22709	102	22693	102
910X11	22958	108	23032	108
910V21	23606	100	29985	90
910X21	24103	103	29713	91
910V22	26504	93	26600	93
910X22	30438	90	30415	90
1210	21639	172	21641	172
1210V11	25902	133	25902	133
1210X11	No performance point.			
1210V21	26571	133	33399	119
1210X21	No performance point.			
1210V22	30873	121	30799	121
1210X22	31352	122	31407	121

The total drift ratios of all structures are shown in Table 4.12 and the comparisons of these drift ratios for 3-, 6-, 9-, and 12-story building models are shown in figures between Figure 4.43 and Figure 4.50.

Table 4.12 Drift Ratios According to Pushover Analysis Method

Modal	Drift Ratios	
	X	Y
310	7,78E-03	7,78E-03
310V11	4,89E-03	4,78E-03
310X11	4,89E-03	4,78E-03
310V21	5,33E-03	4,44E-03
310X21	5,00E-03	4,56E-03
310V22	4,33E-03	4,33E-03
310X22	4,11E-03	4,11E-03
610	4,72E-03	4,72E-03
610V11	4,00E-03	4,00E-03
610X11	4,06E-03	4,11E-03
610V21	4,56E-03	3,67E-03
610X21	4,28E-03	3,89E-03
610V22	3,61E-03	3,61E-03
610X22	3,89E-03	3,89E-03
910	4,26E-03	4,26E-03
910V11	3,78E-03	3,78E-03
910X11	4,00E-03	4,00E-03
910V21	3,70E-03	3,33E-03
910X21	3,81E-03	3,37E-03
910V22	3,44E-03	3,44E-03
910X22	3,33E-03	3,33E-03
1210	4,78E-03	4,78E-03
1210V11	3,69E-03	3,69E-03
1210X11	No performance point.	
1210V21	3,69E-03	3,31E-03
1210X21	No performance point.	
1210V22	3,36E-03	3,36E-03
1210X22	3,39E-03	3,36E-03

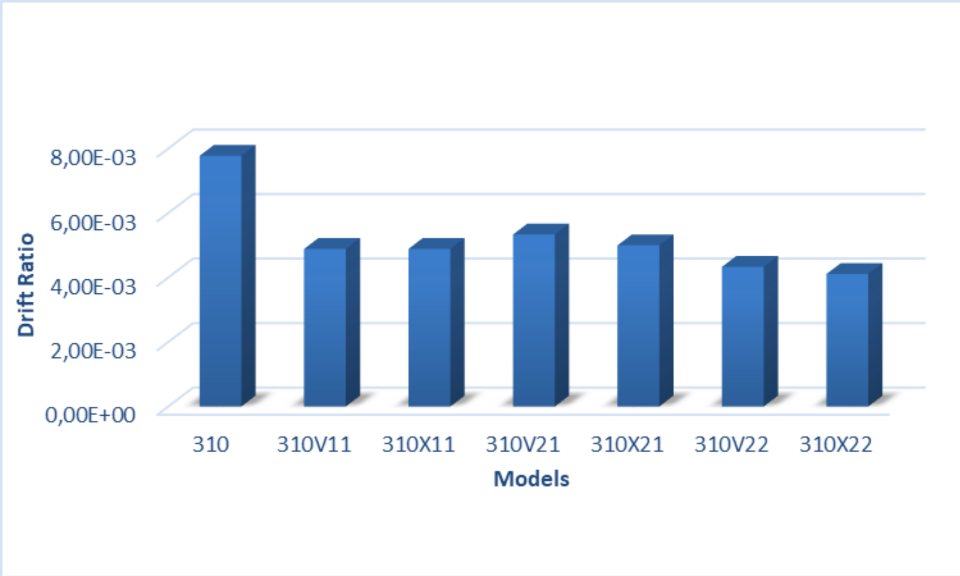

Figure 4.43 Drift Ratios for 3-Story Models for Pushover Analysis in X-Direction

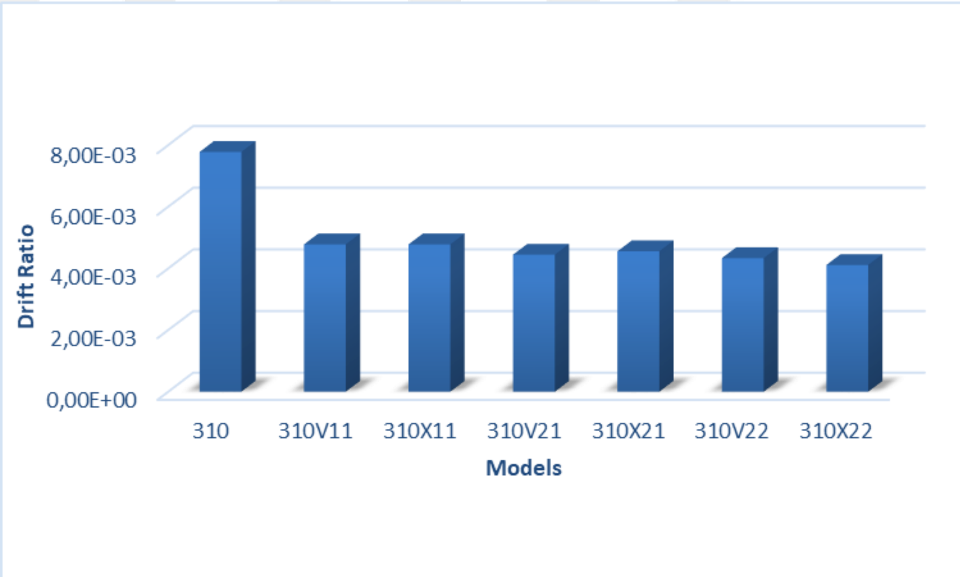

Figure 4.44 Drift Ratios for 3-Story Models for Pushover Analysis in Y-Direction

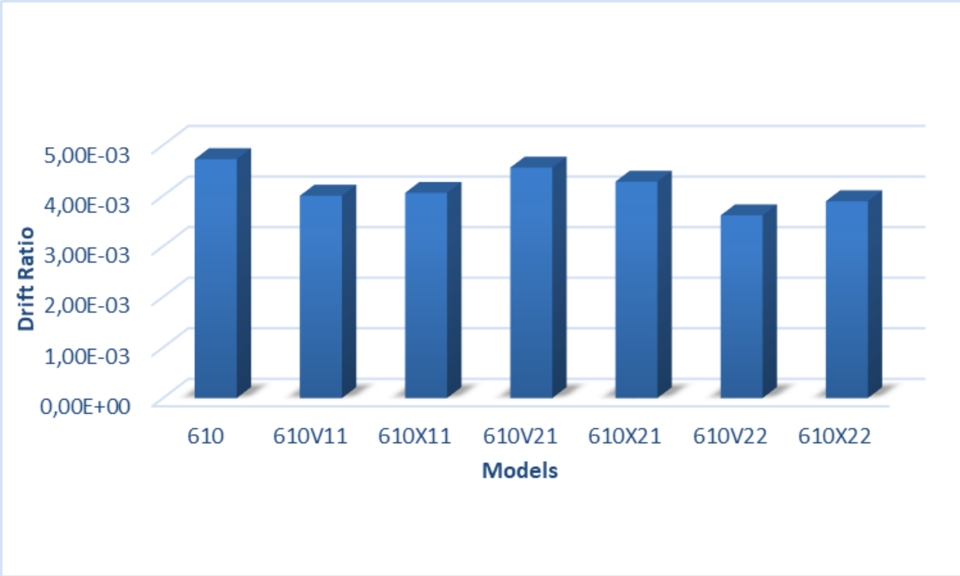

Figure 4.45 Drift Ratios for 6-Story Models for Pushover Analysis in X-Direction

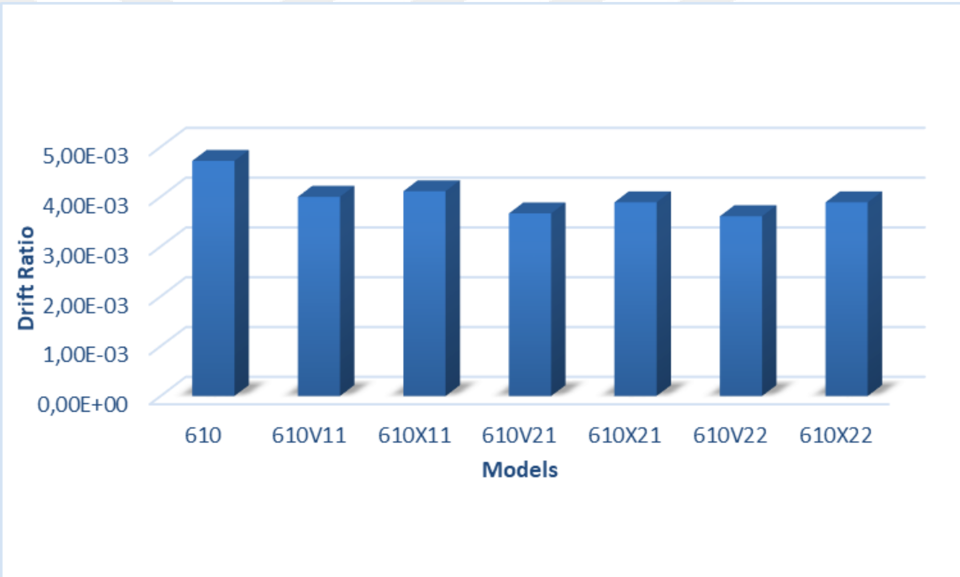

Figure 4.46 Drift Ratios for 6-Story Models for Pushover Analysis in Y-Direction

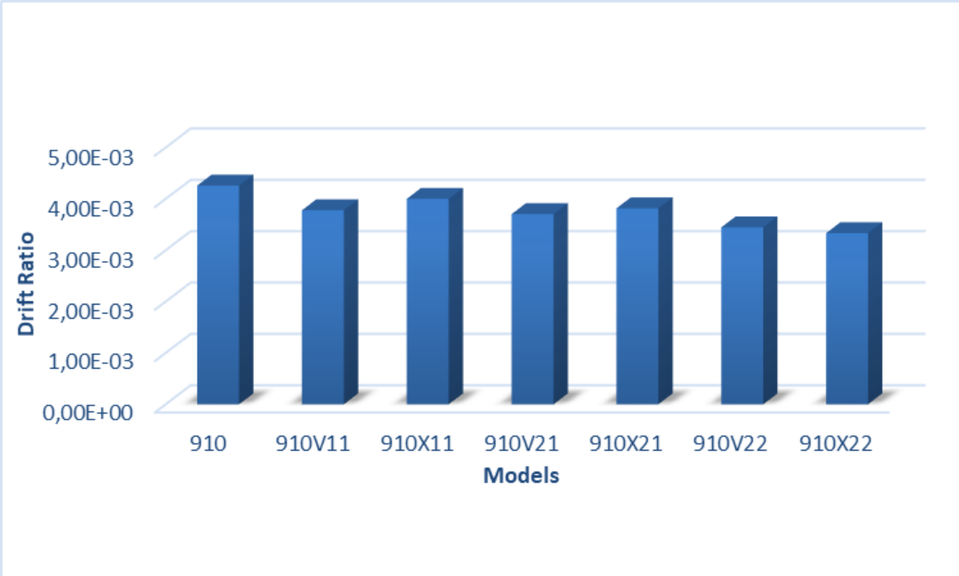

Figure 4.47 Drift Ratios for 9-Story Models for Pushover Analysis in X-Direction

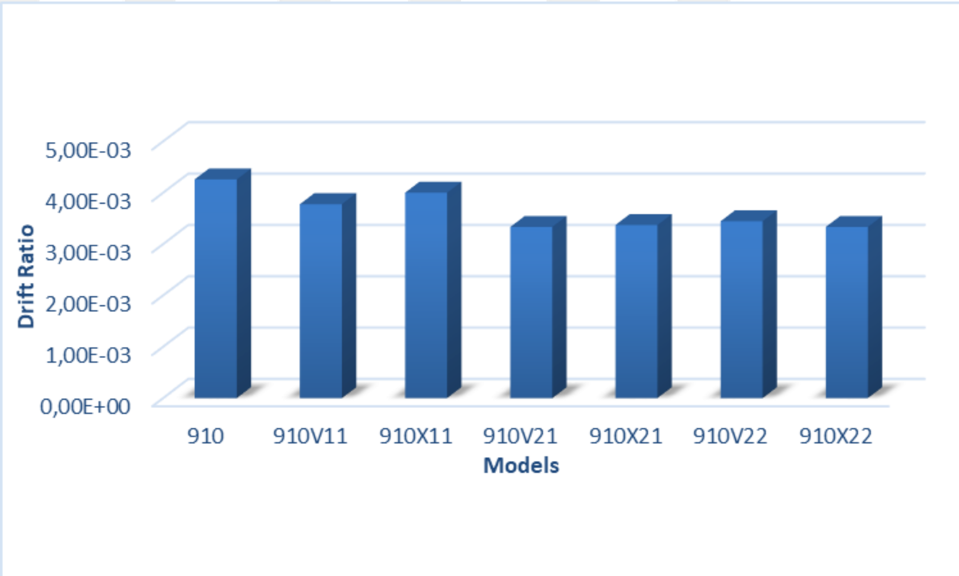

Figure 4.48 Drift Ratios for 9-Story Models for Pushover Analysis in Y-Direction

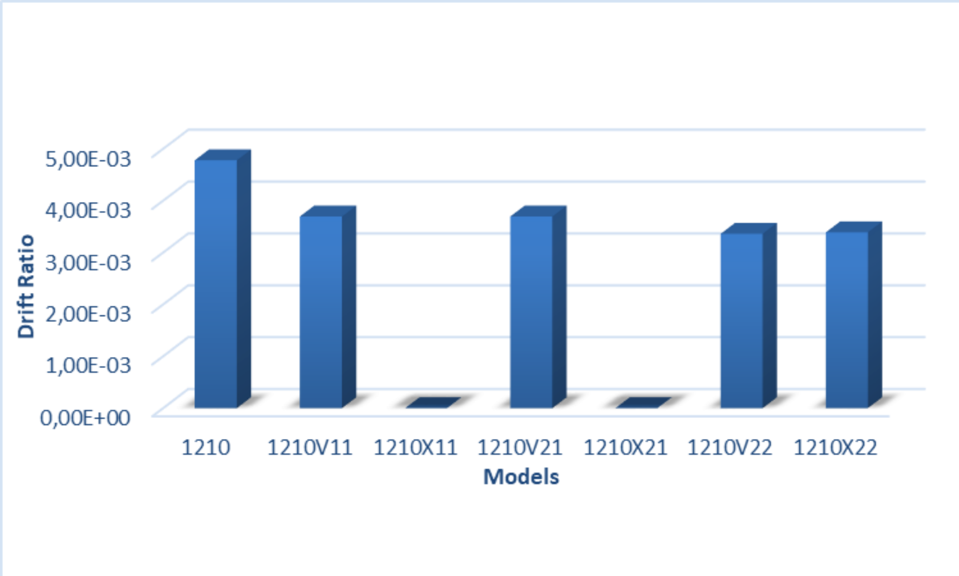

Figure 4.49 Drift Ratios for 12-Story Models for Pushover Analysis in X-Direction

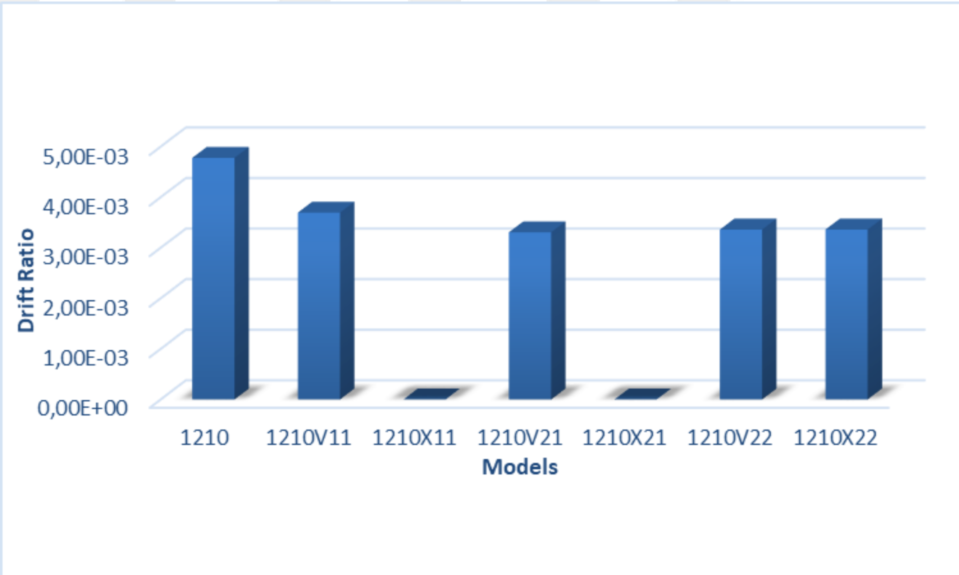

Figure 4.50 Drift Ratios for 12-Story Models for Pushover Analysis in Y-Direction

4.5 Analysis and Design of Strengthened Building Using Time History Analysis Method

Time-history analysis of past earthquakes was used to calculate the earthquake for the strengthened buildings. In this section, maximum deflections and maximum base shear forces in both X- and Y-directions (results of 11 different ground motion data are shown in Table 3.23) are shown in tables between Table 4.13 and Table 4.18. The results of the deficient building models were also presented in these tables for comparison purposes. Results of 11 different ground motion data and earthquake cases, which were calculated based on TBEC (2018) [11], were compared to each other in terms of base reaction forces and maximum deflections in both X- and Y-directions. The results indicated that the base reaction forces due to earthquakes of the building models decreased significantly when the models were strengthened, except for 3-story models, because X- and Y- periods of 3-story structure models were relatively low based on the deficient 3-story structure. This decrease on periods of 3-story structure caused higher base reaction forces.

Table 4.13 Total Base Shears and Maximum Deflections based on Time-History Analysis for EQ1 and EQ2

Modal	EQ1				EQ2			
	Fx (kN)	Δ_x (mm)	Fy (kN)	Δ_y (mm)	Fx (kN)	Δ_x (mm)	Fy (kN)	Δ_y (mm)
310	2460	15,037	738	4,511	2665	15,262	800	4,590
310V11	2431	5,389	729	1,693	2672	6,159	802	1,881
310X11	2353	5,888	706	1,794	2581	6,427	774	1,956
310V21	2334	6,119	851	1,613	2531	6,479	746	1,385
310X21	2500	5,504	866	1,518	2704	6,022	870	1,442
310V22	2885	5,206	866	1,594	2552	4,526	766	1,389
310X22	2914	4,868	874	1,493	3024	4,752	907	1,457
610	3969	19,755	1191	5,946	4606	24,751	1382	7,444
610V11	2760	8,315	828	2,529	2626	8,604	788	2,616
610X11	2763	8,356	829	2,541	2607	8,642	782	2,524
610V21	2699	8,140	946	2,491	2487	8,628	878	2,404
610X21	2776	8,252	946	2,492	2589	8,757	878	2,407
610V22	3252	8,082	976	2,459	2975	7,732	892	2,355
610X22	3260	8,087	978	2,461	2978	7,737	893	2,356
910	4598	30,000	1379	9,022	5384	29,134	1615	8,764
910V11	3254	11,183	976	3,394	3311	13,797	993	4,178
910X11	3304	11,187	991	3,395	3333	13,799	1000	4,178
910V21	3604	10,817	1060	3,271	3432	13,578	1021	3,640
910X21	3634	10,796	1051	3,269	3453	13,583	1029	3,622
910V22	4018	10,490	1205	3,186	3537	12,672	1061	3,842
910X22	3383	10,648	1015	3,235	3559	11,586	1068	3,516
1210	4549	39,922	1365	12,003	5835	34,148	1750	10,268
1210V11	3403	16,155	1021	4,885	3858	15,121	1157	4,578
1210X11	3375	16,322	1012	4,934	3903	15,072	1171	4,561
1210V21	3554	16,174	1110	4,063	3910	15,115	1463	4,524
1210X21	3605	15,925	1041	4,549	4465	15,085	1398	4,536
1210V22	3641	14,665	1092	4,442	4739	15,139	1422	4,584
1210X22	3705	14,393	1111	4,360	4783	15,210	1435	4,604

Table 4.14 Total Base Shears and Maximum Deflections based on Time-History Analysis for EQ3 and EQ4

Modal	**EQ3**				**EQ4**			
	Fx (kN)	**Δ_x (mm)**	**Fy (kN)**	**Δ_y (mm)**	**Fx (kN)**	**Δ_x (mm)**	**Fy (kN)**	**Δ_y (mm)**
310	3017	17,411	905	5,234	3310	18,335	992	5,510
310V11	2325	5,514	698	1,686	2781	6,351	834	1,938
310X11	2147	5,323	644	1,624	2694	6,679	808	2,032
310V21	2236	5,564	844	1,524	2670	6,845	893	1,631
310X21	2439	5,546	780	1,343	2842	6,261	890	1,479
310V22	2817	4,819	845	1,477	2982	5,198	895	1,591
310X22	2571	4,257	771	1,308	2995	4,744	899	1,455
610	4020	23,891	1206	7,186	3999	23,537	1200	7,080
610V11	3099	9,711	930	2,949	3003	10,712	901	3,252
610X11	3106	9,758	932	2,962	2975	10,783	893	3,271
610V21	3162	9,693	1061	2,804	2883	10,852	1028	3,159
610X21	3137	9,669	1060	2,806	2938	10,864	1026	3,161
610V22	3638	9,156	1091	2,783	3536	10,368	1061	3,150
610X22	3644	9,165	1093	2,786	3538	10,382	1062	3,154
910	4642	36,810	1392	11,067	4352	29,658	1306	8,920
910V11	2843	13,048	853	3,952	3218	13,068	965	3,958
910X11	2844	12,994	853	3,936	3231	13,078	969	3,961
910V21	2935	12,462	1308	3,257	3354	12,894	1176	3,704
910X21	2965	12,433	1321	3,263	3382	12,894	1185	3,710
910V22	3904	11,378	1171	3,660	3900	12,069	1170	3,660
910X22	4579	10,802	1374	3,281	3962	12,226	1189	3,709
1210	4643	46,613	1393	14,013	4401	37,834	1320	11,375
1210V11	3730	18,256	1119	5,517	3536	15,250	1061	4,613
1210X11	3786	18,155	1136	5,485	3669	15,292	1101	4,624
1210V21	3733	18,024	1169	4,494	3627	15,165	1329	4,271
1210X21	3688	17,021	1069	4,771	3962	14,955	1231	4,374
1210V22	3731	15,305	1119	4,633	4208	14,411	1262	4,364
1210X22	3846	14,939	1154	4,523	4269	14,408	1281	4,363

Table 4.15 Total Base Shears and Maximum Deflections based on Time-History Analysis for EQ5 and EQ6

Modal	EQ5				EQ6			
	Fx (kN)	Δ_x (mm)	Fy (kN)	Δ_y (mm)	Fx (kN)	Δ_x (mm)	Fy (kN)	Δ_y (mm)
310	2565	14,197	770	4,270	2546	14,382	764	4,307
310V11	2404	5,643	721	1,674	2456	5,802	737	1,773
310X11	2252	5,737	676	1,749	2358	5,999	708	1,827
310V21	2270	5,814	831	1,590	2372	6,205	783	1,464
310X21	2448	5,540	896	1,571	2495	5,684	833	1,404
310V22	2863	5,237	859	1,604	2640	4,719	792	1,447
310X22	3046	5,103	914	1,564	2853	4,558	856	1,399
610	4170	21,800	1251	6,559	3313	19,277	994	5,802
610V11	2770	8,118	831	2,471	2524	8,094	757	2,463
610X11	2778	8,148	833	2,479	2518	8,161	755	2,482
610V21	2508	8,319	860	2,447	2558	8,605	891	2,573
610X21	2723	8,327	862	2,450	2546	8,389	890	2,571
610V22	2888	7,775	867	2,369	3062	8,604	919	2,619
610X22	2899	7,775	870	2,369	3066	8,619	920	2,624
910	3937	25,211	1181	7,585	4242	29,969	1273	9,013
910V11	3155	11,933	946	3,618	2807	10,688	842	3,243
910X11	3183	11,994	955	3,636	2810	10,746	843	3,261
910V21	3234	12,270	1009	3,075	2694	10,902	1007	3,050
910X21	3255	12,307	1015	3,067	2693	10,926	1015	3,068
910V22	3136	11,307	941	3,430	2928	9,533	879	2,897
910X22	3457	9,847	1037	2,991	3522	10,180	1057	3,092
1210	4187	39,401	1256	11,846	4646	38,307	1394	11,517
1210V11	2871	12,651	861	3,832	3635	13,734	1091	4,158
1210X11	2915	12,847	875	3,890	3669	13,289	1101	4,023
1210V21	3118	12,815	1140	4,015	3773	12,916	1225	4,085
1210X21	3454	12,657	1085	3,809	4043	13,781	1205	4,172
1210V22	3689	12,883	1107	3,905	4122	13,819	1237	4,192
1210X22	3636	13,079	1091	3,963	4161	13,817	1248	4,192

Table 4.16 Total Base Shears and Maximum Deflections based on Time-History Analysis for EQ7 and EQ8

Modal	EQ7				EQ8			
	Fx (kN)	Δ_x (mm)	Fy (kN)	Δ_y (mm)	Fx (kN)	Δ_x (mm)	Fy (kN)	Δ_y (mm)
310	2854	16,265	856	4,891	3010	17,173	904	5,161
310V11	2689	6,376	807	1,946	2746	6,313	824	1,927
310X11	2532	6,303	760	1,985	2621	6,419	786	1,954
310V21	2463	6,465	850	1,597	2579	6,479	892	1,687
310X21	2733	6,251	897	1,559	2794	6,272	914	1,562
310V22	2905	5,227	872	1,601	3034	5,394	910	1,651
310X22	3028	4,336	908	1,540	3078	4,998	924	1,532
610	4633	22,019	1390	6,625	5029	25,263	1509	7,598
610V11	2760	9,214	828	2,787	2995	9,696	898	2,945
610X11	2754	9,249	826	2,810	2987	9,754	896	2,962
610V21	2765	9,457	959	2,873	2981	9,760	1024	2,676
610X21	2766	9,287	957	2,874	3012	9,600	1023	2,678
610V22	3319	9,436	996	2,868	3554	8,746	1066	2,660
610X22	3324	9,448	997	2,872	3564	8,758	1069	2,663
910	4961	27,467	1488	8,262	6450	36,659	1935	11,021
910V11	3637	12,085	1091	3,662	4180	14,091	1254	4,266
910X11	3650	12,087	1095	3,663	4199	14,073	1260	4,260
910V21	3673	11,985	1211	3,120	4300	13,732	1280	3,763
910X21	3684	11,995	1211	3,106	4302	13,725	1282	3,751
910V22	4004	11,190	1201	3,395	4372	12,770	1312	3,871
910X22	3978	9,950	1193	3,022	4325	12,194	1298	3,700
1210	6009	42,053	1803	12,644	5055	50,657	1516	15,225
1210V11	3761	14,836	1128	4,491	4881	18,793	1464	5,679
1210X11	3712	14,856	1114	4,495	4920	18,830	1476	5,688
1210V21	3800	14,725	1389	4,065	5163	18,487	1705	4,945
1210X21	3801	13,915	1249	4,144	5520	17,926	1672	5,176
1210V22	4361	13,681	1308	4,142	5690	16,941	1707	5,125
1210X22	4436	13,685	1331	4,143	5732	16,794	1720	5,081

Table 4.17 Total Base Shears and Maximum Deflections based on Time-History Analysis for EQ9 and EQ10

Modal	EQ9				EQ10			
	Fx (kN)	Δ_x (mm)	Fy (kN)	Δ_y (mm)	Fx (kN)	Δ_x (mm)	Fy (kN)	Δ_y (mm)
310	3078	17,090	923	5,118	3002	16,745	901	5,035
310V11	2333	5,302	700	1,622	2399	5,409	720	1,654
310X11	2176	5,463	653	1,666	2321	5,633	696	1,717
310V21	2138	5,553	723	1,420	2328	5,799	772	1,485
310X21	2380	5,234	816	1,401	2460	5,307	866	1,496
310V22	2513	4,732	754	1,452	2704	4,901	811	1,502
310X22	2825	4,606	847	1,414	2945	4,820	884	1,478
610	4105	25,286	1231	7,605	4186	23,801	1256	7,160
610V11	3051	9,556	915	2,902	2988	9,491	897	2,883
610X11	3063	9,611	919	2,918	2975	9,540	893	2,897
610V21	3055	9,642	971	2,636	2899	9,444	956	2,758
610X21	3061	9,683	971	2,638	2950	9,586	956	2,761
610V22	3236	8,529	971	2,595	3207	8,916	962	2,713
610X22	3239	8,536	972	2,597	3208	8,929	962	2,716
910	3989	27,561	1197	8,290	4998	32,894	1499	9,890
910V11	3028	14,229	908	4,307	3560	13,388	1068	4,057
910X11	3031	14,253	909	4,314	3552	13,337	1066	4,041
910V21	2991	14,186	1067	3,736	3591	12,605	1019	2,988
910X21	2983	14,196	1081	3,716	3605	12,557	1026	2,998
910V22	3356	13,156	1007	3,986	3246	10,412	974	3,164
910X22	3837	11,900	1151	3,609	3527	9,960	1058	3,029
1210	5126	38,473	1538	11,567	5925	44,400	1778	13,346
1210V11	3415	12,956	1025	3,923	3839	16,614	1152	5,020
1210X11	3474	12,886	1042	3,900	3873	16,541	1162	4,997
1210V21	3606	12,950	1178	4,262	4142	16,580	1517	4,694
1210X21	3954	12,997	1190	4,059	4629	16,308	1421	4,791
1210V22	4067	13,604	1220	4,124	4908	15,820	1472	4,789
1210X22	4078	13,785	1223	4,177	4966	15,867	1490	4,803

Table 4.18 Total Base Shears and Maximum Deflections based on Time-History Analysis for EQ11

Modal	**EQ11**			
	Fx (kN)	**Δ_x (mm)**	**Fy (kN)**	**Δ_y (mm)**
310	3074	17,853	922	5,367
310V11	2121	4,888	636	1,497
310X11	2078	5,213	623	1,591
310V21	2099	5,427	695	1,350
310X21	2195	4,957	755	1,317
310V22	2384	4,282	715	1,316
310X22	2585	4,339	775	1,333
610	3640	21,472	1092	6,460
610V11	3322	9,767	997	2,965
610X11	3304	9,840	991	2,987
610V21	3206	9,889	1090	2,530
610X21	3296	9,656	1091	2,534
610V22	3676	8,030	1103	2,443
610X22	3684	8,029	1105	2,443
910	5664	27,246	1699	8,195
910V11	3191	11,640	957	3,532
910X11	3211	11,631	963	3,528
910V21	3228	11,568	1059	3,677
910X21	3244	11,595	1075	3,695
910V22	3198	11,593	959	3,516
910X22	3839	12,209	1152	3,703
1210	5022	46,117	1507	13,862
1210V11	4057	14,050	1217	4,254
1210X11	3964	14,280	1189	4,321
1210V21	4012	14,335	1387	3,673
1210X21	4352	14,288	1328	4,083
1210V22	4628	13,223	1388	4,007
1210X22	4688	13,063	1406	3,958

CHAPTER 5

5. CONCLUSIONS AND RECOMMENDATIONS

5.1 Conclusions

The purpose of this research was to determine the effectiveness of external strengthening method using steel braces for existing reinforced concrete buildings that would not disturb/replace the occupants of the building during the construction process. Based on this purpose, external steel braces were used to strengthen existing deficient 3- ,6-, 9-, and 12- story reinforced concrete structures and these structures modelled in SAP2000 [7]. 3-, 6-, 9-, and 12-story reinforced concrete structure models were analyzed using linear and nonlinear analysis methods which are Equivalent Earthquake Load Method based on criteria specified by TBEC (2018) [11], Pushover Analysis Method, and Time History Analysis Method using past earthquakes.

Based on the results, following conclusions may be drawn:

- Deficient 3-, 6-, 9-, and 12-story reinforced concrete structures had problems against earthquake loads based on TS500 (2000) [8] and TBEC (2018) [11]. These buildings were strengthened using external steel braces. Strengthened buildings were analyzed using Equivalent Earthquake Load Method, Pushover Analysis Method, and Time History Analysis Method. The results indicated that all these deficient buildings can be strengthened effectively using external steel braces.
- Periods (T_x and T_y) in both directions of strengthened structures with external steel braces were lower than those of deficient buildings.
- Based on results of TBEC (2018) [11], maximum joint displacements (U_x and U_y) in both directions of strengthened structures using external steel braces were less than maximum joint displacements of deficient structures.
- Based on pushover curves produced using coefficients according to ATC-40 [22], performance point V and Δ were calculated. When deficient and strengthened structures with external steel braces were compared,

- performances of strengthened structures were better than those of the deficient structures.
- Based on time history analysis of past earthquakes, earthquake forces were determined. Results of Equivalent Earthquake Load Method based on TBEC (2018) [11] and time history analysis method using past earthquake data were similar and produced similar performances.
- Based on the results of bracing weight ratio per total area of structures, the most cost-effective strengthening system was the one having one steel frame on each side (V11 steel configuration along building height) of the building.
- Based on Equivalent Earthquake Load Method, pushover analysis method, and time history analysis method using past earthquakes, deficient reinforced concrete structures had a low performance under earthquake loads. Strengthened structures using external steel braces had better performances and structural elements according to load combinations were strong enough against earthquake loads.
- Based on the three methods used in this study, all building models can effectively be strengthened using inverted-V configured external steel bracing system. Buildings up to 9 stories can be effectively strengthened using X configured steel bracing system. No performance point was achieved for 12-story building models for the two cases during the pushover analysis. Other two methods reached as solution.
- Performances based on linear and nonlinear analysis of strengthened structure models using external steel braces had better behavior than those of deficient reinforced concrete structures. These results indicated that strengthening using external steel braces method can successfully be used to enhance the earthquake behavior of deficient buildings.

5.2 Recommendations for Future Research Work

- This study was performed on regular reinforced concrete buildings. The findings of this study may be extended to irregular reinforced concrete structures.

- In this study, steel sections used to strengthen the reinforced concrete buildings were selected to have sufficient member strength. For future research, selection of the structural steel sections can be optimized by program codes.
- Two different configuration of steel braces were used in the research. In the future research, number of different configurations can be increased and compared to each other to evaluate the advantages and disadvantages based configurations.
- No importance was given to the aesthetic view of the strengthening system in this study. In the future studies, the aesthetic concerns may also be added in the design of such bracing systems.

REFERENCES

[1] Disaster and Emergency Management Presidency (AFAD), "Earthquake Catalog of Turkey", Internet: https://deprem.afad.gov.tr/depremkatalogu [1-Feb-2022].

[2] Disaster and Emergency Management Presidency (AFAD), "Earthquake Map of Turkey" Internet: https://deprem.afad.gov.tr/deprem-tehlike-haritasi [1-Feb-2022].

[3] I. Ileri, "Can an Earthquake say That It is Coming?" *Journal of Blue Planet Popular Geoscience*, vol. 13, pp. 19-24, 2016: (in Turkish).

[4] Republic of Turkey Ministry of Environment, Urbanization and Climate Change. "Urban Transformation Report" 2015: (in Turkish)

[5] Republic of Turkey Ministry of Environment, Urbanization and Climate Change, "Turkish Earthquake Code 2007" Ankara, Turkey, 2007.

[6] Strengthening of Existing Reinforced Concrete Parking Garage Using External Steel Braces, Internet: https://www.wikiwand.com/en/Seismic_retrofit [15-Dec-2021]

[7] CSI America, "SAP2000 v19 | STRUCTURAL ANALYSIS AND DESIGN." Internet: https://www.csiamerica.com/products/sap2000. [15-Dec-2021].

[8] Turkish Standards Institute, "TS500: Requirements for design and construction of reinforced concrete structures." Ankara, Turkey, 2000.

[9] American Institute of Steel Construction, "AISC 360-10, Specification for Structural Steel Buildings" Chicago, Illinois, USA, 2010.

[10] Turkish Standards Institute, "TS498: Design Loads for Buildings" Ankara, Turkey, 1987.

[11] Disaster and Emergency Management Presidency (AFAD), “TBDY 2018: Turkish Building Earthquake Code” Ankara, Turkey, 2018.

[12] A. Balagopal, “Design Proposal and Analysis of Curved Brace System to Reduce Drift in Moment Frame Structures” M.S Thesis, Faculty of the USC School of Architecture, University of Southern California, California, 2012.

[13] C. Haikal and M. Muca, “Seismic Analysis and Retrofitting of Existing Multi-Storey Building in Stockholm” M.S Thesis, School of Architecture and the Built Environment Department of Concrete Structures, KTH Royal Institute of Technology, Stockholm,2018.

[14] MIDAS Structure, “Midas Gen | MIDAS Engineering Software” Internet: http://en.midasuser.com, [15-Dec-2021].

[15] H. Abou-Elfath and A. Ghobarah, “Behaviour of reinforced concrete frames rehabilitated with concentric steel bracing” *Canadian Journal of Civil Engineering*, 2000.

[16] M. Agar, “Strengthening of Reinforced Concrete Frames by Using Steel Bracings” M.S Thesis, Civil Engineering Department, Middle East Technical University, Ankara, 2008.

[17] C. Balkaya, “Invention: Seismic Retrofitting by Exterior Steel Brace Structural Building Jacketing System” presented at 5th International Symposium on Innovative Technologies in Engineering and Science, Baku, Azerbaijan, 2017.

[18] Tunc G., Mertol H.C., and Akıs T., *Ege Denizi Deprem Raporu (30.10.2020)* Hiperlink Yayınları, 2021, 116 p.

[19] American Society for Testing and Materials, “American Society for Testing and Materials ASTM A992.” West Conshohocken, PA, 2009.

[20] Turkish Standards Institute, “TS ISO9194: Bases for Design of Structures; Actions due to the Self-Weight of Structures, Non-Structural Elements and Stored Materials; Density” Ankara,Turkey, 1997.

[21] European Standards “EN 1993, Eurocode 3: Design of Steel Structures” Italy, 2005.

[22] Applied Technology Council, “ATC-40. Seismic evaluation and retrofit of concrete buildings, vols. 1 and 2” California, 1996.

[23] American Society of Civil Engineering ASCE, “Seismic evaluation and retrofit of existing buildings,” 2014.

[24] M.G. Kalibhat and Y.M Kumar and K. Kamath. and S.K Prasad, “Seismic performance of R. C. frames with vertical stiffness irregularity from pushover analysis” *IOSR Journal of Mechanical and Civil Engineering* pp. 61-66, 2014.

[25] Pacific Earthquake Engineering Research Center, “PEER Ground Motion Database.” Internet: https://ngawest2.berkeley.edu/ [10-May-2021].

[26] CSI America, “SAP2000 v22 | STRUCTURAL ANALYSIS AND DESIGN.” Internet: https://www.csiamerica.com/products/sap2000 [15-Dec-2021].

APPENDICIES

A. DEFINED MATERIAL PROPERTIES AND TYPICAL RESULTS FOR DESIGN

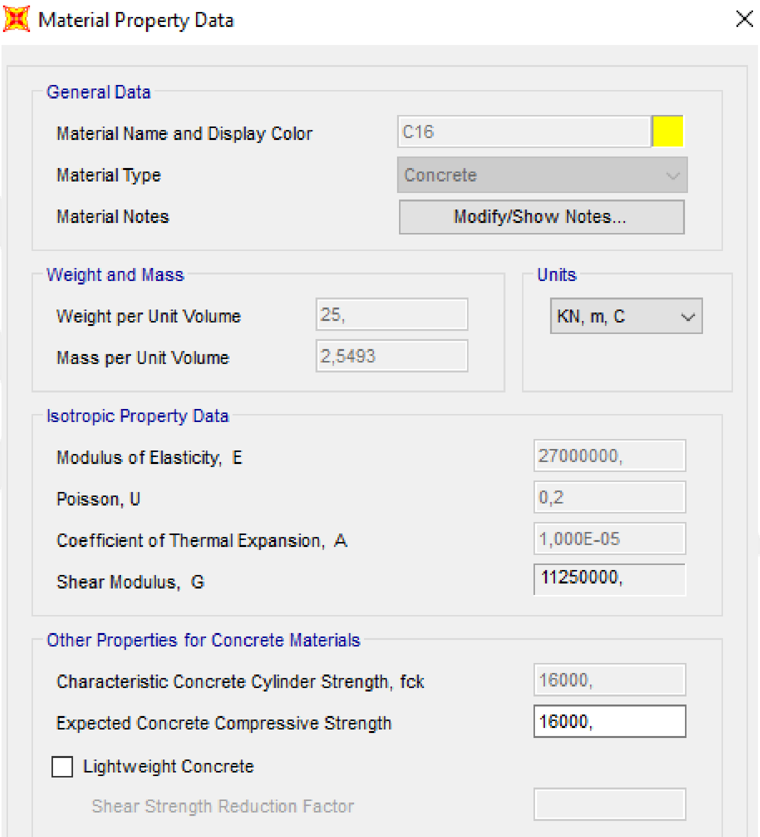

Figure A.1 Defined Properties for Concrete

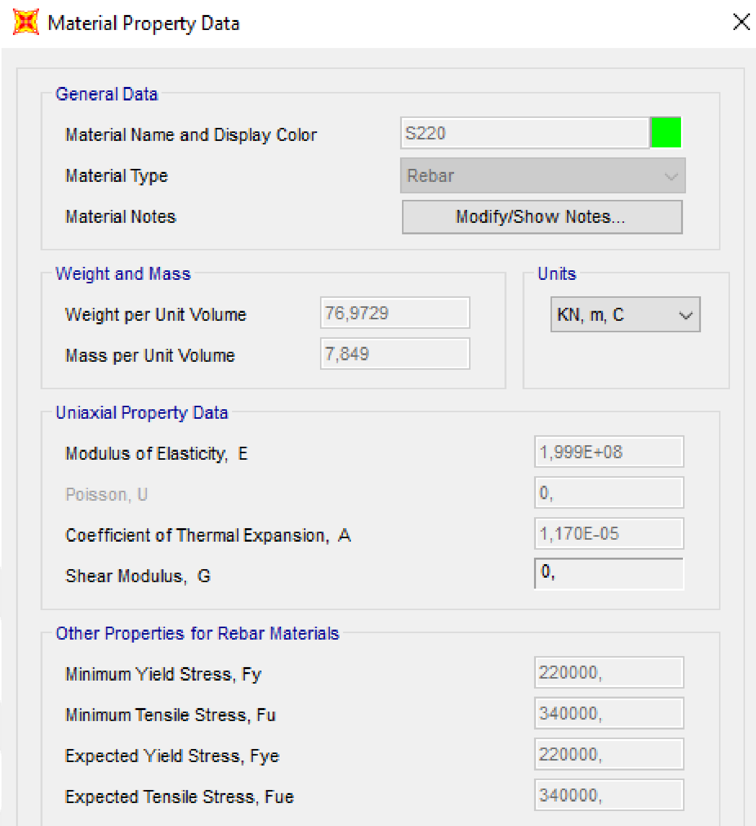

Figure A.2 Defined Properties for S220 Steel Reinforcement

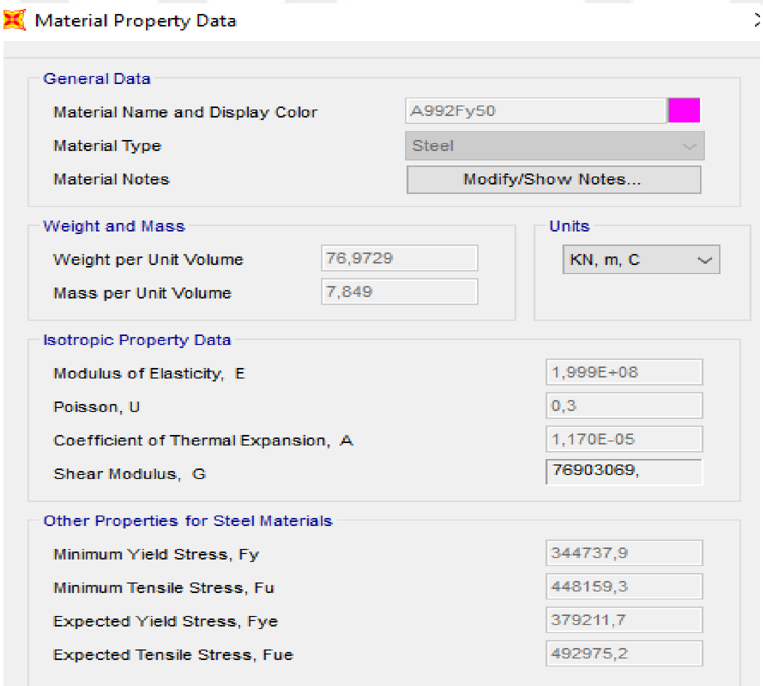

Figure A.3 Defined Properties for Structural Steel Sections

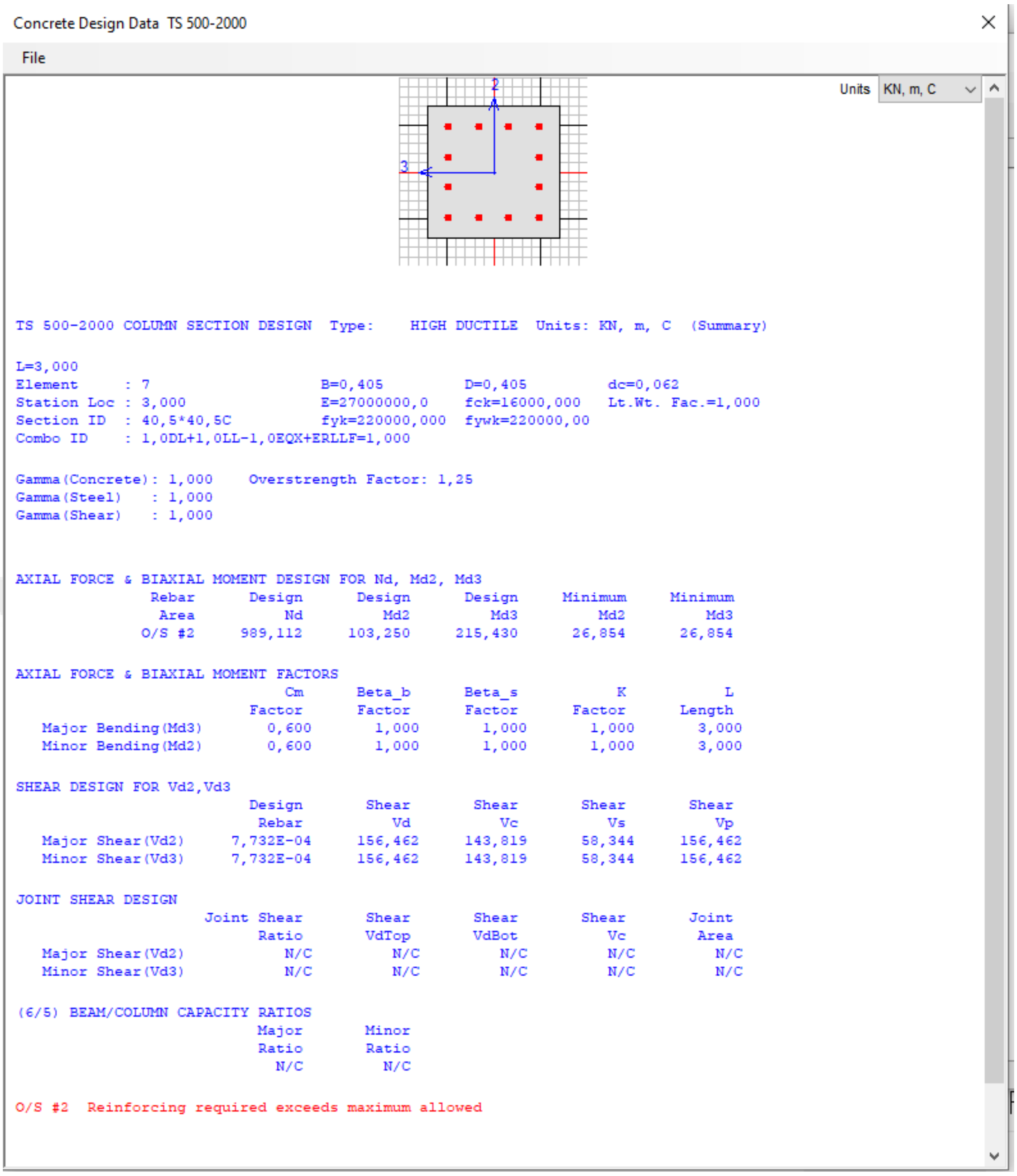

```
Concrete Design Data  TS 500-2000
File                                                                  Units  KN, m, C

TS 500-2000 COLUMN SECTION DESIGN  Type:    HIGH DUCTILE  Units: KN, m, C  (Summary)

L=3,000
Element      : 7                 B=0,405         D=0,405         dc=0,062
Station Loc  : 3,000             E=27000000,0    fck=16000,000   Lt.Wt. Fac.=1,000
Section ID   : 40,5*40,5C        fyk=220000,000  fywk=220000,00
Combo ID     : 1,0DL+1,0LL-1,0EQX+ERLLF=1,000

Gamma(Concrete): 1,000    Overstrength Factor: 1,25
Gamma(Steel)   : 1,000
Gamma(Shear)   : 1,000


AXIAL FORCE & BIAXIAL MOMENT DESIGN FOR Nd, Md2, Md3
               Rebar      Design      Design      Design     Minimum     Minimum
                Area          Nd         Md2         Md3         Md2         Md3
              O/S #2     989,112     103,250     215,430      26,854      26,854

AXIAL FORCE & BIAXIAL MOMENT FACTORS
                              Cm      Beta_b      Beta_s           K           L
                          Factor      Factor      Factor      Factor      Length
   Major Bending(Md3)      0,600       1,000       1,000       1,000       3,000
   Minor Bending(Md2)      0,600       1,000       1,000       1,000       3,000

SHEAR DESIGN FOR Vd2,Vd3
                          Design       Shear       Shear       Shear       Shear
                           Rebar          Vd          Vc          Vs          Vp
   Major Shear(Vd2)    7,732E-04     156,462     143,819      58,344     156,462
   Minor Shear(Vd3)    7,732E-04     156,462     143,819      58,344     156,462

JOINT SHEAR DESIGN
                     Joint Shear       Shear       Shear       Shear       Joint
                           Ratio       VdTop       VdBot          Vc        Area
   Major Shear(Vd2)          N/C         N/C         N/C         N/C         N/C
   Minor Shear(Vd3)          N/C         N/C         N/C         N/C         N/C

(6/5) BEAM/COLUMN CAPACITY RATIOS
                           Major       Minor
                           Ratio       Ratio
                             N/C         N/C

O/S #2  Reinforcing required exceeds maximum allowed
```

Figure A.4 Typical Results of Basement Column Design of 3-Story Deficient Building

Concrete Design Data TS 500-2000

File

Units KN, m, C

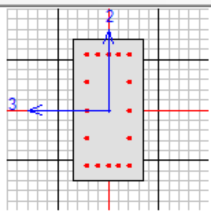


```
TS 500-2000 COLUMN SECTION DESIGN  Type:   HIGH DUCTILE  Units: KN, m, C  (Summary)

L=6,000
Element      : 139                 B=0,300          D=0,600         dc=0,062
Station Loc  : 6,000               E=27000000,0     fck=16000,000   Lt.Wt. Fac.=1,000
Section ID   : 30*60B              fyk=220000,000   fywk=220000,00
Combo ID     : 1,0DL+1,0LL+1,0EQX-ERLLF=1,000

Gamma(Concrete): 1,000    Overstrength Factor: 1,25
Gamma(Steel)   : 1,000
Gamma(Shear)   : 1,000


AXIAL FORCE & BIAXIAL MOMENT DESIGN FOR Nd, Md2, Md3
               Rebar      Design      Design      Design      Minimum     Minimum
                Area          Nd         Md2         Md3          Md2         Md3
              O/S #2       7,389      -0,254    -402,235        0,177       0,244

AXIAL FORCE & BIAXIAL MOMENT FACTORS
                              Cm      Beta_b      Beta_s            K           L
                          Factor      Factor      Factor       Factor      Length
   Major Bending(Md3)      1,000       1,001       1,000        1,000       6,000
   Minor Bending(Md2)      1,000       1,005       1,000        1,000       6,000

SHEAR DESIGN FOR Vd2,Vd3
                          Design       Shear       Shear        Shear       Shear
                           Rebar          Vd          Vc           Vs          Vp
   Major Shear(Vd2)        0,001     153,452       0,000      153,452     153,452
   Minor Shear(Vd3)        0,001      62,011       0,000       59,976      62,011

JOINT SHEAR DESIGN
                     Joint Shear       Shear       Shear        Shear       Joint
                           Ratio       VdTop       VdBot           Vc        Area
   Major Shear(Vd2)          N/C         N/C         N/C          N/C         N/C
   Minor Shear(Vd3)          N/C         N/C         N/C          N/C         N/C

(6/5) BEAM/COLUMN CAPACITY RATIOS
                           Major       Minor
                           Ratio       Ratio
                             N/C         N/C

O/S #2  Reinforcing required exceeds maximum allowed
```

Figure A.5 Typical Results of 1st Story Beam Design of 3-Story Deficient Building

Concrete Design Data TS 500-2000

File

Units KN, m, C

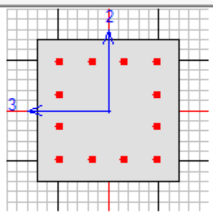


```
TS 500-2000 COLUMN SECTION DESIGN  Type:    HIGH DUCTILE  Units: KN, m, C  (Summary)

L=3,000
Element      : 7                   B=0,405         D=0,405         dc=0,062
Station Loc  : 3,000               E=27000000,0    fck=16000,000   Lt.Wt. Fac.=1,000
Section ID   : 40,5*40,5C          fyk=220000,000  fywk=220000,00
Combo ID     : 1,0DL+1,0LL-1,0EQX-ERLLF=1,000

Gamma(Concrete): 1,500    Overstrength Factor: 1,25
Gamma(Steel)   : 1,150
Gamma(Shear)   : 1,250


AXIAL FORCE & BIAXIAL MOMENT DESIGN FOR Nd, Md2, Md3
               Rebar      Design      Design      Design     Minimum     Minimum
                Area          Nd         Md2         Md3         Md2         Md3
               0,002     470,645      11,203      82,311      12,778      12,778

AXIAL FORCE & BIAXIAL MOMENT FACTORS
                              Cm      Beta_b      Beta_s           K           L
                          Factor      Factor      Factor      Factor      Length
   Major Bending(Md3)      0,600       1,000       1,000       1,000       3,000
   Minor Bending(Md2)      0,600       1,000       1,000       1,000       3,000

SHEAR DESIGN FOR Vd2,Vd3
                          Design       Shear       Shear       Shear       Shear
                           Rebar          Vd          Vc          Vs          Vp
   Major Shear(Vd2)    5,928E-04      89,208      80,962      38,896      89,208
   Minor Shear(Vd3)    5,928E-04      89,208      80,962      38,896      89,208

JOINT SHEAR DESIGN
                     Joint Shear       Shear       Shear       Shear       Joint
                           Ratio       VdTop       VdBot          Vc        Area
   Major Shear(Vd2)          N/C         N/C         N/C         N/C         N/C
   Minor Shear(Vd3)          N/C         N/C         N/C         N/C         N/C

(6/5) BEAM/COLUMN CAPACITY RATIOS
                           Major       Minor
                           Ratio       Ratio
                             N/C         N/C


Notes:
   N/A: Not Applicable
   N/C: Not Calculated
```

Figure A.6 Typical Results of Basement Column Design of 3-Story Strengthened (V11) Building

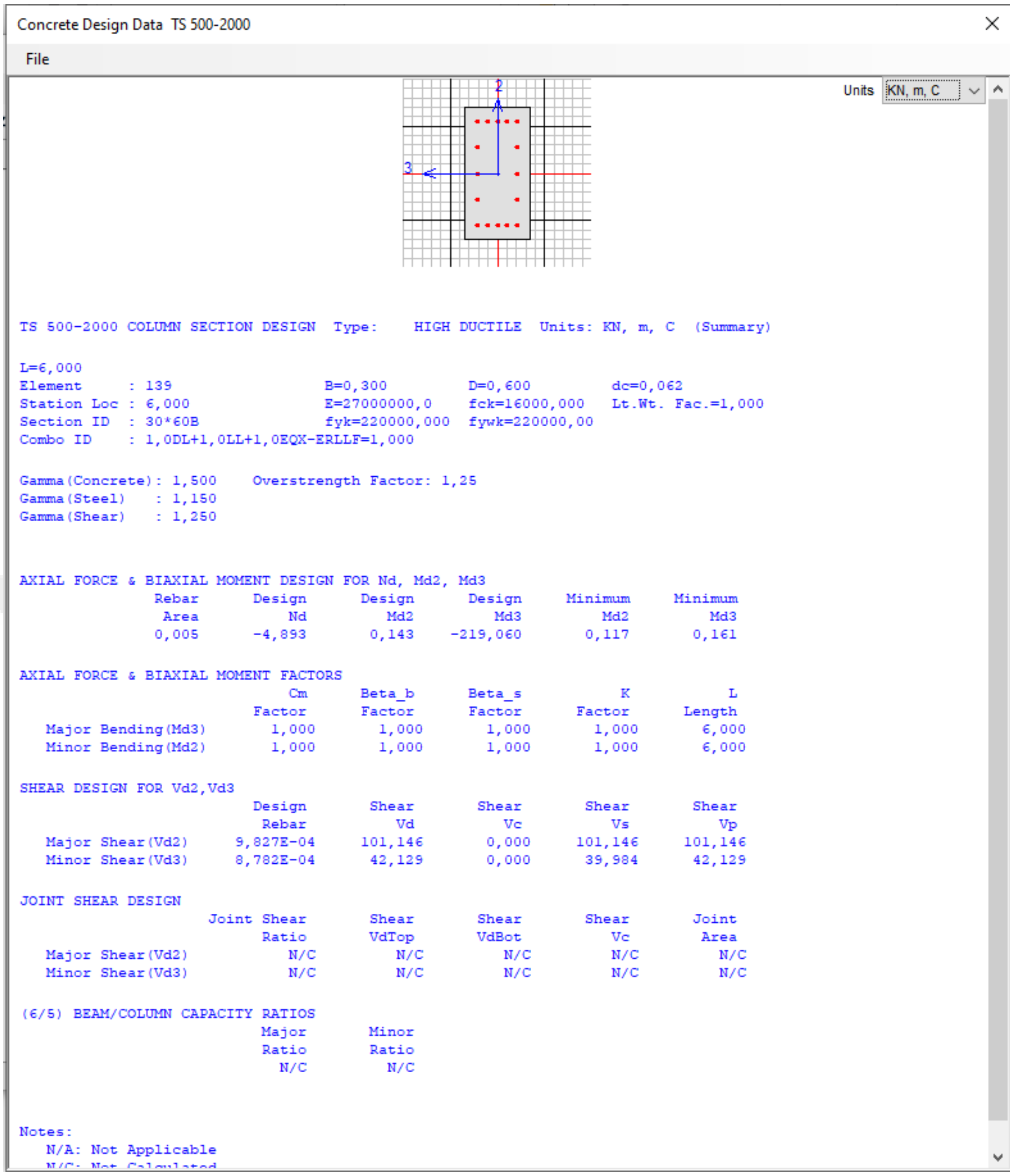

```
Concrete Design Data  TS 500-2000
File
Units  KN, m, C

TS 500-2000 COLUMN SECTION DESIGN  Type:    HIGH DUCTILE  Units: KN, m, C  (Summary)

L=6,000
Element      : 139                B=0,300          D=0,600          dc=0,062
Station Loc  : 6,000              E=27000000,0     fck=16000,000    Lt.Wt. Fac.=1,000
Section ID   : 30*60B             fyk=220000,000   fywk=220000,00
Combo ID     : 1,0DL+1,0LL+1,0EQX-ERLLF=1,000

Gamma(Concrete): 1,500    Overstrength Factor: 1,25
Gamma(Steel)   : 1,150
Gamma(Shear)   : 1,250


AXIAL FORCE & BIAXIAL MOMENT DESIGN FOR Nd, Md2, Md3
               Rebar      Design      Design      Design     Minimum     Minimum
                Area          Nd         Md2         Md3         Md2         Md3
               0,005      -4,893       0,143    -219,060       0,117       0,161

AXIAL FORCE & BIAXIAL MOMENT FACTORS
                              Cm      Beta_b      Beta_s           K           L
                          Factor      Factor      Factor      Factor      Length
   Major Bending(Md3)      1,000       1,000       1,000       1,000       6,000
   Minor Bending(Md2)      1,000       1,000       1,000       1,000       6,000

SHEAR DESIGN FOR Vd2,Vd3
                          Design       Shear       Shear       Shear       Shear
                           Rebar          Vd          Vc          Vs          Vp
   Major Shear(Vd2)    9,827E-04     101,146       0,000     101,146     101,146
   Minor Shear(Vd3)    8,782E-04      42,129       0,000      39,984      42,129

JOINT SHEAR DESIGN
                    Joint Shear       Shear       Shear       Shear       Joint
                           Ratio       VdTop       VdBot          Vc        Area
   Major Shear(Vd2)          N/C         N/C         N/C         N/C         N/C
   Minor Shear(Vd3)          N/C         N/C         N/C         N/C         N/C

(6/5) BEAM/COLUMN CAPACITY RATIOS
                           Major       Minor
                           Ratio       Ratio
                             N/C         N/C


Notes:
   N/A: Not Applicable
```

Figure A.7 Typical Results of 1st Story Beam Design of 3-Story Strengthened (V11) Building

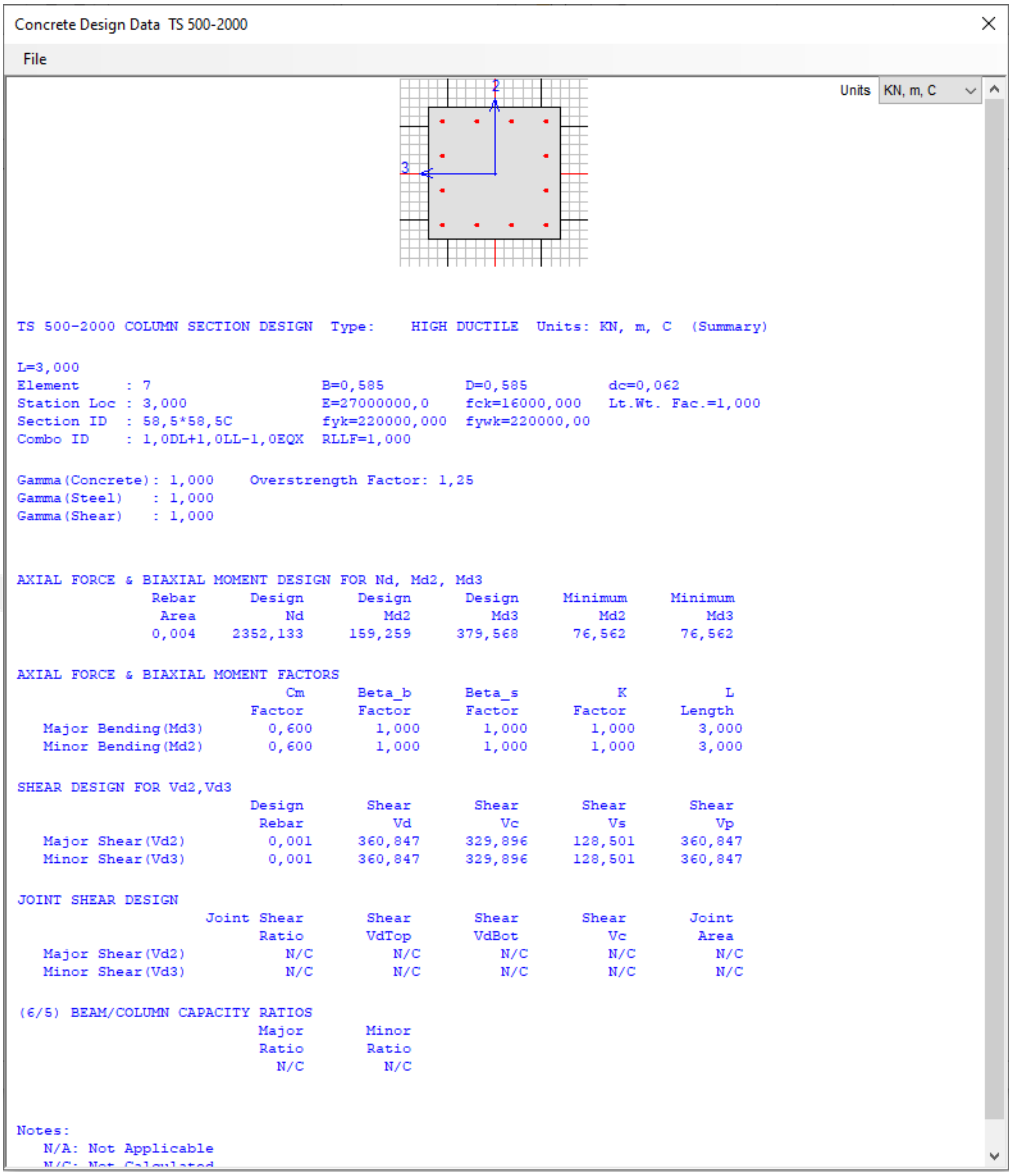

Figure A.8 Typical Results of Basement Column Design of 6-Story Deficient Building

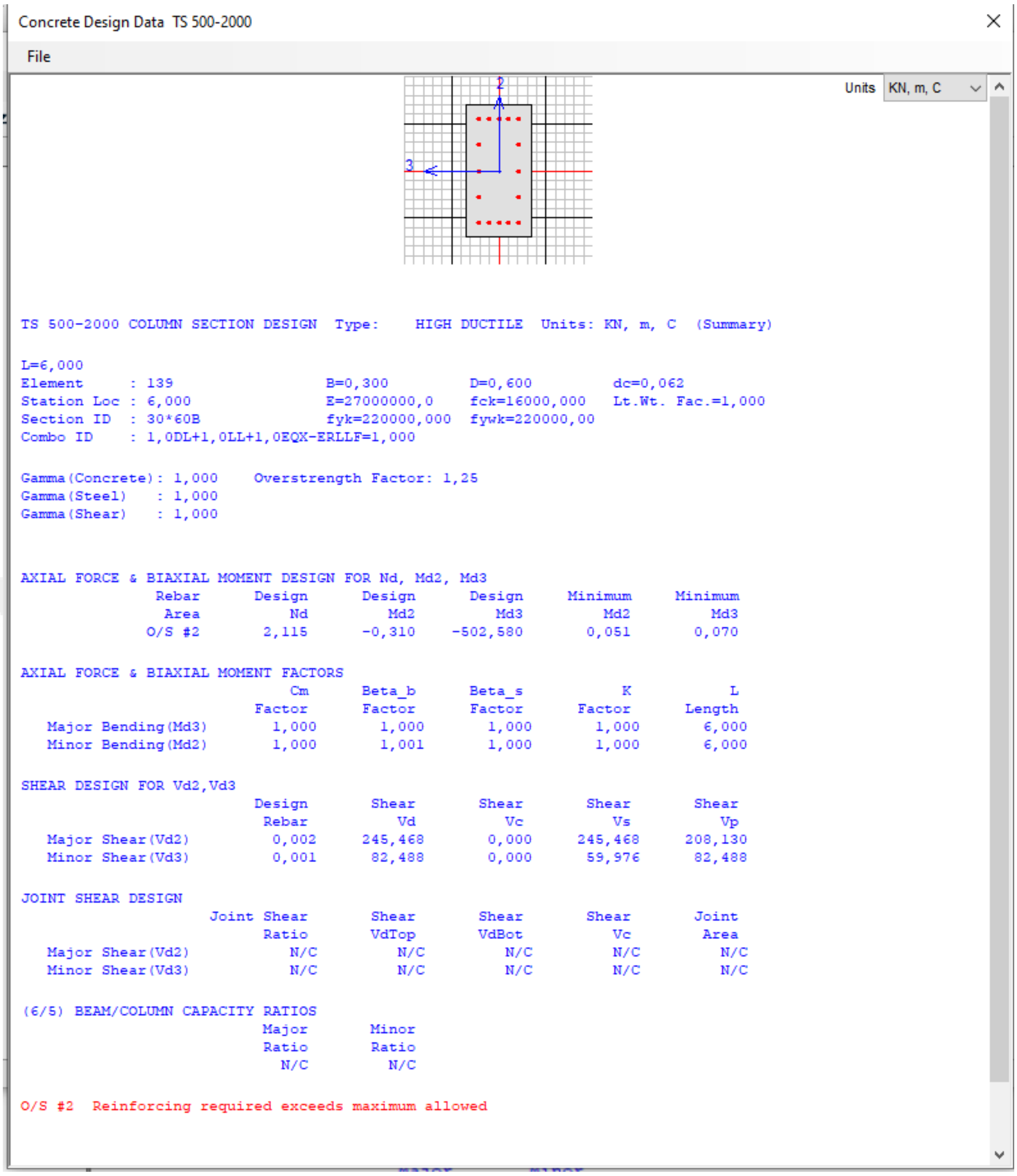

TS 500-2000 COLUMN SECTION DESIGN Type: HIGH DUCTILE Units: KN, m, C (Summary)

L=6,000
Element : 139 B=0,300 D=0,600 dc=0,062
Station Loc : 6,000 E=27000000,0 fck=16000,000 Lt.Wt. Fac.=1,000
Section ID : 30*60B fyk=220000,000 fywk=220000,00
Combo ID : 1,0DL+1,0LL+1,0EQX-ERLLF=1,000

Gamma(Concrete): 1,000 Overstrength Factor: 1,25
Gamma(Steel) : 1,000
Gamma(Shear) : 1,000

AXIAL FORCE & BIAXIAL MOMENT DESIGN FOR Nd, Md2, Md3

Rebar Area	Design Nd	Design Md2	Design Md3	Minimum Md2	Minimum Md3
O/S #2	2,115	-0,310	-502,580	0,051	0,070

AXIAL FORCE & BIAXIAL MOMENT FACTORS

	Cm Factor	Beta_b Factor	Beta_s Factor	K Factor	L Length
Major Bending(Md3)	1,000	1,000	1,000	1,000	6,000
Minor Bending(Md2)	1,000	1,001	1,000	1,000	6,000

SHEAR DESIGN FOR Vd2,Vd3

	Design Rebar	Shear Vd	Shear Vc	Shear Vs	Shear Vp
Major Shear(Vd2)	0,002	245,468	0,000	245,468	208,130
Minor Shear(Vd3)	0,001	82,488	0,000	59,976	82,488

JOINT SHEAR DESIGN

	Joint Shear Ratio	Shear VdTop	Shear VdBot	Shear Vc	Joint Area
Major Shear(Vd2)	N/C	N/C	N/C	N/C	N/C
Minor Shear(Vd3)	N/C	N/C	N/C	N/C	N/C

(6/5) BEAM/COLUMN CAPACITY RATIOS

Major Ratio	Minor Ratio
N/C	N/C

O/S #2 Reinforcing required exceeds maximum allowed

Figure A.9 Typical Results of 1st Story Beam Design of 6-Story Deficient Building

Concrete Design Data TS 500-2000

File

Units KN, m, C

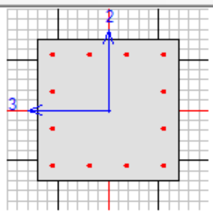


```
TS 500-2000 COLUMN SECTION DESIGN  Type:    HIGH DUCTILE  Units: KN, m, C  (Summary)

L=3,000
Element      : 7                      B=0,585         D=0,585         dc=0,062
Station Loc  : 3,000                  E=27000000,0    fck=16000,000   Lt.Wt. Fac.=1,000
Section ID   : 58,5*58,5C             fyk=220000,000  fywk=220000,00
Combo ID     : 1,0DL+1,0LL-1,0EQY-ERLLF=1,000

Gamma(Concrete): 1,500    Overstrength Factor: 1,25
Gamma(Steel)   : 1,150
Gamma(Shear)   : 1,250


AXIAL FORCE & BIAXIAL MOMENT DESIGN FOR Nd, Md2, Md3
               Rebar      Design      Design      Design     Minimum     Minimum
                Area          Nd         Md2         Md3         Md2         Md3
               0,003    1558,801     106,058      81,701      50,739      50,739

AXIAL FORCE & BIAXIAL MOMENT FACTORS
                              Cm      Beta_b      Beta_s           K           L
                          Factor      Factor      Factor      Factor      Length
   Major Bending(Md3)      0,600       1,000       1,000       1,000       3,000
   Minor Bending(Md2)      0,600       1,000       1,000       1,000       3,000

SHEAR DESIGN FOR Vd2,Vd3
                          Design       Shear       Shear       Shear       Shear
                           Rebar          Vd          Vc          Vs          Vp
   Major Shear(Vd2)        0,001     318,144     195,835     122,309     318,144
   Minor Shear(Vd3)        0,001     318,144     195,835     122,309     318,144

JOINT SHEAR DESIGN
                     Joint Shear       Shear       Shear       Shear       Joint
                           Ratio       VdTop       VdBot          Vc        Area
   Major Shear(Vd2)          N/C         N/C         N/C         N/C         N/C
   Minor Shear(Vd3)          N/C         N/C         N/C         N/C         N/C

(6/5) BEAM/COLUMN CAPACITY RATIOS
                           Major       Minor
                           Ratio       Ratio
                             N/C         N/C


Notes:
   N/A: Not Applicable
   N/C: Not Calculated
```

Figure A.10 Typical Results of Basement Column Design of 6-Story Strengthened (V11) Building

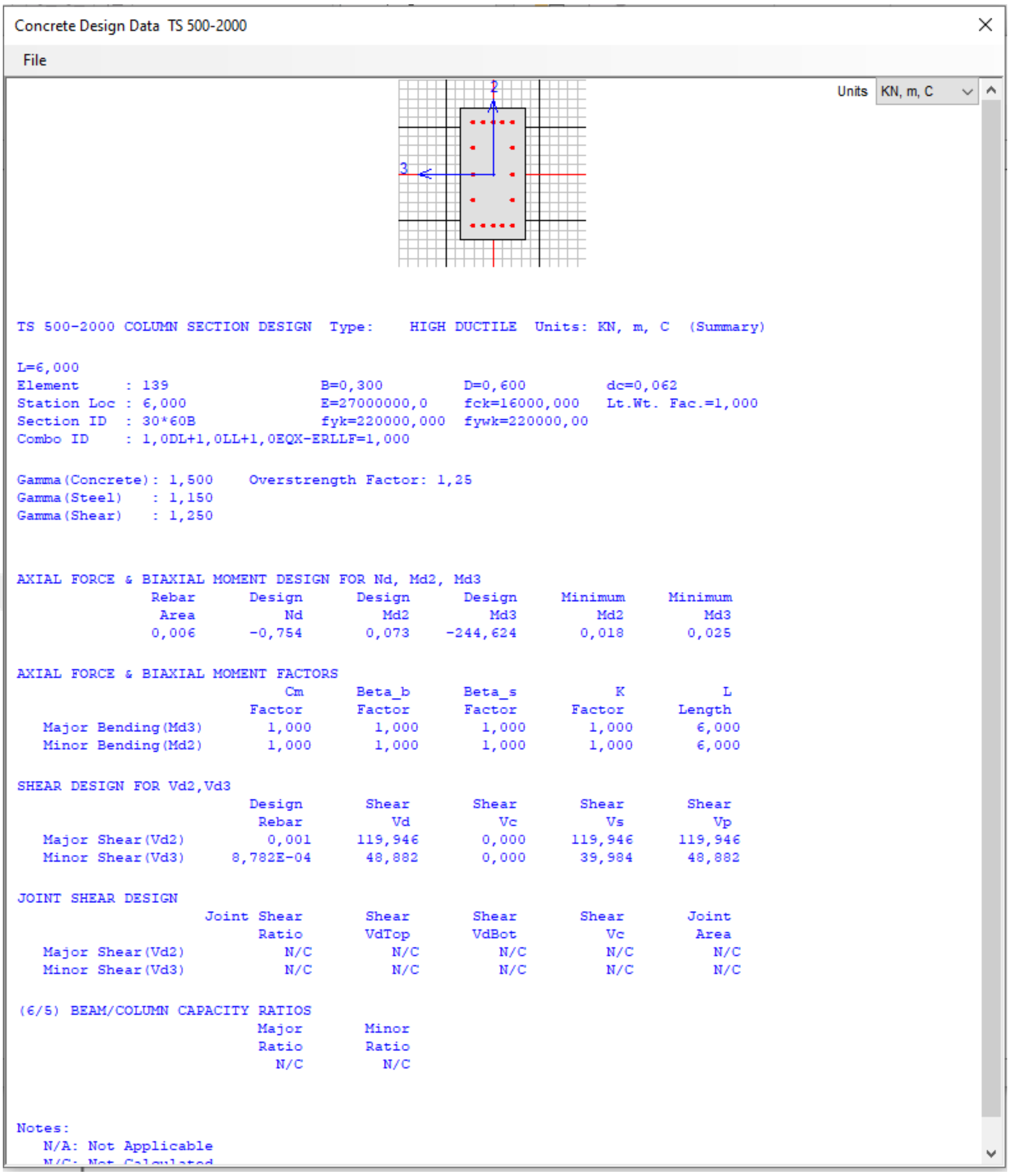

Concrete Design Data TS 500-2000

File

Units KN, m, C

TS 500-2000 COLUMN SECTION DESIGN Type: HIGH DUCTILE Units: KN, m, C (Summary)

L=6,000

Element : 139	B=0,300	D=0,600	dc=0,062
Station Loc : 6,000	E=27000000,0	fck=16000,000	Lt.Wt. Fac.=1,000
Section ID : 30*60B	fyk=220000,000	fywk=220000,00	
Combo ID : 1,0DL+1,0LL+1,0EQX-ERLLF=1,000			

Gamma(Concrete): 1,500 Overstrength Factor: 1,25
Gamma(Steel) : 1,150
Gamma(Shear) : 1,250

AXIAL FORCE & BIAXIAL MOMENT DESIGN FOR Nd, Md2, Md3

Rebar Area	Design Nd	Design Md2	Design Md3	Minimum Md2	Minimum Md3
0,006	-0,754	0,073	-244,624	0,018	0,025

AXIAL FORCE & BIAXIAL MOMENT FACTORS

	Cm Factor	Beta_b Factor	Beta_s Factor	K Factor	L Length
Major Bending(Md3)	1,000	1,000	1,000	1,000	6,000
Minor Bending(Md2)	1,000	1,000	1,000	1,000	6,000

SHEAR DESIGN FOR Vd2,Vd3

	Design Rebar	Shear Vd	Shear Vc	Shear Vs	Shear Vp
Major Shear(Vd2)	0,001	119,946	0,000	119,946	119,946
Minor Shear(Vd3)	8,782E-04	48,882	0,000	39,984	48,882

JOINT SHEAR DESIGN

	Joint Shear Ratio	Shear VdTop	Shear VdBot	Shear Vc	Joint Area
Major Shear(Vd2)	N/C	N/C	N/C	N/C	N/C
Minor Shear(Vd3)	N/C	N/C	N/C	N/C	N/C

(6/5) BEAM/COLUMN CAPACITY RATIOS

Major Ratio	Minor Ratio
N/C	N/C

Notes:
N/A: Not Applicable

Figure A.11 Typical Results of 1st Story Beam Design of 6-Story Strengthened (V11) Building

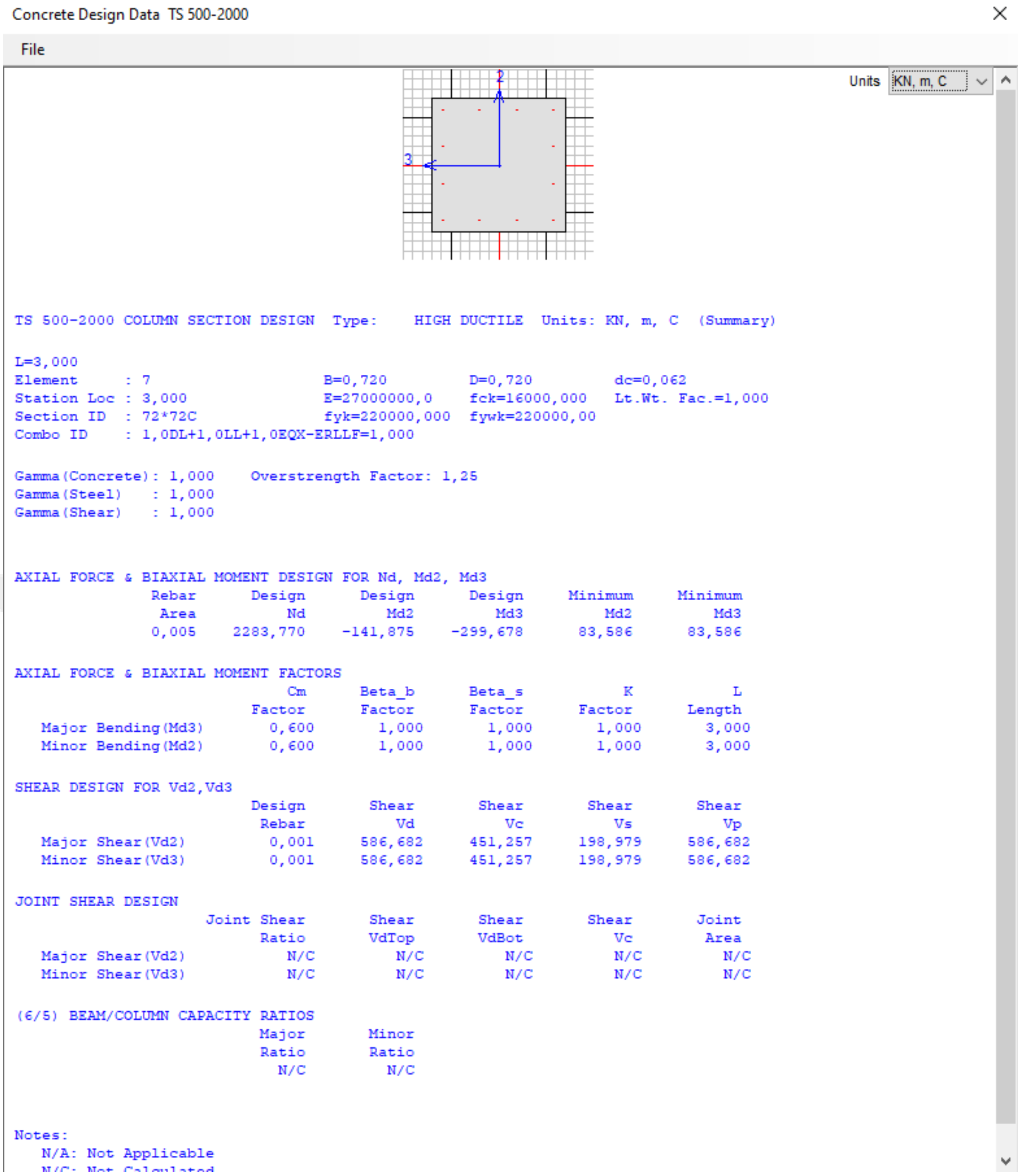


```
TS 500-2000 COLUMN SECTION DESIGN  Type:    HIGH DUCTILE  Units: KN, m, C  (Summary)

L=3,000
Element      : 7                    B=0,720          D=0,720          dc=0,062
Station Loc  : 3,000                E=27000000,0     fck=16000,000    Lt.Wt. Fac.=1,000
Section ID   : 72*72C               fyk=220000,000   fywk=220000,00
Combo ID     : 1,0DL+1,0LL+1,0EQX-ERLLF=1,000

Gamma(Concrete): 1,000    Overstrength Factor: 1,25
Gamma(Steel)   : 1,000
Gamma(Shear)   : 1,000


AXIAL FORCE & BIAXIAL MOMENT DESIGN FOR Nd, Md2, Md3
               Rebar      Design      Design      Design     Minimum     Minimum
                Area          Nd         Md2         Md3         Md2         Md3
               0,005    2283,770    -141,875    -299,678      83,586      83,586

AXIAL FORCE & BIAXIAL MOMENT FACTORS
                              Cm      Beta_b      Beta_s           K           L
                          Factor      Factor      Factor      Factor      Length
   Major Bending(Md3)      0,600       1,000       1,000       1,000       3,000
   Minor Bending(Md2)      0,600       1,000       1,000       1,000       3,000

SHEAR DESIGN FOR Vd2,Vd3
                          Design       Shear       Shear       Shear       Shear
                           Rebar          Vd          Vc          Vs          Vp
   Major Shear(Vd2)        0,001     586,682     451,257     198,979     586,682
   Minor Shear(Vd3)        0,001     586,682     451,257     198,979     586,682

JOINT SHEAR DESIGN
                     Joint Shear       Shear       Shear       Shear       Joint
                           Ratio      VdTop       VdBot          Vc        Area
   Major Shear(Vd2)          N/C         N/C         N/C         N/C         N/C
   Minor Shear(Vd3)          N/C         N/C         N/C         N/C         N/C

(6/5) BEAM/COLUMN CAPACITY RATIOS
                           Major       Minor
                           Ratio       Ratio
                             N/C         N/C


Notes:
   N/A: Not Applicable
   N/C: Not Calculated
```

Figure A.12 Typical Results of Basement Column Design of 9-Story Deficient Building

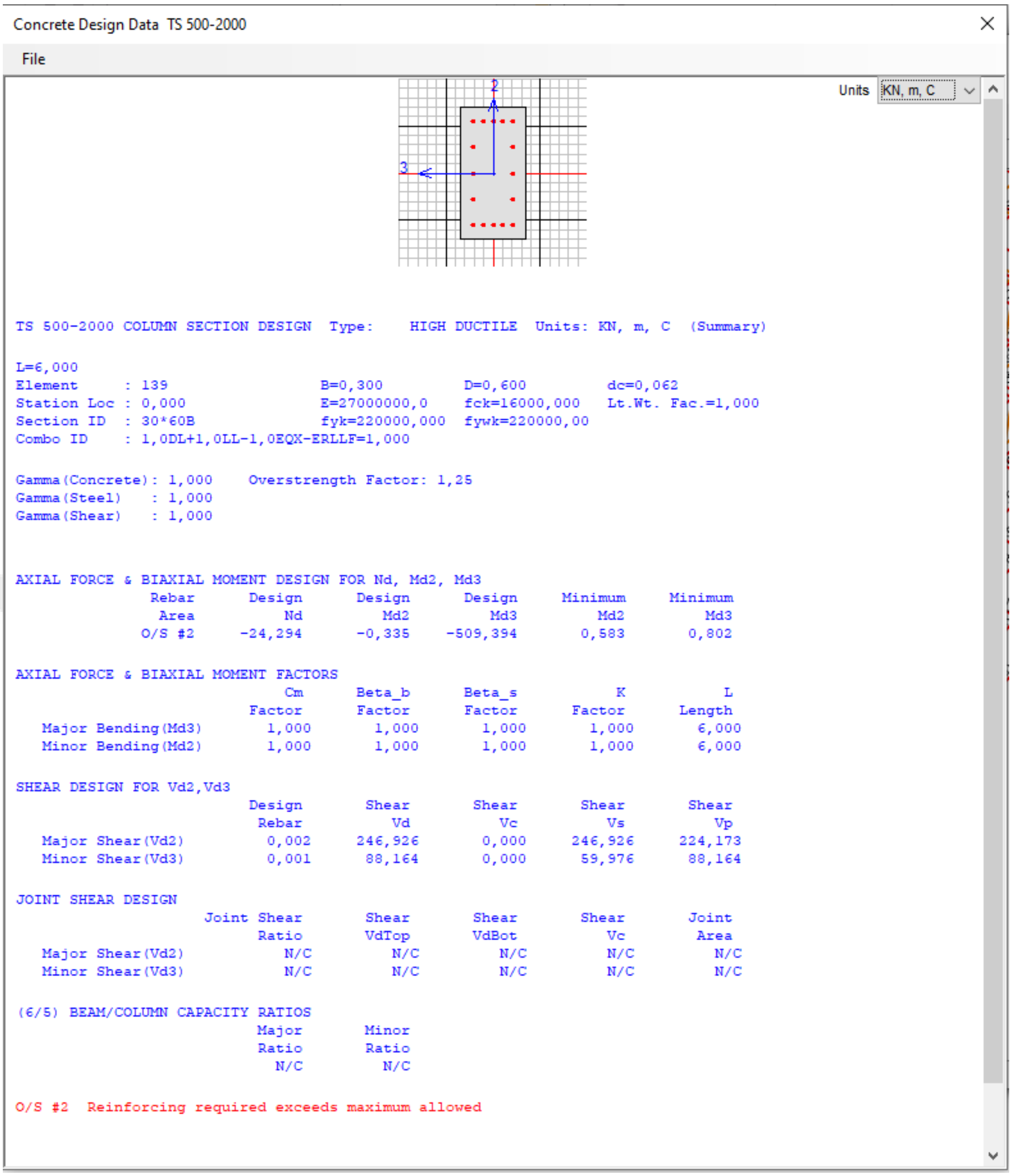

```
Concrete Design Data  TS 500-2000
File                                                        Units  KN, m, C

TS 500-2000 COLUMN SECTION DESIGN  Type:   HIGH DUCTILE  Units: KN, m, C  (Summary)

L=6,000
Element      : 139                B=0,300        D=0,600        dc=0,062
Station Loc  : 0,000              E=27000000,0   fck=16000,000  Lt.Wt. Fac.=1,000
Section ID   : 30*60B             fyk=220000,000 fywk=220000,00
Combo ID     : 1,0DL+1,0LL-1,0EQX-ERLLF=1,000

Gamma(Concrete): 1,000    Overstrength Factor: 1,25
Gamma(Steel)   : 1,000
Gamma(Shear)   : 1,000


AXIAL FORCE & BIAXIAL MOMENT DESIGN FOR Nd, Md2, Md3
               Rebar      Design      Design      Design      Minimum     Minimum
                Area          Nd         Md2         Md3         Md2         Md3
              O/S #2     -24,294      -0,335    -509,394       0,583       0,802

AXIAL FORCE & BIAXIAL MOMENT FACTORS
                            Cm      Beta_b      Beta_s           K           L
                        Factor      Factor      Factor      Factor      Length
   Major Bending(Md3)    1,000       1,000       1,000       1,000       6,000
   Minor Bending(Md2)    1,000       1,000       1,000       1,000       6,000

SHEAR DESIGN FOR Vd2,Vd3
                        Design       Shear       Shear       Shear       Shear
                         Rebar          Vd          Vc          Vs          Vp
   Major Shear(Vd2)      0,002     246,926       0,000     246,926     224,173
   Minor Shear(Vd3)      0,001      88,164       0,000      59,976      88,164

JOINT SHEAR DESIGN
                   Joint Shear       Shear       Shear       Shear       Joint
                         Ratio       VdTop       VdBot          Vc        Area
   Major Shear(Vd2)        N/C         N/C         N/C         N/C         N/C
   Minor Shear(Vd3)        N/C         N/C         N/C         N/C         N/C

(6/5) BEAM/COLUMN CAPACITY RATIOS
                         Major       Minor
                         Ratio       Ratio
                           N/C         N/C

O/S #2  Reinforcing required exceeds maximum allowed
```

Figure A.13 Typical Results of 1st Story Beam Design of 9-Story Deficient Building

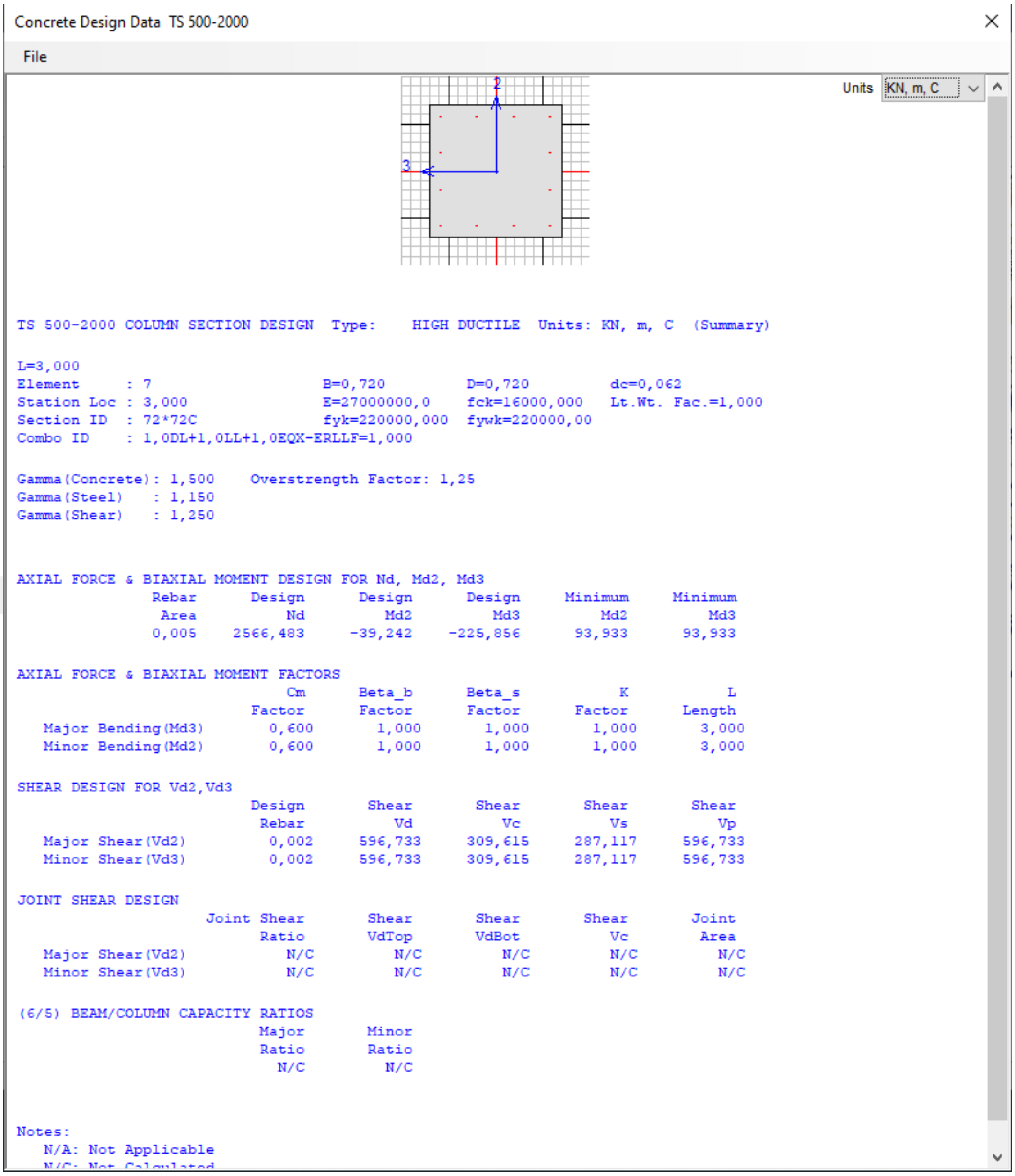

Figure A.14 Typical Results of Basement Column Design of 9-Story Strengthened (V11) Building

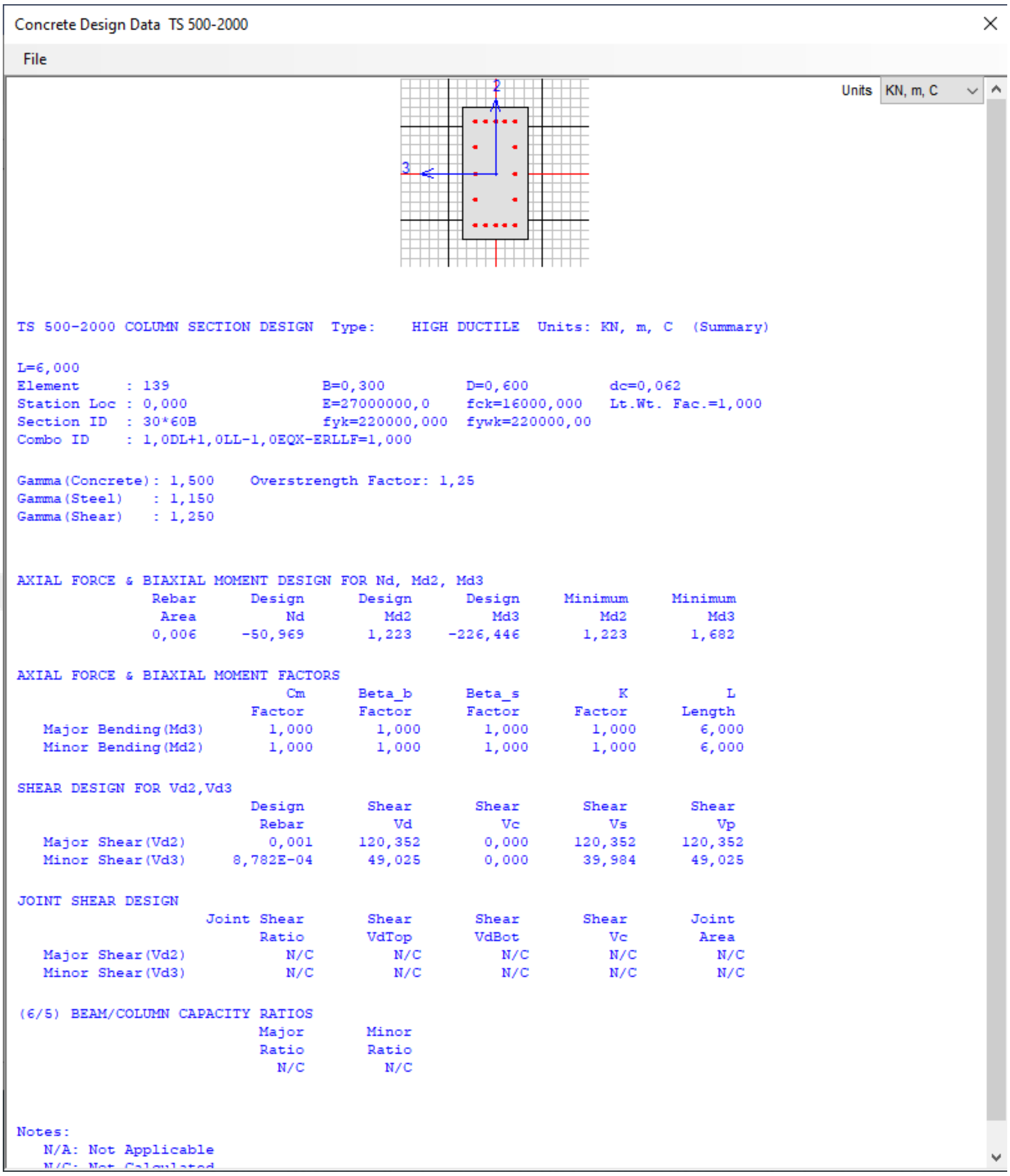

Concrete Design Data TS 500-2000

File

Units KN, m, C

```
TS 500-2000 COLUMN SECTION DESIGN  Type:   HIGH DUCTILE  Units: KN, m, C  (Summary)

L=6,000
Element     : 139                B=0,300         D=0,600         dc=0,062
Station Loc : 0,000              E=27000000,0    fck=16000,000   Lt.Wt. Fac.=1,000
Section ID  : 30*60B             fyk=220000,000  fywk=220000,00
Combo ID    : 1,0DL+1,0LL-1,0EQX-ERLLF=1,000

Gamma(Concrete): 1,500    Overstrength Factor: 1,25
Gamma(Steel)   : 1,150
Gamma(Shear)   : 1,250


AXIAL FORCE & BIAXIAL MOMENT DESIGN FOR Nd, Md2, Md3
               Rebar      Design      Design      Design      Minimum     Minimum
                Area          Nd         Md2         Md3          Md2         Md3
               0,006     -50,969       1,223    -226,446        1,223       1,682

AXIAL FORCE & BIAXIAL MOMENT FACTORS
                              Cm      Beta_b      Beta_s            K           L
                          Factor      Factor      Factor       Factor      Length
   Major Bending(Md3)      1,000       1,000       1,000        1,000       6,000
   Minor Bending(Md2)      1,000       1,000       1,000        1,000       6,000

SHEAR DESIGN FOR Vd2,Vd3
                          Design       Shear       Shear        Shear       Shear
                           Rebar          Vd          Vc           Vs          Vp
   Major Shear(Vd2)        0,001     120,352       0,000      120,352     120,352
   Minor Shear(Vd3)   8,782E-04       49,025       0,000       39,984      49,025

JOINT SHEAR DESIGN
                     Joint Shear       Shear       Shear        Shear       Joint
                           Ratio       VdTop       VdBot           Vc        Area
   Major Shear(Vd2)          N/C         N/C         N/C          N/C         N/C
   Minor Shear(Vd3)          N/C         N/C         N/C          N/C         N/C

(6/5) BEAM/COLUMN CAPACITY RATIOS
                           Major       Minor
                           Ratio       Ratio
                             N/C         N/C


Notes:
   N/A: Not Applicable
   N/C: Not Calculated
```

Figure A.15 Typical Results of 1st Story Beam Design of 9-Story Strengthened (V11) Building

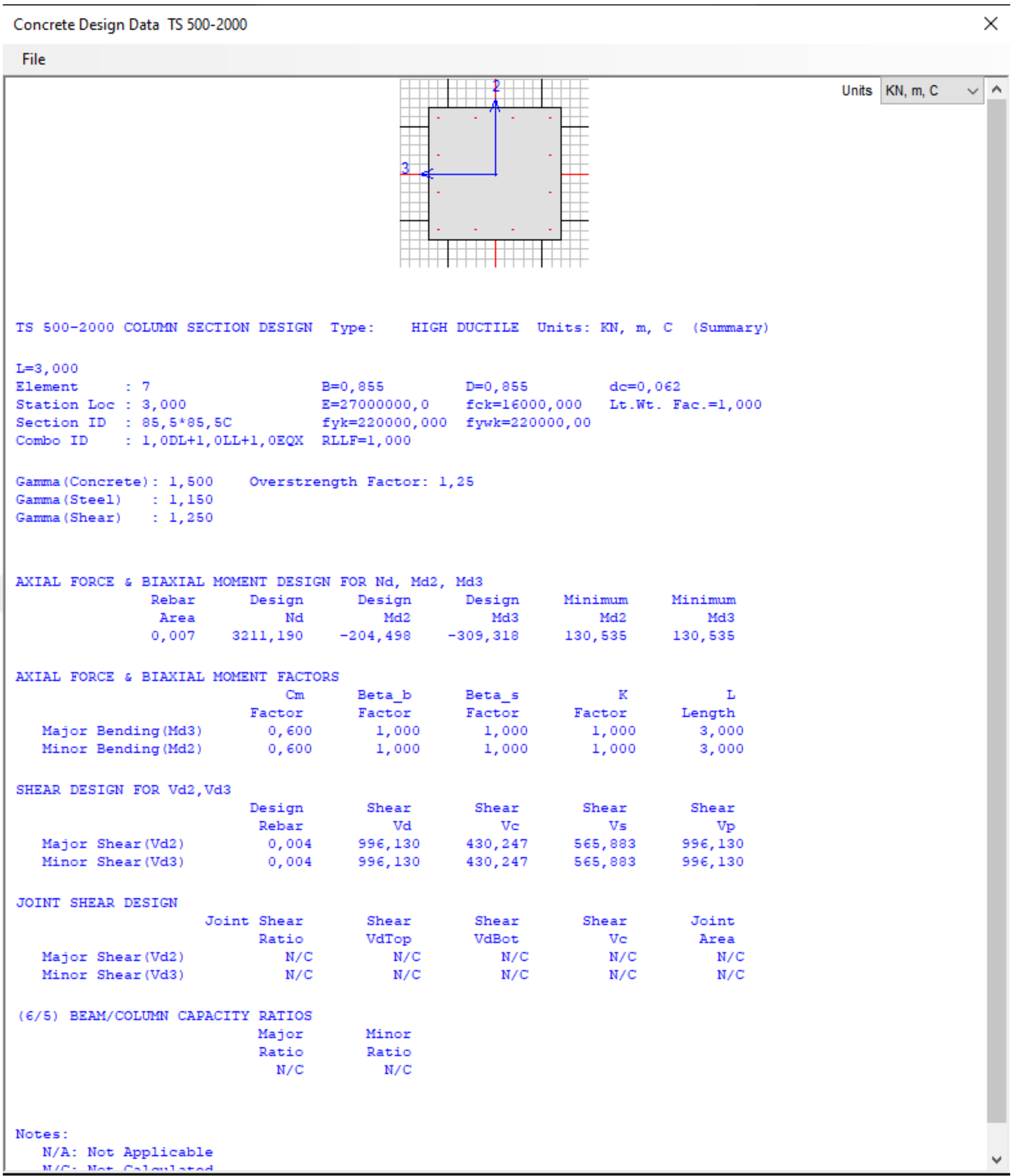

Concrete Design Data TS 500-2000

File

Units KN, m, C

TS 500-2000 COLUMN SECTION DESIGN Type: HIGH DUCTILE Units: KN, m, C (Summary)

L=3,000
Element : 7 B=0,855 D=0,855 dc=0,062
Station Loc : 3,000 E=27000000,0 fck=16000,000 Lt.Wt. Fac.=1,000
Section ID : 85,5*85,5C fyk=220000,000 fywk=220000,00
Combo ID : 1,0DL+1,0LL+1,0EQX RLLF=1,000

Gamma(Concrete): 1,500 Overstrength Factor: 1,25
Gamma(Steel) : 1,150
Gamma(Shear) : 1,250

AXIAL FORCE & BIAXIAL MOMENT DESIGN FOR Nd, Md2, Md3

Rebar Area	Design Nd	Design Md2	Design Md3	Minimum Md2	Minimum Md3
0,007	3211,190	-204,498	-309,318	130,535	130,535

AXIAL FORCE & BIAXIAL MOMENT FACTORS

	Cm Factor	Beta_b Factor	Beta_s Factor	K Factor	L Length
Major Bending(Md3)	0,600	1,000	1,000	1,000	3,000
Minor Bending(Md2)	0,600	1,000	1,000	1,000	3,000

SHEAR DESIGN FOR Vd2,Vd3

	Design Rebar	Shear Vd	Shear Vc	Shear Vs	Shear Vp
Major Shear(Vd2)	0,004	996,130	430,247	565,883	996,130
Minor Shear(Vd3)	0,004	996,130	430,247	565,883	996,130

JOINT SHEAR DESIGN

	Joint Shear Ratio	Shear VdTop	Shear VdBot	Shear Vc	Joint Area
Major Shear(Vd2)	N/C	N/C	N/C	N/C	N/C
Minor Shear(Vd3)	N/C	N/C	N/C	N/C	N/C

(6/5) BEAM/COLUMN CAPACITY RATIOS

Major Ratio	Minor Ratio
N/C	N/C

Notes:
N/A: Not Applicable

Figure A.16 Typical Results of Basement Column Design of 12-Story Deficient Building

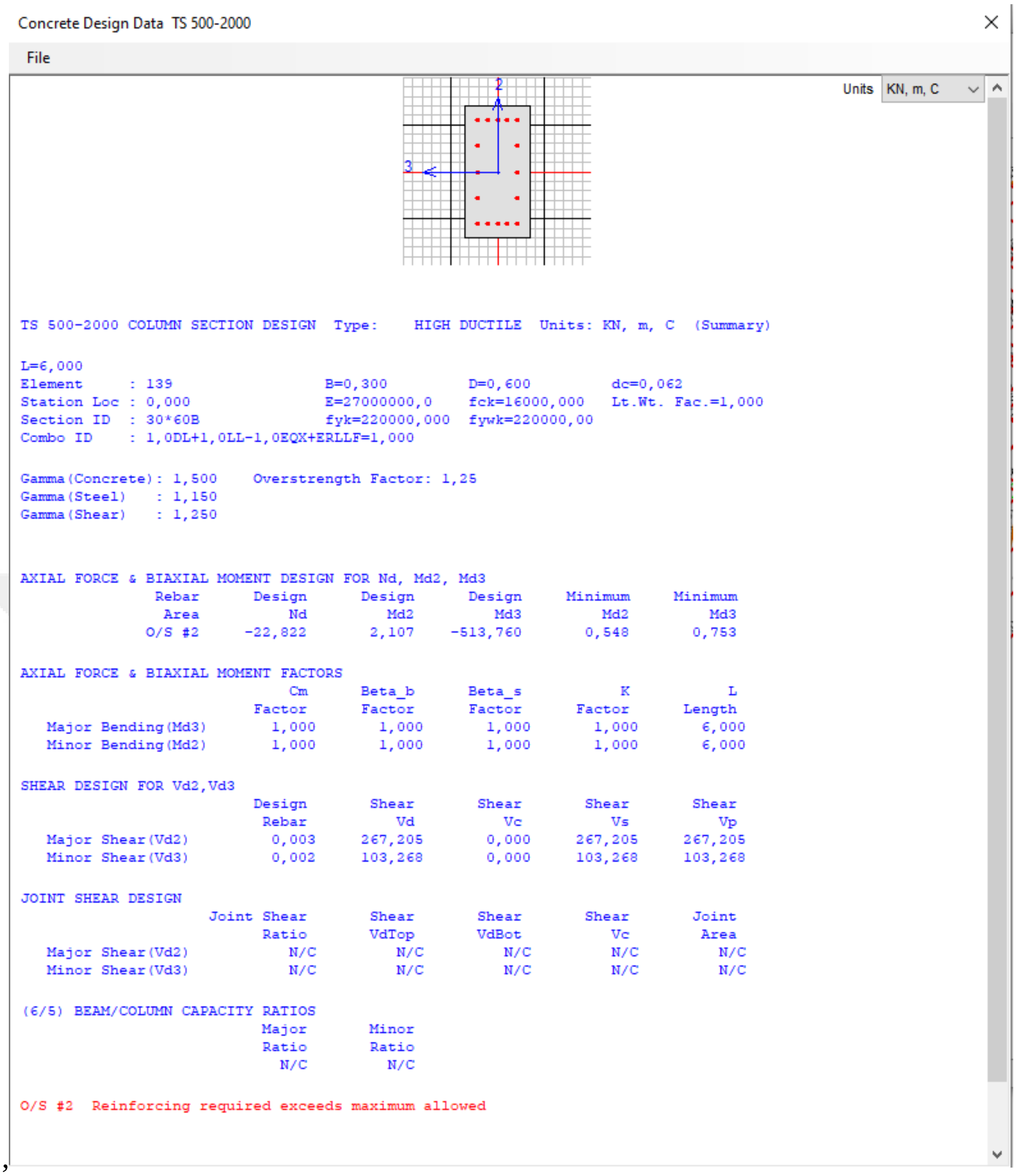

Figure A.17 Typical Results of 1st Story Beam Design of 12-Story Deficient Building

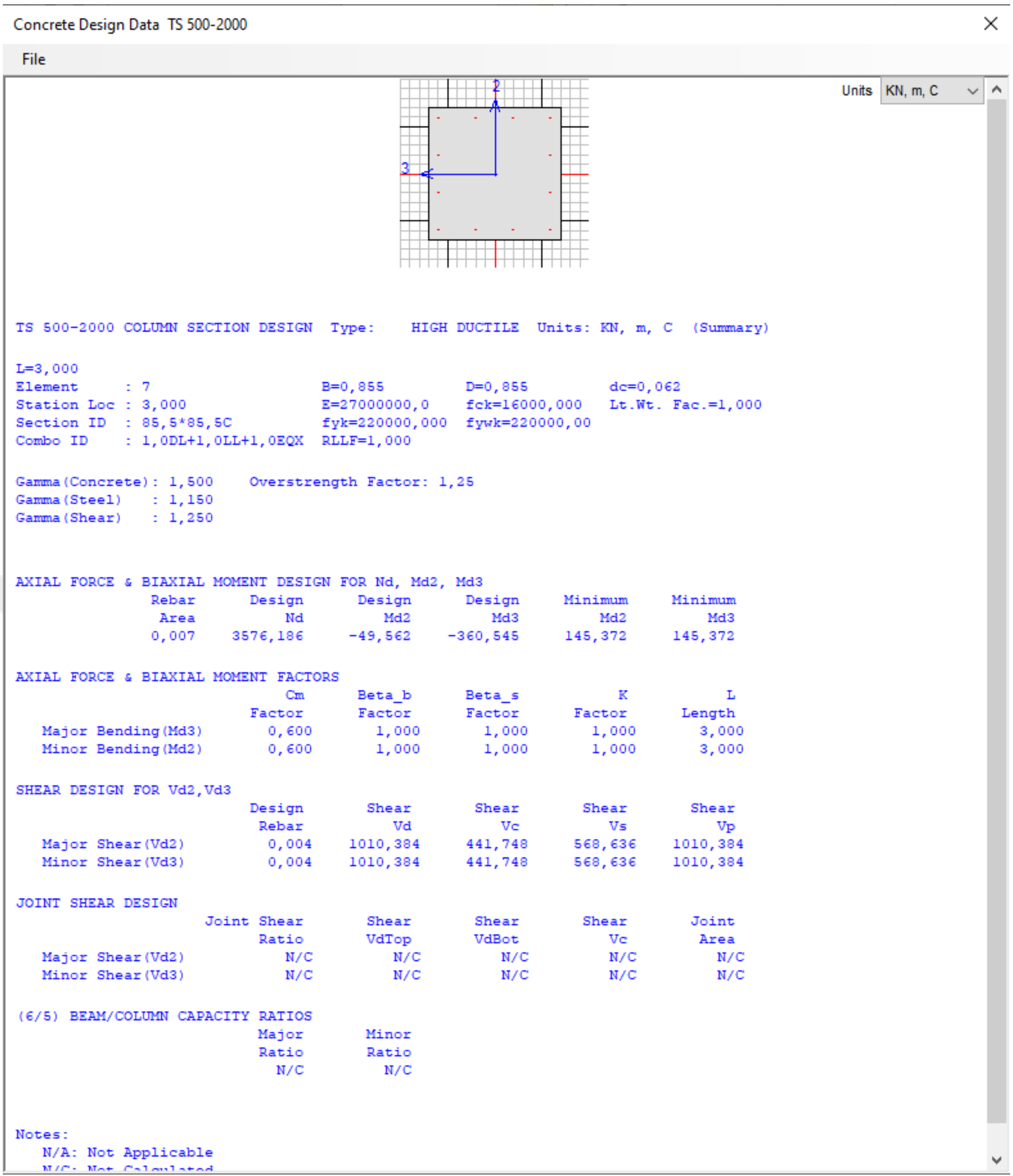

Concrete Design Data TS 500-2000

File

Units KN, m, C

```
TS 500-2000 COLUMN SECTION DESIGN  Type:   HIGH DUCTILE  Units: KN, m, C  (Summary)

L=3,000
Element      : 7                 B=0,855         D=0,855         dc=0,062
Station Loc  : 3,000             E=27000000,0    fck=16000,000   Lt.Wt. Fac.=1,000
Section ID   : 85,5*85,5C        fyk=220000,000  fywk=220000,00
Combo ID     : 1,0DL+1,0LL+1,0EQX  RLLF=1,000

Gamma(Concrete): 1,500    Overstrength Factor: 1,25
Gamma(Steel)   : 1,150
Gamma(Shear)   : 1,250


AXIAL FORCE & BIAXIAL MOMENT DESIGN FOR Nd, Md2, Md3
               Rebar      Design      Design      Design     Minimum     Minimum
                Area          Nd         Md2         Md3         Md2         Md3
               0,007    3576,186     -49,562    -360,545     145,372     145,372

AXIAL FORCE & BIAXIAL MOMENT FACTORS
                              Cm      Beta_b      Beta_s           K           L
                          Factor      Factor      Factor      Factor      Length
   Major Bending(Md3)      0,600       1,000       1,000       1,000       3,000
   Minor Bending(Md2)      0,600       1,000       1,000       1,000       3,000

SHEAR DESIGN FOR Vd2,Vd3
                          Design       Shear       Shear       Shear       Shear
                           Rebar          Vd          Vc          Vs          Vp
   Major Shear(Vd2)        0,004    1010,384     441,748     568,636    1010,384
   Minor Shear(Vd3)        0,004    1010,384     441,748     568,636    1010,384

JOINT SHEAR DESIGN
                     Joint Shear       Shear       Shear       Shear       Joint
                           Ratio       VdTop       VdBot          Vc        Area
   Major Shear(Vd2)          N/C         N/C         N/C         N/C         N/C
   Minor Shear(Vd3)          N/C         N/C         N/C         N/C         N/C

(6/5) BEAM/COLUMN CAPACITY RATIOS
                           Major       Minor
                           Ratio       Ratio
                             N/C         N/C


Notes:
   N/A: Not Applicable
```

Figure A.18 Typical Results of Basement Column Design of 12-Story Strengthened (V11) Building

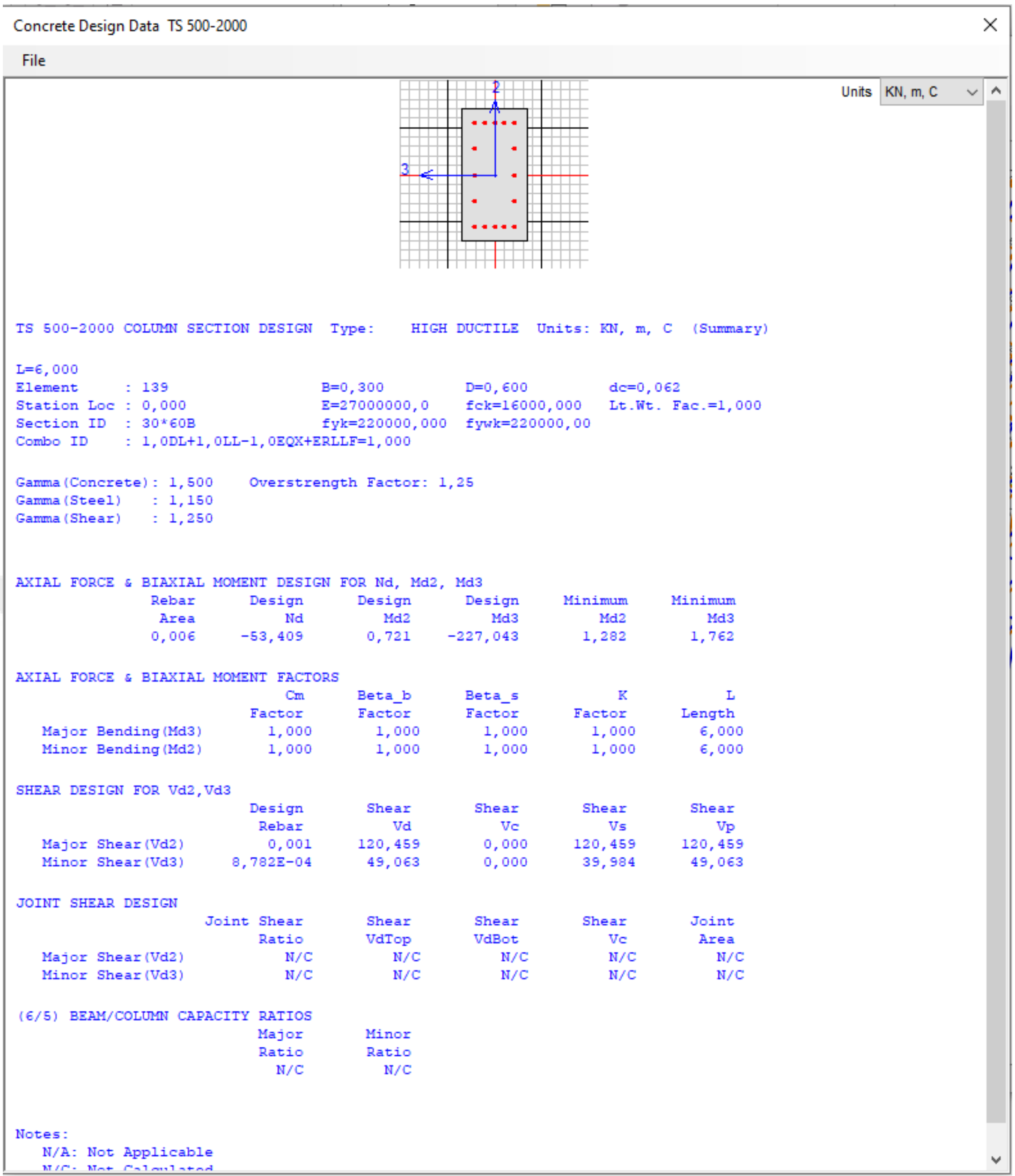

```
Concrete Design Data  TS 500-2000
File
                                                              Units  KN, m, C

TS 500-2000 COLUMN SECTION DESIGN  Type:   HIGH DUCTILE  Units: KN, m, C  (Summary)

L=6,000
Element      : 139                 B=0,300          D=0,600          dc=0,062
Station Loc  : 0,000               E=27000000,0     fck=16000,000    Lt.Wt. Fac.=1,000
Section ID   : 30*60B              fyk=220000,000   fywk=220000,00
Combo ID     : 1,0DL+1,0LL-1,0EQX+ERLLF=1,000

Gamma(Concrete): 1,500    Overstrength Factor: 1,25
Gamma(Steel)   : 1,150
Gamma(Shear)   : 1,250


AXIAL FORCE & BIAXIAL MOMENT DESIGN FOR Nd, Md2, Md3
               Rebar      Design      Design      Design     Minimum     Minimum
                Area          Nd         Md2         Md3         Md2         Md3
               0,006     -53,409       0,721    -227,043       1,282       1,762

AXIAL FORCE & BIAXIAL MOMENT FACTORS
                              Cm      Beta_b      Beta_s           K           L
                          Factor      Factor      Factor      Factor      Length
   Major Bending(Md3)      1,000       1,000       1,000       1,000       6,000
   Minor Bending(Md2)      1,000       1,000       1,000       1,000       6,000

SHEAR DESIGN FOR Vd2,Vd3
                          Design       Shear       Shear       Shear       Shear
                           Rebar          Vd          Vc          Vs          Vp
   Major Shear(Vd2)        0,001     120,459       0,000     120,459     120,459
   Minor Shear(Vd3)   8,782E-04       49,063       0,000      39,984      49,063

JOINT SHEAR DESIGN
                     Joint Shear       Shear       Shear       Shear       Joint
                           Ratio       VdTop       VdBot          Vc        Area
   Major Shear(Vd2)          N/C         N/C         N/C         N/C         N/C
   Minor Shear(Vd3)          N/C         N/C         N/C         N/C         N/C

(6/5) BEAM/COLUMN CAPACITY RATIOS
                           Major       Minor
                           Ratio       Ratio
                             N/C         N/C


Notes:
   N/A: Not Applicable
   N/C: Not Calculated
```

Figure A.19 Typical Results of 1st Story Beam Design of 12-Story Strengthened (V11) Building

B. RESULTS OF STEEL FRAME DESIGN

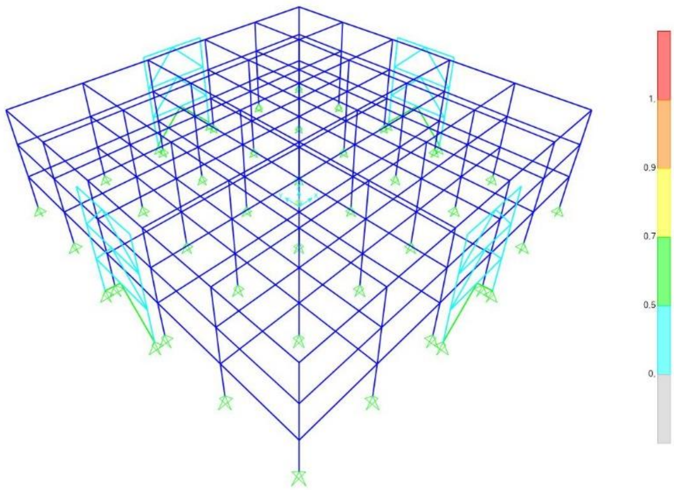

Figure B.1 Results of Steel Frame Design of Model 310V11

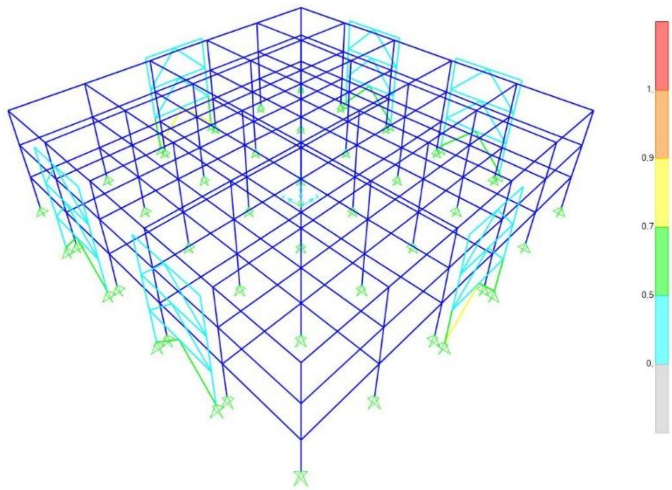

Figure B.2 Results of Steel Frame Design of Model 310V21

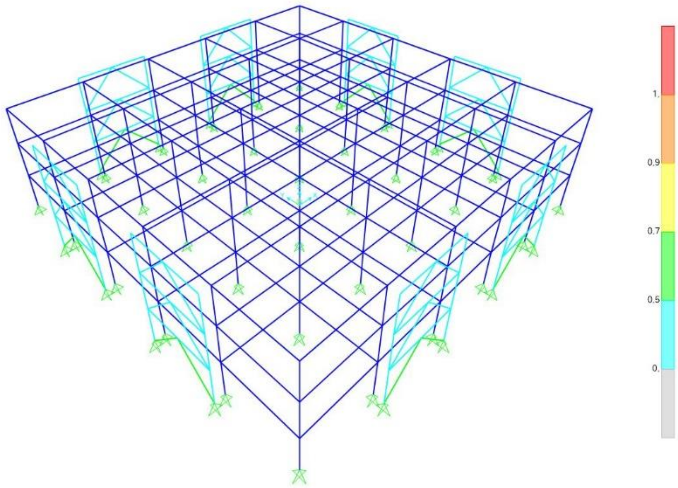

Figure B.3 Results of Steel Frame Design of Model 310V22

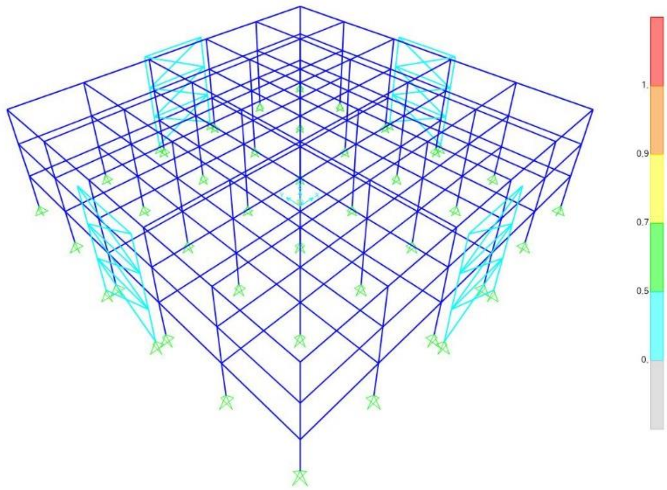

Figure B.4 Results of Steel Frame Design of Model 310X11

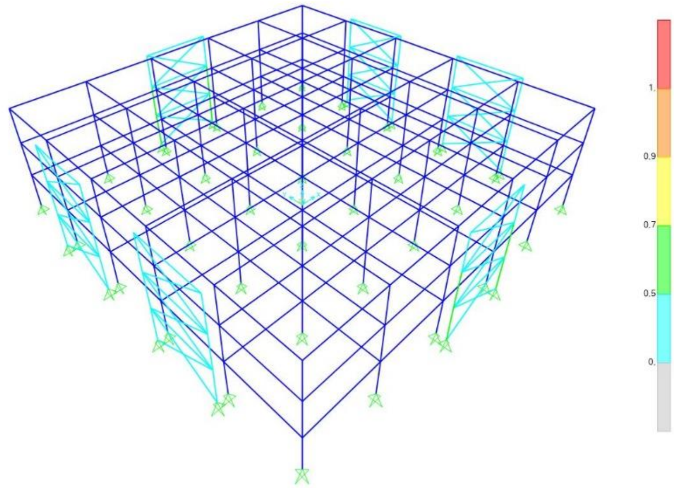

Figure B.5 Results of Steel Frame Design of Model 310X21

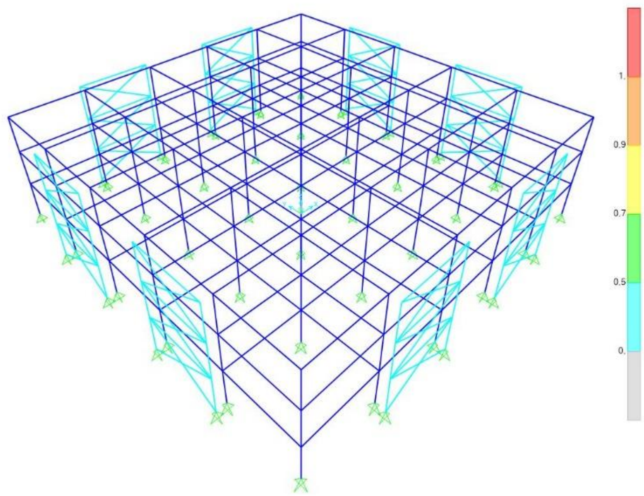

Figure B.6 Results of Steel Frame Design of Model 310X22

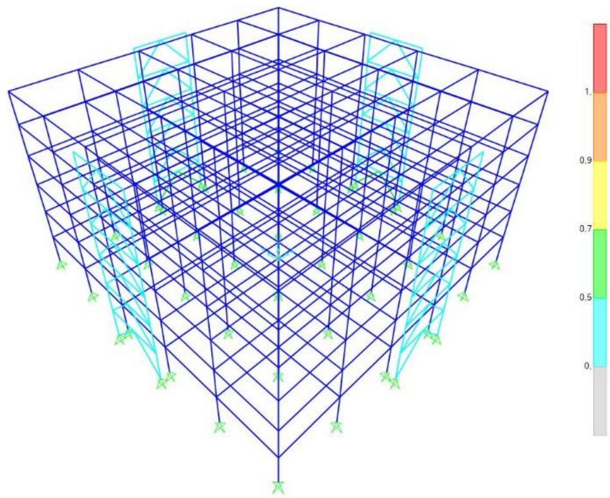

Figure B.7 Results of Steel Frame Design of Model 610V11

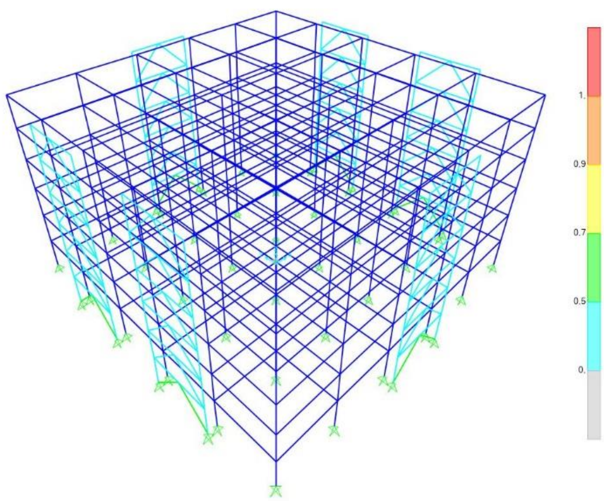

Figure B.8 Results of Steel Frame Design of Model 610V21

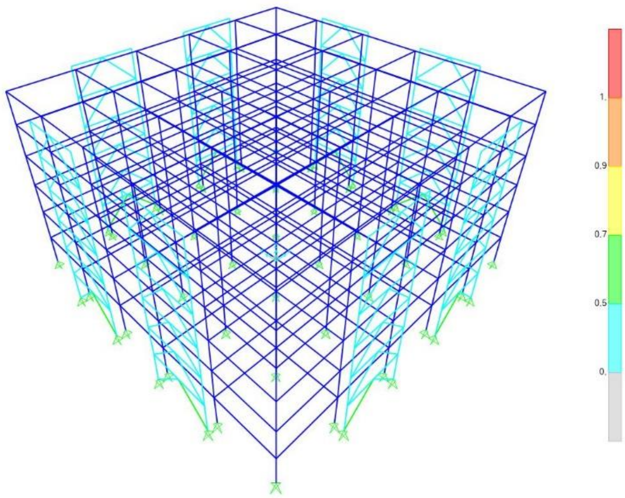

Figure B.9 Results of Steel Frame Design of Model 610V22

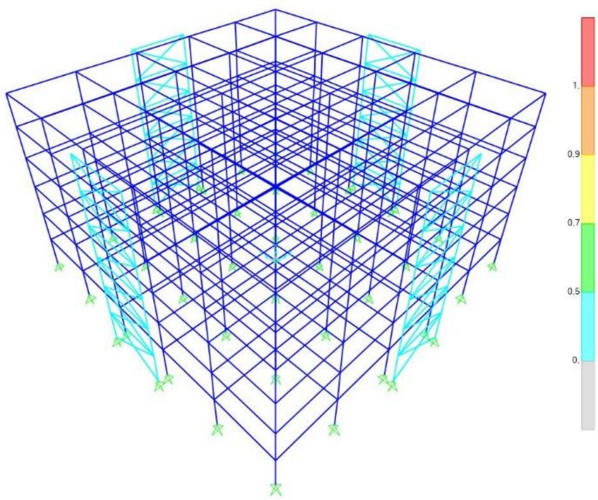

Figure B.10 Results of Steel Frame Design of Model 610X11

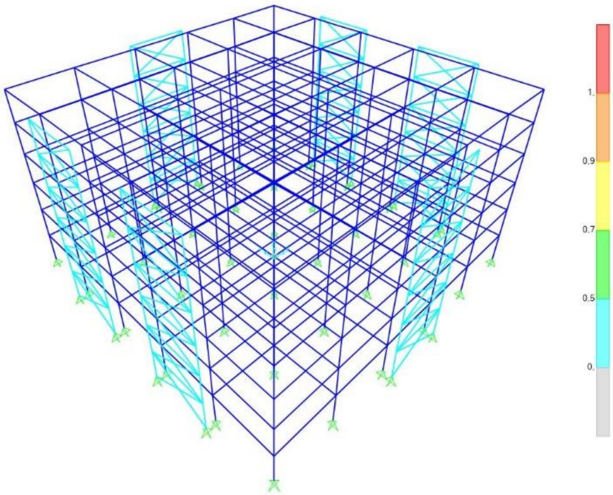

Figure B.11 Results of Steel Frame Design of Model 610X21

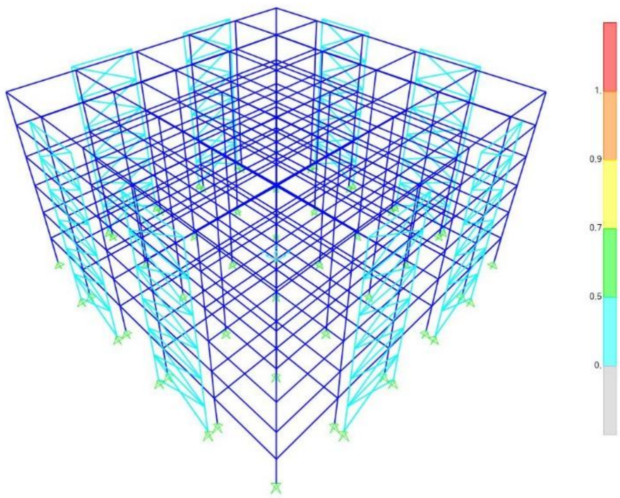

Figure B.12 Results of Steel Frame Design of Model 610X22

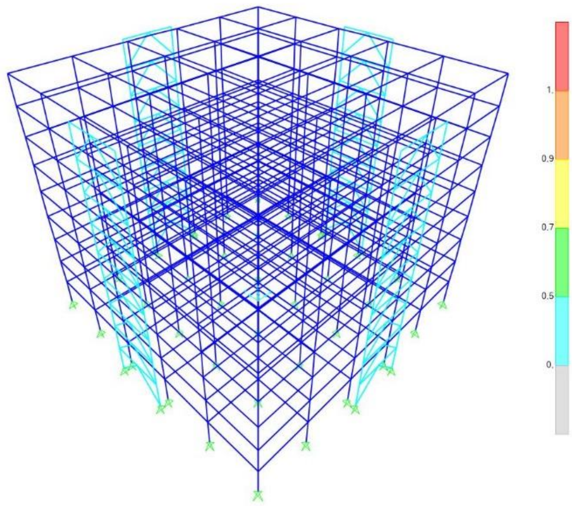

Figure B.13 Results of Steel Frame Design of Model 910V11

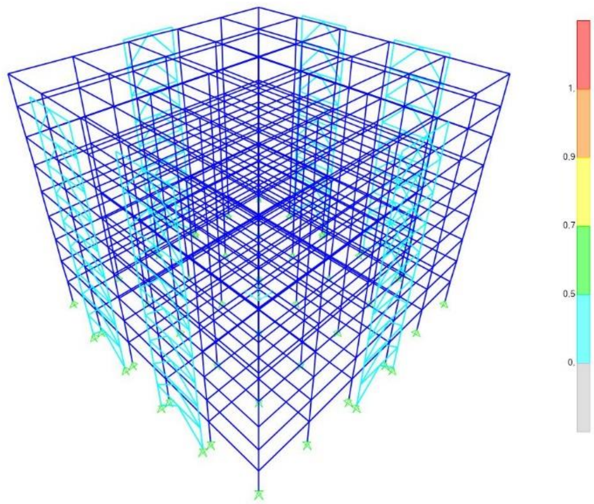

Figure B.14 Results of Steel Frame Design of Model 910V21

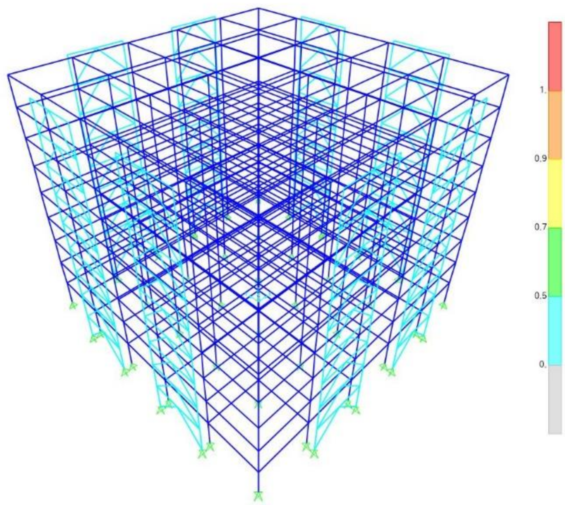

Figure B.15 Results of Steel Frame Design of Model 910V22

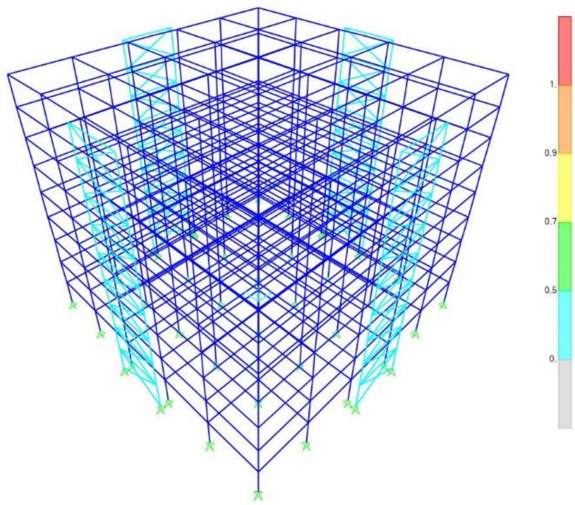

Figure B.16 Results of Steel Frame Design of Model 910X11

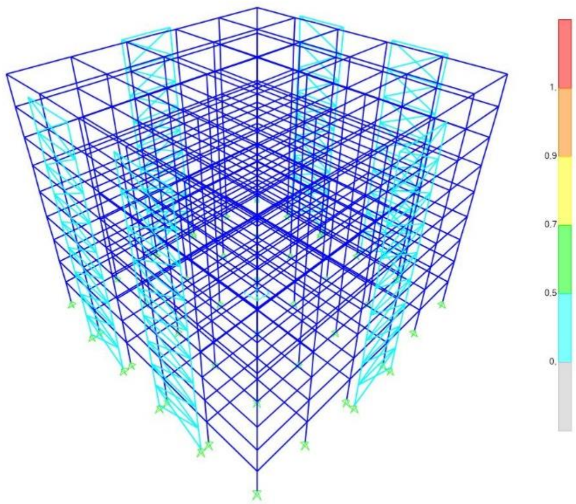

Figure B.17 Results of Steel Frame Design of Model 910X21

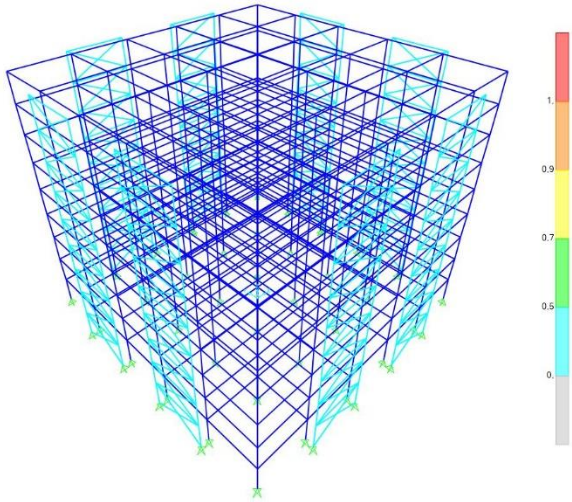

Figure B.18 Results of Steel Frame Design of Model 910X22

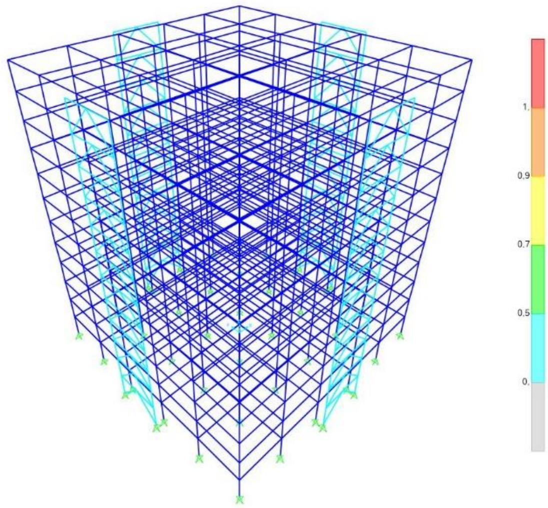

Figure B.19 Results of Steel Frame Design of Model 1210V11

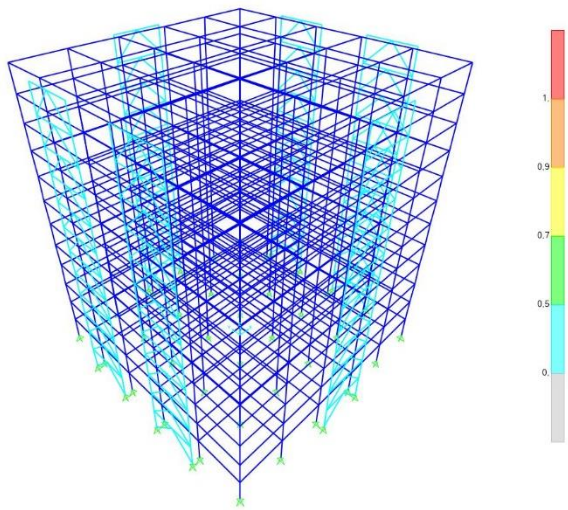

Figure B.20 Results of Steel Frame Design of Model 1210V21

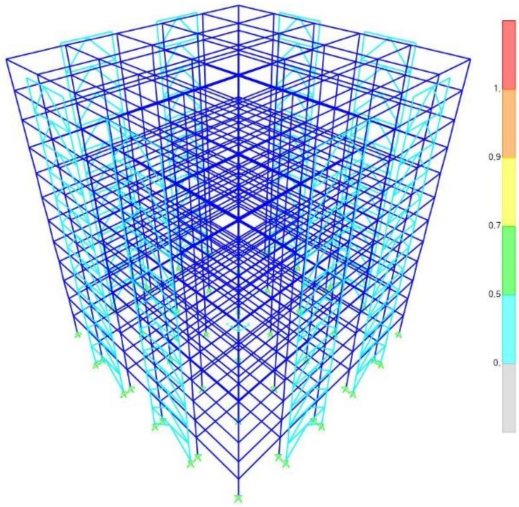

Figure B.21 Results of Steel Frame Design of Model 1210V22

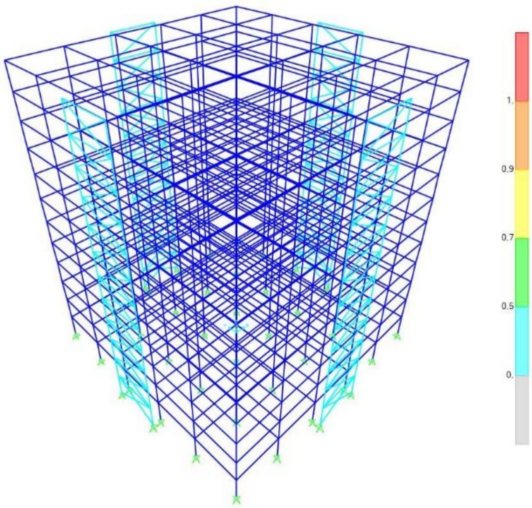

Figure B.22 Results of Steel Frame Design of Model 1210X11

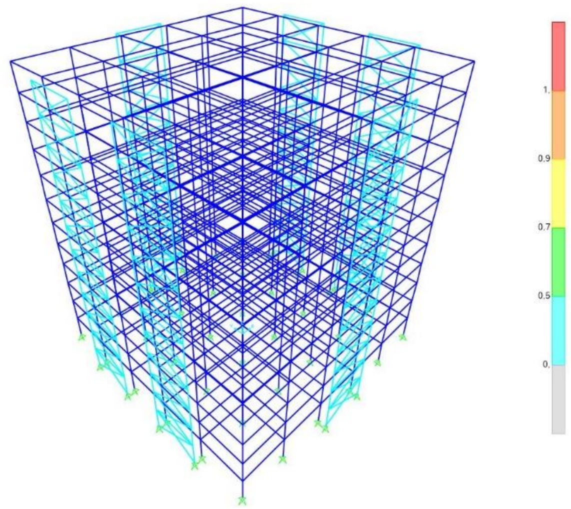

Figure B.23 Results of Steel Frame Design of Model 1210X21

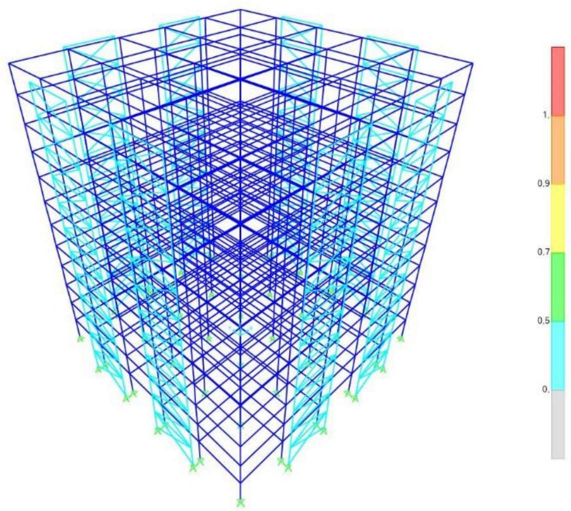

Figure B.24 Results of Steel Frame Design of Model 1210X22

C. CALCULATED SEISMIC LOAD BASED ON EQUIVALENT EARTHQUAKE LOAD METHOD FOR ALL THE MODELS

Table C.1 – Seismic Load of Model 310

EQX				
Story No	**Hi (m)**	**wi (kN)**	**Hi*wi (kN.m)**	**Fi (kN)**
1	3	10762	32286	682,1
2	6	10762	64572	1364,2
3	9	8442	75979,89	1689,3
∑		29966	172837,9	3735,7
EQY				
Story No	**Hi (m)**	**wi (kN)**	**Hi*wi (kN.m)**	**Fi (kN)**
1	3	10762	32286	682,1
2	6	10762	64572	1364,2
3	9	8442	75980	1689,3
∑		29966	172838	3735,7

Table C.2 Seismic Load of Model 310V11

EQX				
Story No	**Hi (m)**	**wi (kN)**	**Hi*wi (kN.m)**	**Fi (kN)**
1	3	10908	32725	544,7
2	6	10908	65451	1089,4
3	9	8515	76639	1342,6
∑		30332	174815	2976,8
EQY				
Story No	**Hi (m)**	**wi (kN)**	**Hi*wi (kN.m)**	**Fi (kN)**
1	3	10908	32725	544,7
2	6	10908	65451	1089,4
3	9	8515	76639	1342,6
∑		30332	174815	2976,8

Table C.3 Seismic Load of Model 310V21

EQX				
Story No	**Hi (m)**	**wi (kN)**	**Hi*wi (kN.m)**	**Fi (kN)**
1	3	10971	32914	515,1
2	6	10971	65827	1030,3
3	9	8547	76921	1267,2
∑		30489	175662	2812,6
EQY				
Story No	**Hi (m)**	**wi (kN)**	**Hi*wi (kN.m)**	**Fi (kN)**
1	3	10971	32914	613,3
2	6	10971	65827	1226,5
3	9	8547	76921	1508,6
∑		30489	175662	3348,4

Table C.4 Seismic Load of Model 310V22

EQX				
Story No	**Hi (m)**	**wi (kN)**	**Hi*wi (kN.m)**	**Fi (kN)**
1	3	11045	33136	632,7
2	6	11045	66272	1265,4
3	9	8584	77254	1552,7
∑		30674	176661	3450,9
EQY				
Story No	**Hi (m)**	**wi (kN)**	**Hi*wi (kN.m)**	**Fi (kN)**
1	3	11045	33136	632,7
2	6	11045	66272	1265,4
3	9	8584	77254	1552,7
∑		30674	176661	3450,9

Table C.5 Seismic Load of Model 310X11

EQX				
Story No	**Hi (m)**	**wi (kN)**	**Hi*wi (kN.m)**	**Fi (kN)**
1	3	10914	32742	522,8
2	6	10914	65483	1045,5
3	9	8518	76663	1288,3
∑		30346	174889	2856,5
EQY				
Story No	**Hi (m)**	**wi (kN)**	**Hi*wi (kN.m)**	**Fi (kN)**
1	3	10914	32742	522,8
2	6	10914	65483	1045,5
3	9	8518	76663	1288,3
∑		30346	174889	2856,5

Table C.6 Seismic Load of Model 310X21

EQX				
Story No	**Hi (m)**	**wi (kN)**	**Hi*wi (kN.m)**	**Fi (kN)**
1	3	11028	33084	563,0
2	6	11028	66168	1126,0
3	9	8575	77177	1382,4
∑		30631	176429	3071,4
EQY				
Story No	**Hi (m)**	**wi (kN)**	**Hi*wi (kN.m)**	**Fi (kN)**
1	3	11028	33084	647,4
2	6	11028	66168	1294,9
3	9	8575	77177	1589,8
∑		30631	176429	3532,2

Table C.7 Seismic Load of Model 310X22

EQX				
Story No	**Hi (m)**	**wi (kN)**	**Hi*wi (kN.m)**	**Fi (kN)**
1	3	11066	33197	666,5
2	6	11066	66395	1332,9
3	9	8594	77347	1634,5
∑		30726	176939	3633,9
EQY				
Story No	**Hi (m)**	**wi (kN)**	**Hi*wi (kN.m)**	**Fi (kN)**
1	3	11066	33197	666,5
2	6	11066	66395	1332,9
3	9	8594	77347	1634,5
∑		30726	176939	3633,9

Table C.8 Seismic Load of Model 610

EQX				
Story No	**Hi (m)**	**wi (kN)**	**Hi*wi (kN.m)**	**Fi (kN)**
1	3	11275	33825	286,3
2	6	11276	67654	572,7
3	9	11275	101479	859,0
4	12	11275	135305	1145,4
5	15	11275	169130	1431,7
6	18	8699	156580	1590,3
∑		65076	663972	5885,5
EQY				
Story No	**Hi (m)**	**wi (kN)**	**Hi*wi (kN.m)**	**Fi (kN)**
1	3	11275	33825	286,3
2	6	11276	67654	572,7
3	9	11275	101479	859,0
4	12	11275	135305	1145,4
5	15	11275	169130	1431,7
6	18	8699	156580	1590,3
∑		65076	663972	5885,5

Table C.9 Seismic Load of Model 610V11

EQX				
Story No	**Hi (m)**	**wi (kN)**	**Hi*wi (kN.m)**	**Fi (kN)**
1	3	11456	34368	198,0
2	6	11456	68736	396,1
3	9	11441	102973	593,3
4	12	11427	137123	790,1
5	15	11427	171404	987,6
6	18	8775	157947	1092,7
∑		65982	672550	4057,9
EQY				
Story No	**Hi (m)**	**wi (kN)**	**Hi*wi (kN.m)**	**Fi (kN)**
1	3	11456	34368	198,0
2	6	11456	68736	396,1
3	9	11441	102973	593,3
4	12	11427	137123	790,1
5	15	11427	171404	987,6
6	18	8775	157947	1092,7
∑		65982	672550	4057,9

Table C.10 Seismic Load of Model 610V21

EQX				
Story No	**Hi (m)**	**wi (kN)**	**Hi*wi (kN.m)**	**Fi (kN)**
1	3	11536	34607	194,3
2	6	11536	69213	388,6
3	9	11520	103676	582,0
4	12	11503	138042	775,0
5	15	11503	172552	968,7
6	18	8813	158636	1069,6
∑		66411	676726	3978,2
EQY				
Story No	**Hi (m)**	**wi (kN)**	**Hi*wi (kN.m)**	**Fi (kN)**
1	3	11536	34607	216,8
2	6	11536	69213	433,6
3	9	11520	103676	649,5
4	12	11503	138042	864,8
5	15	11503	172552	1081,0
6	18	8813	158636	1193,6
∑		66411	676726	4439,4

Table C.11 Seismic Load of Model 610V22

EQX				
Story No	**Hi (m)**	**wi (kN)**	**Hi*wi (kN.m)**	**Fi (kN)**
1	3	11612	34835	221,5
2	6	11612	69670	443,1
3	9	11589	104303	663,3
4	12	11567	138802	882,7
5	15	11567	173502	1103,4
6	18	8845	159206	1216,4
∑		66791	680318	4530,5
EQY				
Story No	**Hi (m)**	**wi (kN)**	**Hi*wi (kN.m)**	**Fi (kN)**
1	3	11612	34835	221,5
2	6	11612	69670	443,1
3	9	11589	104303	663,3
4	12	11567	138802	882,7
5	15	11567	173502	1103,4
6	18	8845	159206	1216,4
∑		66791	680318	4530,5

Table C.12 Seismic Load of Model 610X11

EQX				
Story No	**Hi (m)**	**wi (kN)**	**Hi*wi (kN.m)**	**Fi (kN)**
1	3	11468	34403	198,3
2	6	11468	68806	396,6
3	9	11446	103010	593,7
4	12	11423	137081	790,1
5	15	11423	171351	987,6
6	18	8773	157915	1092,8
∑		66001	672565	4059,0
EQY				
Story No	**Hi (m)**	**wi (kN)**	**Hi*wi (kN.m)**	**Fi (kN)**
1	3	11468	34403	198,3
2	6	11468	68806	396,6
3	9	11446	103010	593,7
4	12	11423	137081	790,1
5	15	11423	171351	987,6
6	18	8773	157915	1092,8
∑		66001	672565	4059,0

Table C.13 Seismic Load of Model 610X21

EQX				
Story No	**Hi (m)**	**wi (kN)**	**Hi*wi (kN.m)**	**Fi (kN)**
1	3	11542	34626	199,6
2	6	11542	69251	399,2
3	9	11522	103701	597,8
4	12	11503	138032	795,7
5	15	11503	172541	994,6
6	18	8813	158629	1098,2
∑		66424	676780	4085,1
EQY				
Story No	**Hi (m)**	**wi (kN)**	**Hi*wi (kN.m)**	**Fi (kN)**
1	3	11542	34626	217,0
2	6	11542	69251	433,9
3	9	11522	103701	649,8
4	12	11503	138032	864,9
5	15	11503	172541	1081,1
6	18	8813	158629	1193,7
∑		66424	676780	4440,3

Table C.14 Seismic Load of Model 610X22

EQX				
Story No	**Hi (m)**	**wi (kN)**	**Hi*wi (kN.m)**	**Fi (kN)**
1	3	11628	34884	221,9
2	6	11628	69768	443,8
3	9	11603	104429	664,2
4	12	11579	138943	883,7
5	15	11579	173679	1104,7
6	18	8851	159312	1217,4
∑		66867	681015	4535,6
EQY				
Story No	**Hi (m)**	**wi (kN)**	**Hi*wi (kN.m)**	**Fi (kN)**
1	3	11628	34884	221,9
2	6	11628	69768	443,8
3	9	11603	104429	664,2
4	12	11579	138943	883,7
5	15	11579	173679	1104,7
6	18	8851	159312	1217,4
∑		66867	681015	4535,6

Table C.15 Seismic Load of Model 910

EQX				
Story No	**Hi (m)**	**wi (kN)**	**Hi*wi (kN.m)**	**Fi (kN)**
1	3	11875	35625	151,4
2	6	11875	71250	302,8
3	9	11875	106875	454,2
4	12	11875	142500	605,6
5	15	11875	178125	757,0
6	18	11875	213750	908,4
7	21	11875	249375	1059,8
8	24	11875	285000	1211,2
9	27	8999	242964	1501,8
∑		103999	1525464	6952,1
EQY				
Story No	**Hi (m)**	**wi (kN)**	**Hi*wi (kN.m)**	**Fi (kN)**
1	3	11875	35625	151,4
2	6	11875	71250	302,8
3	9	11875	106875	454,2
4	12	11875	142500	605,6
5	15	11875	178125	757,0
6	18	11875	213750	908,4
7	21	11875	249375	1059,8
8	24	11875	285000	1211,2
9	27	8999	242964	1501,8
∑		103999	1525464	6952,1

Table C.16 Seismic Load of Model 910V11

EQX				
Story No	**Hi (m)**	**wi (kN)**	**Hi*wi (kN.m)**	**Fi (kN)**
1	3	12102	36306	103,5
2	6	12102	72612	207,0
3	9	12084	108759	310,1
4	12	12067	144800	412,8
5	15	12067	181000	516,0
6	18	12051	216917	618,4
7	21	12035	252739	720,5
8	24	12035	288844	823,5
9	27	9079	245127	1018,1
∑		105622	1547103	4729,9
EQY				
Story No	**Hi (m)**	**wi (kN)**	**Hi*wi (kN.m)**	**Fi (kN)**
1	3	12102	36306	103,5
2	6	12102	72612	207,0
3	9	12084	108759	310,1
4	12	12067	144800	412,8
5	15	12067	181000	516,0
6	18	12051	216917	618,4
7	21	12035	252739	720,5
8	24	12035	288844	823,5
9	27	9079	245127	1018,1
∑		105622	1547103	4729,9

Table C.17 Seismic Load of Model 910V21

EQX				
Story No	**Hi (m)**	**wi (kN)**	**Hi*wi (kN.m)**	**Fi (kN)**
1	3	12215	36646	107,7
2	6	12215	73293	215,4
3	9	12189	109701	322,3
4	12	12163	145950	428,9
5	15	12163	182438	536,1
6	18	12139	218500	642,0
7	21	12115	254420	747,6
8	24	12115	290766	854,4
9	27	9119	246208	1054,8
∑		106433	1557923	4909,2
EQY				
Story No	**Hi (m)**	**wi (kN)**	**Hi*wi (kN.m)**	**Fi (kN)**
1	3	12215	36646	122,4
2	6	12215	73293	244,7
3	9	12189	109701	366,3
4	12	12163	145950	487,3
5	15	12163	182438	609,2
6	18	12139	218500	729,6
7	21	12115	254420	849,5
8	24	12115	290766	970,9
9	27	9119	246208	1198,7
∑		106433	1557923	5578,7

Table C.18 Seismic Load of Model 910V22

EQX				
Story No	**Hi (m)**	**wi (kN)**	**Hi*wi (kN.m)**	**Fi (kN)**
1	3	12310	36930	116,7
2	6	12310	73860	233,5
3	9	12278	110504	349,3
4	12	12246	146956	464,5
5	15	12246	183695	580,6
6	18	12219	219945	695,2
7	21	12192	256031	809,3
8	24	12192	292607	924,9
9	27	9157	247243	1140,2
∑		107151	1567771	5314,4
EQY				
Story No	**Hi (m)**	**wi (kN)**	**Hi*wi (kN.m)**	**Fi (kN)**
1	3	12310	36930	116,7
2	6	12310	73860	233,5
3	9	12278	110504	349,3
4	12	12246	146956	464,5
5	15	12246	183695	580,6
6	18	12219	219945	695,2
7	21	12192	256031	809,3
8	24	12192	292607	924,9
9	27	9157	247243	1140,2
∑		107151	1567771	5314,4

Table C.19 Seismic Load of Model 910X11

EQX				
Story No	**Hi (m)**	**wi (kN)**	**Hi*wi (kN.m)**	**Fi (kN)**
1	3	12119	36357	104,7
2	6	12119	72715	209,4
3	9	12099	108889	313,5
4	12	12078	144940	417,3
5	15	12078	181175	521,7
6	18	12060	217083	625,1
7	21	12042	252883	728,1
8	24	12042	289009	832,2
9	27	9082	245220	1028,8
∑		105720	1548271	4780,7
EQY				
Story No	**Hi (m)**	**wi (kN)**	**Hi*wi (kN.m)**	**Fi (kN)**
1	3	12119	36357	104,7
2	6	12119	72715	209,4
3	9	12099	108889	313,5
4	12	12078	144940	417,3
5	15	12078	181175	521,7
6	18	12060	217083	625,1
7	21	12042	252883	728,1
8	24	12042	289009	832,2
9	27	9082	245220	1028,8
∑		105720	1548271	4780,7

Table C.20 Seismic Load of Model 910X21

EQX				
Story No	**Hi (m)**	**wi (kN)**	**Hi*wi (kN.m)**	**Fi (kN)**
1	3	12241	36724	107,9
2	6	12241	73447	215,9
3	9	12211	109895	323,0
4	12	12180	146160	429,6
5	15	12180	182700	537,0
6	18	12153	218750	643,0
7	21	12126	254637	748,4
8	24	12126	291014	855,4
9	27	9124	246347	1055,9
∑		106581	1559675	4916,0
EQY				
Story No	**Hi (m)**	**wi (kN)**	**Hi*wi (kN.m)**	**Fi (kN)**
1	3	12241	36724	122,7
2	6	12241	73447	245,3
3	9	12211	109895	367,1
4	12	12180	146160	488,2
5	15	12180	182700	610,2
6	18	12153	218750	730,6
7	21	12126	254637	850,5
8	24	12126	291014	972,0
9	27	9124	246347	1199,9
∑		106581	1559675	5586,4

Table C.21 Seismic Load of Model 910X22

EQX				
Story No	**Hi (m)**	**wi (kN)**	**Hi*wi (kN.m)**	**Fi (kN)**
1	3	12363	37090	125,4
2	6	12363	74180	250,8
3	9	12322	110902	375,0
4	12	12282	147380	498,3
5	15	12282	184225	622,9
6	18	12245	220417	745,2
7	21	12209	256391	866,9
8	24	12209	293018	990,7
9	27	9166	247475	1221,2
∑		107442	1571078	5696,3
EQY				
Story No	**Hi (m)**	**wi (kN)**	**Hi*wi (kN.m)**	**Fi (kN)**
1	3	12363	37090	125,4
2	6	12363	74180	250,8
3	9	12322	110902	375,0
4	12	12282	147380	498,3
5	15	12282	184225	622,9
6	18	12245	220417	745,2
7	21	12209	256391	866,9
8	24	12209	293018	990,7
9	27	9166	247475	1221,2
∑		107442	1571078	5696,3

Table C.22 Seismic Load of Model 1210

EQX				
Story No	**Hi (m)**	**wi (kN)**	**Hi*wi (kN.m)**	**Fi (kN)**
1	3	12607	37821	92,9
2	6	12607	75642	185,8
3	9	12607	113463	278,7
4	12	12607	151284	371,6
5	15	12607	189105	464,5
6	18	12607	226926	557,4
7	21	12607	264747	650,3
8	24	12607	302568	743,2
9	27	12607	340389	836,1
10	30	12607	378210	929,0
11	33	12607	416031	1021,9
12	36	8960	322549	1477,1
∑		147637	2818735	7608,7
EQY				
Story No	**Hi (m)**	**wi (kN)**	**Hi*wi (kN.m)**	**Fi (kN)**
1	3	12607	37821	92,9
2	6	12607	75642	185,8
3	9	12607	113463	278,7
4	12	12607	151284	371,6
5	15	12607	189105	464,5
6	18	12607	226926	557,4
7	21	12607	264747	650,3
8	24	12607	302568	743,2
9	27	12607	340389	836,1
10	30	12607	378210	929,0
11	33	12607	416031	1021,9
12	36	8960	322549	1477,1
∑		147637	2818735	7608,7

Table C.23 Seismic Load of Model 1210V11

EQX				
Story No	**Hi (m)**	**wi (kN)**	**Hi*wi (kN.m)**	**Fi (kN)**
1	3	12878	38634	64,9
2	6	12878	77267	129,8
3	9	12868	115815	194,6
4	12	12859	154306	259,2
5	15	12859	192882	324,0
6	18	12850	231294	388,6
7	21	12841	269652	453,0
8	24	12841	308174	517,7
9	27	12831	346444	582,0
10	30	12822	384660	646,2
11	33	12822	423126	710,9
12	36	9067	326419	1025,0
∑		150415	2868671	5296,1
EQY				
Story No	**Hi (m)**	**wi (kN)**	**Hi*wi (kN.m)**	**Fi (kN)**
1	3	12878	38634	64,9
2	6	12878	77267	129,8
3	9	12868	115815	194,6
4	12	12859	154306	259,2
5	15	12859	192882	324,0
6	18	12850	231294	388,6
7	21	12841	269652	453,0
8	24	12841	308174	517,7
9	27	12831	346444	582,0
10	30	12822	384660	646,2
11	33	12822	423126	710,9
12	36	9067	326419	1025,0
∑		150415	2868671	5296,1

Table C.24 Seismic Load of Model 1210V21

EQX				
Story No	**Hi (m)**	**wi (kN)**	**Hi*wi (kN.m)**	**Fi (kN)**
1	3	12999	38997	66,6
2	6	12999	77994	133,1
3	9	12985	116867	199,5
4	12	12971	155657	265,7
5	15	12971	194571	332,1
6	18	12957	233232	398,1
7	21	12943	271808	464,0
8	24	12943	310638	530,3
9	27	12928	349064	595,9
10	30	12913	387401	661,3
11	33	12913	426141	727,4
12	36	9113	328064	1048,0
∑		151638	2890432	5421,9
EQY				
Story No	**Hi (m)**	**wi (kN)**	**Hi*wi (kN.m)**	**Fi (kN)**
1	3	12999	38997	75,3
2	6	12999	77994	150,7
3	9	12985	116867	225,7
4	12	12971	155657	300,7
5	15	12971	194571	375,8
6	18	12957	233232	450,5
7	21	12943	271808	525,0
8	24	12943	310638	600,0
9	27	12928	349064	674,3
10	30	12913	387401	748,3
11	33	12913	426141	823,1
12	36	9113	328064	1185,9
∑		151638	2890432	6135,3

Table C.25 Seismic Load of Model 1210V22

EQX				
Story No	**Hi (m)**	**wi (kN)**	**Hi*wi (kN.m)**	**Fi (kN)**
1	3	13258	39773	74,3
2	6	13258	79545	148,6
3	9	13236	119126	222,5
4	12	13215	158580	296,2
5	15	13215	198225	370,3
6	18	13187	237359	443,4
7	21	13158	276322	516,2
8	24	13158	315797	589,9
9	27	13138	354739	662,7
10	30	13119	393562	735,2
11	33	13119	432918	808,7
12	36	9216	331760	1162,5
∑		154276	2937705	6030,5
EQY				
Story No	**Hi (m)**	**wi (kN)**	**Hi*wi (kN.m)**	**Fi (kN)**
1	3	13258	39773	74,3
2	6	13258	79545	148,6
3	9	13236	119126	222,5
4	12	13215	158580	296,2
5	15	13215	198225	370,3
6	18	13187	237359	443,4
7	21	13158	276322	516,2
8	24	13158	315797	589,9
9	27	13138	354739	662,7
10	30	13119	393562	735,2
11	33	13119	432918	808,7
12	36	9216	331760	1162,5
∑		154276	2937705	6030,5

Table C.26 Seismic Load of Model 1210X11

EQX				
Story No	**Hi (m)**	**wi (kN)**	**Hi*wi (kN.m)**	**Fi (kN)**
1	3	12890	38669	65,5
2	6	12890	77338	131,0
3	9	12878	115906	196,3
4	12	12867	154407	261,5
5	15	12867	193009	326,9
6	18	12857	231432	392,0
7	21	12847	269795	456,9
8	24	12847	308338	522,2
9	27	12824	346256	586,5
10	30	12801	384036	650,4
11	33	12801	422440	715,5
12	36	9057	326045	1032,6
∑		150428	2867671	5337,3
EQY				
Story No	**Hi (m)**	**wi (kN)**	**Hi*wi (kN.m)**	**Fi (kN)**
1	3	12890	38669	65,5
2	6	12890	77338	131,0
3	9	12878	115906	196,3
4	12	12867	154407	261,5
5	15	12867	193009	326,9
6	18	12857	231432	392,0
7	21	12847	269795	456,9
8	24	12847	308338	522,2
9	27	12824	346256	586,5
10	30	12801	384036	650,4
11	33	12801	422440	715,5
12	36	9057	326045	1032,6
∑		150428	2867671	5337,3

Table C.27 Seismic Load of Model 1210X21

EQX				
Story No	**Hi (m)**	**wi (kN)**	**Hi*wi (kN.m)**	**Fi (kN)**
1	3	13057	39172	70,2
2	6	13057	78345	140,3
3	9	13037	117334	210,2
4	12	13017	156202	279,8
5	15	13017	195252	349,7
6	18	13001	234013	419,1
7	21	12985	272679	488,4
8	24	12985	311633	558,2
9	27	12962	349980	626,8
10	30	12940	388192	695,3
11	33	12940	427011	764,8
12	36	9126	328538	1101,9
∑		152124	2898350	5704,6
EQY				
Story No	**Hi (m)**	**wi (kN)**	**Hi*wi (kN.m)**	**Fi (kN)**
1	3	13057	39172	71,9
2	6	13057	78345	143,8
3	9	13037	117334	215,4
4	12	13017	156202	286,8
5	15	13017	195252	358,5
6	18	13001	234013	429,6
7	21	12985	272679	500,6
8	24	12985	311633	572,1
9	27	12962	349980	642,5
10	30	12940	388192	712,7
11	33	12940	427011	783,9
12	36	9126	328538	1129,4
∑		152124	2898350	5847,2

Table C.28 Seismic Load of Model 1210X22

EQX				
Story No	**Hi (m)**	**wi (kN)**	**Hi*wi (kN.m)**	**Fi (kN)**
1	3	13185	39556	74,5
2	6	13185	79112	149,0
3	9	13159	118435	223,1
4	12	13134	157602	296,9
5	15	13134	197003	371,1
6	18	13113	236033	444,6
7	21	13092	274940	517,9
8	24	13092	314217	591,9
9	27	13072	352931	664,8
10	30	13051	391519	737,5
11	33	13051	430671	811,2
12	36	9182	330535	1167,1
∑		153449	2922553	6049,4
EQY				
Story No	**Hi (m)**	**wi (kN)**	**Hi*wi (kN.m)**	**Fi (kN)**
1	3	13185	39556	74,5
2	6	13185	79112	149,0
3	9	13159	118435	223,1
4	12	13134	157602	296,9
5	15	13134	197003	371,1
6	18	13113	236033	444,6
7	21	13092	274940	517,9
8	24	13092	314217	591,9
9	27	13072	352931	664,8
10	30	13051	391519	737,5
11	33	13051	430671	811,2
12	36	9182	330535	1167,1
∑		153449	2922553	6049,4

D. RESULTS OF PUSHOVER ANALYSIS

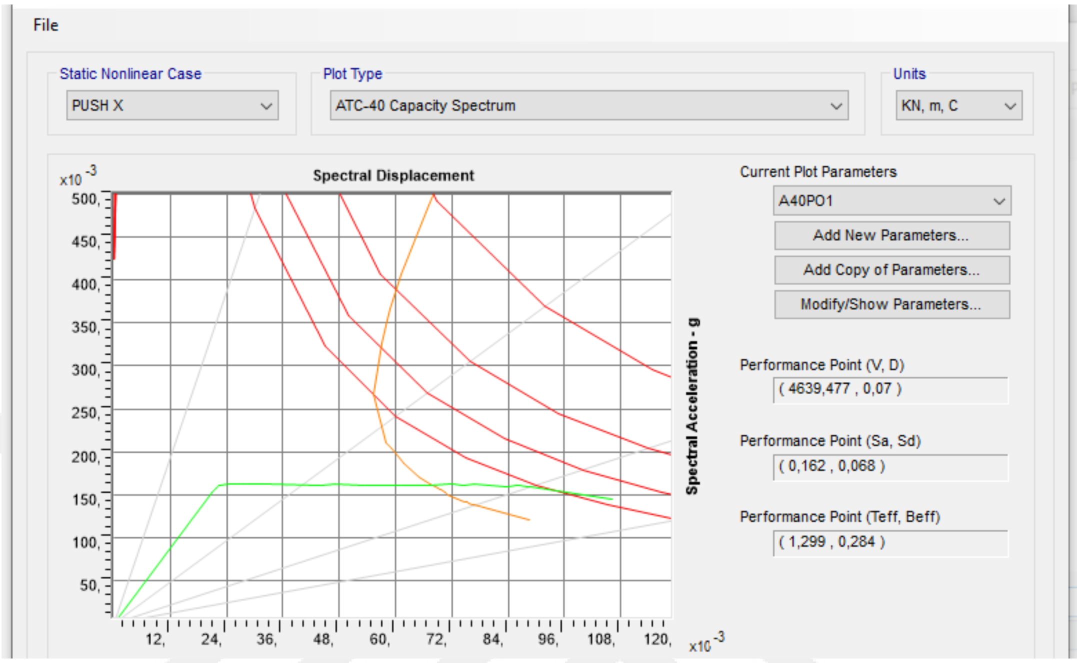

Figure D.1 Performance Point based on Pushover Analysis in X-Direction for Model 310

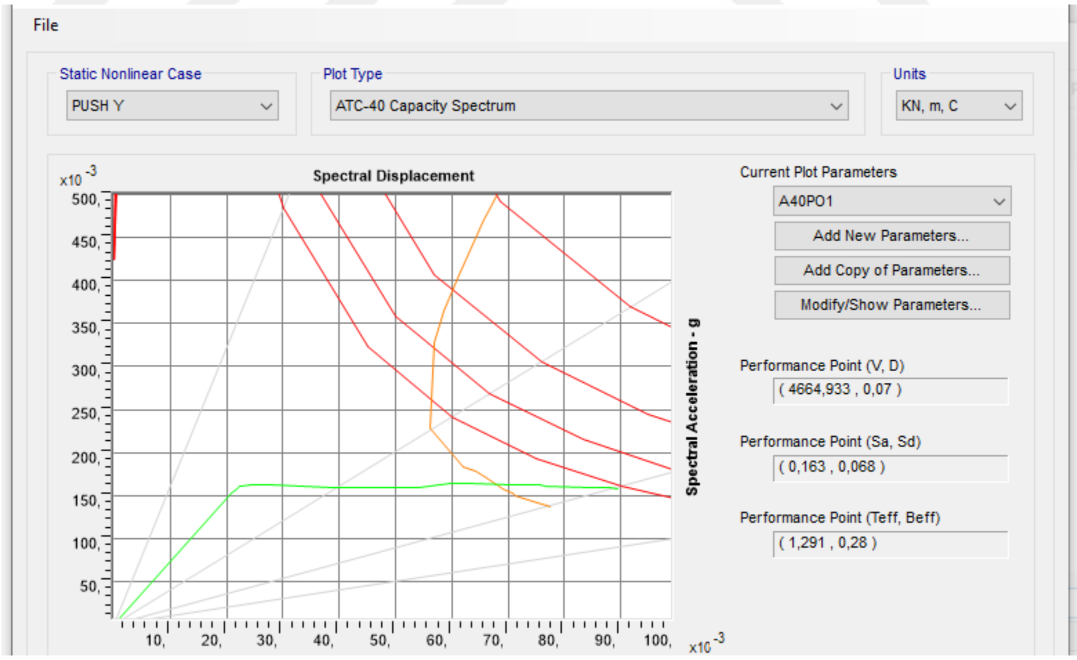

Figure D.2 Performance Point based on Pushover Analysis in Y-Direction for Model 310

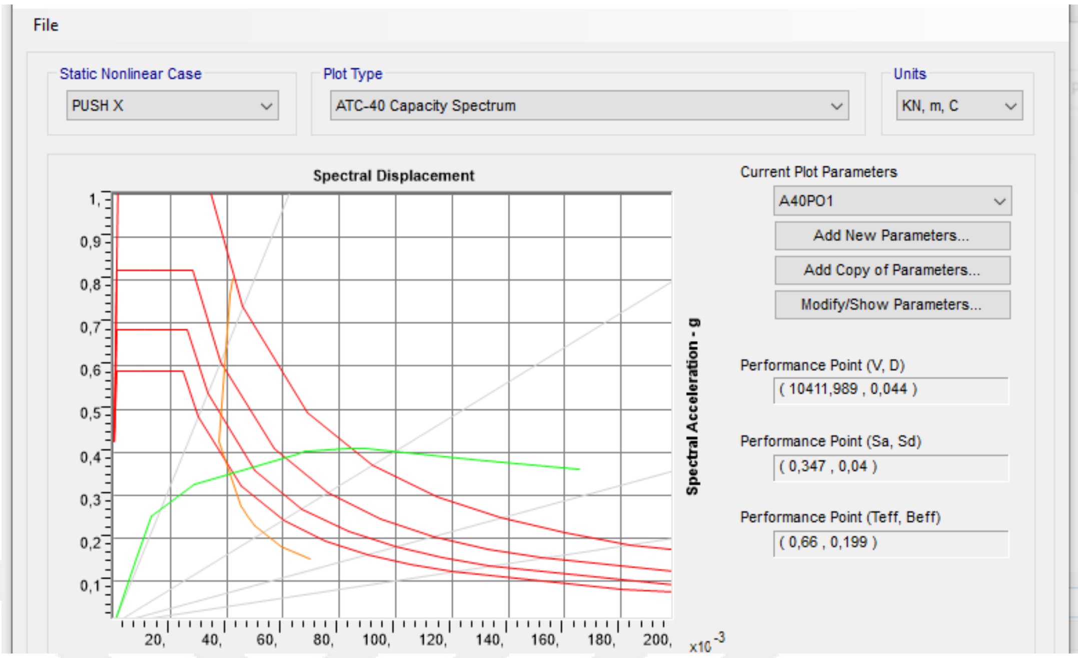

Figure D.3 Performance Point based on Pushover Analysis in X-Direction for Model 310V11

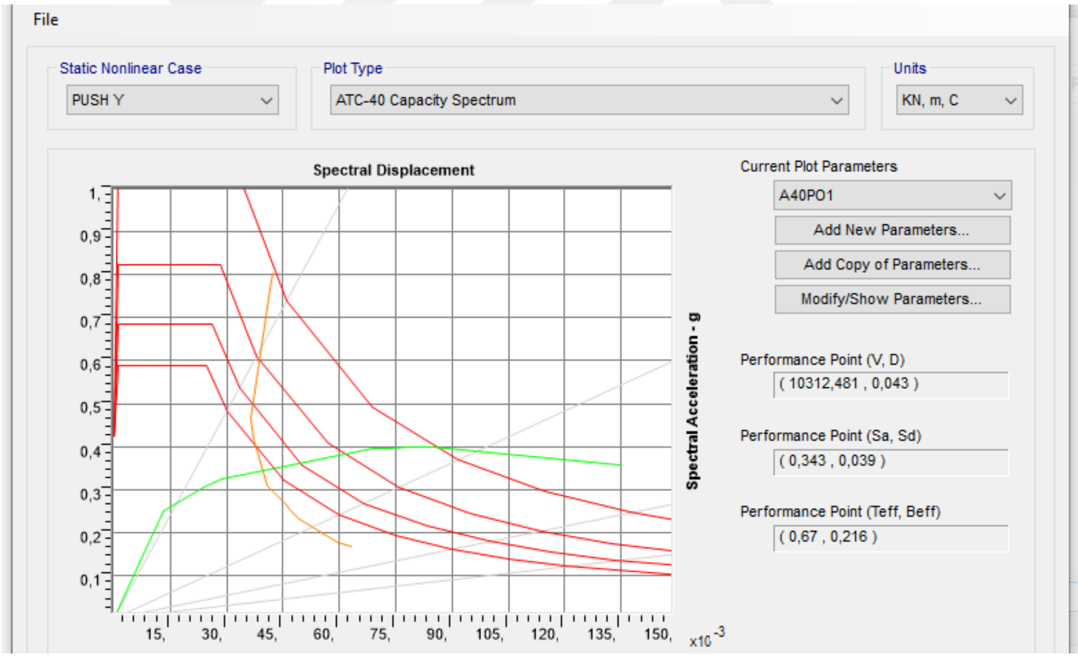

Figure D.4 Performance Point based on Pushover Analysis in Y-Direction for Model 310V11

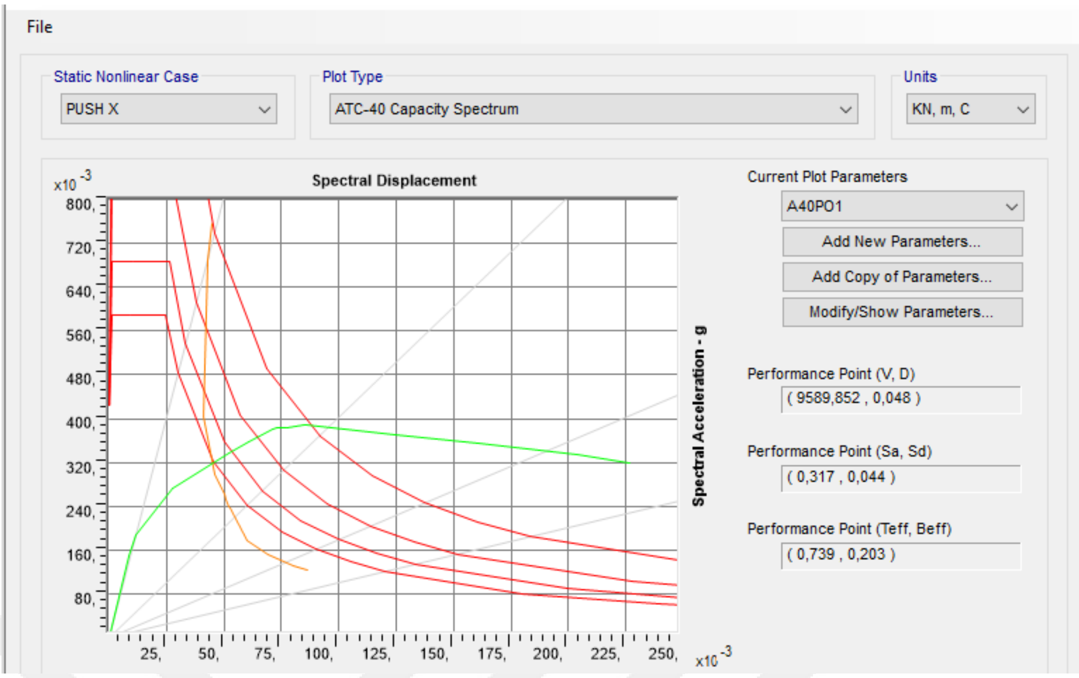

Figure D.5 Performance Point based on Pushover Analysis in X-Direction for Model 310V21

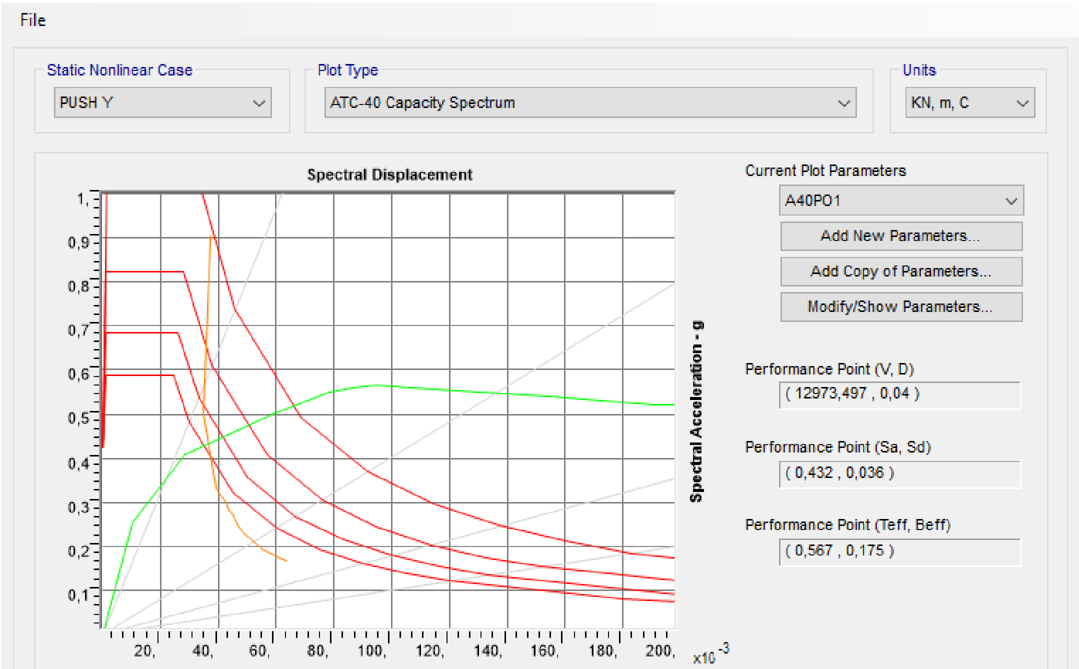

Figure D.6 Performance Point based on Pushover Analysis in Y-Direction for Model 310V21

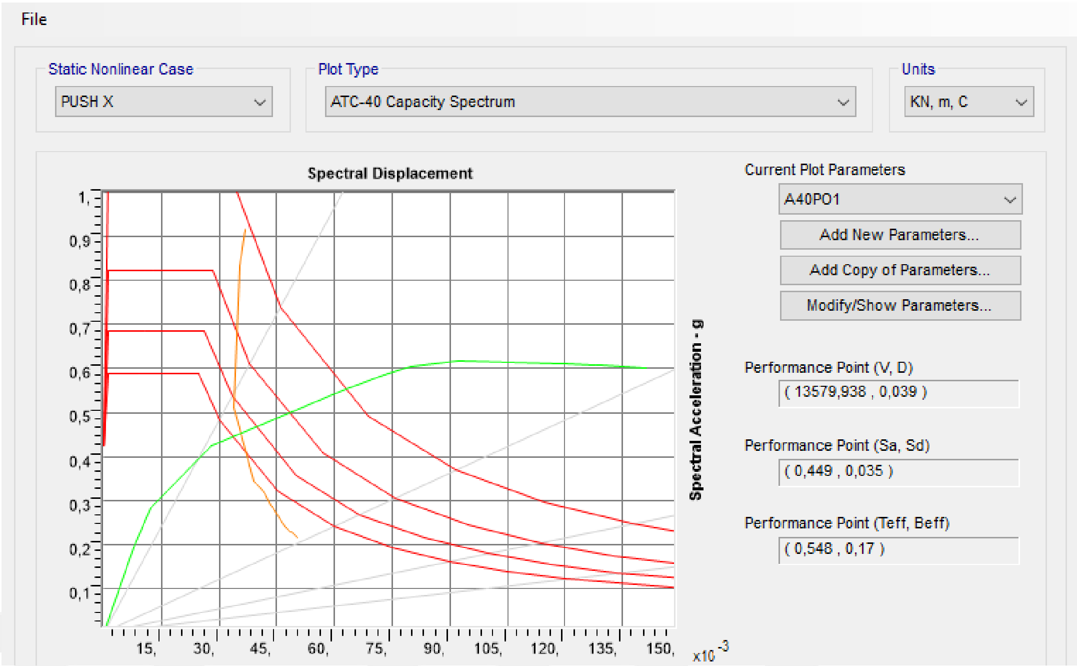

Figure D.7 Performance Point based on Pushover Analysis in X-Direction for Model 310V22

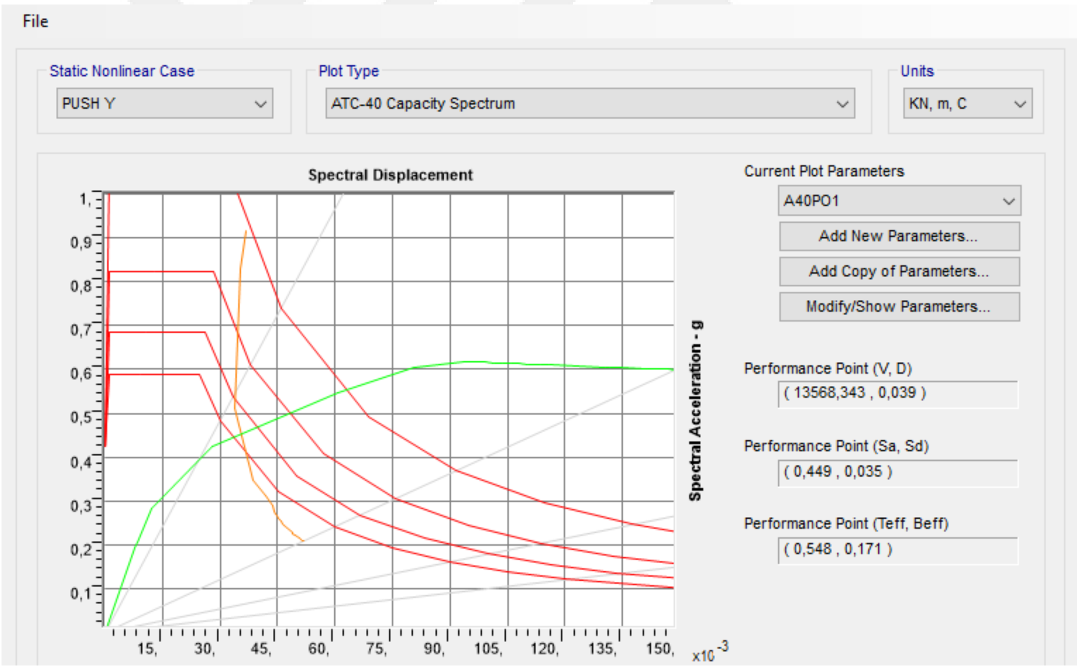

Figure D.8 Performance Point based on Pushover Analysis in Y-Direction for Model 310V22

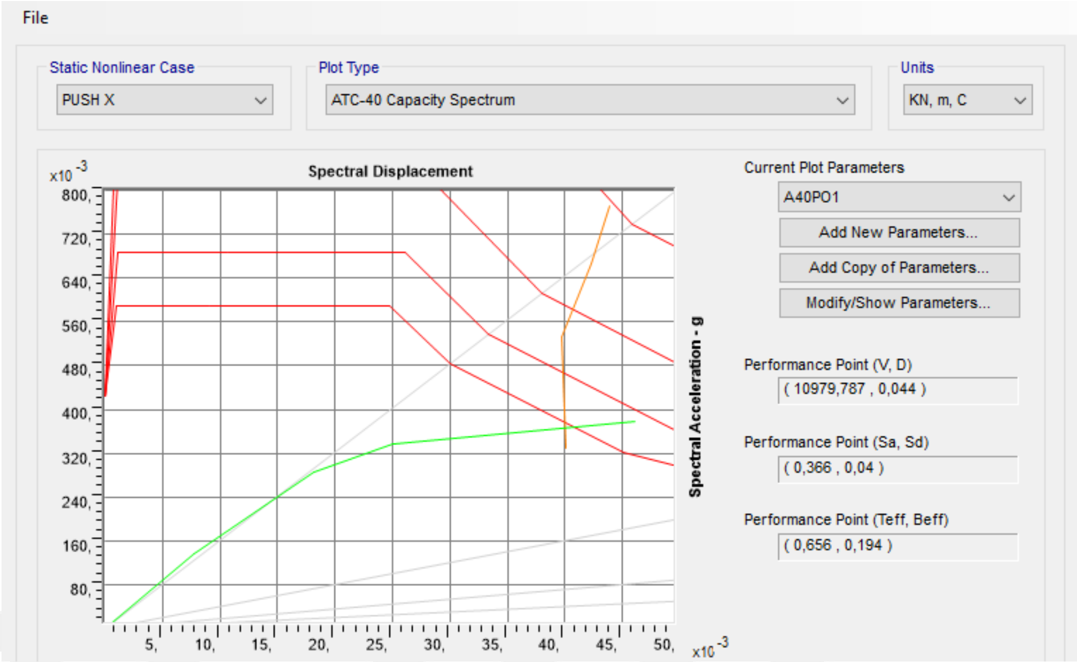

Figure D.9 Performance Point based on Pushover Analysis in X-Direction for Model 310X11

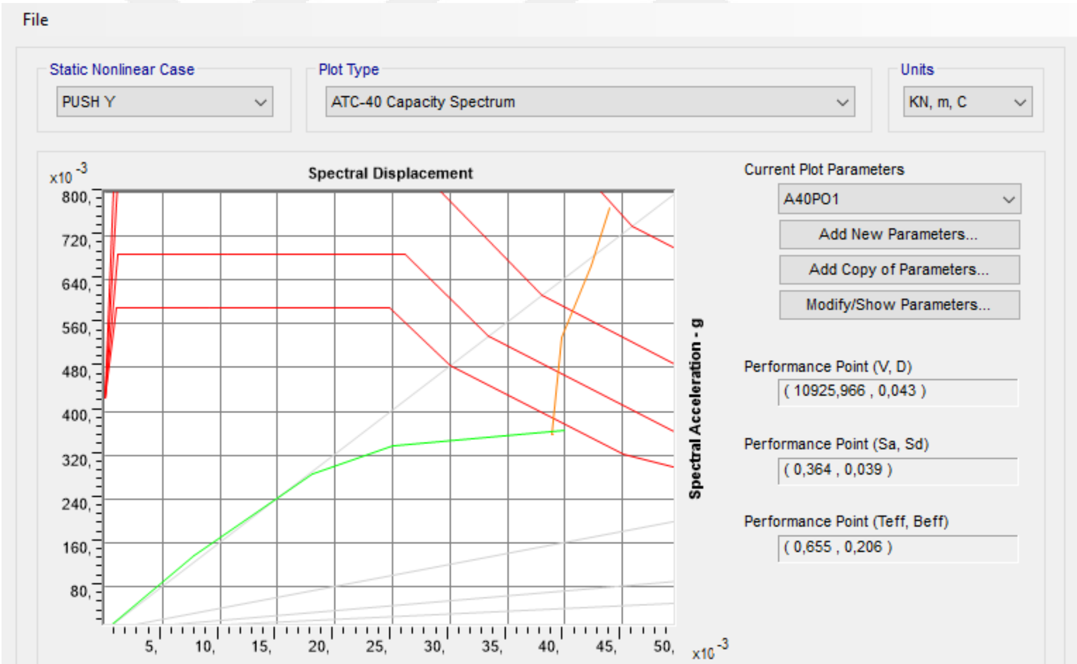

Figure D.10 Performance Point based on Pushover Analysis in Y-Direction for Model 310X11

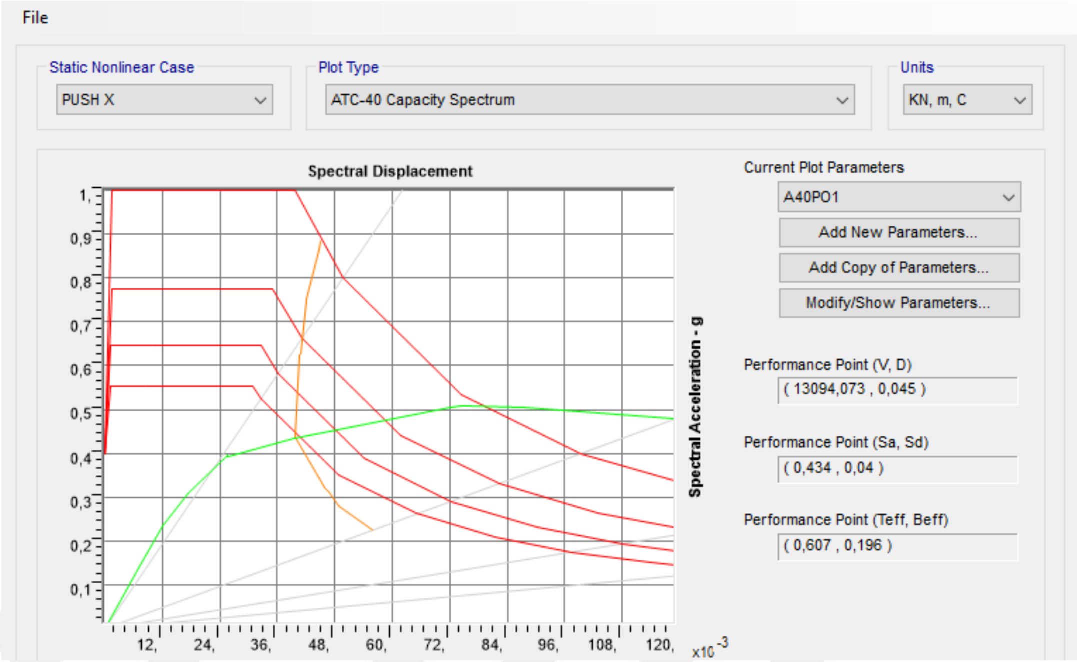

Figure D.11 Performance Point based on Pushover Analysis in X-Direction for Model 310X21

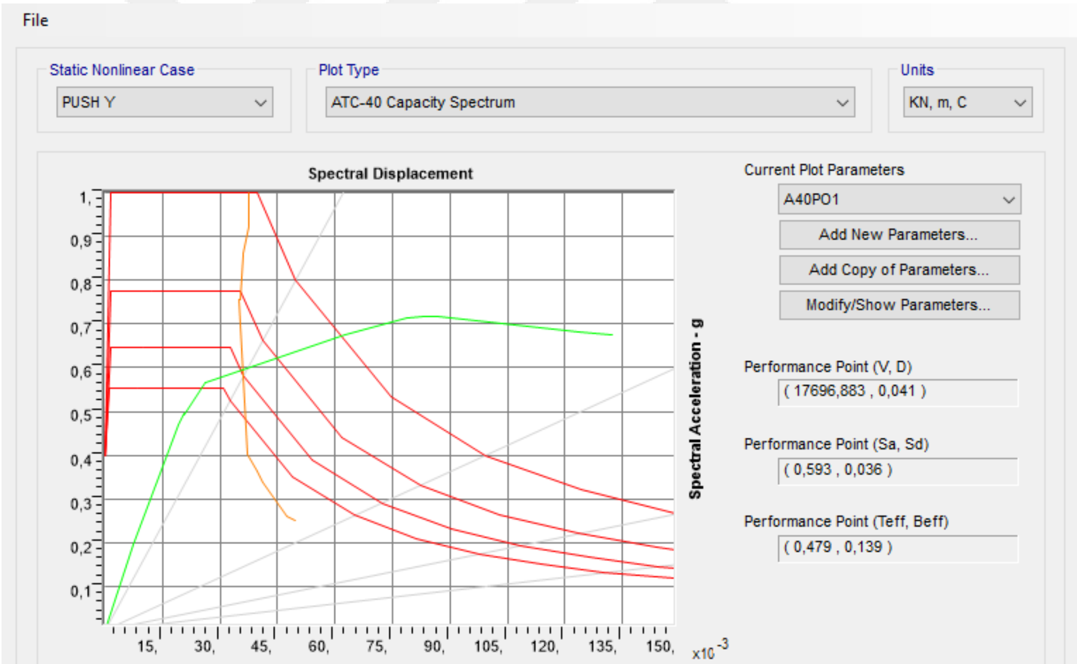

Figure D.12 Performance Point based on Pushover Analysis in Y-Direction for Model 310X21

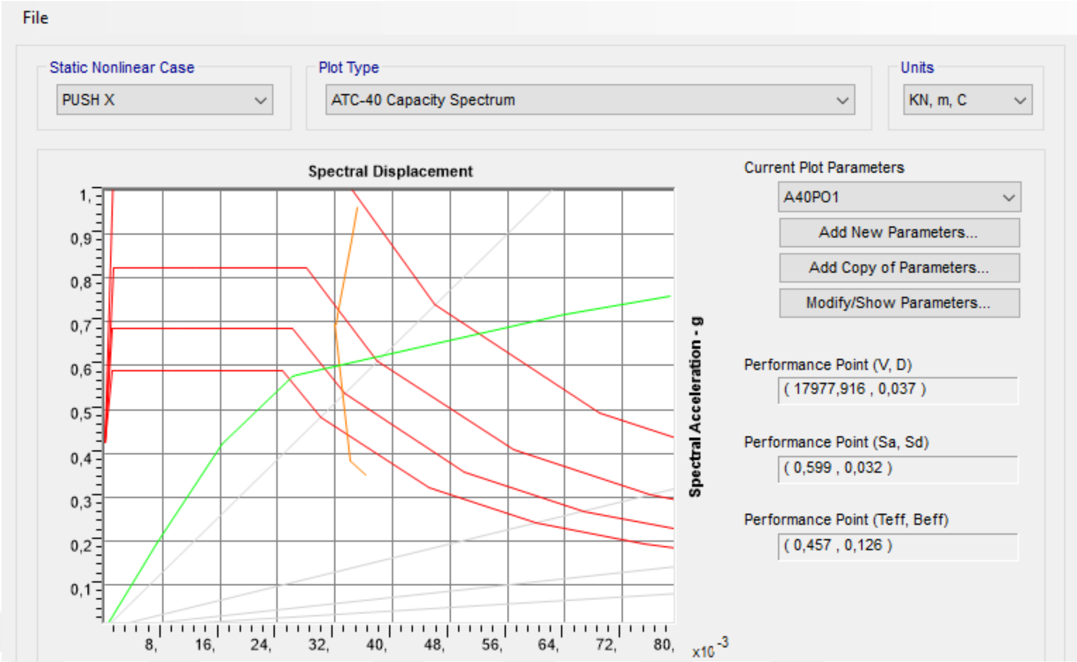

Figure D.13 Performance Point based on Pushover Analysis in X-Direction for Model 310X22

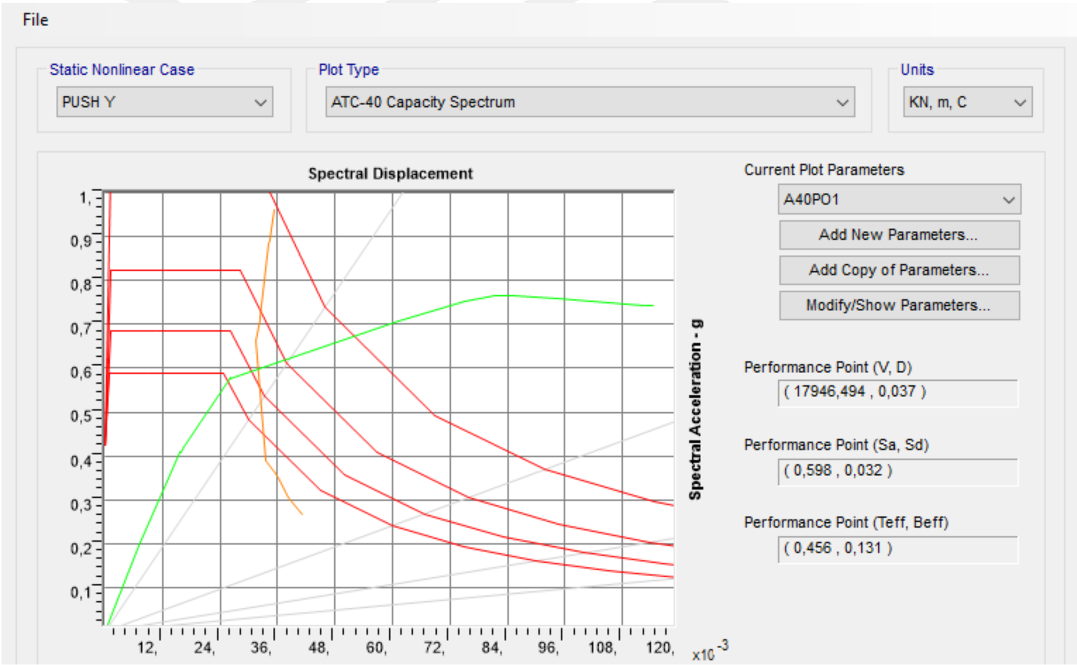

Figure D.14 Performance Point based on Pushover Analysis in Y-Direction for Model 310X22

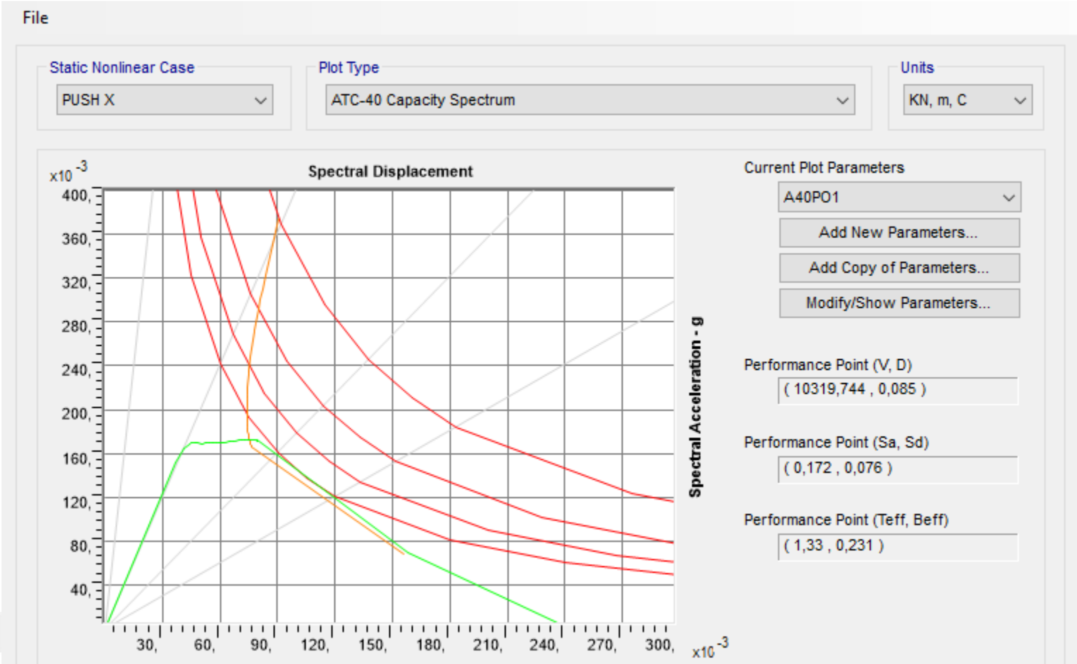

Figure D.15 Performance Point based on Pushover Analysis in X-Direction for Model 610

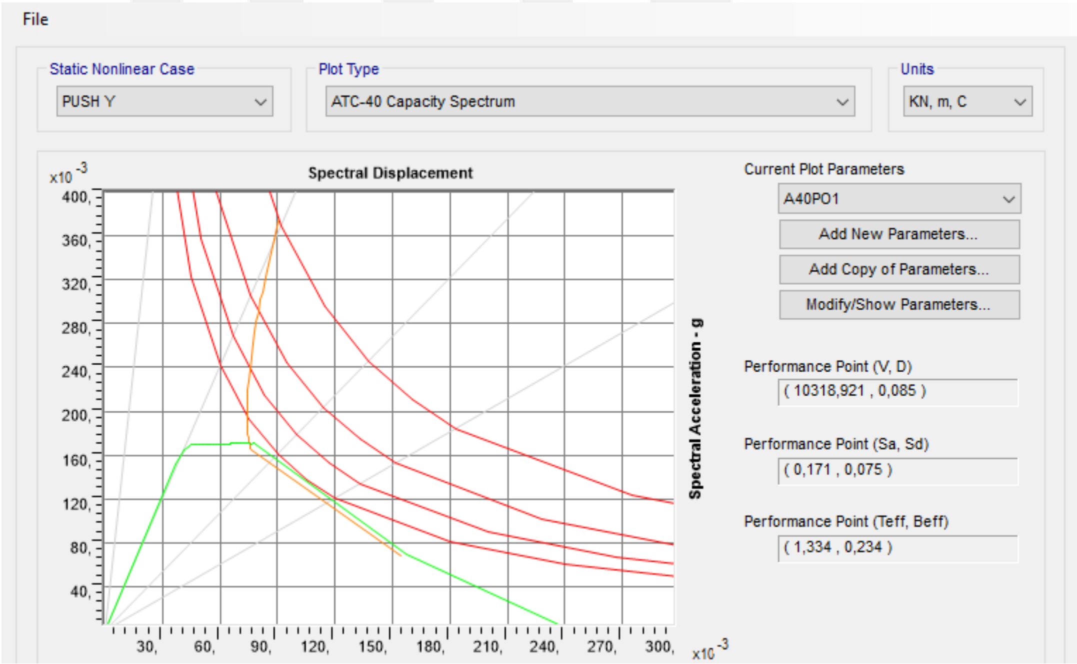

Figure D.16 Performance Point based on Pushover Analysis in Y-Direction for Model 610

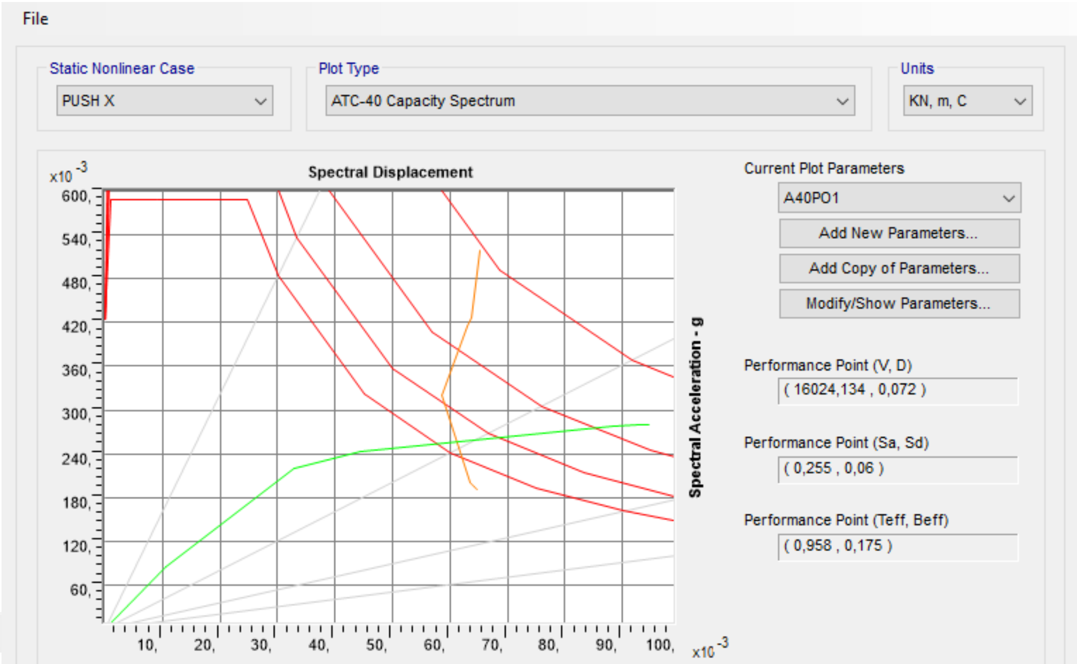

Figure D.17 Performance Point based on Pushover Analysis in X-Direction for Model 610V11

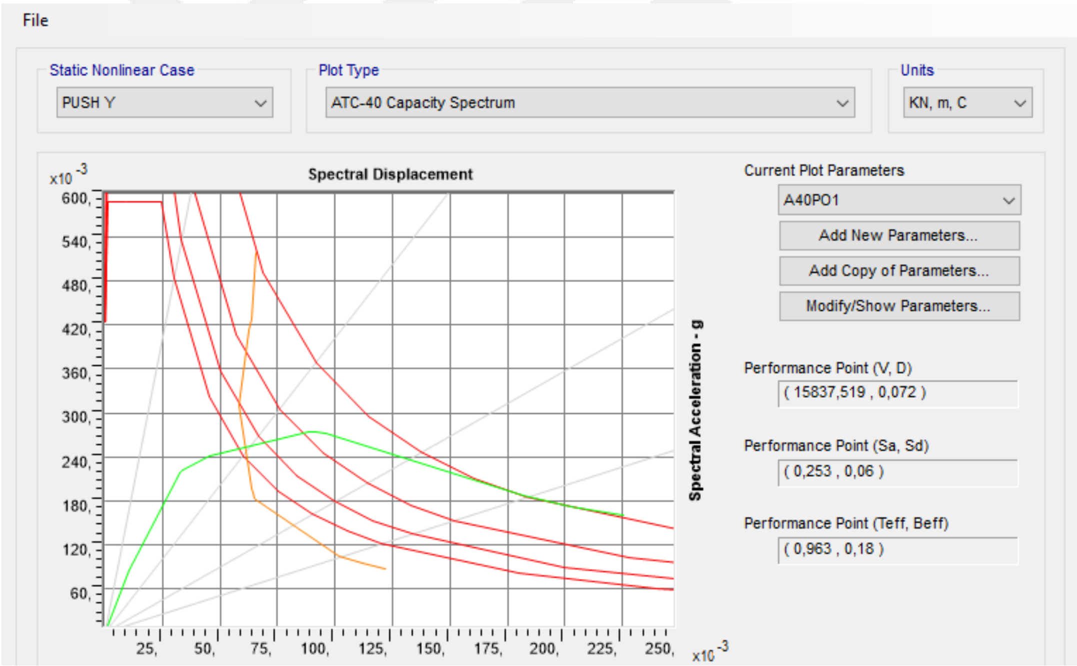

Figure D.18 Performance Point based on Pushover Analysis in Y-Direction for Model 610V11

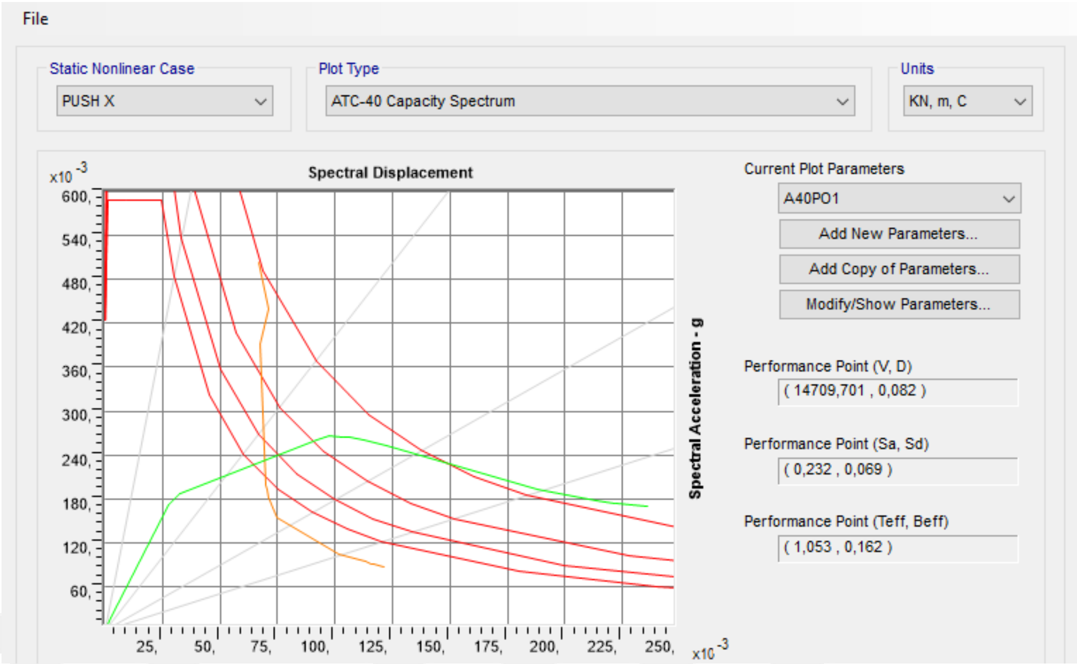

Figure D.19 Performance Point based on Pushover Analysis in X-Direction for Model 610V21

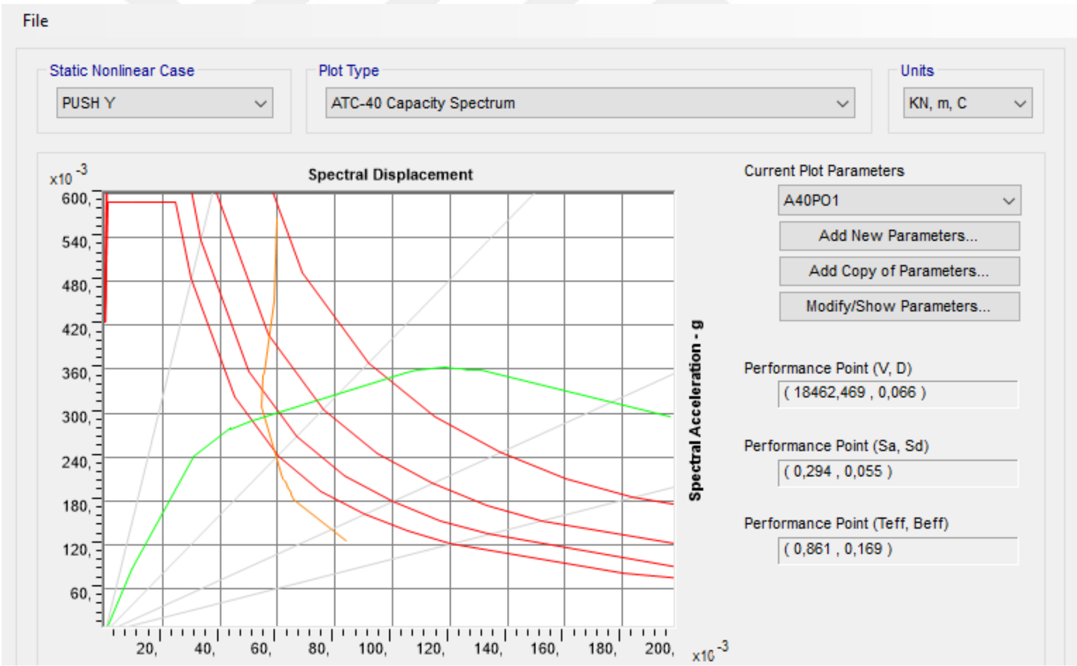

Figure D.20 Performance Point based on Pushover Analysis in Y-Direction for Model 610V21

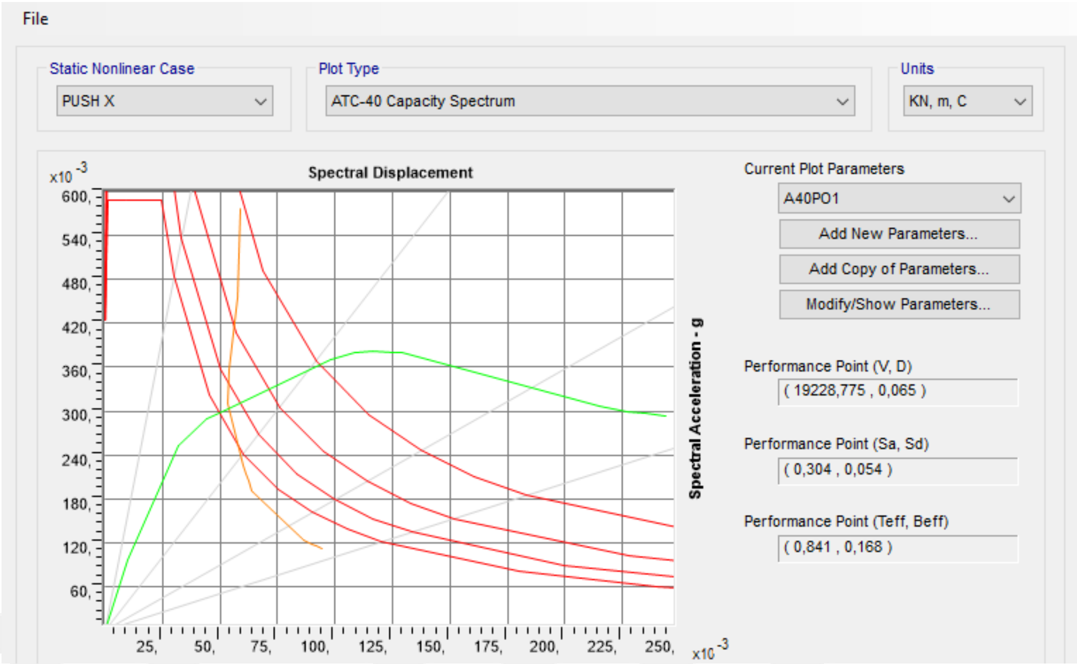

Figure D.21 Performance Point based on Pushover Analysis in X-Direction for Model 610V22

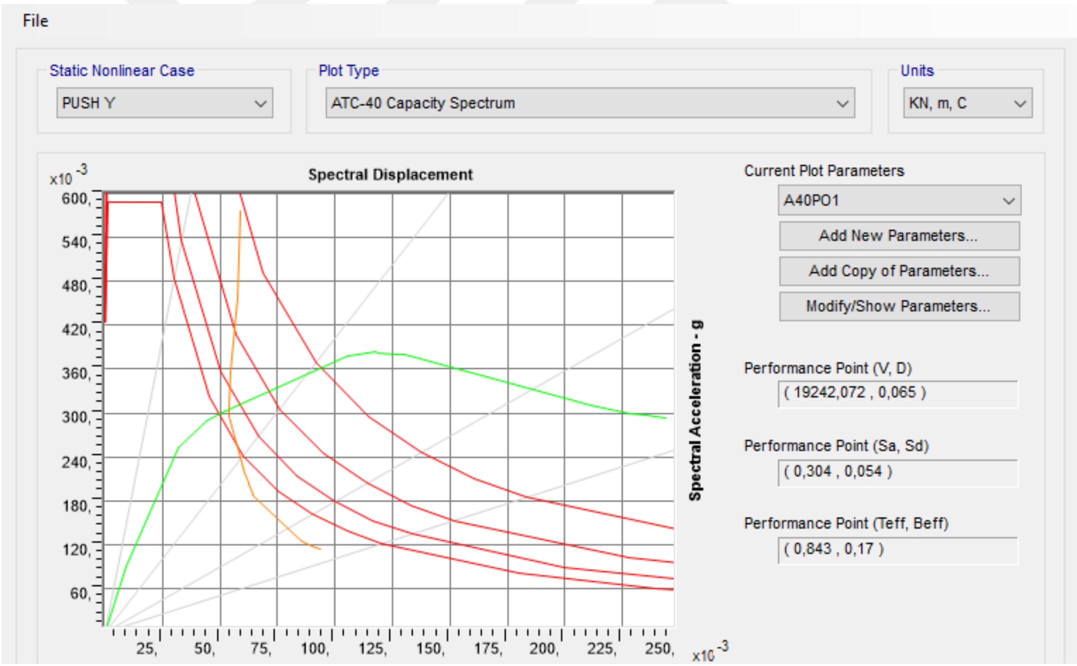

Figure D.22 Performance Point based on Pushover Analysis in Y-Direction for Model 610V22

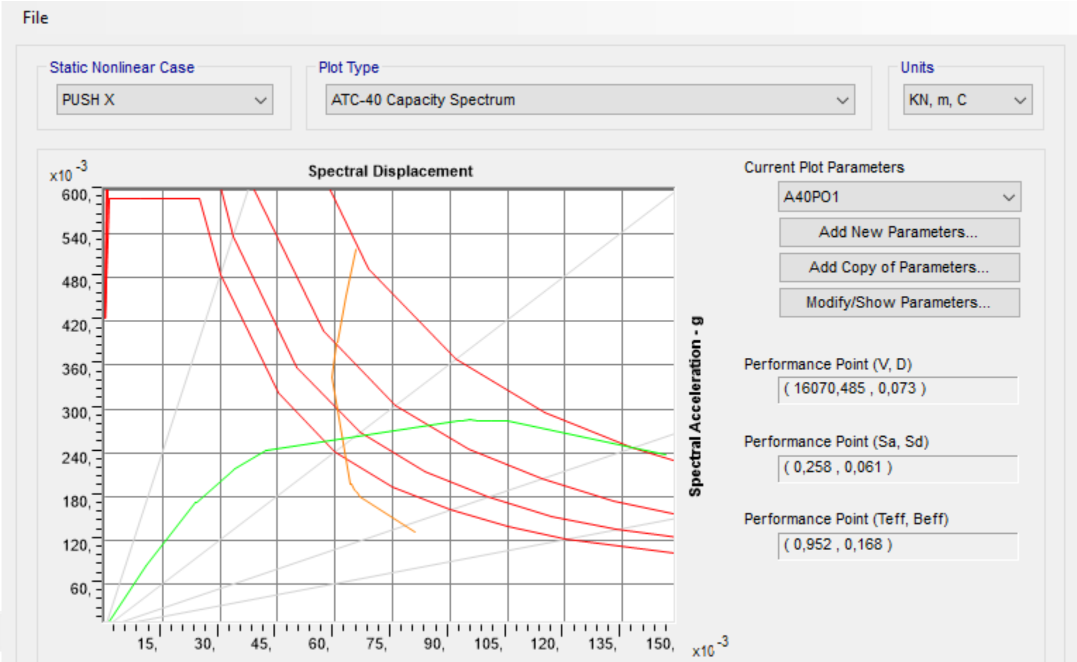

Figure D.23 Performance Point based on Pushover Analysis in X-Direction for Model 610X11

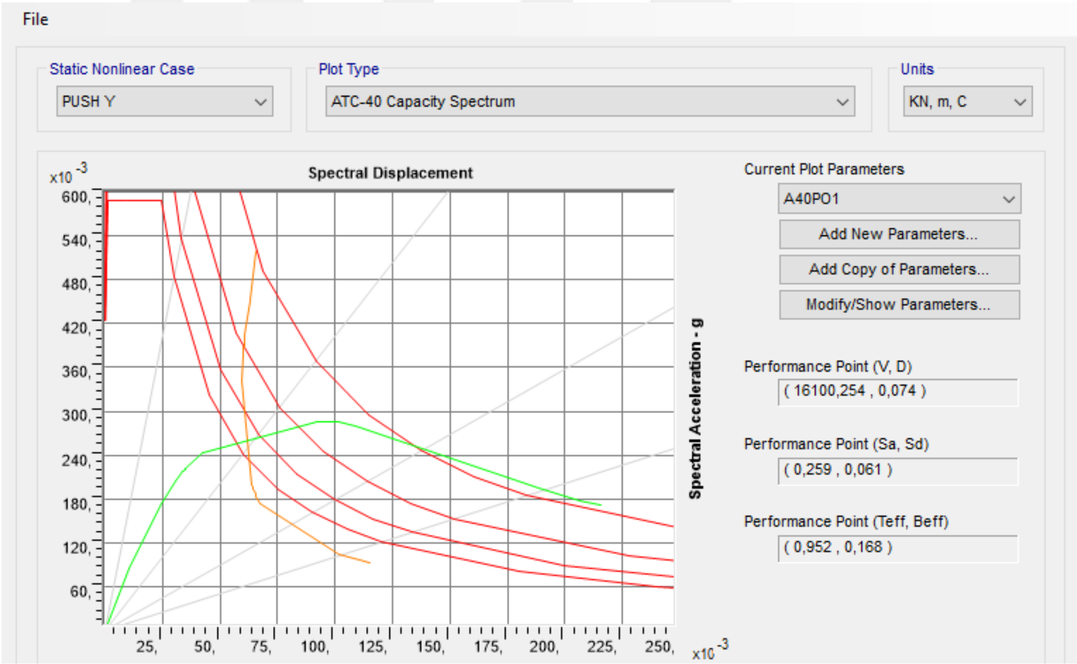

Figure D.24 Performance Point based on Pushover Analysis in Y-Direction for Model 610X11

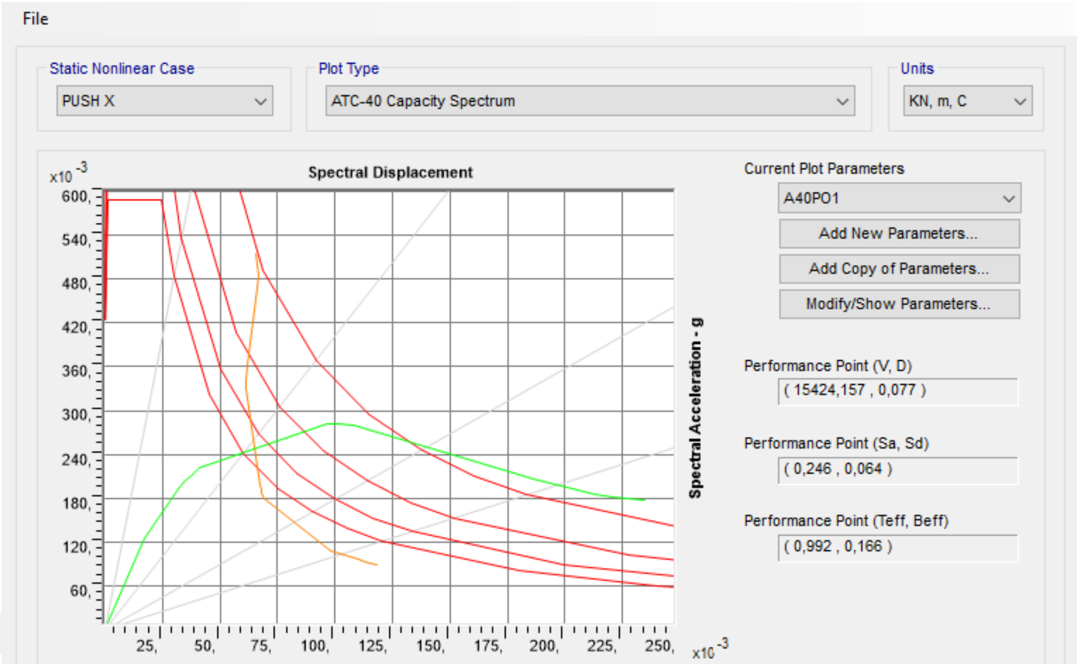

Figure D.25 Performance Point based on Pushover Analysis in X-Direction for Model 610X21

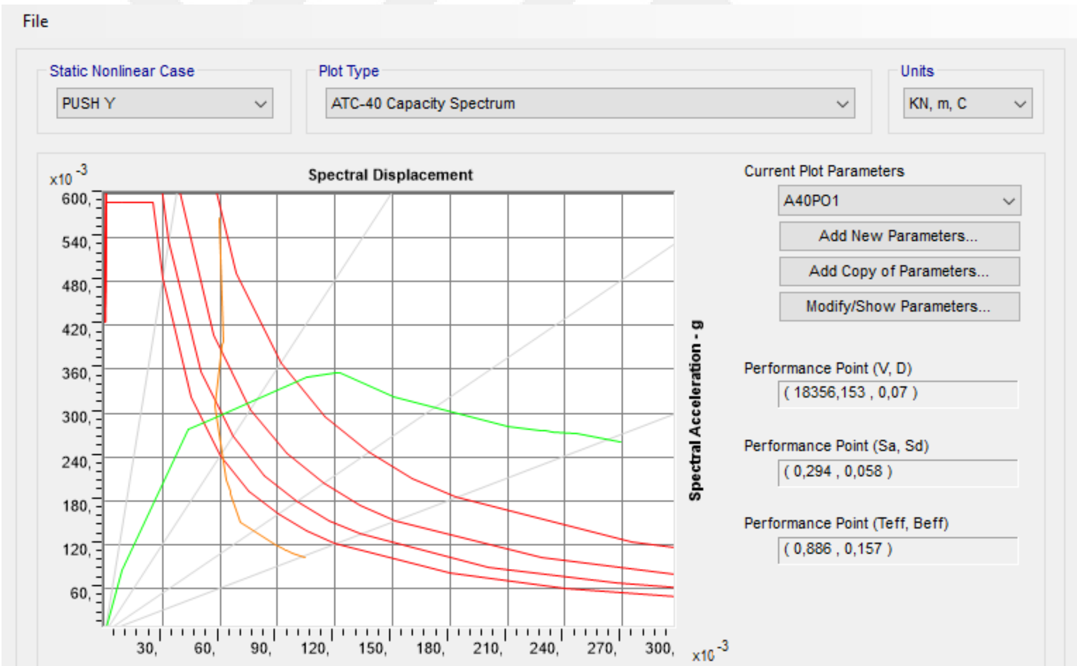

Figure D.26 Performance Point based on Pushover Analysis in Y-Direction for Model 610X21

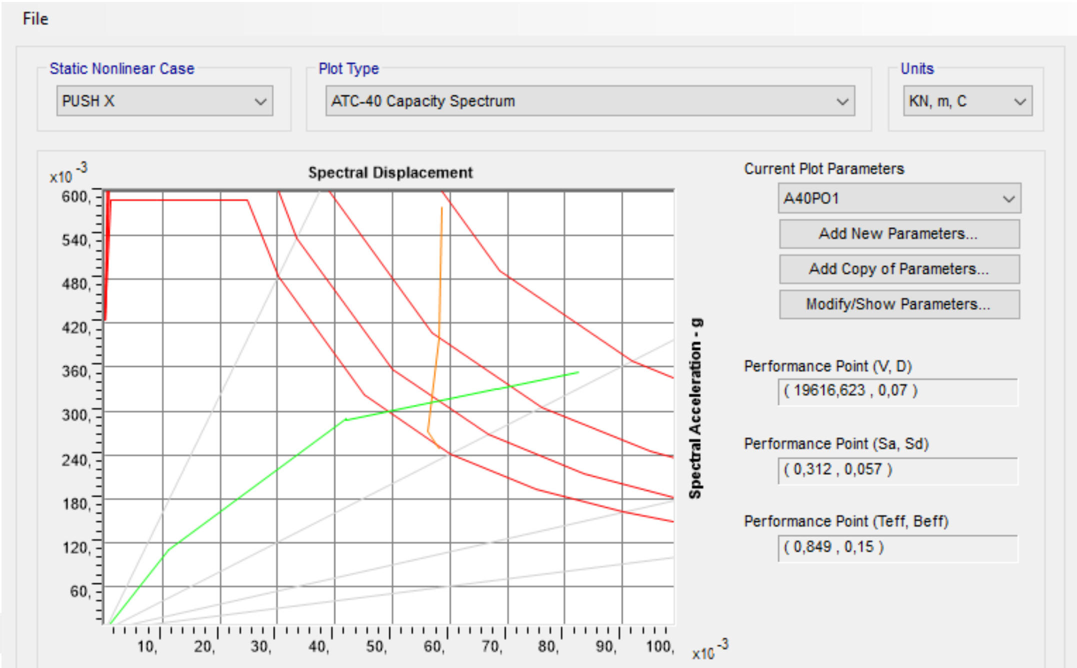

Figure D.27 Performance Point based on Pushover Analysis in X-Direction for Model 610X22

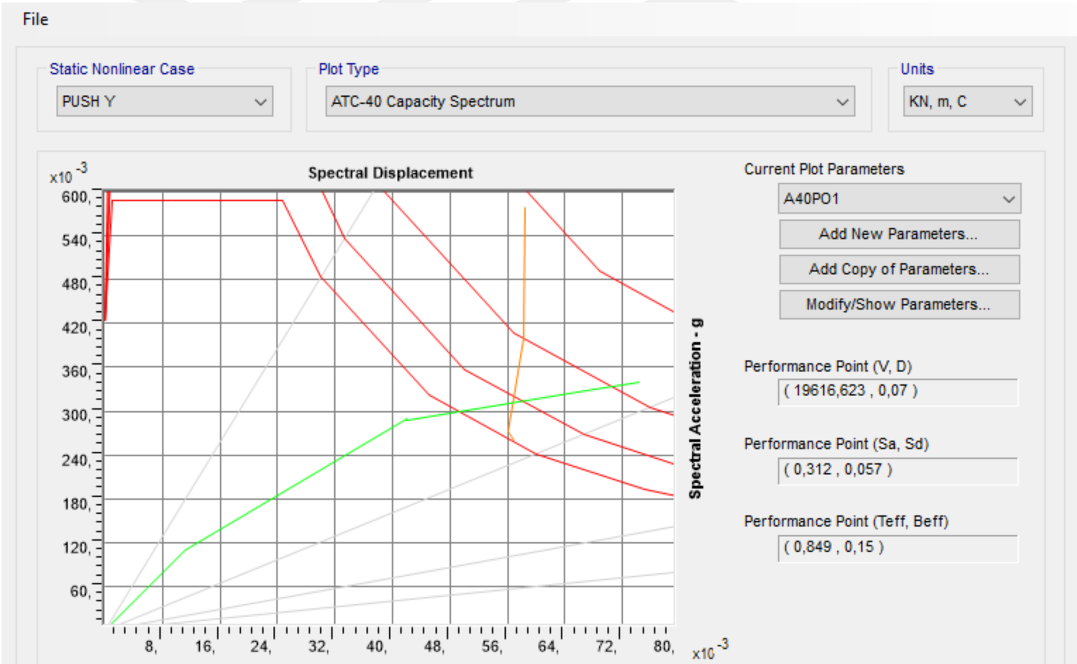

Figure D.28 Performance Point based on Pushover Analysis in Y-Direction for Model 610X22

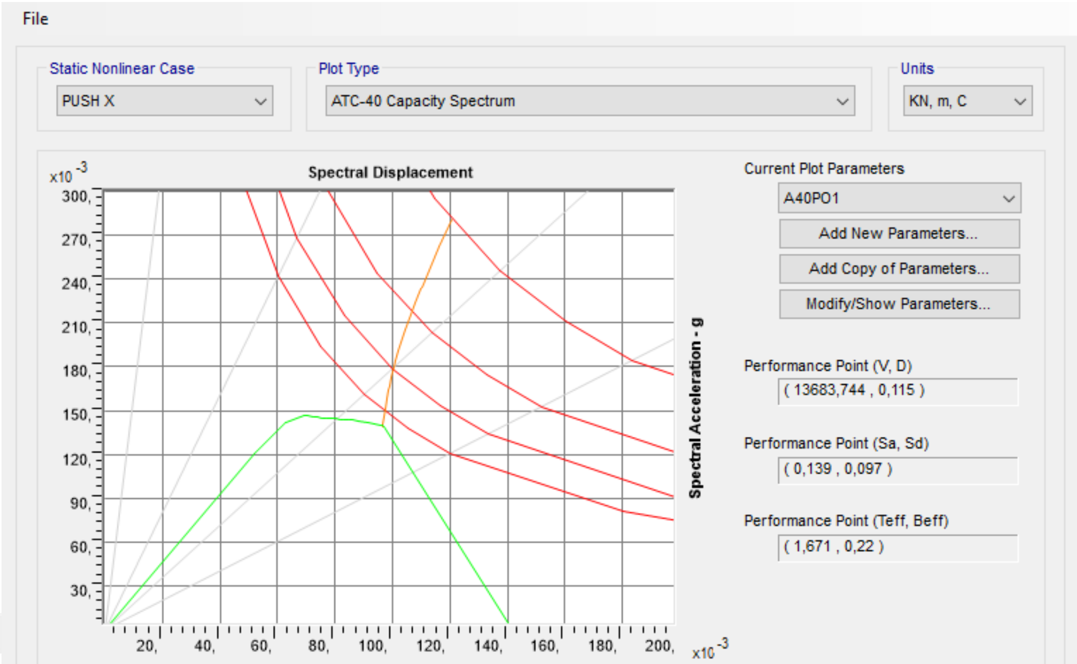

Figure D.29 Performance Point based on Pushover Analysis in X-Direction for Model 910

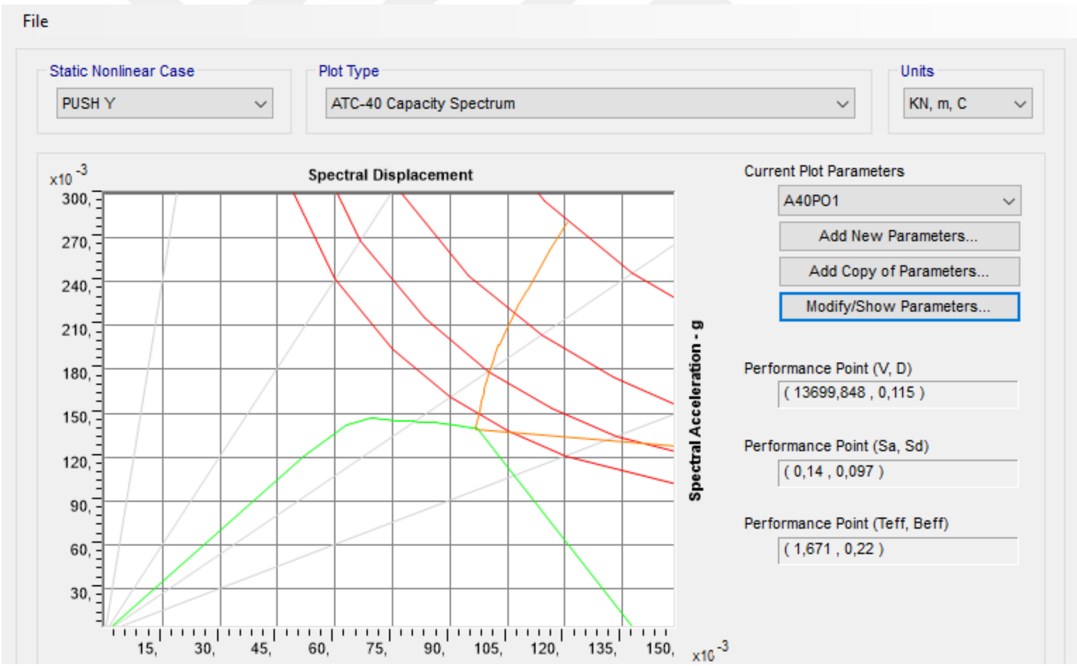

Figure D.30 Performance Point based on Pushover Analysis in Y-Direction for Model 910

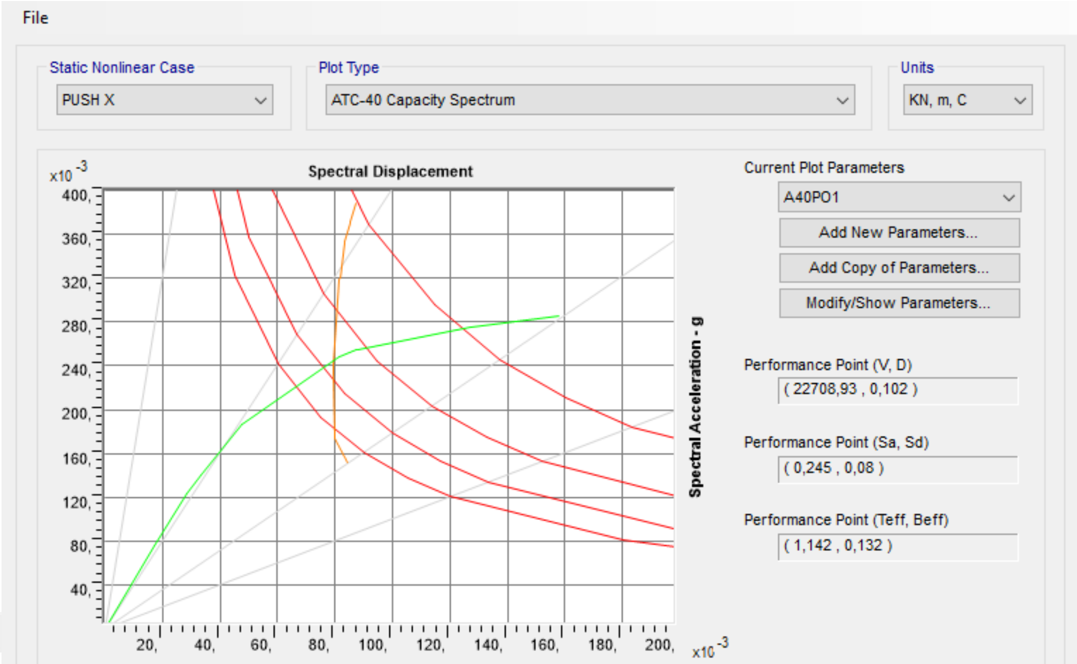

Figure D.31 Performance Point based on Pushover Analysis in X-Direction for Model 910V11

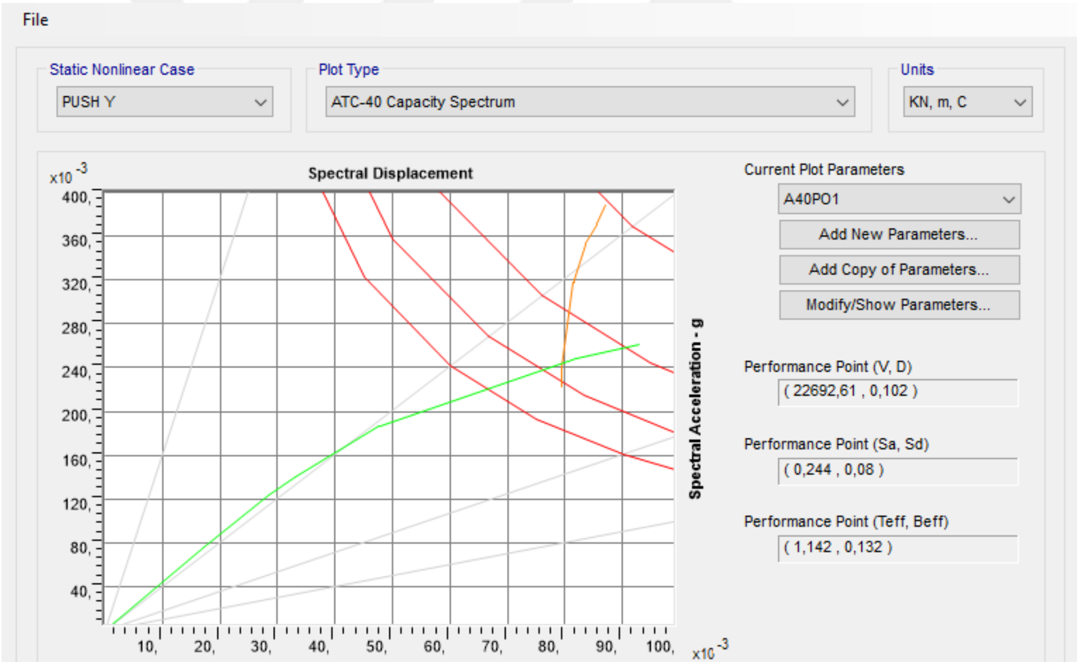

Figure D.32 Performance Point based on Pushover Analysis in Y-Direction for Model 910V11

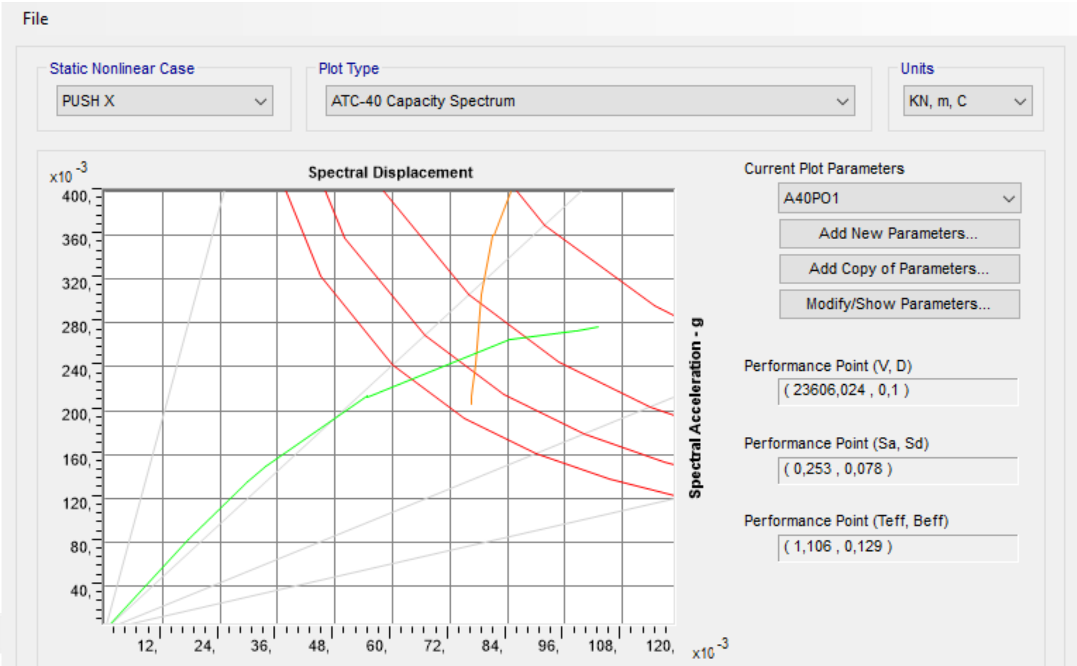

Figure D.33 Performance Point based on Pushover Analysis in X-Direction for Model 910V21

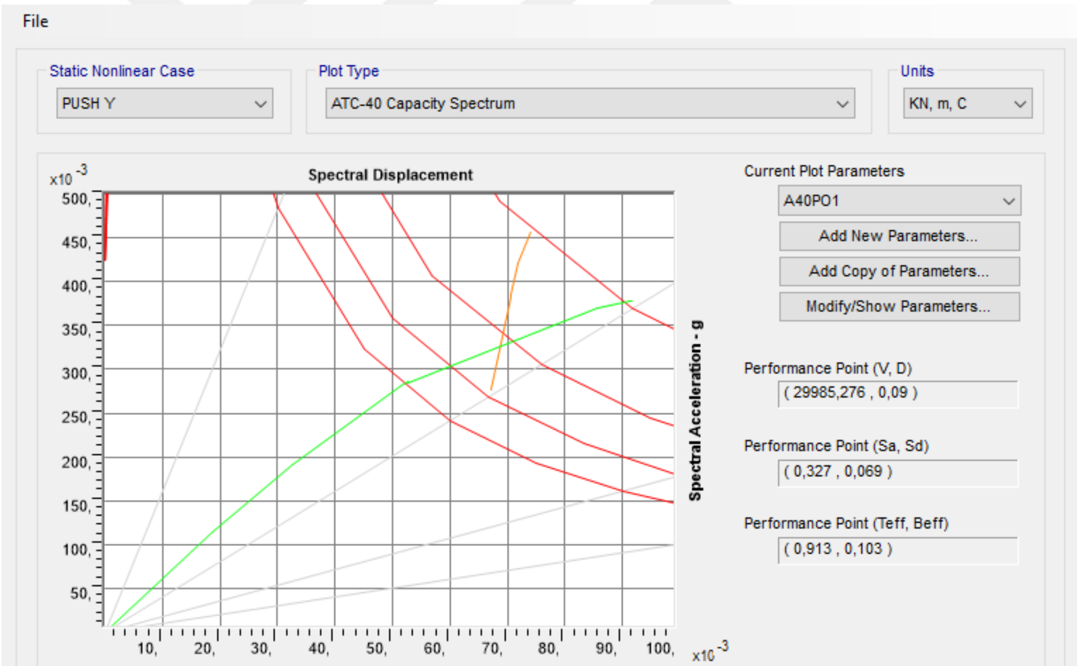

Figure D.34 Performance Point based on Pushover Analysis in Y-Direction for Model 910V21

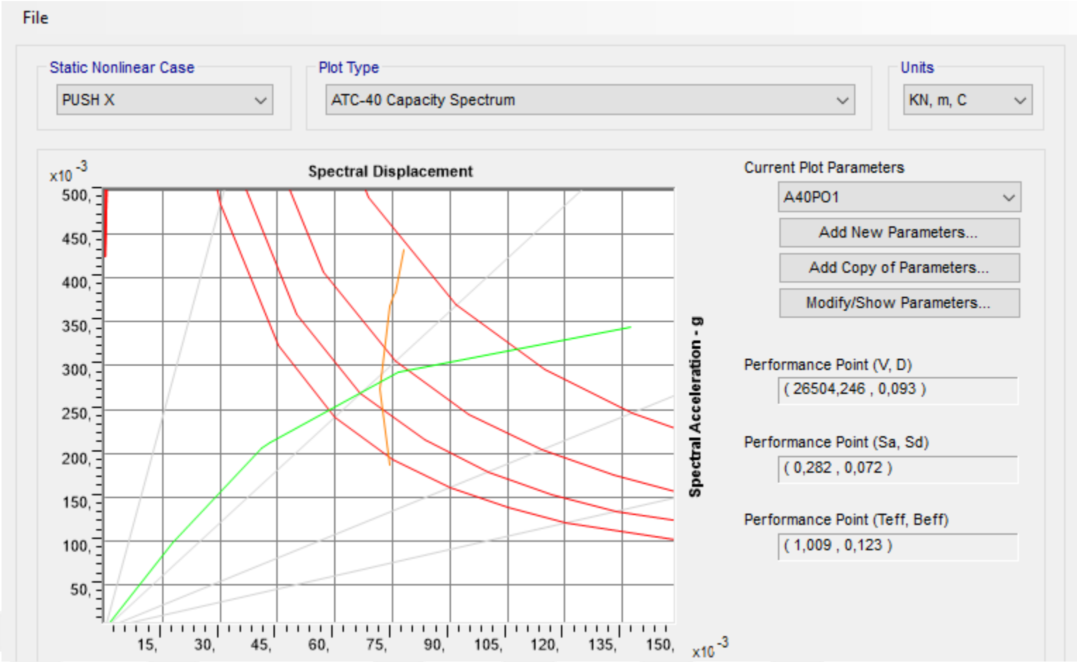

Figure D.35 Performance Point based on Pushover Analysis in X-Direction for Model 910V22

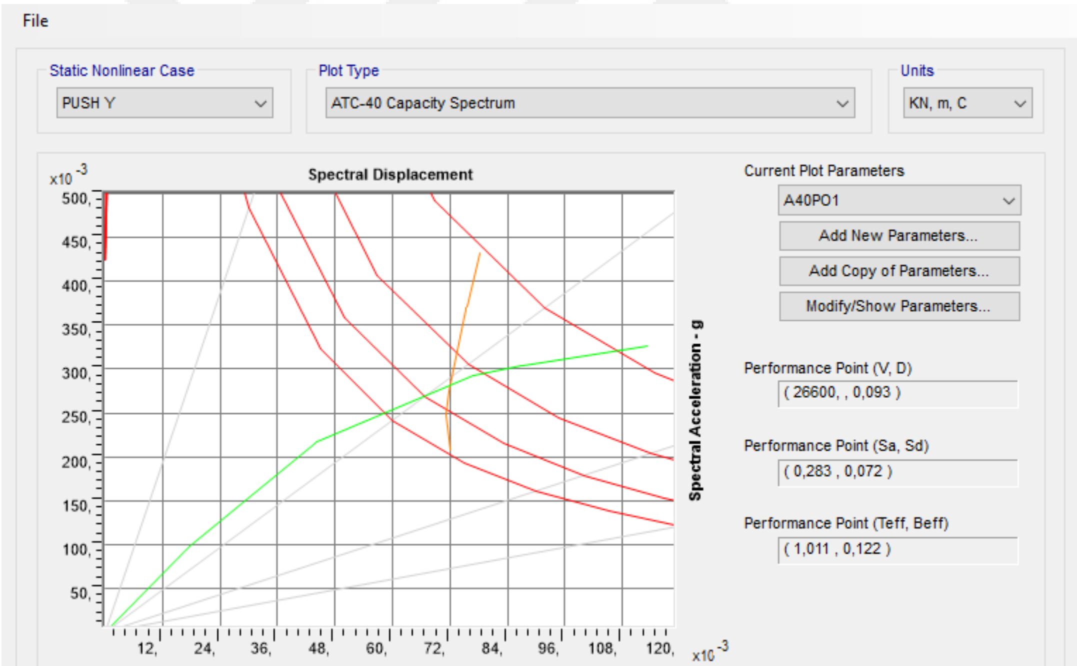

Figure D.36 Performance Point based on Pushover Analysis in Y-Direction for Model 910V22

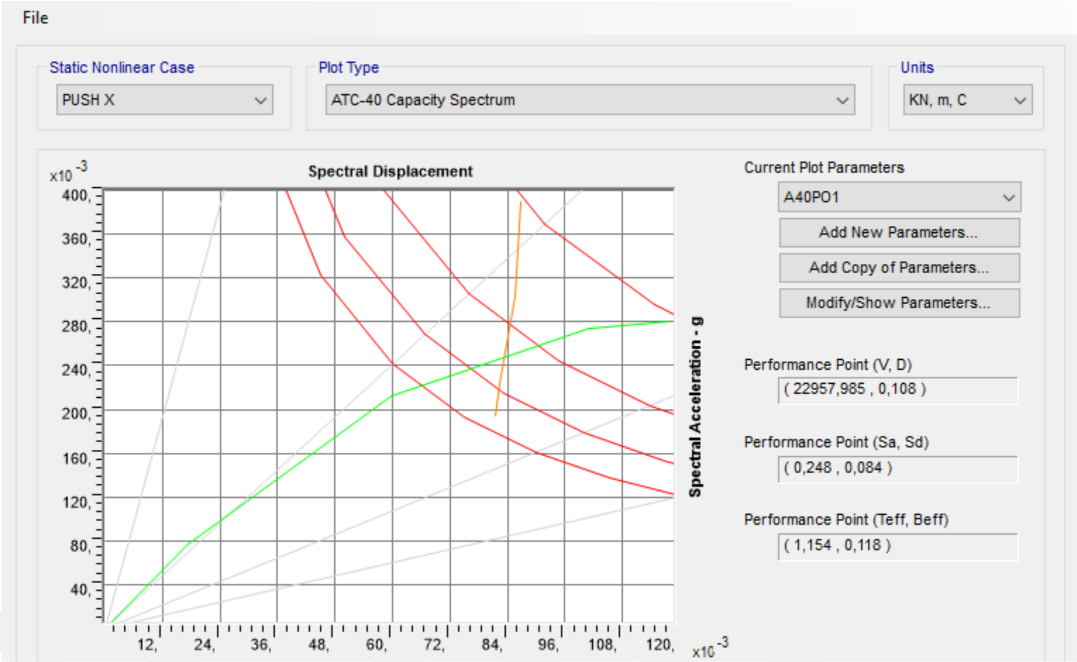

Figure D.37 Performance Point based on Pushover Analysis in X-Direction for Model 910X11

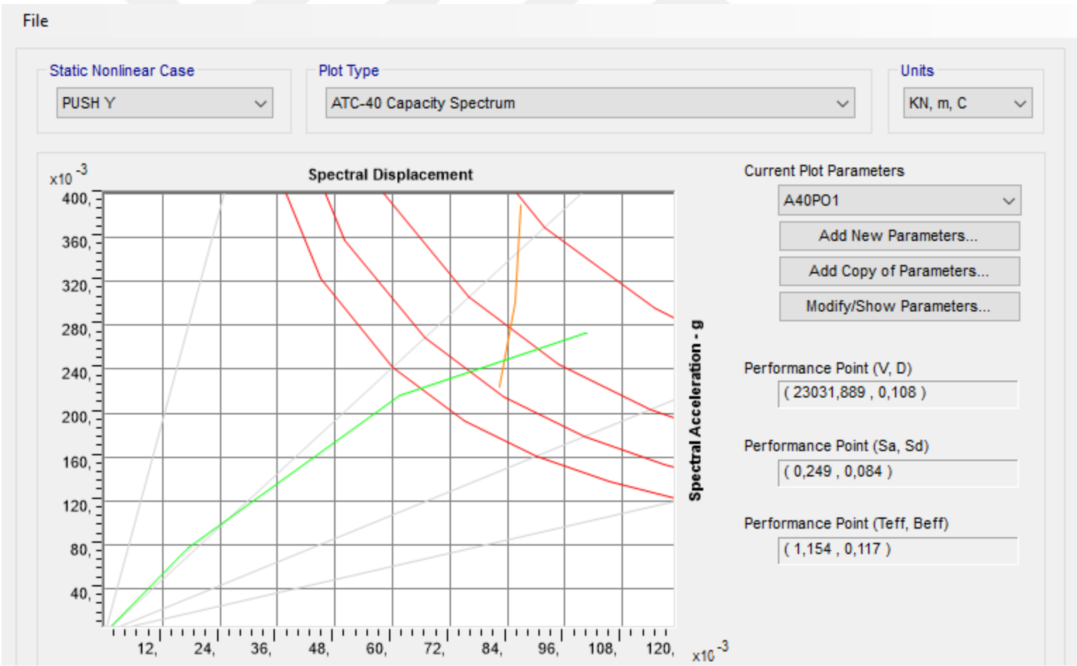

Figure D.38 Performance Point based on Pushover Analysis in Y-Direction for Model 910X11

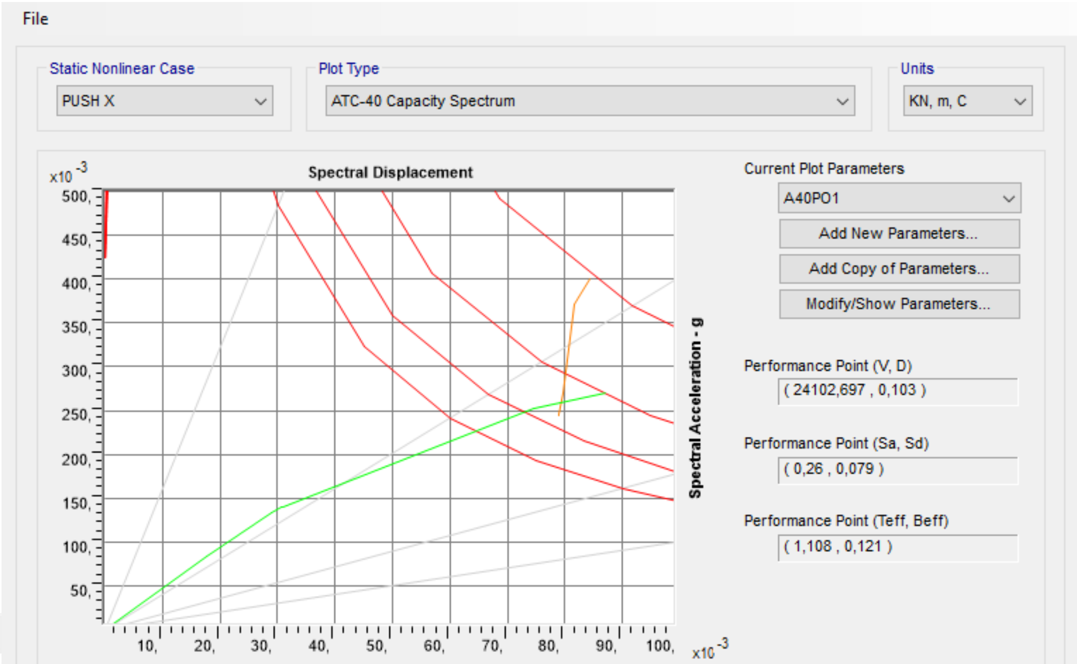

Figure D.39 Performance Point based on Pushover Analysis in X-Direction for Model 910X21

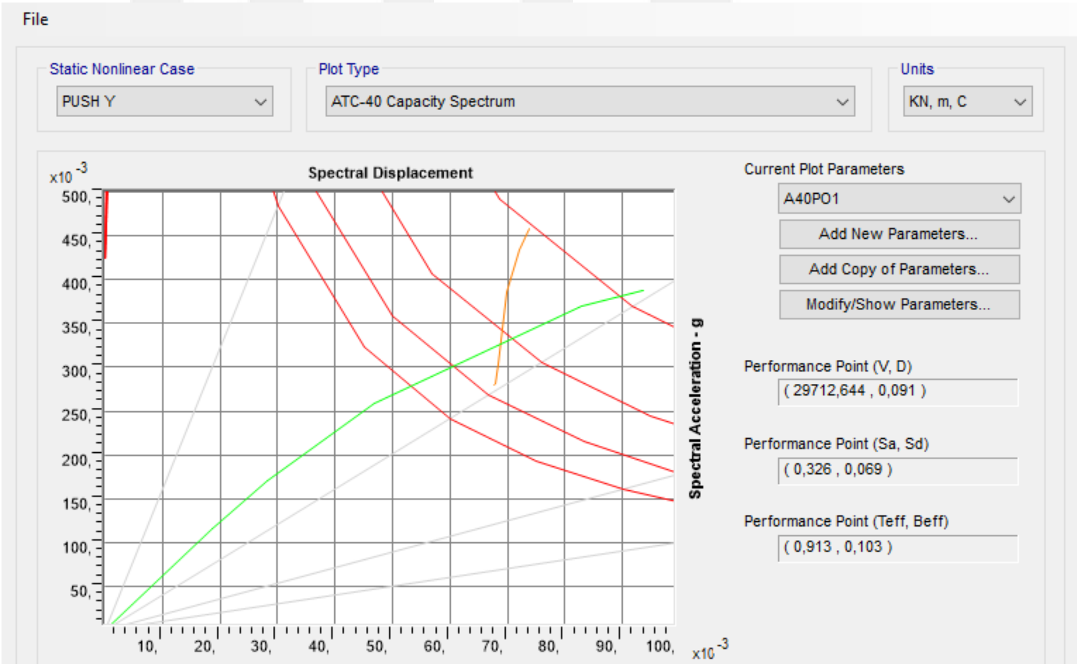

Figure D.40 Performance Point based on Pushover Analysis in Y-Direction for Model 910X21

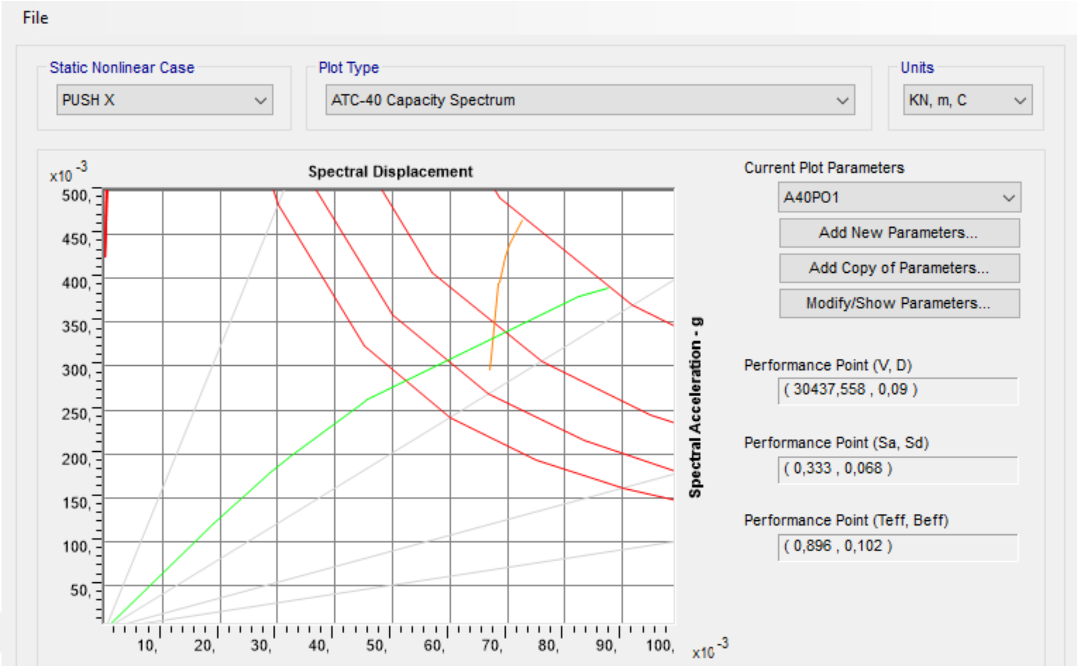

Figure D.41 Performance Point based on Pushover Analysis in X-Direction for Model 910X22

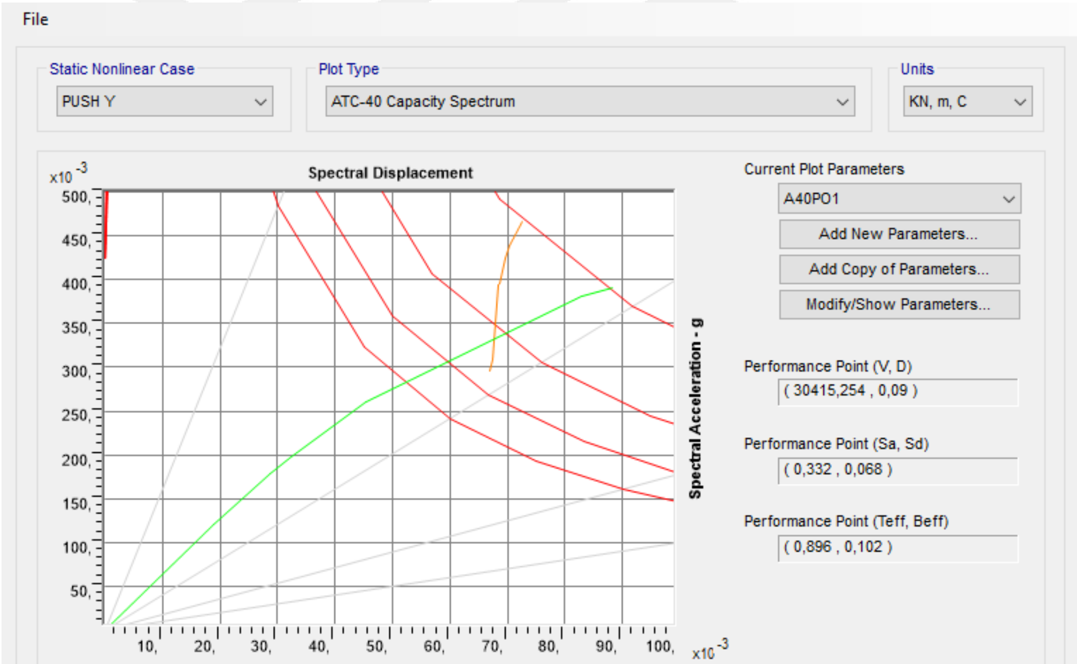

Figure D.42 Performance Point based on Pushover Analysis in Y-Direction for Model 910X22

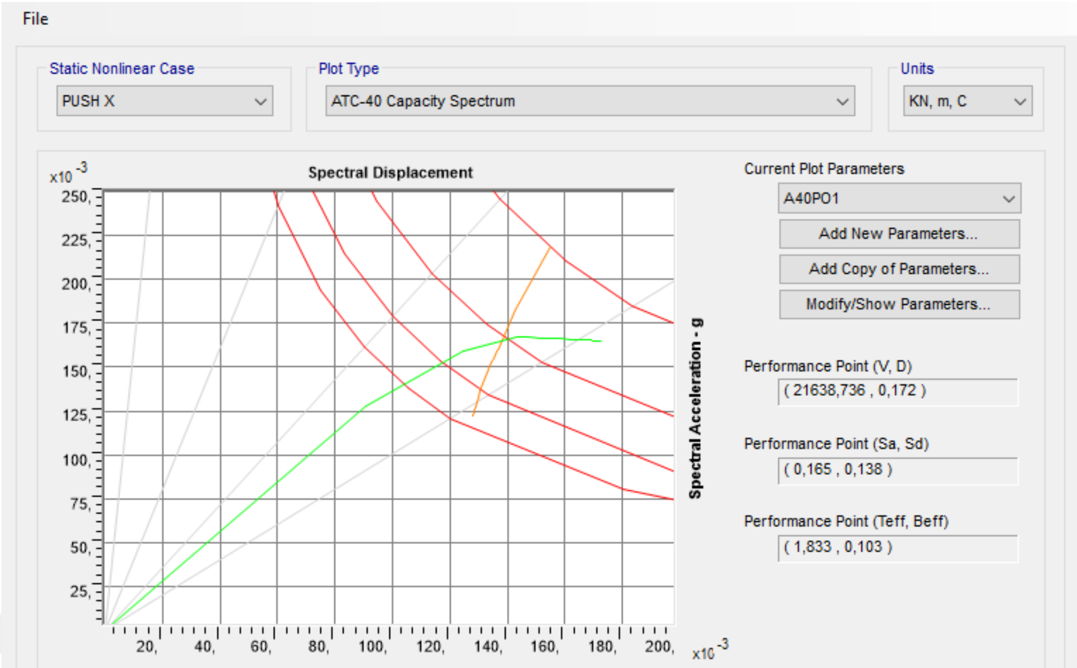

Figure D.43 Performance Point based on Pushover Analysis in X-Direction for Model 1210

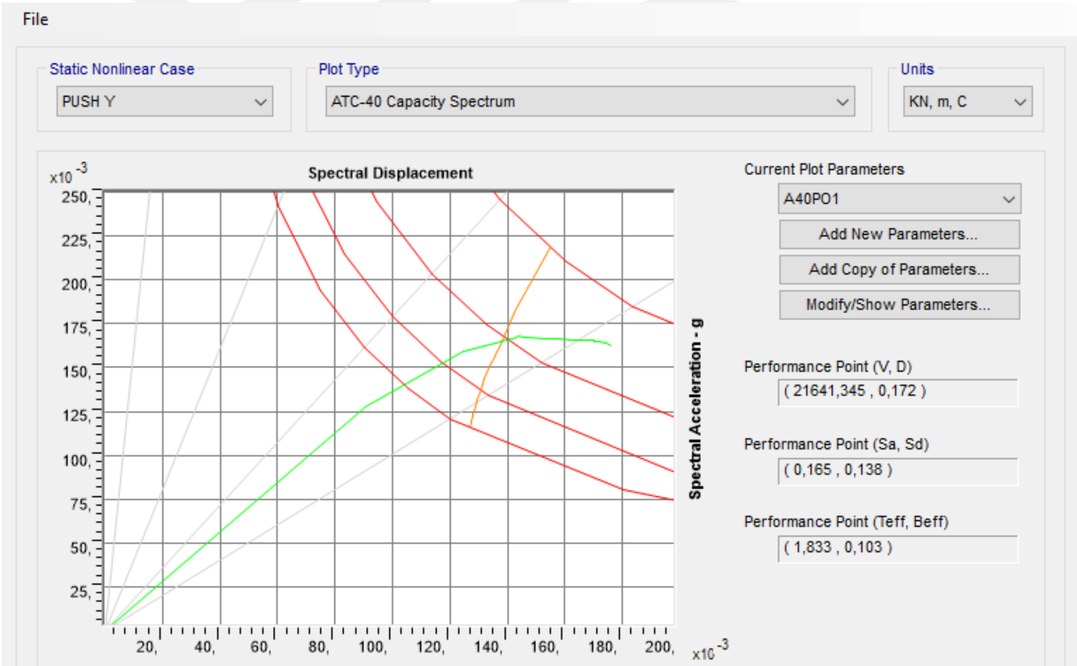

Figure D.44 Performance Point based on Pushover Analysis in Y-Direction for Model 1210

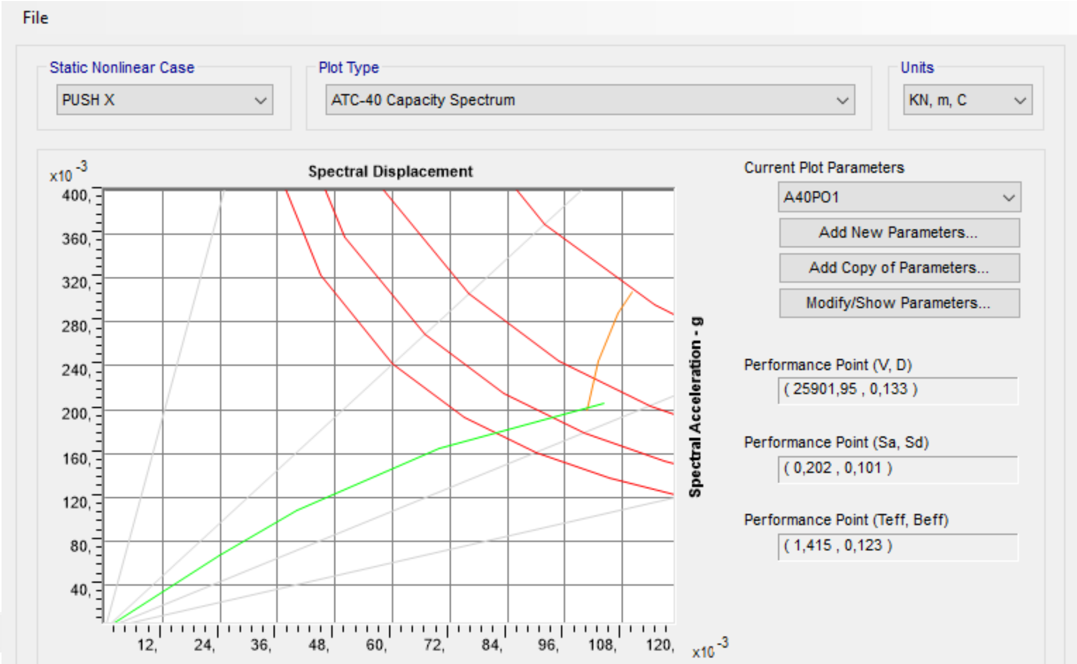

Figure D.45 Performance Point based on Pushover Analysis in X-Direction for Model 1210V11

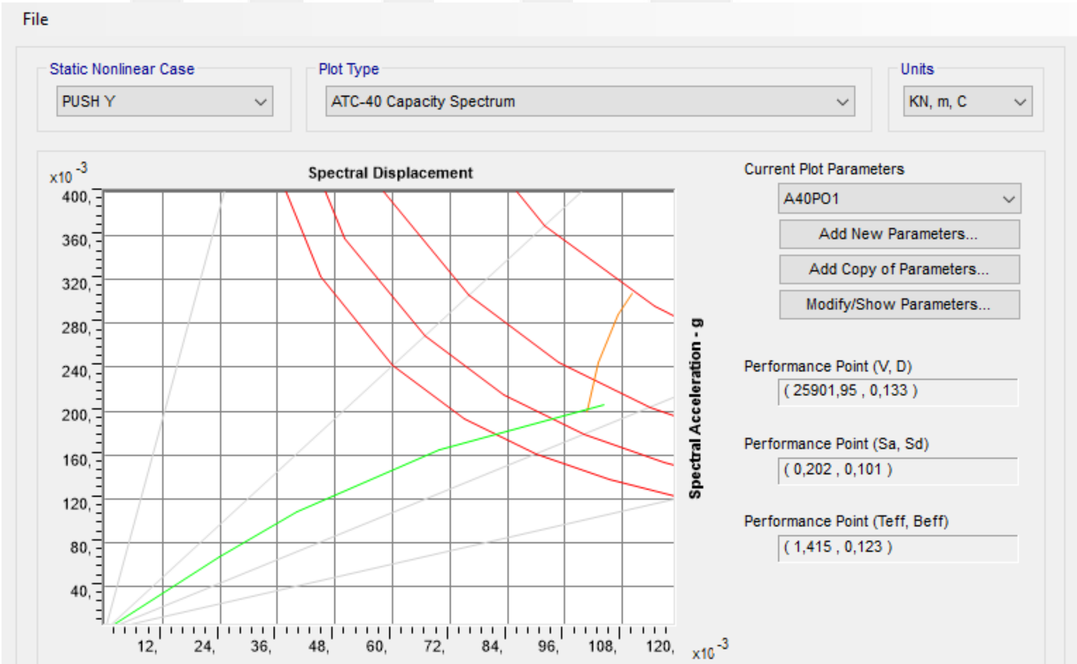

Figure D.46 Performance Point based on Pushover Analysis in X-Direction for Model 1210V11

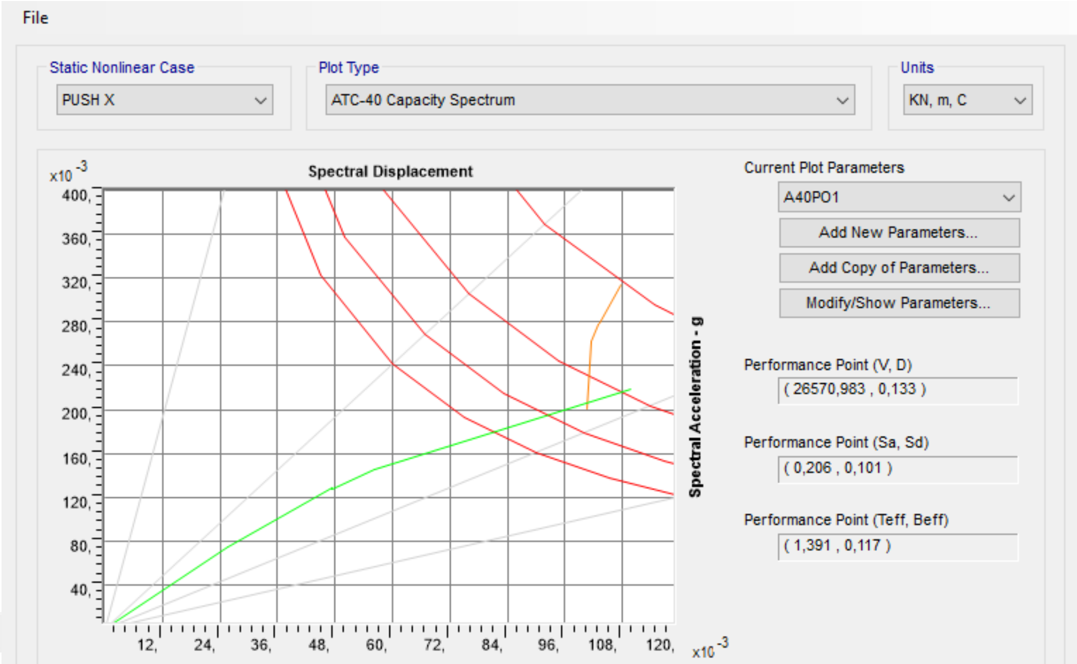

Figure D.47 Performance Point based on Pushover Analysis in X-Direction for Model 1210V21

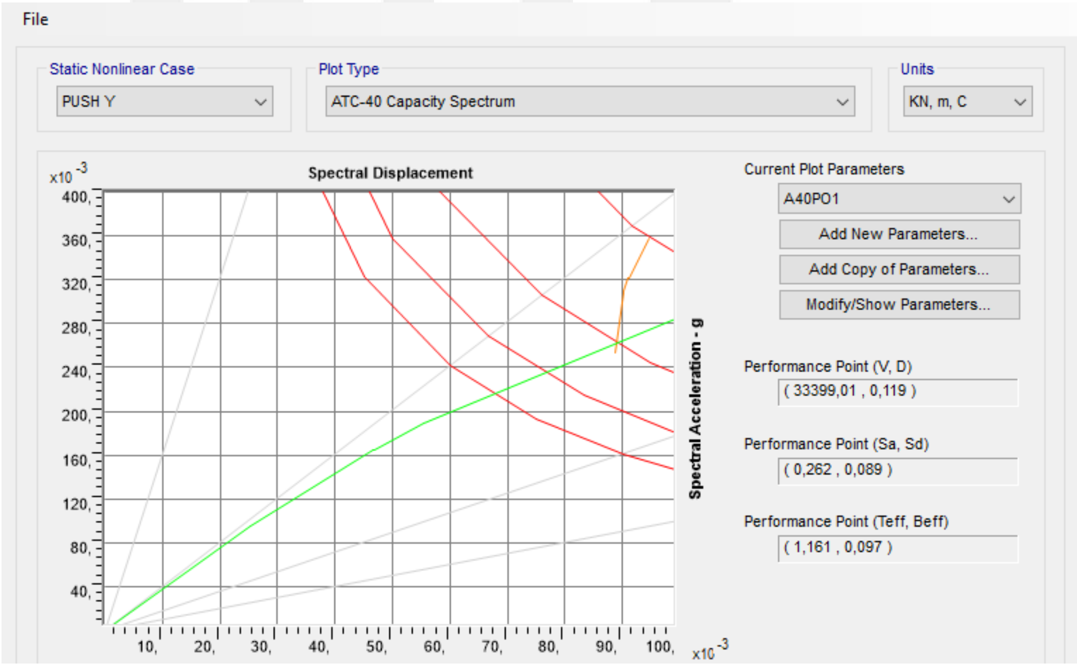

Figure D.48 Performance Point based on Pushover Analysis in Y-Direction for Model 1210V21

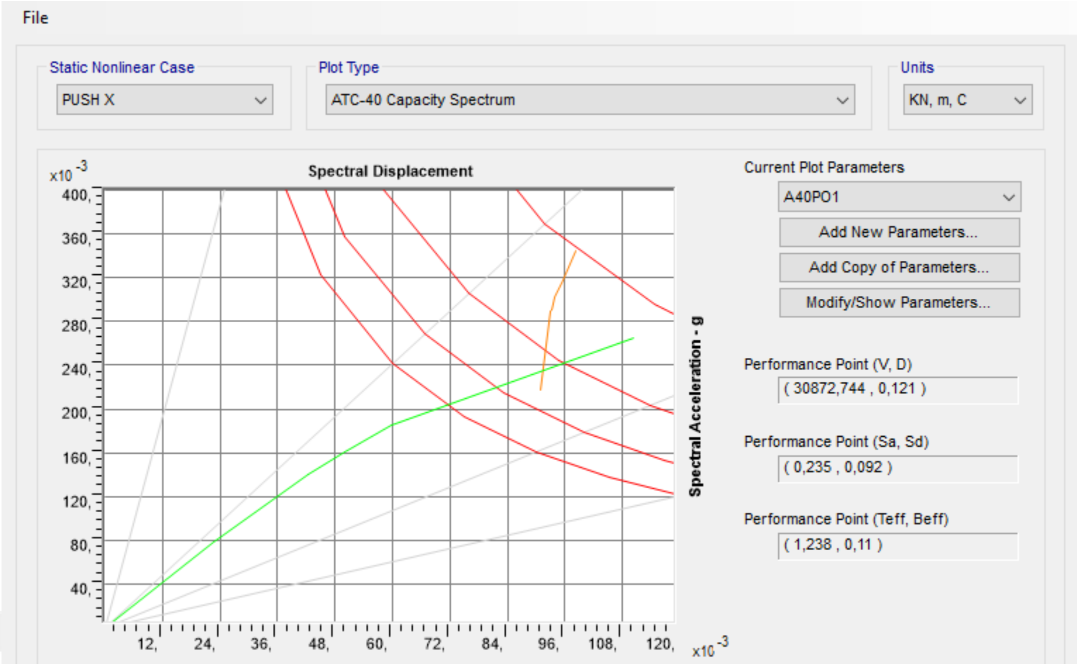

Figure D.49 Performance Point based on Pushover Analysis in X-Direction for Model 1210V22

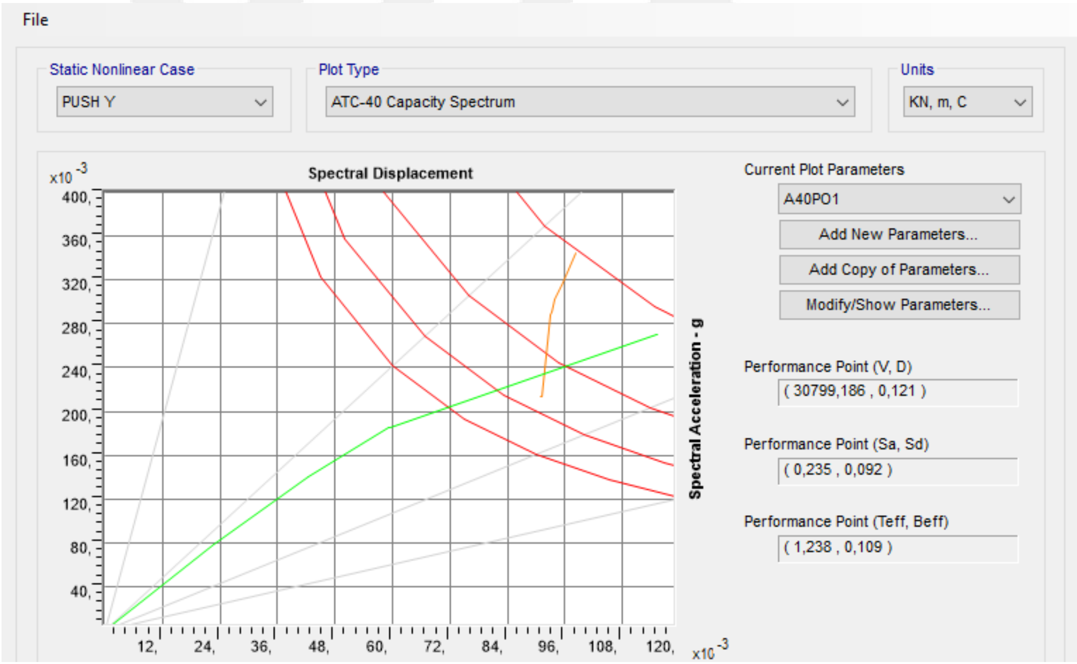

Figure D.50 Performance Point based on Pushover Analysis in Y-Direction for Model 1210V22

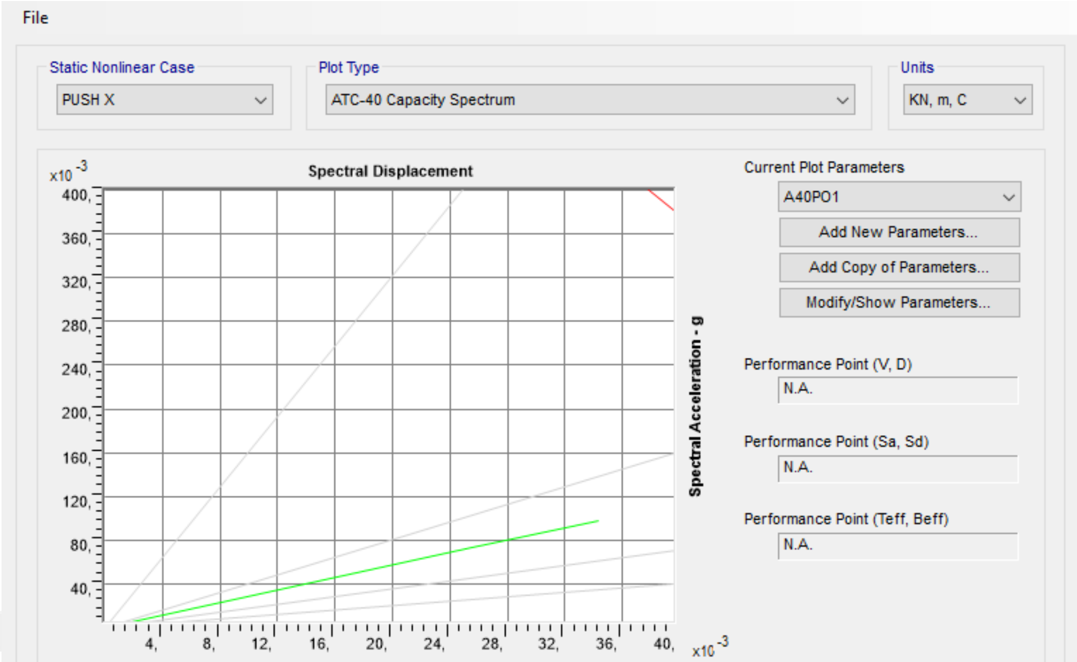

Figure D.51 Performance Point based on Pushover Analysis in X-Direction for Model 1210X11

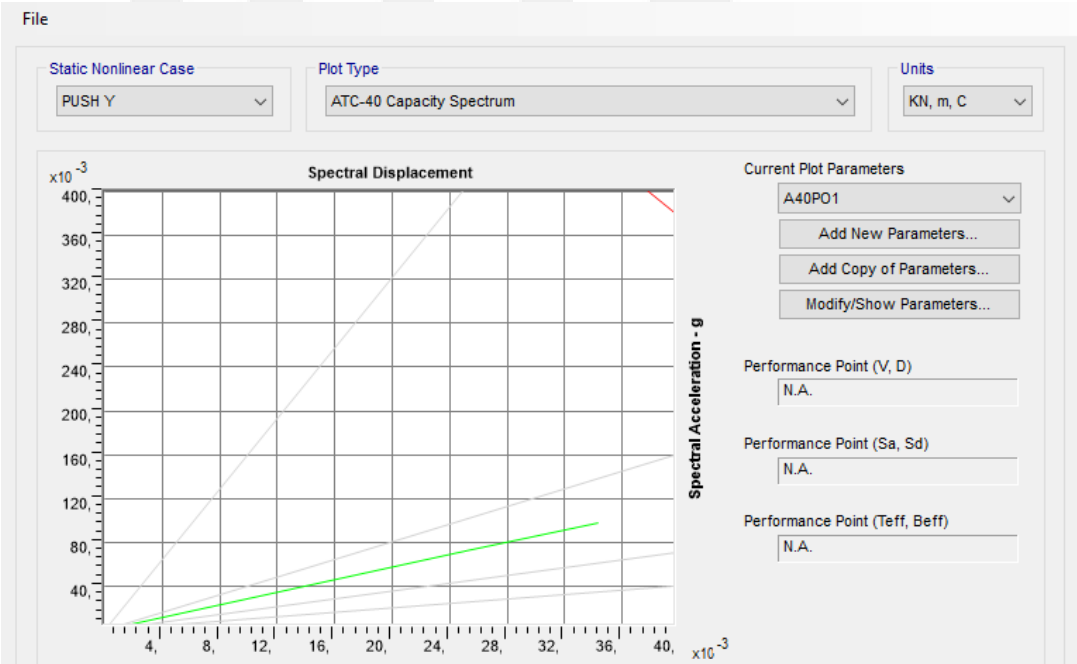

Figure D.52 Performance Point based on Pushover Analysis in Y-Direction for Model 1210X11

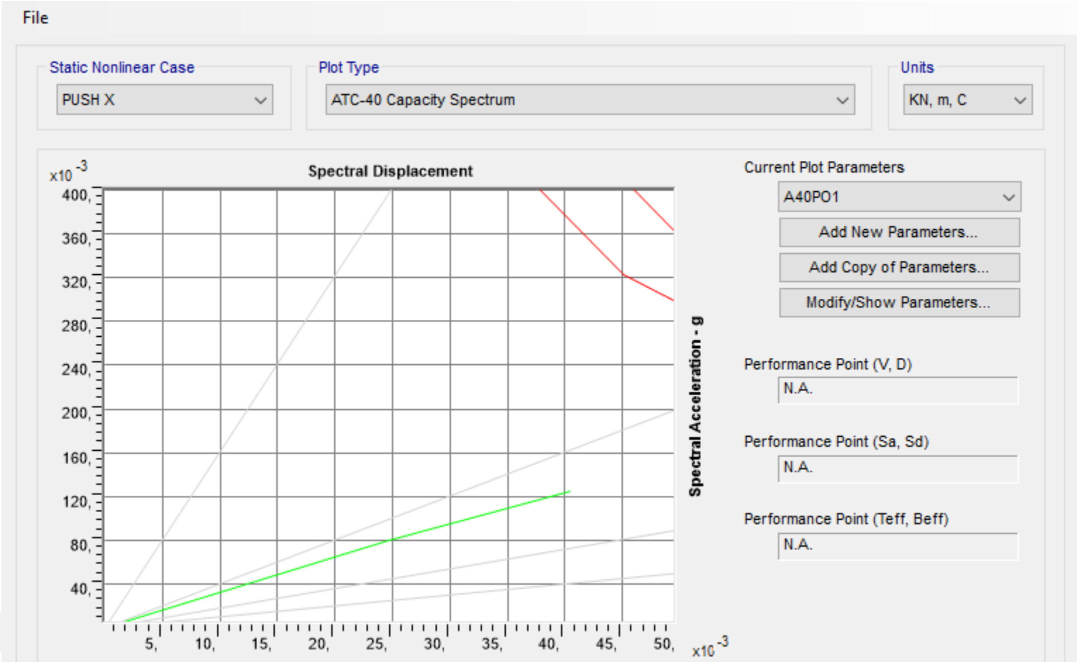

Figure D.53 Performance Point based on Pushover Analysis in X-Direction for Model 1210X21

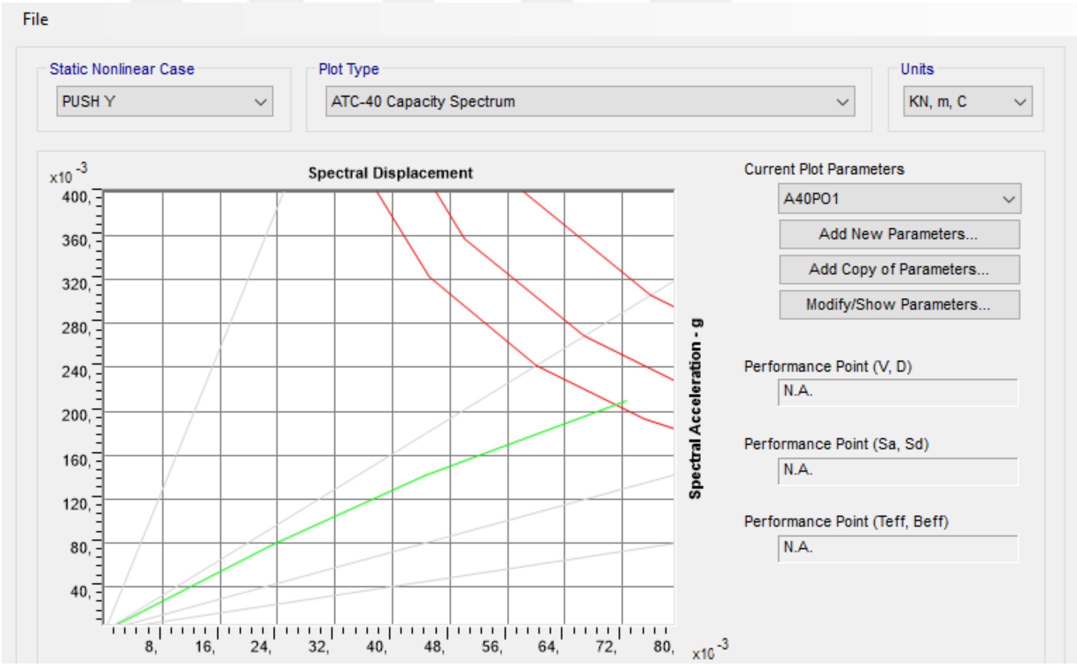

Figure D.54 Performance Point based on Pushover Analysis in Y-Direction for Model 1210X21

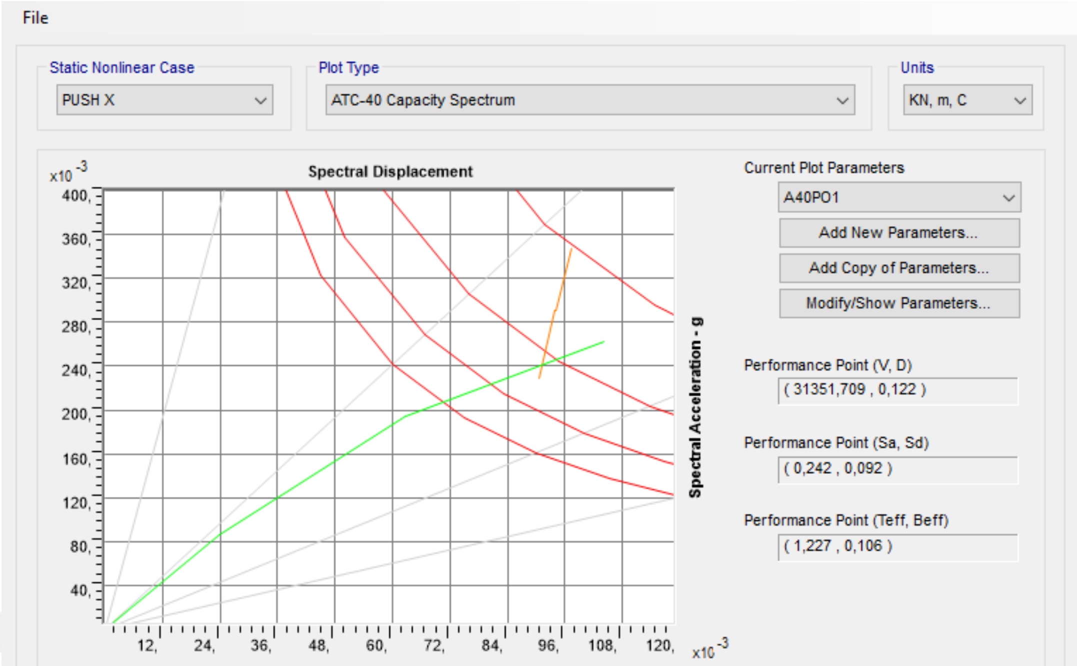

Figure D.55 Performance Point based on Pushover Analysis in X-Direction for Model 1210X22

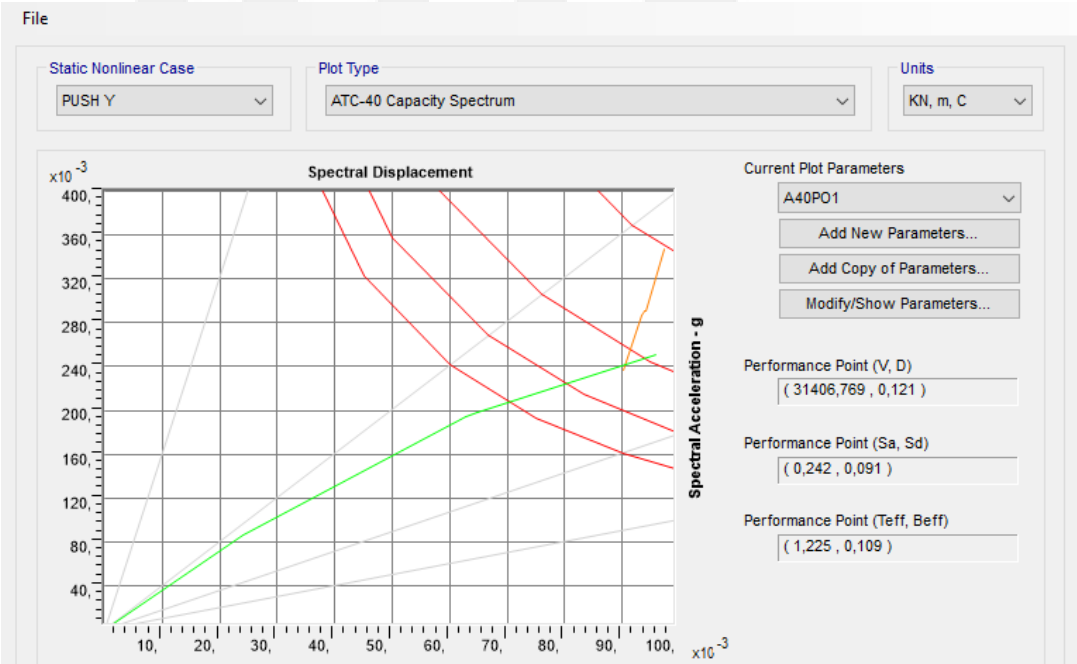

Figure D.56 Performance Point based on Pushover Analysis in Y-Direction for Model 1210X22

E. PLASTIC HINGE FORMATIONS FOR ALL MODELS BASED ON PUSHOVER ANALYSIS

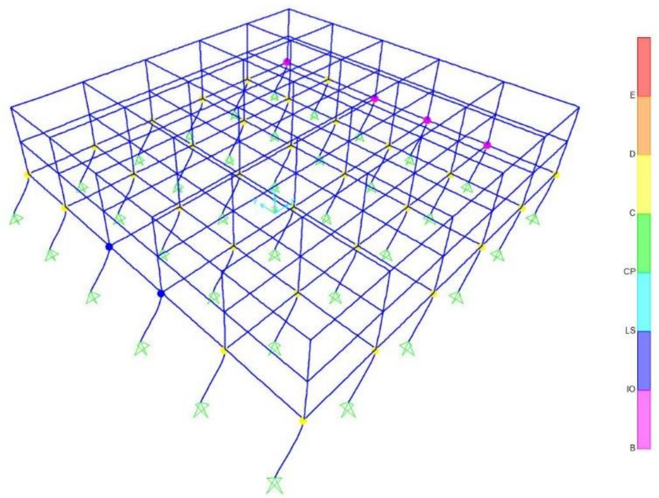

Figure E.1 Plastic Hinge Formation of Push X Load Case for Model 310

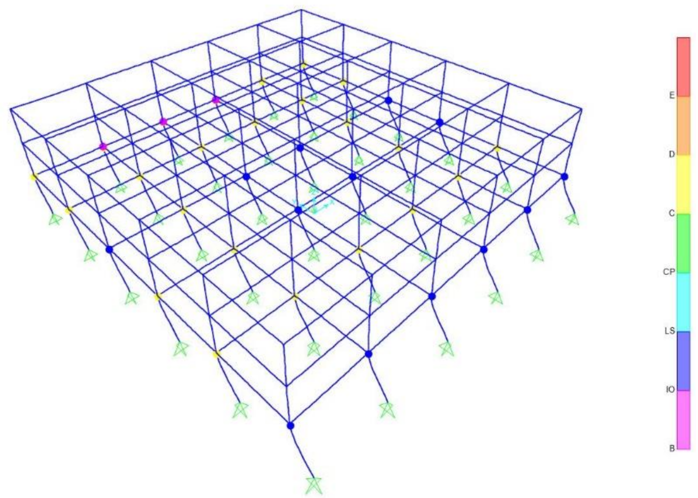

Figure E.2 Plastic Hinge Formation of Push Y Load Case for 310

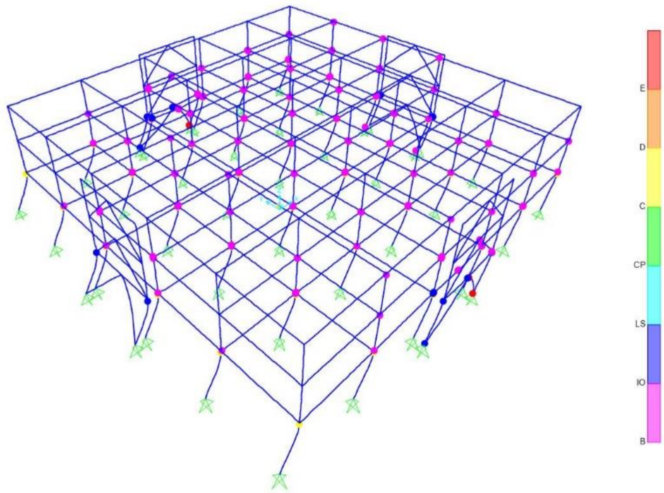

Figure E.3 Plastic Hinge Formation of Push X Load Case for 310V11

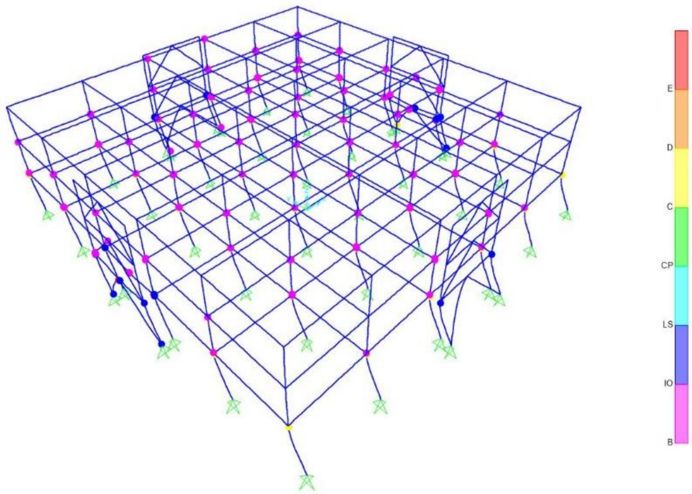

Figure E.4 Plastic Hinge Formation of Push Y Load Case for 310V11

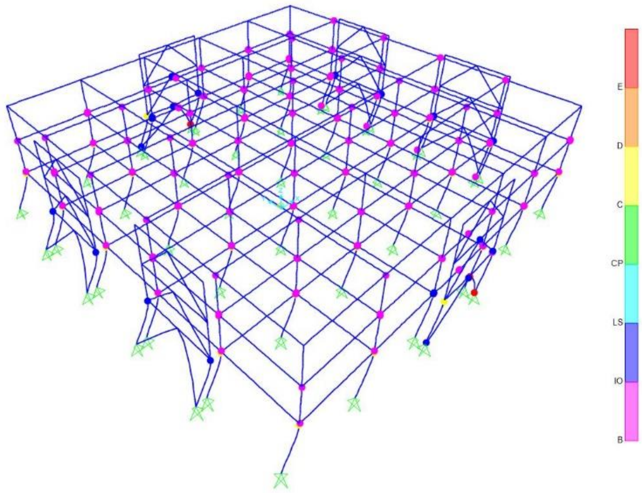

Figure E.5 Plastic Hinge Formation of Push X Load Case for 310V21

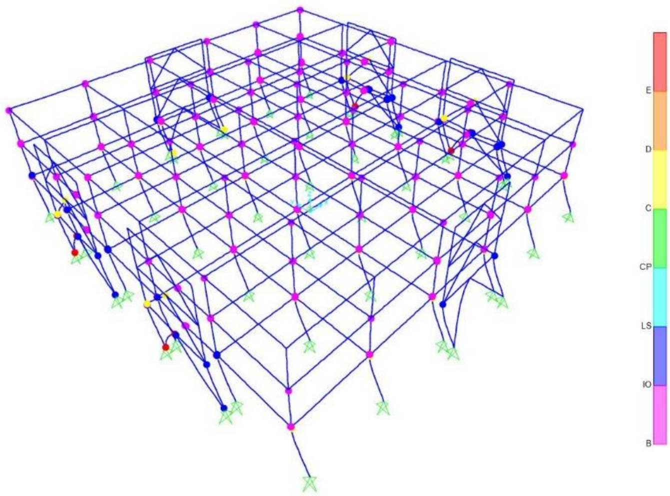

Figure E.6 Plastic Hinge Formation of Push Y Load Case for 310V21

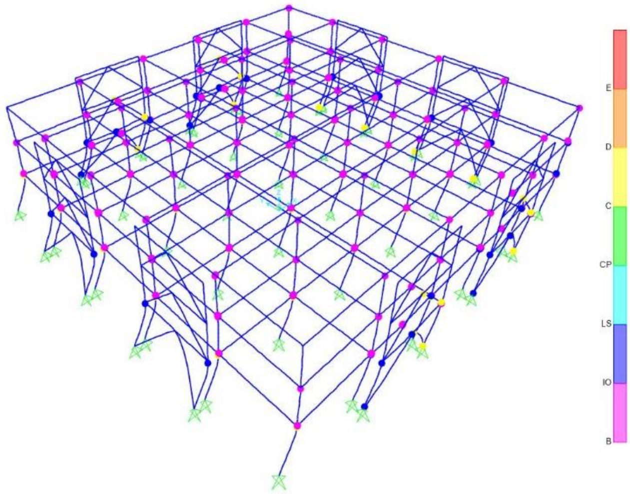

Figure E.7 Plastic Hinge Formation of Push X Load Case for 310V22

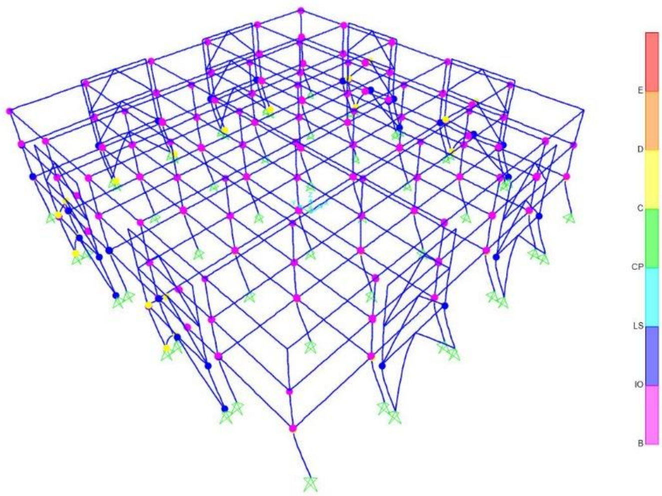

Figure E.8 Plastic Hinge Formation of Push Y Load Case for 310V22

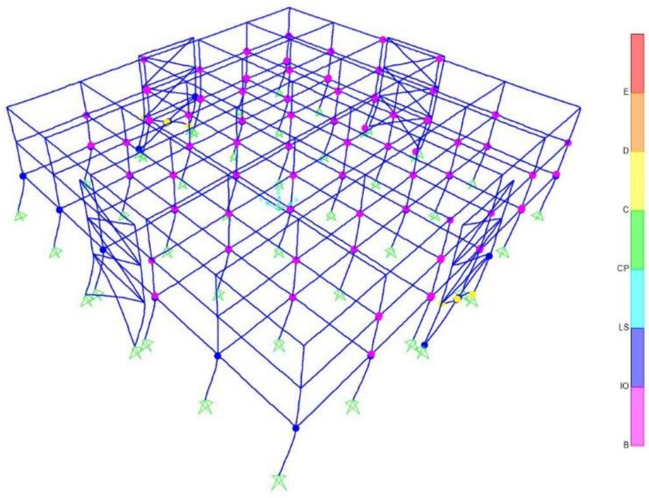

Figure E.9 Plastic Hinge Formation of Push X Load Case for 310X11

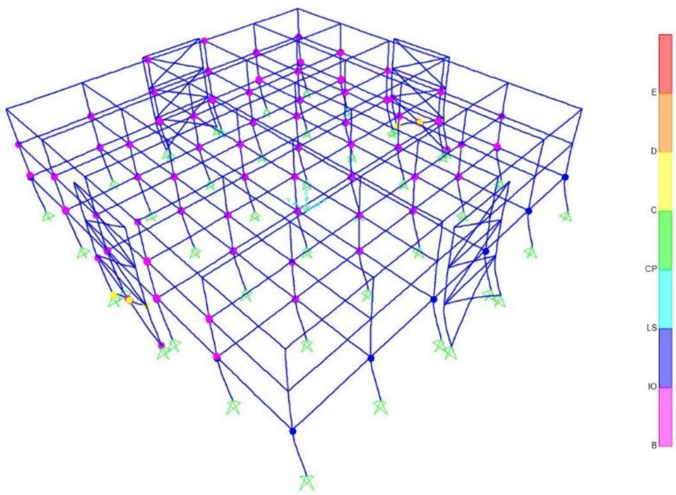

Figure E.10 Plastic Hinge Formation of Push Y Load Case for 310X11

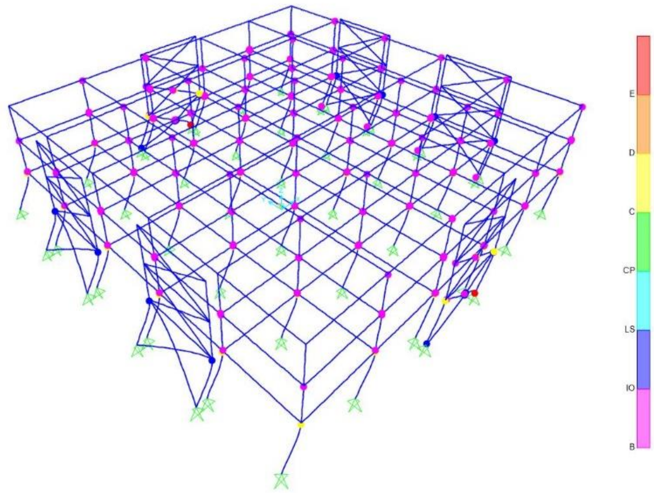

Figure E.11 Plastic Hinge Formation of Push X Load Case for 310X21

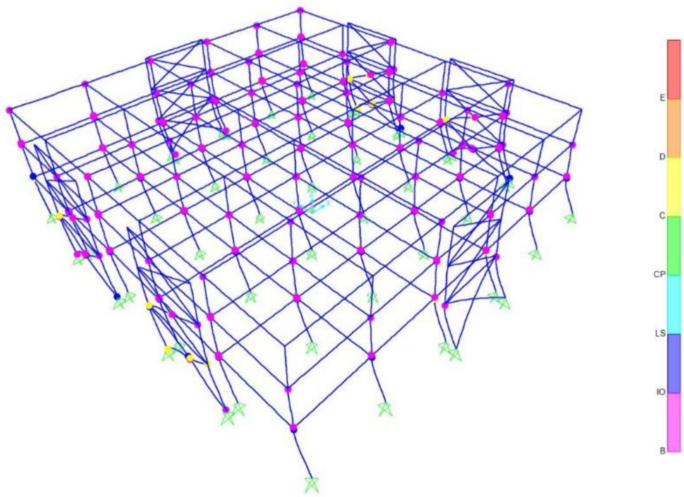

Figure E.12 Plastic Hinge Formation of Push Y Load Case for 310X21

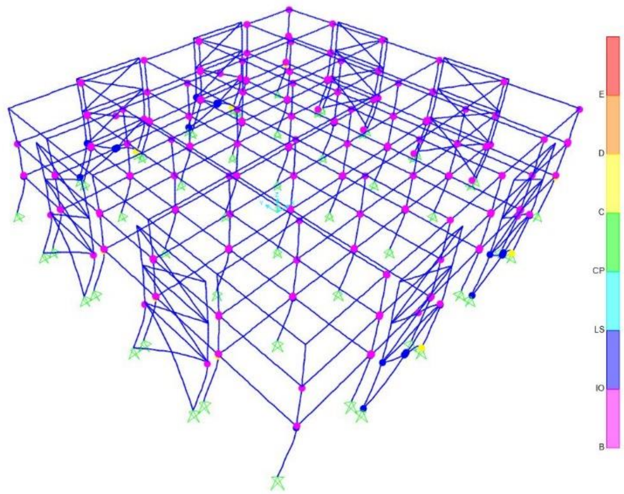

Figure E.13 Plastic Hinge Formation of Push X Load Case for 310X22

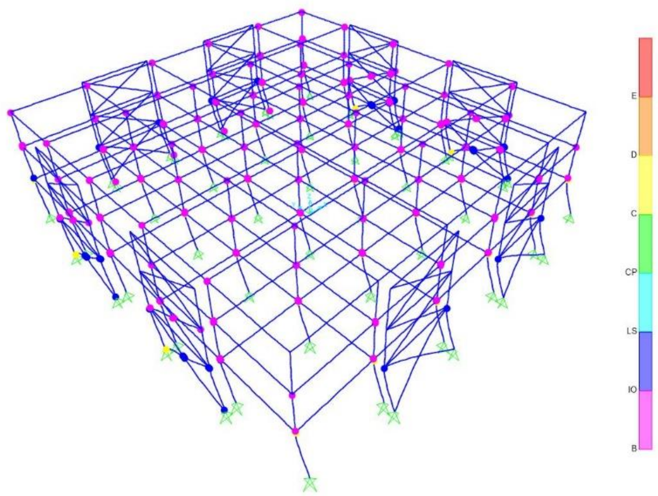

Figure E.14 Plastic Hinge Formation of Push Y Load Case for 310X22

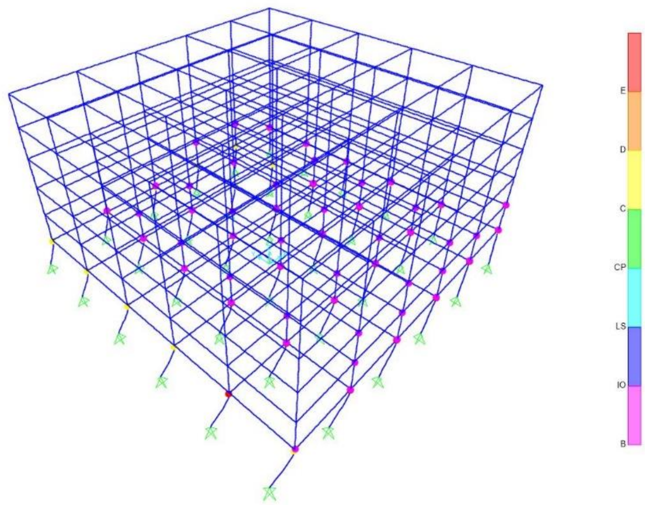

Figure E.15 Plastic Hinge Formation of Push X Load Case for 610

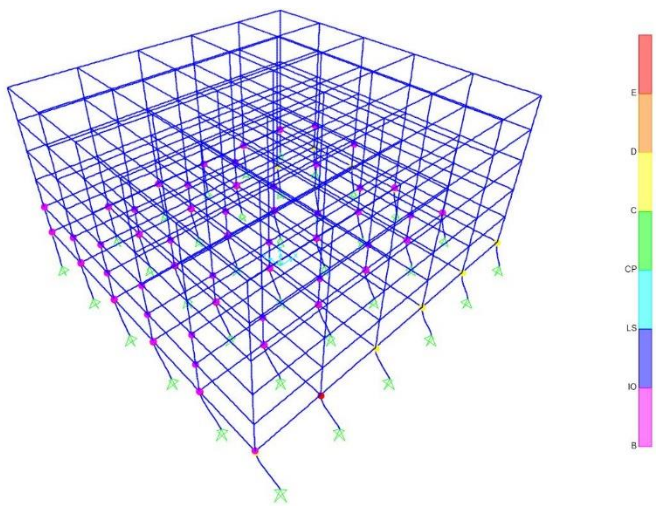

Figure E.16 Plastic Hinge Formation of Push Y Load Case for 610

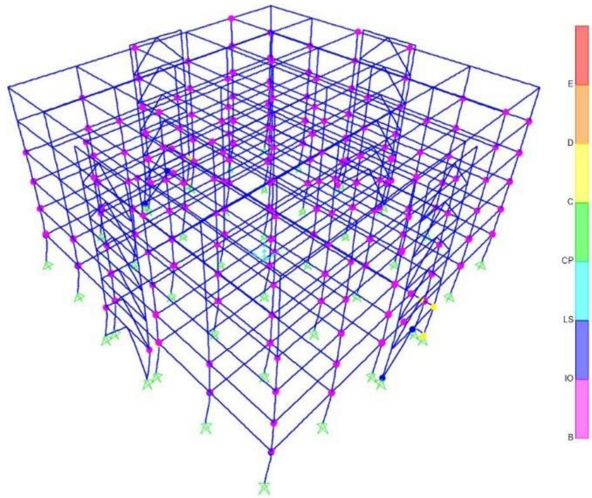

Figure E.17 Plastic Hinge Formation of Push X Load Case for 610V11

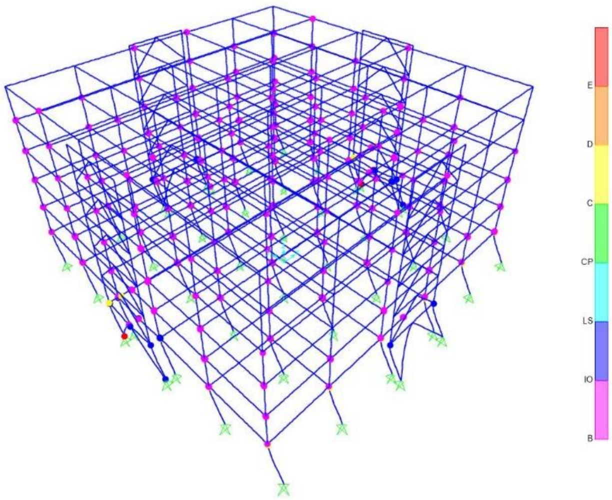

Figure E.18 Plastic Hinge Formation of Push Y Load Case for 610V11

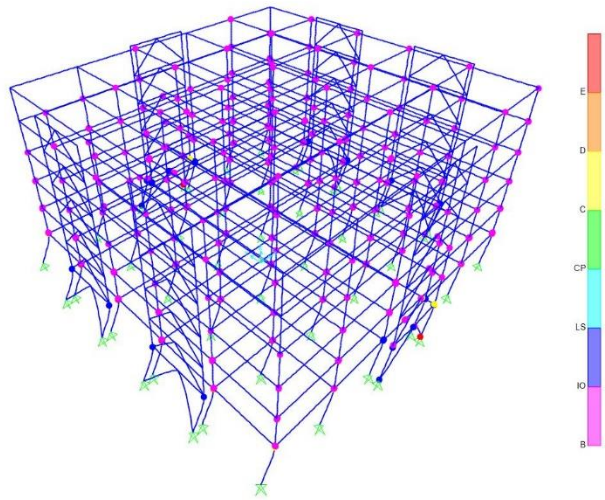

Figure E.19 Plastic Hinge Formation of Push X Load Case for 610V21

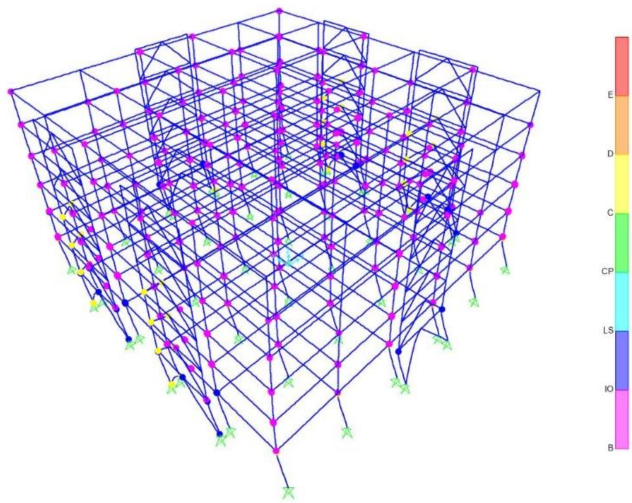

Figure E.20 Plastic Hinge Formation of Push Y Load Case for 610V21

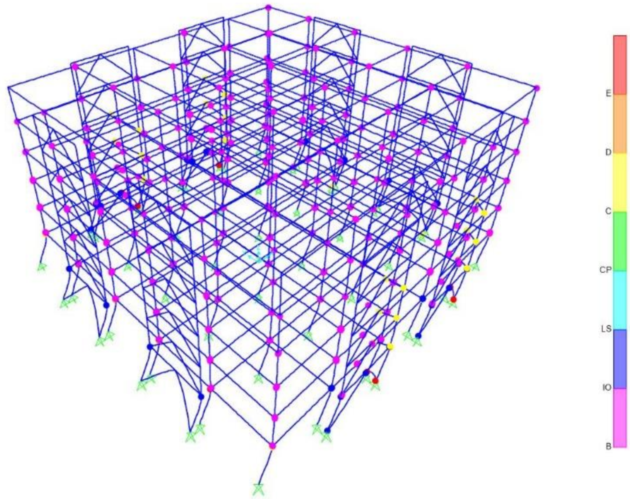

Figure E.21 Plastic Hinge Formation of Push X Load Case for 610V22

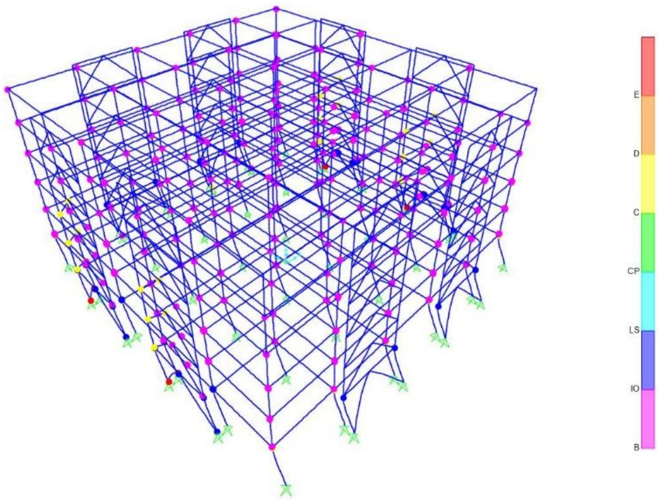

Figure E.22 Plastic Hinge Formation of Push Y Load Case for 610V22

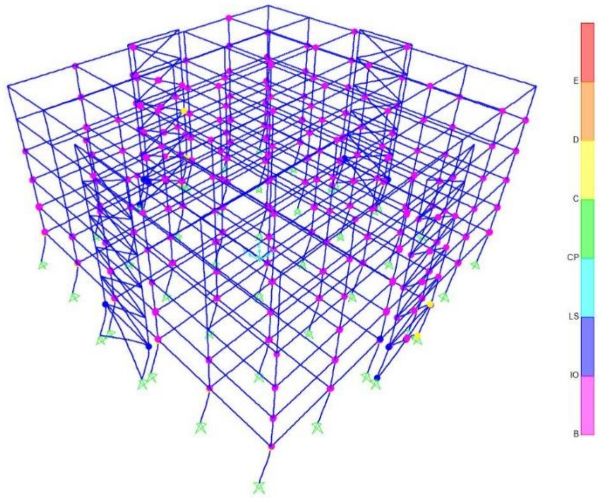

Figure E.23 Plastic Hinge Formation of Push X Load Case for 610X11

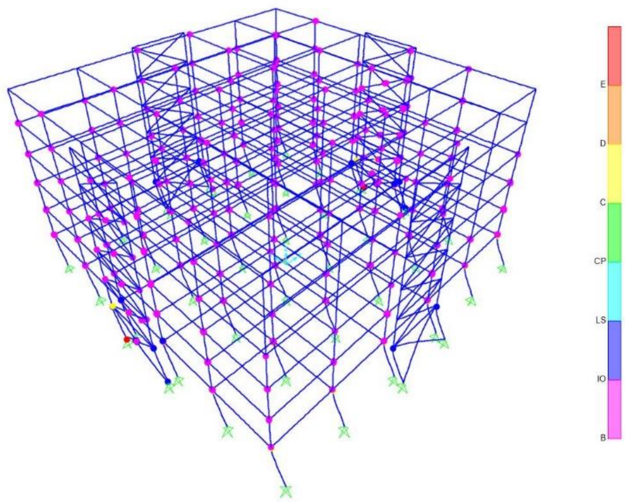

Figure E.24 Plastic Hinge Formation of Push Y Load Case for 610X11

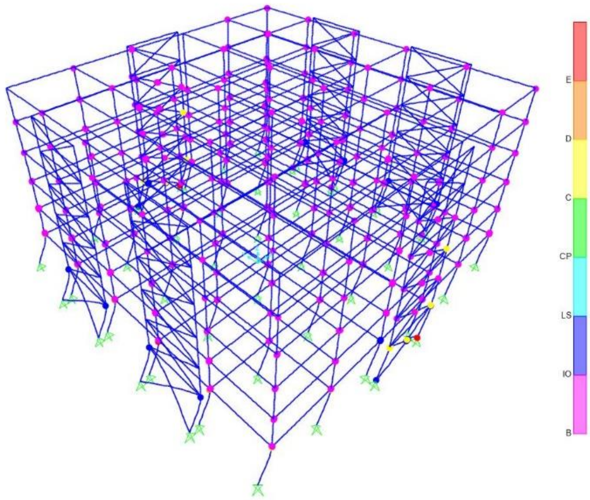

Figure E.25 Plastic Hinge Formation of Push X Load Case for 610X21

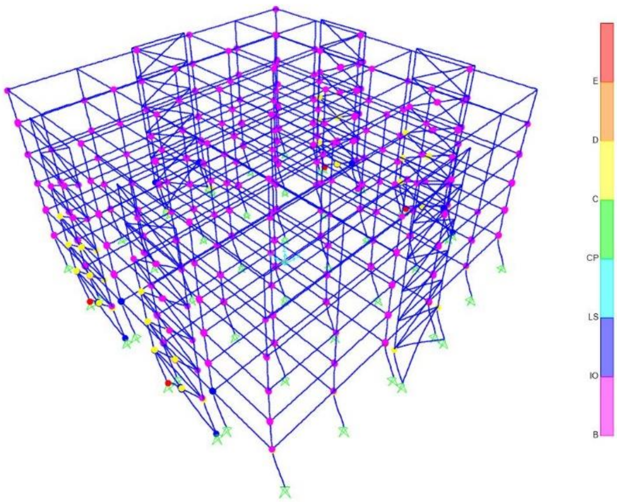

Figure E.26 Plastic Hinge Formation of Push Y Load Case for 610X21

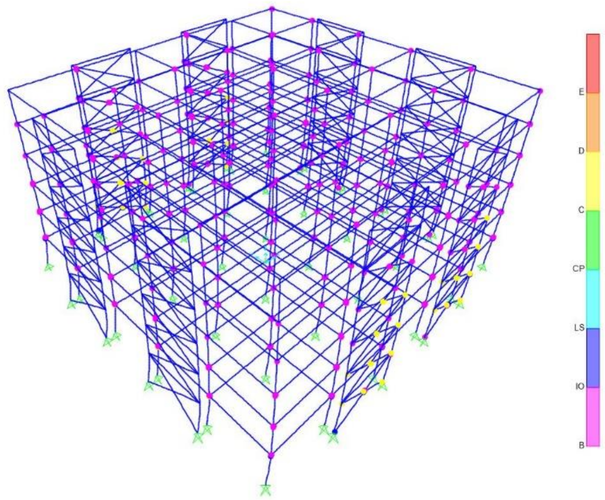

Figure E.27 Plastic Hinge Formation of Push X Load Case for 610X22

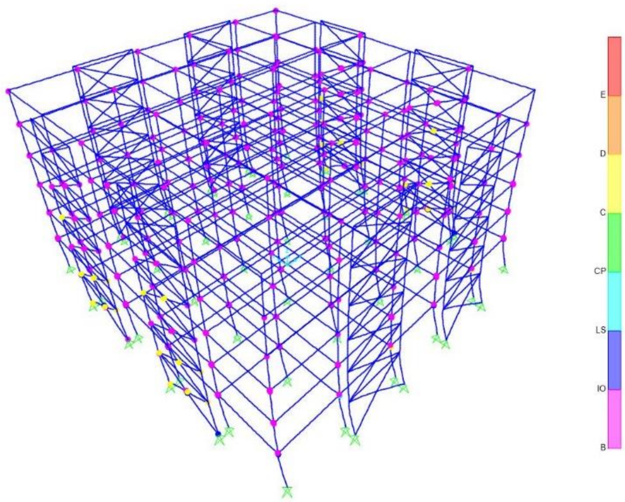

Figure E.28 Plastic Hinge Formation of Push Y Load Case for 610X22

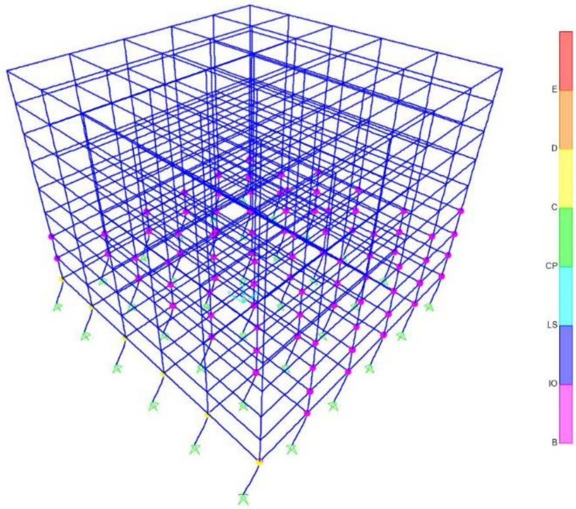

Figure E.29 Plastic Hinge Formation of Push X Load Case for 910

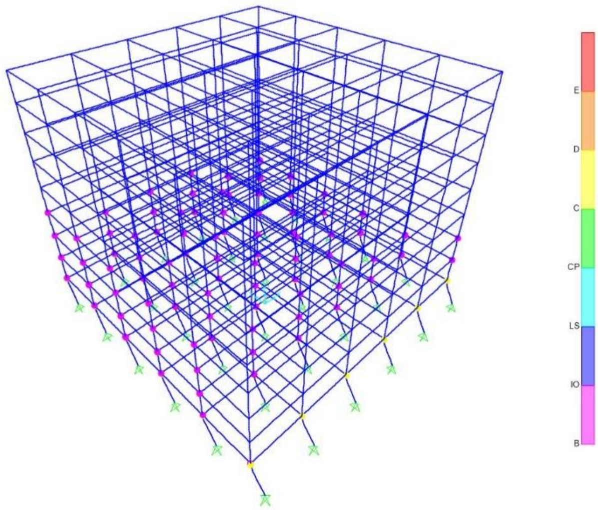

Figure E.30 Plastic Hinge Formation of Push Y Load Case for 910

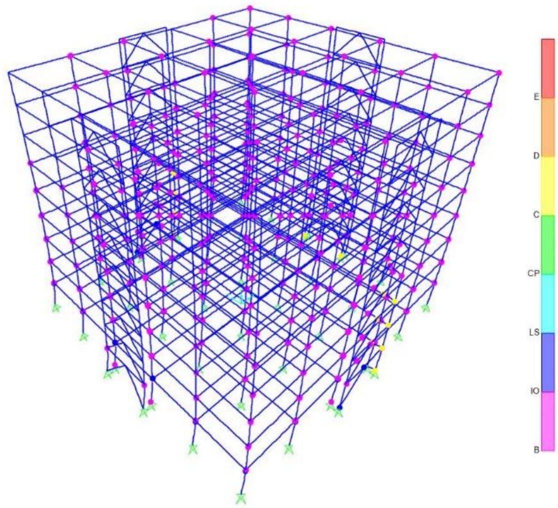

Figure E.31 Plastic Hinge Formation of Push X Load Case for 910V11

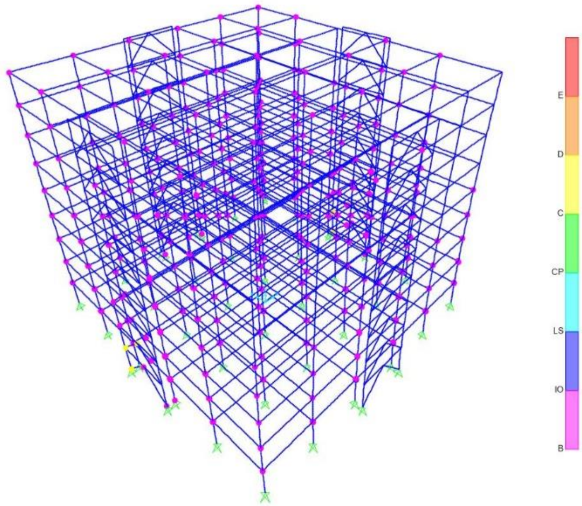

Figure E.32 Plastic Hinge Formation of Push Y Load Case for 910V11

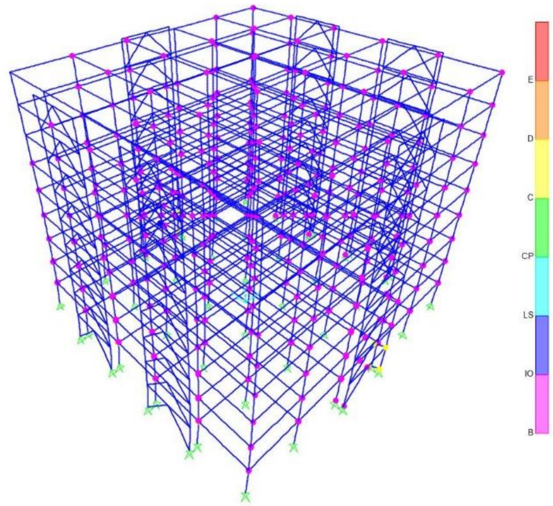

Figure E.33 Plastic Hinge Formation of Push X Load Case for 910V21

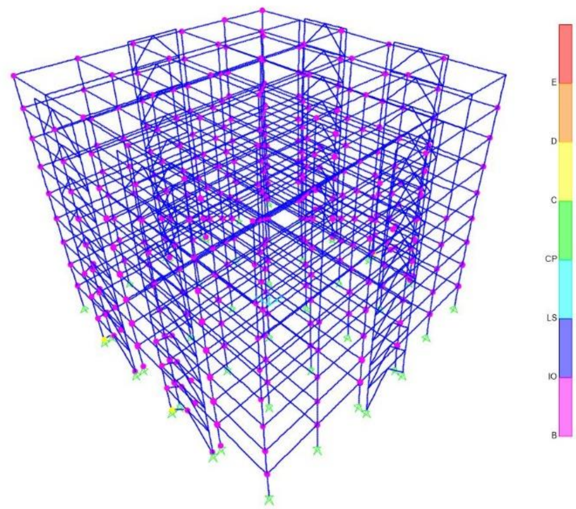

Figure E.34 Plastic Hinge Formation of Push Y Load Case for 910V21

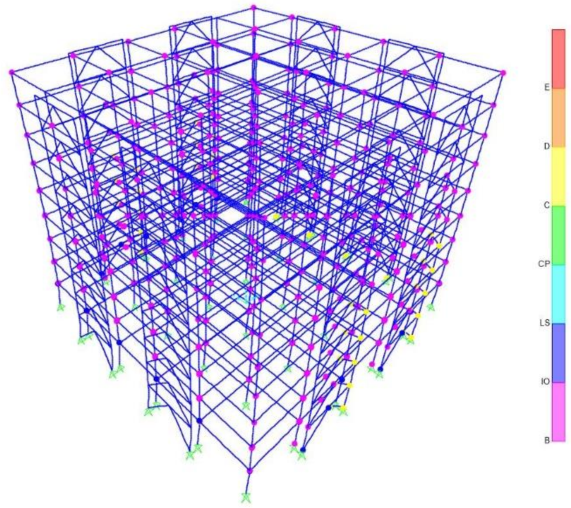

Figure E.35 Plastic Hinge Formation of Push X Load Case for 910V22

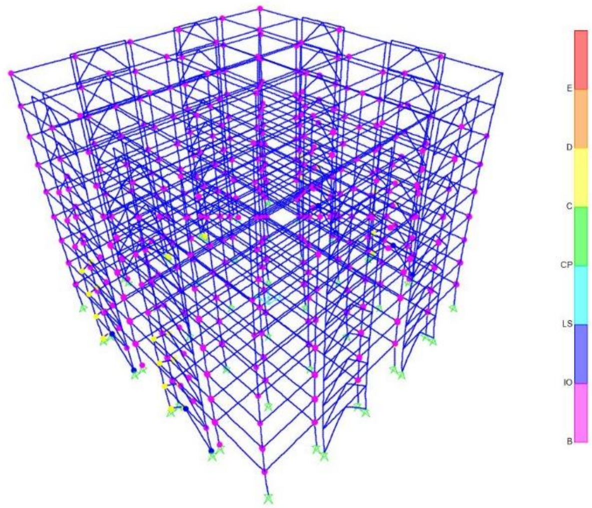

Figure E.36 Plastic Hinge Formation of Push Y Load Case for 910V22

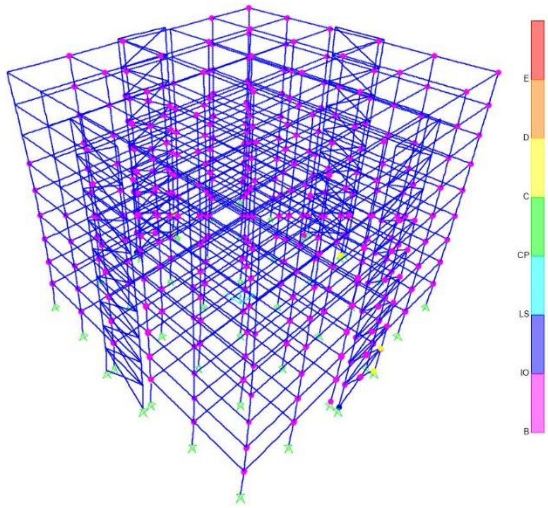

Figure E.37 Plastic Hinge Formation of Push X Load Case for 910X11

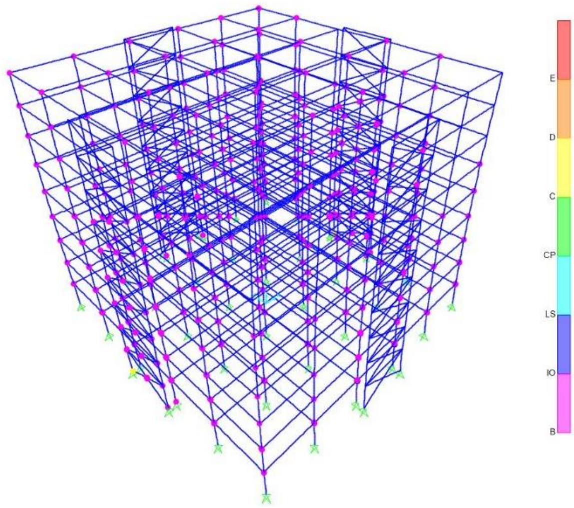

Figure E.38 Plastic Hinge Formation of Push Y Load Case for 910X11

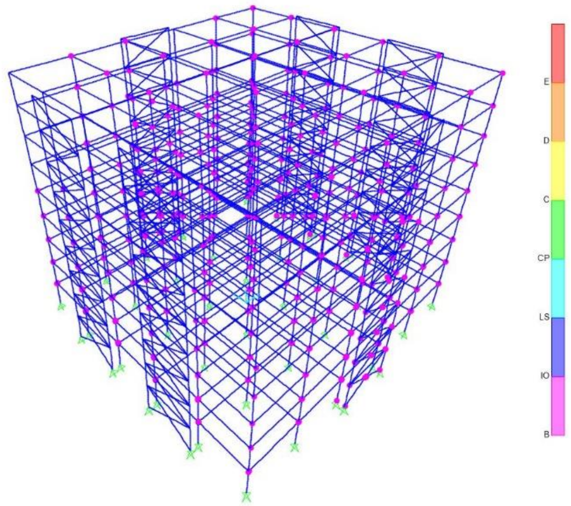

Figure E.39 Plastic Hinge Formation of Push X Load Case for 910X21

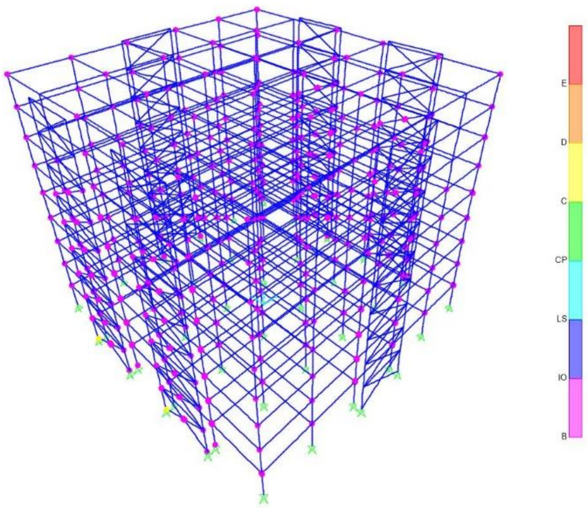

Figure E.40 Plastic Hinge Formation of Push X Load Case for 910X21

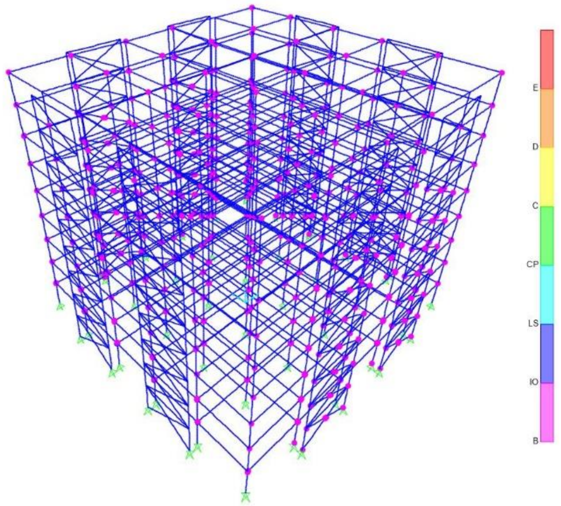

Figure E.41 Plastic Hinge Formation of Push X Load Case for 910X22

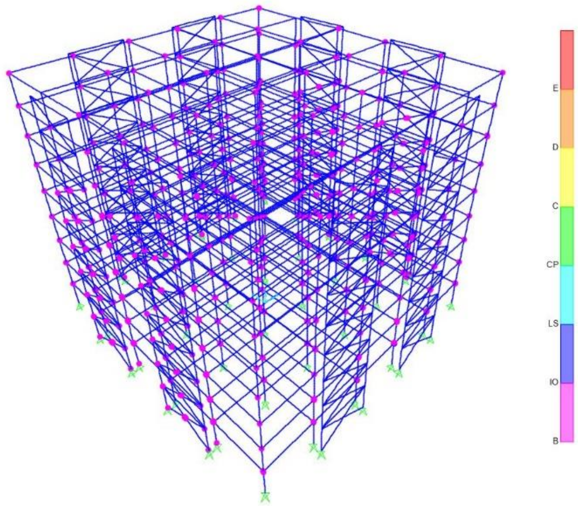

Figure E.42 Plastic Hinge Formation of Push Y Load Case for 910X22

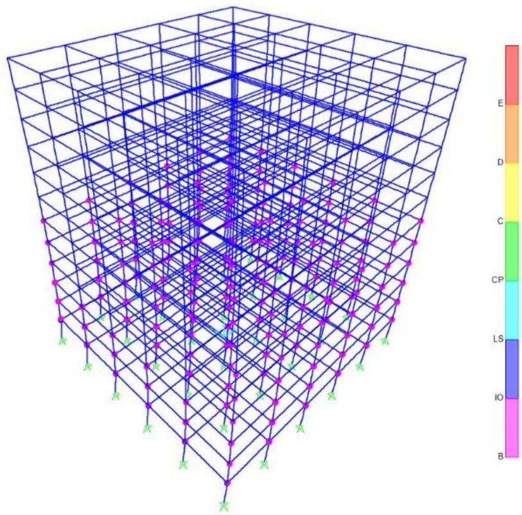

Figure E.43 Plastic Hinge Formation of Push X Load Case for 1210

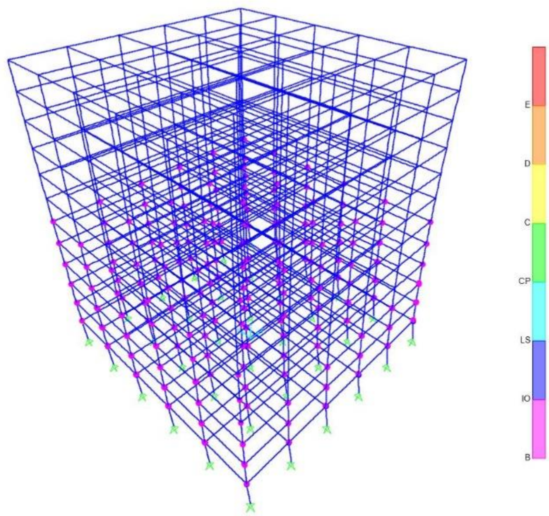

Figure E.44 Plastic Hinge Formation of Push Y Load Case for 1210

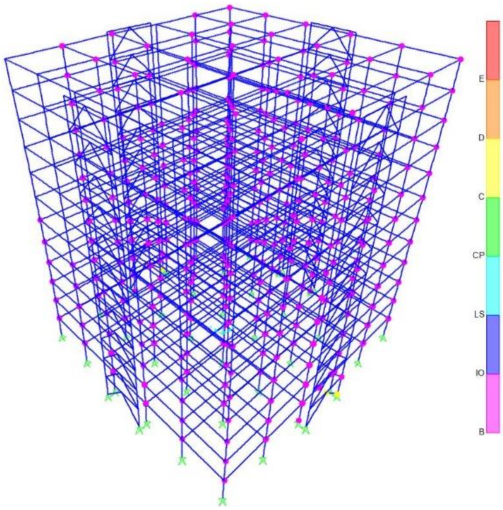

Figure E.45 Plastic Hinge Formation of Push X Load Case for 1210V11

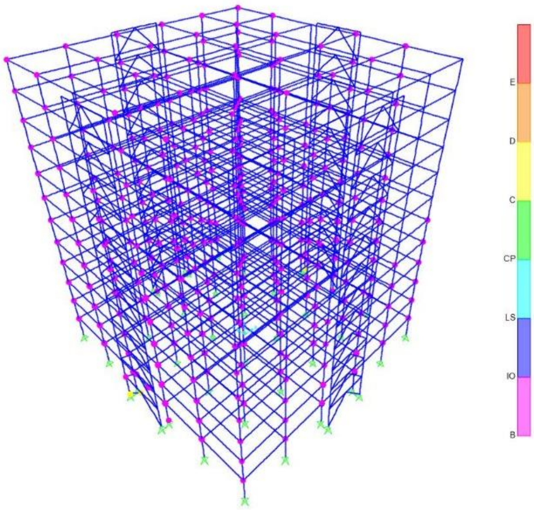

Figure E.46 Plastic Hinge Formation of Push Y Load Case for 1210V11

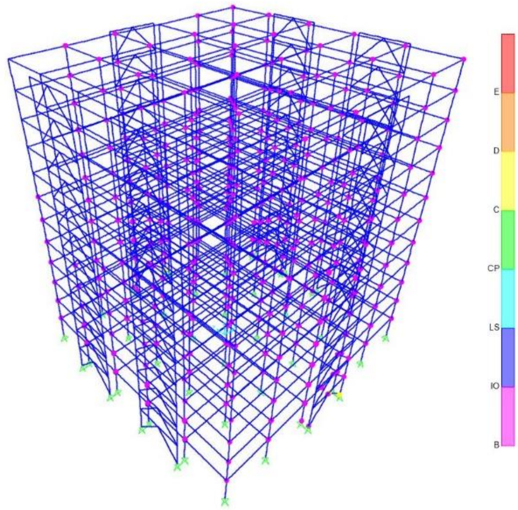

Figure E.47 Plastic Hinge Formation of Push X Load Case for 1210V21

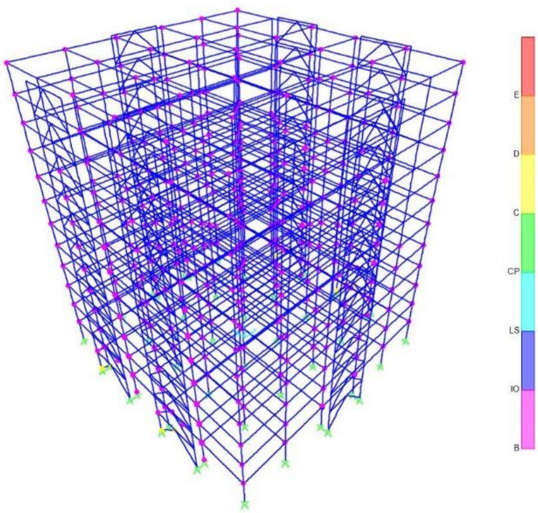

Figure E.48 Plastic Hinge Formation of Push Y Load Case for 1210V21

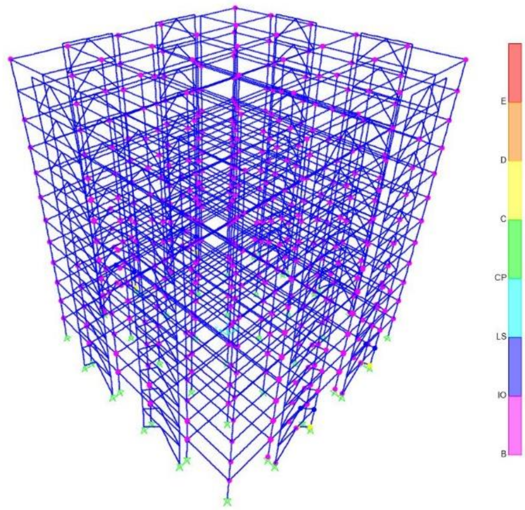

Figure E.49 Plastic Hinge Formation of Push X Load Case for 1210V22

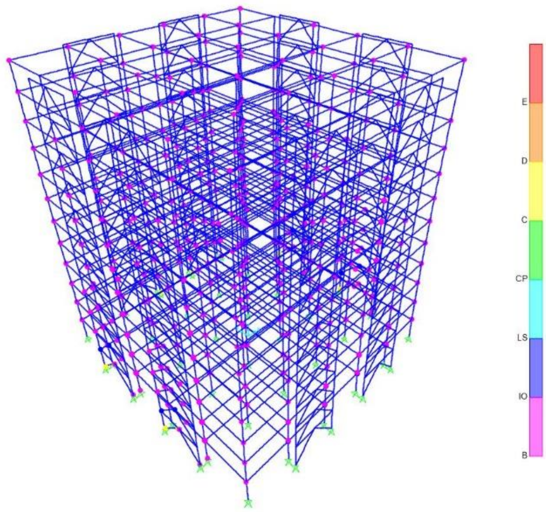

Figure E.50 Plastic Hinge Formation of Push Y Load Case for 1210V22

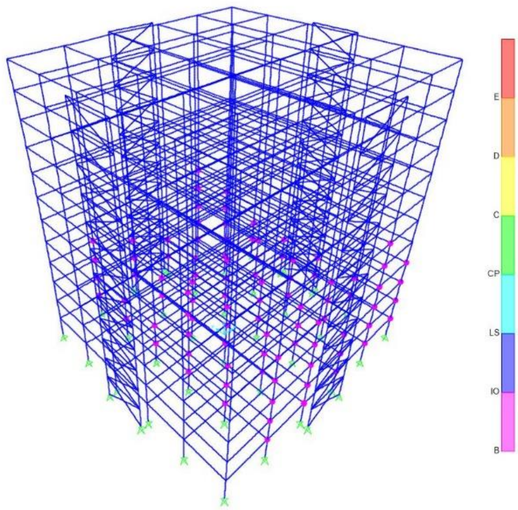

Figure E.51 Plastic Hinge Formation of Push X Load Case for 1210X11

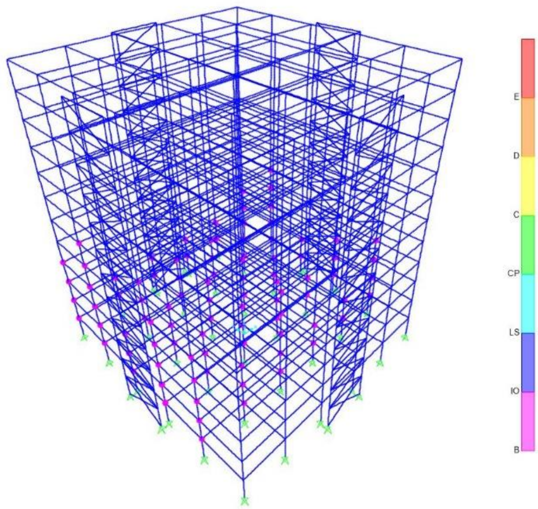

Figure E.52 Plastic Hinge Formation of Push Y Load Case for 1210X11

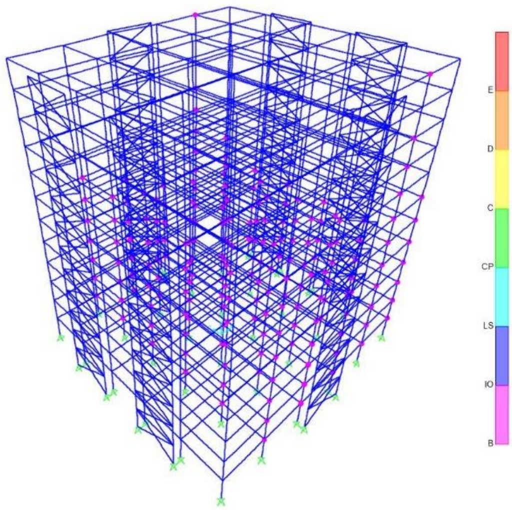

Figure E.53 Plastic Hinge Formation of Push X Load Case for 1210X21

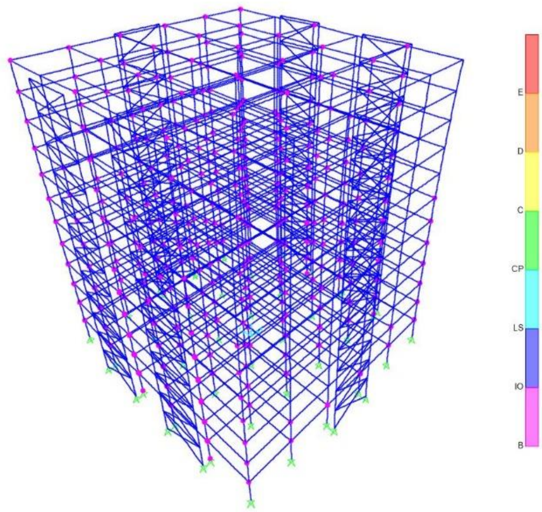

Figure E.54 Plastic Hinge Formation of Push Y Load Case for 1210X21

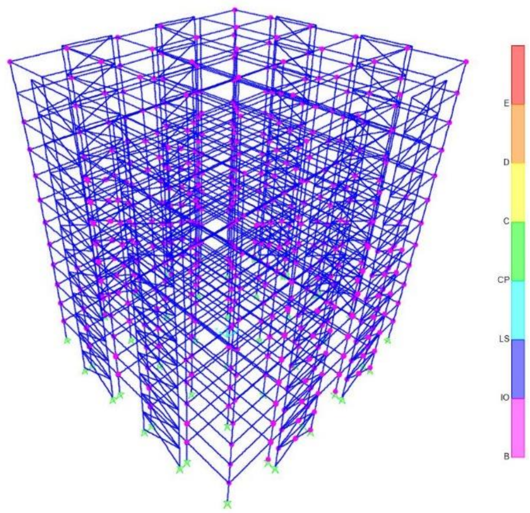

Figure E.55 Plastic Hinge Formation of Push X Load Case for 1210X22

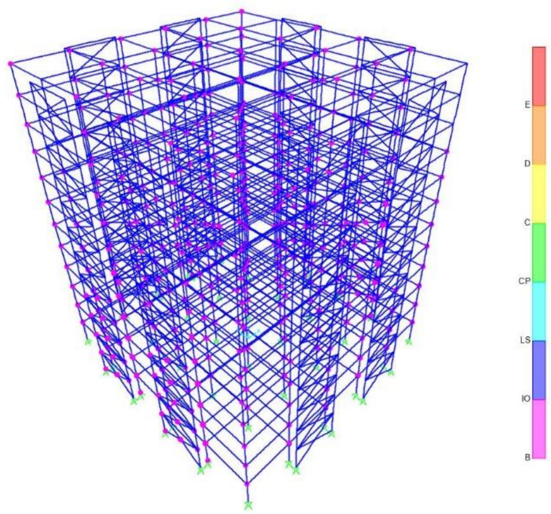

Figure E.56 Plastic Hinge Formation of Push Y Load Case for 1210X22